

**From Main Group to Transition Metal-containing Brønsted Acid Initiators for the  
Cationic Polymerization of Olefin Monomers**

by

Khatera Hazin

M.Sc., Freie Universität Berlin, 2010

A THESIS SUBMITTED IN PARTIAL FULFILLMENT OF  
THE REQUIREMENTS FOR THE DEGREE OF

Doctor of Philosophy

in

THE FACULTY OF GRADUATE AND POSTDOCTORAL STUDIES

(Chemistry)

THE UNIVERSITY OF BRITISH COLUMBIA

(Vancouver)

July 2018

© Khatera Hazin, 2018

The following individuals certify that they have read, and recommend to the Faculty of Graduate and Postdoctoral Studies for acceptance, the dissertation entitled:

From Main Group to Transition Metal-containing Brønsted Acid Initiators for the Cationic Polymerization of Olefin Monomers

---

submitted by Khatera Hazin in partial fulfillment of the requirements for

the degree of Doctor of Philosophy

in Chemistry

**Examining Committee:**

Derek Gates

---

Supervisor

Laurel Schafer

---

Supervisory Committee Member

---

Supervisory Committee Member

Mark MacLachlan

---

University Examiner

Glenn Sammis

---

University Examiner

**Additional Supervisory Committee Members:**

Chris Orvig

---

Supervisory Committee Member

George Sawatzky

---

Supervisory Committee Member

## Abstract

This dissertation outlines the development of Brønsted acids and their application as single-component initiators for the cationic polymerization of olefins. Solid weighable Brønsted acids are of particular interest in the generation and stabilization of highly reactive cations. Weakly coordinating anions (WCAs) facilitate the isolation of Brønsted acids and play a critical role in the carbocationic polymerization of vinyl monomers.

Chapter 1 gives an introduction to the mechanism of cationic polymerization and the challenges associated with it. The chapter also describes important initiator systems that are used in cationic polymerization and provides an overview of main group element-based WCAs that have been previously reported.

Chapter 2 outlines the application of the known tris(tetrachlorobenzenediolato)phosphate,  $[\text{P}(1,2\text{-O}_2\text{C}_6\text{Cl}_4)_3]^-$ , as a WCA in the stabilization of reactive cations. The isolated Brønsted acids  $\text{H}(\text{L})_2[\text{P}(1,2\text{-O}_2\text{C}_6\text{Cl}_4)_3]$  ( $\text{L} = \text{THF}, \text{DMF}$ ) were employed as effective single-component initiators for the cationic polymerization of *n*-butyl vinyl ether and *p*-methoxystyrene at various temperatures. Notably, high molecular weight poly(*p*-methoxystyrene) was obtained with an unexpected branched structure.

Chapter 3 describes three potential routes to afford Hellwinkel's salt,  $[\text{P}(\text{C}_{12}\text{H}_8)_2][\text{P}(\text{C}_{12}\text{H}_8)_3]$ . A pentavalent phosphorane,  $\text{P}(\text{C}_{12}\text{H}_8)_2(\text{C}_{12}\text{H}_9)$ , and an unprecedented product,  $[\text{P}(\text{C}_{12}\text{H}_8)(\text{C}_{24}\text{H}_{16})][\text{P}(\text{C}_{12}\text{H}_8)_3]$ , were isolated and characterized. The cation  $[\text{P}(\text{C}_{12}\text{H}_8)(\text{C}_{24}\text{H}_{16})]^+$  is formally derived from the insertion of an additional biphenyl unit into the known  $[\text{P}(\text{C}_{12}\text{H}_8)_2]^+$ .

Chapter 4 highlights the synthesis and characterization of several amine salts and an alkali metal salt featuring a hexacoordinate anion,  $[\text{P}(\text{C}_6\text{H}_4\text{CO}_2)_3]^-$ . The basicity of  $[\text{P}(\text{C}_6\text{H}_4\text{CO}_2)_3]^-$  was examined using IR spectroscopy and found to be comparable to  $[\text{ClO}_4]^-$  and  $[\text{N}(\text{SO}_2\text{CF}_3)_2]^-$ .

Chapter 5 describes the synthesis and characterization of two different Brønsted acids with the cation moiety  $[\text{H}(\text{OEt}_2)_2]^+$ . The Brønsted acids were employed as highly effective single-component initiators for the cationic polymerization of *n*-butyl vinyl ether, styrene,  $\alpha$ -methylstyrene and isoprene at different temperatures. Remarkably, high molecular weight polystyrene and poly( $\alpha$ -methylstyrene) were obtained. A predominantly rich syndiotactic poly( $\alpha$ -methylstyrene) (*rr* up to 90%) was isolated from a polymerization at  $-78\text{ }^\circ\text{C}$ .

Chapter 6 provides a summary of the thesis work and postulates future considerations in the field.

## **Lay Summary**

Polymers are produced by a process in which monomers are chemically combined to form long chain molecules composed of many repeated units. Rubber, a synthetic polymer, is produced by a process called cationic polymerization and requires an initiator to start the polymerization. The initiator is comprised of a cation (positively charged ion) and an anion (negatively charged ion). Industrial processes utilize a chemical, in combination with water, as an activator to generate such an initiator. This dissertation details the preparation and characterization of initiators that contain the cation and anion in one system. In order for the initiator to provide desired long polymer chains, the interaction between the cation and anion is of particular interest. The interaction should neither be too strong nor too weak, but just right. There are only a few such systems known due to the challenge in preparing and handling these initiators.

## Preface

Sections of this dissertation have been previously published in peer reviewed journals. Chapter 2 has been published as a full paper in *Dalton Transactions*. Khatera Hazin, Spencer C. Serin, Brian O. Patrick, Maria B. Ezhova, Derek P. Gates. [HL<sub>2</sub>][P(1,2-O<sub>2</sub>C<sub>6</sub>Cl<sub>4</sub>)<sub>3</sub>] (L = THF, DMF): Brønsted acid initiators for the polymerization of *n*-butyl vinyl ether and *p*-methoxystyrene. *Dalton Trans.* **2017**, *46*, 5901–5910. I have performed the syntheses, polymerizations, and characterizations. I wrote the manuscript in collaboration with my supervisor Prof. Derek P. Gates. Dr. Maria B. Ezhova assisted in the collection of the low temperature 2D <sup>1</sup>H-NOESY and <sup>1</sup>H-ROESY NMR spectra. Dr. Spencer C. Serin collected X-ray crystallographic data for compounds H(DMF)<sub>2</sub>[**2.1**], H(THF)<sub>2</sub>[**2.1**] and H(THF)(CH<sub>3</sub>CN)[**2.1**]. The refinements of these three structures were performed by Dr. Spencer C. Serin and Dr. Brian O. Patrick.

Chapter 3 has been published as a full paper in *Canadian Journal of Chemistry*. Khatera Hazin and Derek P. Gates. A twist on Hellwinkel's salt, [P(2,2'-biphenyl)<sub>2</sub>]<sup>+</sup>[P(2,2'-biphenyl)<sub>3</sub>]<sup>-</sup>. *Can. J. Chem.* **2018**, *96*, 526-533. I performed all synthetic work and characterizations. I wrote the manuscript in collaboration with Prof. Derek P. Gates. X-ray crystallographic data for the structures [**3.1'**][**3.2**] and **3.3** were collected by Dr. Spencer C. Serin and solved by both Dr. Spencer C. Serin and Dr. Brian O. Patrick.

A version of Chapter 4 will be submitted as a full paper to a peer reviewed journal. Khatera Hazin, Brian O. Patrick, Derek P. Gates. *To be submitted*. I performed the syntheses and characterizations of the complexes. The manuscript is written in collaboration with Prof. Derek P. Gates. X-ray crystallographic data for the structure [PhNMe<sub>2</sub>H]-*rac-mer*-[**4.1**] was collected and solved by Dr. Spencer C. Serin, while data for the structures [(-)-brucineH]-*Λ-mer*-[**4.1**],

[isoquinolineH]-*rac-mer*-[4.1], [pyH]-*rac-mer*-[4.1], and K-*rac-mer*-[4.1] were collected and solved by Dr. Brian O. Patrick.

A version of Chapter 5 will be submitted for publication to a peer reviewed journal. Khatera Hazin and Derek P. Gates. *To be submitted*. I performed the syntheses, polymerizations, and characterizations. The manuscript is written in collaboration with Prof. Derek P. Gates. The collection of the  $^{13}\text{C}\{^1\text{H}\}$  NMR spectrum of polyisoprene at 44 °C was performed by Dr. Maria B. Ezhova. X-ray crystallographic data for the structure  $\text{H}(\text{OEt}_2)_2$ [5.1] was collected and solved by Dr. Brian O. Patrick.

Chapter 6 was written by me.

# Table of Contents

|  |             |
|--|-------------|
| <b>Abstract.....</b>   | <b>iii</b>  |
| <b>Lay Summary .....</b>   | <b>v</b>    |
| <b>Preface.....</b>  | <b>vi</b>   |
| <b>Table of Contents .....</b>   | <b>viii</b> |
| <b>List of Tables .....</b>  | <b>xiii</b> |
| <b>List of Figures.....</b>  | <b>xv</b>   |
| <b>List of Schemes .....</b>   | <b>xx</b>   |
| <b>List of Symbols and Abbreviations .....</b>                                   | <b>xxii</b> |
| <b>Acknowledgements .....</b>  | <b>xxix</b> |
| <b>Dedication .....</b>  | <b>xxxi</b> |
| <b>Chapter 1: Introduction .....</b>   | <b>1</b>    |
| <b>1.1 Butyl Rubber .....</b>  | <b>1</b>    |
| <b>1.2 Mechanism of Cationic Polymerization .....</b>                            | <b>4</b>    |
| 1.2.1 Initiation.....  | 5           |
| 1.2.2 Propagation .....  | 7           |
| 1.2.3 Termination and Chain Transfer.....  | 8           |
| <b>1.3 Initiators Used in Cationic Polymerization .....</b>                      | <b>10</b>   |
| 1.3.1 Binary Initiators .....  | 10          |
| 1.3.2 Single-component Initiators.....   | 10          |
| <b>1.4 Weakly Coordinating Anions (WCAs).....</b>                                | <b>12</b>   |
| 1.4.1 Development and Application of WCAs in Cationic Olefin Polymerization..... | 14          |

|  |   |           |
|--|---|-----------|
| 1.5  | Group 15 Element Based WCAs .....   | 26        |
| 1.6  | Outline of Thesis .....   | 28        |
| <b>Chapter 2: [HL<sub>2</sub>][P(1,2-O<sub>2</sub>C<sub>6</sub>Cl<sub>4</sub>)<sub>3</sub>] (L = THF, DMF): Brønsted Acid Initiators for the</b> |   |           |
| <b>Polymerization of <i>n</i>-Butyl Vinyl Ether and <i>p</i>-Methoxystyrene* .....</b>   |   |           |
| <b>2.1</b>   | <b>Introduction.....</b>  | <b>30</b> |
| <b>2.2</b>   | <b>Results and Discussion.....</b>  | <b>32</b> |
| 2.2.1  | Synthesis and Characterization of Initiators .....  | 32        |
| 2.2.2  | Metrical Parameters Determined by X-ray Crystallography .....   | 38        |
| 2.2.3  | H(DMF) <sub>2</sub> [ <b>2.1</b> ] and H(THF) <sub>2</sub> [ <b>2.1</b> ]-initiated Cationic Polymerization ..... | 44        |
| <b>2.3</b>   | <b>Summary.....</b>   | <b>52</b> |
| <b>2.4</b>   | <b>Experimental .....</b>   | <b>53</b> |
| 2.4.1  | General Procedures .....  | 53        |
| 2.4.2  | Synthesis of H(DMF) <sub>2</sub> [ <b>2.1</b> ].....  | 55        |
| 2.4.3  | Synthesis of H(THF) <sub>2</sub> [ <b>2.1</b> ].....  | 55        |
| 2.4.4  | Synthesis of (CH <sub>3</sub> CN)(THF)[ <b>2.1</b> ].....   | 56        |
| 2.4.5  | Representative H(DMF) <sub>2</sub> [ <b>2.1</b> ]-initiated Polymerization of <i>n</i> -Butyl Vinyl Ether .....   | 56        |
| 2.4.6  | Representative H(DMF) <sub>2</sub> [ <b>2.1</b> ]-initiated Polymerization of <i>p</i> -Methoxystyrene .....      | 57        |
| 2.4.7  | X-ray Structure Determination .....   | 57        |
| <b>Chapter 3: A Twist on Hellwinkel's Salt, [P(2,2'-biphenyl)<sub>2</sub>]<sup>+</sup>[P(2,2'-biphenyl)<sub>3</sub>]<sup>-</sup> * .....</b>     |   |           |
| <b>3.1</b>   | <b>Introduction.....</b>  | <b>60</b> |
| <b>3.2</b>   | <b>Results and Discussion.....</b>  | <b>62</b> |
| <b>3.3</b>   | <b>Summary.....</b>   | <b>73</b> |
| <b>3.4</b>   | <b>Experimental .....</b>   | <b>74</b> |

|       |  |    |
|-------|--|----|
| 3.4.1 | General Procedures .....   | 74 |
| 3.4.2 | Synthesis of $[P(C_{12}H_8)(C_{24}H_{16})]^+$ ( <b>[3.1']<sup>+</sup></b> ), $[P(C_{12}H_8)_2]^+$ ( <b>[3.1]<sup>+</sup></b> ), $[P(C_{12}H_8)_3]^-$ ( <b>[3.2]<sup>-</sup></b> ) and $P(C_{12}H_8)_2(C_{12}H_9)$ ( <b>3.3</b> ) ..... | 75 |
| 3.4.3 | Synthesis of $[P(C_{12}H_8)(C_{24}H_{16})]$ <b>[3.2]</b> .....   | 76 |
| 3.4.4 | Synthesis of <b>3.3</b> .....  | 77 |
| 3.4.5 | X-ray Structure Determination .....  | 77 |

## Chapter 4: Ammonium and Potassium Salts of a Hexacoordinate Phosphorus(V) Anion

|   |   |           |
|---|---|-----------|
| <b>Featuring P–O and P–C Bonds.....</b> |   | <b>79</b> |
| <b>4.1</b>                              | <b>Introduction.....</b>  | <b>79</b> |
| <b>4.2</b>                              | <b>Results and Discussion.....</b>  | <b>81</b> |
| 4.2.1                                   | Synthesis and Characterization of Ammonium Salts of <i>mer</i> – <b>[4.1]<sup>-</sup></b> ..... | 81        |
| 4.2.2                                   | Metrical Parameters Determined by X-ray Crystallography .....                                   | 85        |
| 4.2.3                                   | Placement of <i>mer</i> – <b>[4.1]<sup>-</sup></b> on IR Scale for WCAs .....                   | 88        |
| 4.2.4                                   | Preparation of $K^+$ and $H^+$ Salts of <i>mer</i> – <b>[4.1]<sup>-</sup></b> .....             | 89        |
| <b>4.3</b>                              | <b>Summary.....</b>   | <b>93</b> |
| <b>4.4</b>                              | <b>Experimental .....</b>   | <b>94</b> |
| 4.4.1                                   | General Procedures .....  | 94        |
| 4.4.2                                   | X-ray Structure Determination .....   | 95        |
| 4.4.3                                   | Synthesis of $[PhNMe_2H]$ – <i>mer</i> – <b>[4.1]</b> .....                                     | 96        |
| 4.4.4                                   | Synthesis of $[PhNH_3]$ – <i>mer</i> – <b>[4.1]</b> .....                                       | 97        |
| 4.4.5                                   | Synthesis of $[pyH]$ – <i>mer</i> – <b>[4.1]</b> .....  | 98        |
| 4.4.6                                   | Synthesis of $[isoquinolineH]$ – <i>mer</i> – <b>[4.1]</b> .....                                | 99        |
| 4.4.7                                   | Synthesis of $[(-)-brucineH]$ – <i>mer</i> – <b>[4.1]</b> .....                                 | 100       |

|  |  |            |
|--|--|------------|
| 4.4.8  | Synthesis of $[(n\text{-C}_8\text{H}_{17})_3\text{NH}]$ -mer-[4.1].....                                      | 102        |
| 4.4.9  | Synthesis of K-mer-[4.1].....  | 103        |
| 4.4.10   | Attempted Synthesis of $\text{H}(\text{DMF})_n$ [4.1].....   | 104        |
| <b>Chapter 5: Brønsted Acids with Hexacoordinate Tantalum(V) Weakly Coordinating</b>               |  |            |
| <b>Anions as Highly Effective Initiators for the Cationic Polymerization of Vinyl Monomers</b> 106 |  |            |
| 5.1  | <b>Introduction</b> .....  | 106        |
| 5.2  | <b>Results and Discussion</b> .....  | 109        |
| 5.2.1  | Synthesis and Characterization of Initiators .....   | 109        |
| 5.2.2  | Metrical Parameters Determined by X-ray Crystallography .....  | 115        |
| 5.2.3  | $\text{H}(\text{OEt}_2)_2$ [5.1] and $\text{H}(\text{OEt}_2)_2$ [5.2]-initiated Cationic Polymerization..... | 119        |
| 5.3  | <b>Summary</b> .....   | 134        |
| 5.4  | <b>Experimental</b> .....  | 135        |
| 5.4.1  | General Procedures .....   | 135        |
| 5.4.2  | Synthesis of $\text{H}(\text{OEt}_2)_2$ [5.1].....   | 136        |
| 5.4.3  | Synthesis of $\text{H}(\text{OEt}_2)_2$ [5.2].....   | 137        |
| 5.4.4  | Representative $\text{H}(\text{OEt}_2)_2$ [5.1]-initiated Polymerization of <i>n</i> -Butyl Vinyl Ether .... | 138        |
| 5.4.5  | Representative $\text{H}(\text{OEt}_2)_2$ [5.1]-initiated Polymerization of Styrene .....                    | 138        |
| 5.4.6  | Representative $\text{H}(\text{OEt}_2)_2$ [5.1]-initiated Polymerization of $\alpha$ -Methylstyrene .....    | 139        |
| 5.4.7  | Representative $\text{H}(\text{OEt}_2)_2$ [5.1]-initiated Polymerization of Isoprene .....                   | 139        |
| 5.4.8  | Representative $\text{H}(\text{OEt}_2)_2$ [5.2]-initiated Polymerization of <i>n</i> -Butyl Vinyl Ether .... | 140        |
| 5.4.9  | Representative $\text{H}(\text{OEt}_2)_2$ [5.2]-initiated Polymerization of $\alpha$ -Methylstyrene .....    | 141        |
| 5.4.10   | X-ray Structure Determination of $\text{H}(\text{OEt}_2)_2(\text{H}_2\text{O})$ [5.1].....                   | 141        |
| <b>Chapter 6: Conclusion and Future Work</b> .....   |  | <b>143</b> |

|            |  |            |
|------------|--|------------|
| <b>6.1</b> | <b>Introduction</b> .....                        | 143        |
| <b>6.2</b> | <b>Hexacoordinate WCAs</b> .....                 | 143        |
| <b>6.3</b> | <b>Concluding Remarks</b> .....                  | 148        |
|            | <b>References</b> .....                          | <b>149</b> |
|            | <b>Appendices</b> .....                          | <b>166</b> |
|            | <b>Appendix A</b> .....                          | 166        |
| <b>A.1</b> | <b>Supplementary Spectra for Chapter 2</b> ..... | 166        |
|            | <b>Appendix B</b> .....                          | 173        |
| <b>B.1</b> | <b>Supplementary Spectra for Chapter 3</b> ..... | 173        |
|            | <b>Appendix C</b> .....                          | 176        |
| <b>C.1</b> | <b>Supplementary Spectra for Chapter 4</b> ..... | 176        |
|            | <b>Appendix D</b> .....                          | 189        |
| <b>D.1</b> | <b>Supplementary Spectra for Chapter 5</b> ..... | 189        |

## List of Tables

|  |     |
|--|-----|
| Table 2-1. Cationic polymerization of <i>n</i> -butyl vinyl ether using H(DMF) <sub>2</sub> [ <b>2.1</b> ] and H(THF) <sub>2</sub> [ <b>2.1</b> ] as initiator.....  | 48  |
| Table 2-2. Cationic polymerization of <i>p</i> -methoxystyrene using H(DMF) <sub>2</sub> [ <b>2.1</b> ] and H(THF) <sub>2</sub> [ <b>2.1</b> ] as initiator.....   | 50  |
| Table 2-3. X-ray crystallographic data and refinement details for compounds H(DMF) <sub>2</sub> [ <b>2.1</b> ], H(THF) <sub>2</sub> [ <b>2.1</b> ] and H(THF)(CH <sub>3</sub> CN)[ <b>2.1</b> ].....   | 59  |
| Table 3-1. X-ray crystallographic data for [ <b>3.1'</b> ][ <b>3.2</b> ] and <b>3.3</b> . ....   | 78  |
| Table 4-1. <sup>31</sup> P{ <sup>1</sup> H} and <sup>1</sup> H-NMR chemical shifts of [N <sub>base</sub> H]- <i>rac-mer</i> -[ <b>4.1</b> ].....   | 83  |
| Table 4-2. νN-H frequencies for [( <i>n</i> -C <sub>8</sub> H <sub>17</sub> ) <sub>3</sub> NH] <sup>+</sup> [Anion] <sup>-</sup> salts in CCl <sub>4</sub> and solid state. ....   | 89  |
| Table 4-3. X-ray crystallographic data for [PhNMe <sub>2</sub> H]- <i>rac-mer</i> -[ <b>4.1</b> ], [pyH]- <i>rac-mer</i> -[ <b>4.1</b> ], [isoquinolineH]- <i>rac-mer</i> -[ <b>4.1</b> ], [(-)-(brucineH)-Λ- <i>mer</i> -[ <b>4.1</b> ], and K- <i>rac-mer</i> -[ <b>4.1</b> ]. ....                    | 105 |
| Table 5-1. Temperature dependencies of H(OEt <sub>2</sub> ) <sub>2</sub> [ <b>5.1</b> ]-initiated cationic polymerizations of <i>n</i> -butyl vinyl ether, α-methylstyrene, styrene, and isoprene in CH <sub>2</sub> Cl <sub>2</sub> . The results shown are representative of multiple repeat runs..... | 123 |
| Table 5-2. Temperature dependencies of H(OEt <sub>2</sub> ) <sub>2</sub> [ <b>5.2</b> ]-initiated cationic polymerizations of <i>n</i> -butyl vinyl ether and α-methylstyrene in CH <sub>2</sub> Cl <sub>2</sub> .....   | 124 |
| Table 5-3. H(OEt <sub>2</sub> ) <sub>2</sub> [ <b>5.1</b> ]-initiated cationic polymerizations of <i>n</i> -butyl vinyl ether and styrene in CH <sub>2</sub> Cl <sub>2</sub> with varying monomer-to-initiator ratio. ....   | 133 |
| Table 5-4. H(OEt <sub>2</sub> ) <sub>2</sub> [ <b>5.1</b> ]-initiated cationic polymerizations of styrene in CH <sub>2</sub> Cl <sub>2</sub> with varying amounts of added H <sub>2</sub> O (μL).....  | 134 |

|  |     |
|--|-----|
| Table 5-5. X-ray crystallographic parameters for H(OEt <sub>2</sub> )(H <sub>2</sub> O)[ <b>5.1</b> ].   | 142 |
| Table C-1. Selected bond lengths [Å] and bond angles [°] of [PhNMe <sub>2</sub> H]- <i>rac-mer</i> -[ <b>4.1</b> ], [pyH]- <i>rac-mer</i> -[ <b>4.1</b> ], [isoquinolineH]- <i>rac-mer</i> -[ <b>4.1</b> ], [(-)-brucineH]- $\Lambda$ - <i>mer</i> -[ <b>4.1</b> ], and K- <i>rac-mer</i> -[ <b>4.1</b> ]. | 188 |

## List of Figures

|   |    |
|---|----|
| Figure 1.1. Microstructure of natural rubber contains <i>cis</i> -1,4-polyisoprene units.....   | 1  |
| Figure 1.2. Solvation association of the carbocation ( $A^{\oplus}$ ) and counter anion ( $B^{\ominus}$ ). .....  | 7  |
| Figure 1.3. Examples of Brønsted acids used as single-component initiators for cationic polymerization of olefins. ....   | 12 |
| Figure 1.4. Electrostatic interactions between a carbocation and a counterion. ....   | 13 |
| Figure 2.1. Examples of isolable Brønsted acids that have successfully been employed as single-component initiator systems for olefins. ....  | 31 |
| Figure 2.2. $^1H$ NMR (400 MHz, $CD_2Cl_2$ , $-85\text{ }^{\circ}C$ ) spectrum of (a) $H(THF)_2[2.1]$ and (b) $H(DMF)_2[2.1]$ . ....  | 35 |
| Figure 2.3. 2D $^1H$ -NOESY(400 MHz, $CD_2Cl_2$ , $-85\text{ }^{\circ}C$ ) experiment of $H(THF)_2[2.1]$ . ....   | 37 |
| Figure 2.4. Molecular structure of $H(DMF)_2\text{-}rac\text{-}[2.1]\cdot 0.2\text{ }CH_2Cl_2$ ( $\Delta$ isomer is shown; molecule 1 of 5 unique molecules). ....  | 40 |
| Figure 2.5. Molecular structure of $H(THF)_2\text{-}rac\text{-}[2.1]\cdot C_6H_2O_2Cl_4\cdot THF$ ( $\Delta$ isomer is shown)... ..   | 41 |
| Figure 2.6. Molecular structure of $H(THF)(MeCN)\text{-}rac\text{-}[2.1]\cdot 3.35\text{ }MeCN\cdot 1.52\text{ }THF$ ( $\Delta$ isomer is shown). ....  | 43 |
| Figure 2.7. Comparison of C–O and C–C bond length of $[H(THF)_2]^+$ in $H(THF)_2[2.1]$ , $H(THF)_2[CHB_{11}H_5Br_6]$ , $H(THF)_2[Al\{OC(CF_3)_3\}_4]$ and $H(THF)_2[MnCl_4(THF)_2]$ . ....  | 44 |
| Figure 2.8. $^1H$ NMR (400 MHz, $CDCl_3$ , $25\text{ }^{\circ}C$ ) spectra of poly( <i>n</i> -butyl vinyl ether) polymerized using (a) $H(DMF)_2[2.1]$ at $18\text{ }^{\circ}C$ , (b) $H(THF)_2[2.1]$ at $18\text{ }^{\circ}C$ and (c) $H(DMF)_2[2.1]$ at $-50\text{ }^{\circ}C$ . .. | 46 |
| Figure 2.9. Refractive index traces of poly( <i>n</i> -butyl vinyl ether) initiated by $H(DMF)_2[2.1]$ (Table 2.1, entry 5) and $H(THF)_2[2.1]$ (Table 2.1, entry 14). ....   | 47 |

|  |    |
|--|----|
| Figure 2.10. $^1\text{H}$ NMR (400 MHz, $\text{CDCl}_3$ , 25 °C) spectrum of poly( <i>p</i> -methoxystyrene) prepared using $\text{H}(\text{DMF})_2[\mathbf{2.1}]$ at 18°C. ....   | 52 |
| Figure 3.1. Selected examples of boron(III)–, aluminum(III)– and phosphorus(V)–containing WCAs.....  | 60 |
| Figure 3.2. Hellwinkel’s spiro-compound $[\mathbf{3.1}][\mathbf{3.2}]$ .....   | 61 |
| Figure 3.3. $^{31}\text{P}\{^1\text{H}\}$ NMR (162 MHz, 25 °C) spectra of: (a) the reaction mixture obtained by reacting $\text{PCl}_5$ with 2,2’-lithiobiphenyl [obtained from biphenyl, <i>n</i> -BuLi and TMEDA] in THF/ $\text{Et}_2\text{O}$ – Route A in Scheme 3.1; (b) the reaction mixture obtained by reacting a portion of isolated reaction mixture from Route A (above) with 2,2’-dilithiobiphenyl in $\text{Et}_2\text{O}$ ; (c) crystals of isolated $[\mathbf{3.1}'][\mathbf{3.2}]$ dissolved in THF/ $\text{Et}_2\text{O}$ solution; and (d) crystals of isolated $\mathbf{3.3}$ dissolved in THF/ $\text{Et}_2\text{O}$ . .... | 64 |
| Figure 3.4. Spiro-compound $[\text{P}(\text{C}_{12}\text{H}_8)(\text{C}_{24}\text{H}_{16})][\text{P}(\text{C}_{12}\text{H}_8)_3]$ ( $[\mathbf{3.1}'][\mathbf{3.2}]$ ). ....  | 67 |
| Figure 3.5. Molecular structure of the salt ( <i>S</i> )– $[\mathbf{3.1}']$ – $\Delta$ – $[\mathbf{3.2}] \cdot 1.73 \text{ THF} \cdot 0.27 \cdot \text{Et}_2\text{O}$ . ....   | 67 |
| Figure 3.6. Pentacoordinate phosphorane $\mathbf{3.3}$ , $[\text{P}(\text{C}_{12}\text{H}_8)_2(\text{C}_{12}\text{H}_9)]$ . ....   | 69 |
| Figure 3.7. Molecular structure of $\mathbf{3.3}$ . ....   | 69 |
| Figure 3.8. $^{31}\text{P}\{^1\text{H}\}$ NMR (162 MHz, 25 °C) spectrum of $[\mathbf{3.1}][\mathbf{3.2}]$ and $[\mathbf{3.1}'][\mathbf{3.2}]$ via (a) dilithiated 2,2’-diiodobiphenyl recorded in THF/ $\text{Et}_2\text{O}$ solution (Route B); (b) dilithiated 2,2’-dibromobiphenyl recorded in THF/ $\text{Et}_2\text{O}$ solution (Route C).....   | 71 |
| Figure 4.1. Examples of hexacoordinate phosphorus(V) weakly coordinating anions. ....  | 80 |
| Figure 4.2. $^{31}\text{P}\{^1\text{H}\}$ NMR (162 MHz, 25 °C) spectra of a) $[(-)\text{-brucineH}]\text{-rac-mer-}[\mathbf{4.1}]$ recorded in $(\text{CD}_3)_2\text{SO}$ and b) $[(-)\text{-brucineH}]\text{-rac-mer-}[\mathbf{4.1}]$ recorded in $\text{CD}_2\text{Cl}_2$ solvent. ....  | 83 |

|  |     |
|--|-----|
| Figure 4.3. Molecular structures of (a) [PhNMe <sub>2</sub> H]– <i>rac-mer</i> –[4.1]·Me <sub>2</sub> C=O (Δ isomer is shown); (b) [pyH]– <i>rac-mer</i> –[4.1]·0.5 Me <sub>2</sub> C=O (Δ isomer is shown); (c) [isoquinolineH]– <i>rac-mer</i> –[4.1]·(C <sub>9</sub> H <sub>7</sub> N) (Δ isomer is shown); (d) [(–)-brucineH]–Δ– <i>mer</i> –[4.1]·2.02 CH <sub>2</sub> Cl <sub>2</sub> .....          | 86  |
| Figure 4.4. Extended structure showing the coordination polymer formed by K– <i>rac-mer</i> –[4.1]·3 CH <sub>3</sub> OH (K–Δ,Δ– <i>mer</i> –[4.1] is shown).....   | 91  |
| Figure 4.5. <sup>31</sup> P{ <sup>1</sup> H} NMR (162 MHz, 25 °C) spectra of a) reaction mixture of H(DMF) <sub><i>n</i></sub> – <i>mer</i> –[4.1] recorded after 2 days and b) reaction mixture of H(DMF) <sub><i>n</i></sub> – <i>mer</i> –[4.1] recorded after ca. 4 weeks. 4.2 is phosphorane P(C <sub>6</sub> H <sub>4</sub> CO <sub>2</sub> ) <sub>2</sub> (C <sub>6</sub> H <sub>4</sub> COOH)..... | 91  |
| Figure 5.1. Examples of characterized tantalum(V)-containing complexes.....  | 108 |
| Figure 5.2. Brønsted acids H(OEt <sub>2</sub> ) <sub>2</sub> [5.1] and H(OEt <sub>2</sub> ) <sub>2</sub> [5.2].....  | 109 |
| Figure 5.3. <sup>1</sup> H NMR (400 MHz, CD <sub>2</sub> Cl <sub>2</sub> , –85 °C) spectrum of H(OEt <sub>2</sub> ) <sub>2</sub> [5.1].....  | 111 |
| Figure 5.4. Molecular structure of H(OEt <sub>2</sub> )(H <sub>2</sub> O)– <i>cis</i> –[5.1]·OEt <sub>2</sub> ·0.17 CH <sub>2</sub> Cl <sub>2</sub> .....  | 112 |
| Figure 5.5. <sup>1</sup> H NMR (400 MHz, CD <sub>2</sub> Cl <sub>2</sub> , –85 °C) spectrum of H(OEt <sub>2</sub> ) <sub>2</sub> [5.2].....  | 114 |
| Figure 5.6. <sup>13</sup> C{ <sup>1</sup> H} NMR (400 MHz, CD <sub>2</sub> Cl <sub>2</sub> , 25 °C) spectrum of H(OEt <sub>2</sub> ) <sub>2</sub> [5.2].....   | 115 |
| Figure 5.7. Metrical parameters [Å] for the cation in H(OEt <sub>2</sub> )(H <sub>2</sub> O)[5.1]·OEt <sub>2</sub> ·0.17 CH <sub>2</sub> Cl <sub>2</sub> ...   | 117 |
| Figure 5.8. <sup>1</sup> H NMR (400 MHz, CDCl <sub>3</sub> , 25 °C) spectrum of poly( <i>n</i> -butyl vinyl ether); polymerization performed (a) with initiator H(OEt <sub>2</sub> ) <sub>2</sub> [5.1] at 18 °C, (b) with initiator H(OEt <sub>2</sub> ) <sub>2</sub> [5.2] at 19.3 °C, (c) with initiator H(OEt <sub>2</sub> ) <sub>2</sub> [5.1] at –84 °C.....   | 122 |
| Figure 5.9. <sup>1</sup> H NMR (400 MHz, CDCl <sub>3</sub> , 25 °C) spectrum of syndiotactic-rich poly(α-methylstyrene) ( <i>rr</i> = 90%); polymerization performed with initiator H(OEt <sub>2</sub> ) <sub>2</sub> [5.1] at –78 °C.   | 127 |
| Figure 5.10. <sup>1</sup> H NMR (400 MHz, CDCl <sub>3</sub> , 25 °C) spectrum of polystyrene; polymerization performed with initiator H(OEt <sub>2</sub> ) <sub>2</sub> [5.1] at –50 °C.....   | 129 |

|  |     |
|--|-----|
| Figure 5.11. $^{13}\text{C}\{^1\text{H}\}$ NMR (101 MHz, $\text{CDCl}_3$ , 45 °C) spectrum of oligoisoprene; polymerization performed with initiator $\text{H}(\text{OEt}_2)_2[\mathbf{5.1}]$ at 18 °C.....  | 132 |
| Figure A.1. $^{31}\text{P}\{^1\text{H}\}$ NMR (121 MHz, $\text{CD}_3\text{CN}$ , 25 °C) spectrum of $\text{H}(\text{THF})_2[\mathbf{2.1}]$ . ....  | 166 |
| Figure A.2. $^{31}\text{P}\{^1\text{H}\}$ NMR (121 MHz, $\text{CD}_3\text{CN}$ , 25 °C) spectrum of $\text{H}(\text{DMF})_2[\mathbf{2.1}]$ . ....  | 167 |
| Figure A.3. $^{13}\text{C}\{^1\text{H}\}$ NMR (75 MHz, $\text{CD}_3\text{CN}$ , 25 °C) spectrum of $\text{H}(\text{THF})_2[\mathbf{2.1}]$ .....  | 168 |
| Figure A.4. $^{13}\text{C}\{^1\text{H}\}$ NMR (75 MHz, $\text{CD}_3\text{CN}$ , 25 °C) spectrum of $\text{H}(\text{DMF})_2[\mathbf{2.1}]$ .....  | 169 |
| Figure A.5. $^1\text{H}-^1\text{H}$ NOESY (400 MHz, $\text{CD}_2\text{Cl}_2$ , -85 °C) spectrum of $\text{H}(\text{DMF})_2[\mathbf{2.1}]$ .....  | 170 |
| Figure A.6. $^1\text{H}-^1\text{H}$ ROESY (400 MHz, $\text{CD}_2\text{Cl}_2$ , -85 °C) spectrum of $\text{H}(\text{DMF})_2[\mathbf{2.1}]$ . ....   | 171 |
| Figure A.7. $^1\text{H}-^1\text{H}$ ROESY (400 MHz, $\text{CD}_2\text{Cl}_2$ , -85 °C) spectrum of $\text{H}(\text{THF})_2[\mathbf{2.1}]$ . ....   | 172 |
| Figure B.1. LRMS (ESI; positive mode) mass spectrum of $[\mathbf{3.1}]^+$ and $[\mathbf{3.1}']^+$ via Route A.....   | 173 |
| Figure B.2. LRMS (ESI; negative mode) mass spectrum of $[\mathbf{3.2}]^-$ via Route A .....  | 174 |
| Figure B.3. Crystal packing of the molecular structure of $[\mathbf{3.1}'][\mathbf{3.2}]$ is shown with 2 unit cells along the b axis (x,y,z).....   | 175 |
| Figure C.1. $^{31}\text{P}\{^1\text{H}\}$ NMR (162 MHz, $(\text{CD}_3)_2\text{CO}$ , 25 °C) spectra of: a) $[\text{PhNMe}_2\text{H}]-\text{mer}-[\mathbf{4.1}]$ , b) $[\text{pyH}]-\text{mer}-[\mathbf{4.1}]$ , c) $[\text{isoquinolineH}]-\text{mer}-[\mathbf{4.1}]$ , and d) $[(n\text{-C}_8\text{H}_{17})_3\text{NH}]-\text{mer}-[\mathbf{4.1}]$ . .... | 176 |
| Figure C.2. $^{31}\text{P}\{^1\text{H}\}$ NMR (162 MHz, $(\text{CD}_3)_2\text{SO}$ , 25 °C) spectra of a) $[\text{PhNH}_3]-\text{mer}-[\mathbf{4.1}]$ and b) $[(\text{-})\text{-brucineH}]-\text{rac-mer}-[\mathbf{4.1}]$ . $\mathbf{4.2}$ is phosphorane $\text{P}(\text{C}_6\text{H}_4\text{CO}_2)_2(\text{C}_6\text{H}_4\text{COOH})$ . ....            | 177 |
| Figure C.3. $^1\text{H}$ NMR (400 MHz, $(\text{CD}_3)_2\text{CO}$ , 25 °C) spectrum of $[\text{PhNMe}_2\text{H}]-\text{mer}-[\mathbf{4.1}]$ .....  | 177 |
| Figure C.4. $^{13}\text{C}\{^1\text{H}\}$ NMR (101 MHz, $(\text{CD}_3)_2\text{CO}$ , 25 °C) spectrum of $[\text{PhNMe}_2\text{H}]-\text{mer}-[\mathbf{4.1}]$ .<br>.....  | 178 |
| Figure C.5. $^1\text{H}$ NMR (400 MHz, $(\text{CD}_3)_2\text{SO}$ , 25 °C) spectrum of $[\text{PhNH}_3]-\text{mer}-[\mathbf{4.1}]$ . ....  | 179 |
| Figure C.6. $^{13}\text{C}\{^1\text{H}\}$ NMR (101 MHz, $(\text{CD}_3)_2\text{SO}$ , 25 °C) spectrum of $[\text{PhNH}_3]-\text{mer}-[\mathbf{4.1}]$ . ....   | 179 |
| Figure C.7. $^1\text{H}$ NMR (400 MHz, $\text{CD}_2\text{Cl}_2$ , 25 °C) spectrum of $[\text{pyH}]-\text{mer}-[\mathbf{4.1}]$ .....  | 180 |

|  |     |
|--|-----|
| Figure C.8. $^{13}\text{C}\{^1\text{H}\}$ NMR (101 MHz, $\text{CD}_2\text{Cl}_2$ , 25 °C) spectrum of [pyH]- <i>mer</i> -[4.1].....  | 181 |
| Figure C.9. $^1\text{H}$ NMR (400 MHz, $\text{CD}_2\text{Cl}_2$ , 25 °C) spectrum of [isoquinolineH]- <i>mer</i> -[4.1].....   | 182 |
| Figure C.10. $^{13}\text{C}\{^1\text{H}\}$ NMR (101 MHz, $\text{CD}_2\text{Cl}_2$ , 25 °C) spectrum of [isoquinolineH]- <i>mer</i> -[4.1].<br>.....  | 182 |
| Figure C.11. $^1\text{H}$ NMR (400 MHz, $\text{CD}_2\text{Cl}_2$ , 25 °C) spectrum of [(-)-brucineH]- $\Lambda$ - <i>mer</i> -[4.1]..  | 183 |
| Figure C.12. $^{13}\text{C}\{^1\text{H}\}$ NMR (101 MHz, $\text{CD}_2\text{Cl}_2$ , 25 °C) spectrum of [(-)-brucineH]- $\Lambda$ - <i>mer</i> -<br>[4.1].....  | 184 |
| Figure C.13. $^1\text{H}$ NMR (400 MHz, $(\text{CD}_3)_2\text{CO}$ , 25 °C) spectrum of [( <i>n</i> - $\text{C}_8\text{H}_{17}$ ) $_3\text{NH}$ ]- <i>mer</i> -[4.1].  | 185 |
| Figure C.14. $^{13}\text{C}\{^1\text{H}\}$ NMR (101 MHz, $(\text{CD}_3)_2\text{CO}$ , 25 °C) spectrum of [( <i>n</i> - $\text{C}_8\text{H}_{17}$ ) $_3\text{NH}$ ]- <i>mer</i> -<br>[4.1].....   | 186 |
| Figure C.15. $^1\text{H}$ NMR (400 MHz, $\text{CD}_3\text{OD}$ , 25 °C) spectrum of K- <i>mer</i> -[4.1].....  | 187 |
| Figure C.16. $^{13}\text{C}\{^1\text{H}\}$ NMR (101 MHz, $\text{CD}_3\text{OD}$ , 25 °C) spectrum of K- <i>mer</i> -[4.1].....   | 187 |
| Figure D.1. $^1\text{H}$ - $^{13}\text{C}$ HMBC NMR (400 MHz for $^1\text{H}$ , $\text{CD}_2\text{Cl}_2$ , -85 °C) spectrum of $\text{H}(\text{OEt}_2)_2$ [5.1].<br>.....  | 189 |
| Figure D.2. $^{13}\text{C}\{^1\text{H}\}$ NMR (400 MHz, $\text{CD}_2\text{Cl}_2$ , -85 °C) spectrum of $\text{H}(\text{OEt}_2)_2$ [5.1]. .....   | 190 |
| Figure D.3. $^1\text{H}$ NMR (400 MHz, $\text{CD}_2\text{Cl}_2$ , -85 °C) spectrum of $\text{H}(\text{OEt}_2)_2$ [5.1]: a) day 1; b) day 2;<br>c) day 3; d) day 5; e) day 8 (addition of $\text{CD}_2\text{Cl}_2$ <i>ca.</i> 0.9 mL); f) day 12 and g) day 15. † indicates<br>free $\text{Et}_2\text{O}$ ..... | 191 |
| Figure D.4. $^1\text{H}$ NMR (400 MHz, $\text{CDCl}_3$ , 25 °C) spectrum of syndiotactic-rich poly( $\alpha$ -methyl-<br>styrene) ( <i>rr</i> = 86 %); polymerization performed with initiator $\text{H}(\text{OEt}_2)_2$ [5.2] at -78 °C .....  | 192 |

## List of Schemes

|  |    |
|--|----|
| Scheme 1.1. Commercial synthetic process for the production of butyl rubber.....   | 2  |
| Scheme 1.2. General mechanism of cationic chain polymerization of vinyl monomers.....  | 4  |
| Scheme 1.3. General formation of an active initiator ( $A^+B^+$ ).....   | 5  |
| Scheme 1.4. Trend in monomer reactivity in cationic polymerization.....  | 6  |
| Scheme 1.5. The carbocation can be stabilized by resonance (top) and inductive effect (bottom).6   |    |
| Scheme 1.6. Combination of the propagating species with a fragment of the counterion. ....   | 8  |
| Scheme 1.7. Chain transfer reaction can occur via (a) $\beta$ -proton transfer to monomer and (b) chain transfer to counterion, respectively.....  | 9  |
| Scheme 1.8. Side reaction in styrene polymerization can occur via (a) chain transfer to growing polymer chain or (b) branching or cross-linking of styrene during cationic polymerization. ....  | 9  |
| Scheme 1.9. Motifs of different interaction between the carbocation and counter anion during cationic polymerization.....  | 14 |
| Scheme 1.10. Different types of cationic polymerization and their general mechanisms; (a) reveals the mechanism of cationic chain polymerization; (b) shows the mechanism of cationic coordination polymerization, and (c) illustrates the mechanism of cationic ring-opening polymerization. .... | 16 |
| Scheme 2.1. Synthesis of Brønsted acid $H(L)_2[2.1]$ ( $L = DMF, THF$ ).....   | 33 |
| Scheme 2.2. Synthesis of Brønsted acid $H(THF)(MeCN)[2.1]$ .....   | 38 |
| Scheme 2.3. $H(L)_2[2.1]$ ( $L = DMF, THF$ ) initiated cationic polymerization of <i>n</i> -butyl vinyl ether. ....  | 45 |
| Scheme 3.1. Synthesis of $[3.1][3.2]$ via route A–C. ....  | 63 |

|   |     |
|---|-----|
| Scheme 4.1. General synthetic route of $[N_{\text{base}}H][\mathbf{4.1}]$ with $N_{\text{base}} = \text{PhNMe}_2, \text{PhNH}_2, \text{py},$<br>isoquinoline, (-)-brucine and $N(n\text{-C}_8\text{H}_{17})_3$ . $\mathbf{4.2}$ is phosphorane $\text{P}(\text{C}_6\text{H}_4\text{CO}_2)_2(\text{C}_6\text{H}_4\text{COOH})$ ..... | 81  |
| Scheme 4.2. Synthetic route of $K\text{-rac-mer-}[\mathbf{4.1}]$ .....  | 90  |
| Scheme 4.3. Proposed route to $\text{H}(\text{DMF})_n\text{-mer-}[\mathbf{4.1}]$ ( $n \geq 1$ ). .....  | 92  |
| Scheme 5.1. Synthesis of Brønsted acid $\text{H}(\text{OEt}_2)_2[\mathbf{5.1}]$ .....   | 109 |
| Scheme 5.2. Synthesis of Brønsted acid $\text{H}(\text{OEt}_2)_2[\mathbf{5.2}]$ .....   | 113 |
| Scheme 5.3. $\text{H}(\text{OEt}_2)_2[\mathbf{5.1}]$ and $\text{H}(\text{OEt}_2)_2[\mathbf{5.2}]$ -initiated cationic polymerization of <i>n</i> -butyl vinyl<br>ether.....   | 120 |
| Scheme 5.4. $\text{H}(\text{OEt}_2)_2[\mathbf{5.1}]$ and $\text{H}(\text{OEt}_2)_2[\mathbf{5.2}]$ -initiated cationic polymerization of $\alpha$ -<br>methylstyrene.....  | 125 |
| Scheme 5.5. $\text{H}(\text{OEt}_2)_2[\mathbf{5.1}]$ -initiated cationic polymerization of styrene. ....  | 127 |
| Scheme 5.6. $\text{H}(\text{OEt}_2)_2[\mathbf{5.1}]$ -initiated cationic polymerization of isoprene. ....   | 130 |
| Scheme 6.1. Synthesis of Brønsted acid $\text{H}(\text{L})_2[\mathbf{6.1}]$ ( $\text{L} = \text{DMF}, \text{THF}$ ).....  | 144 |
| Scheme 6.2. Proposed synthetic route of compound $\text{Li}[\mathbf{6.4}]$ and $\text{H}(\text{L})_2[\mathbf{6.4}]$ ( $\text{L} = \text{DMF}$ or $\text{Et}_2\text{O}$ ).<br>.....  | 145 |
| Scheme 6.3. Synthesis of Brønsted acids $\text{H}(\text{OEt}_2)_2[\mathbf{6.6}]$ and $\text{H}(\text{OEt}_2)_2[\mathbf{6.7}]$ .....   | 147 |

## List of Symbols and Abbreviations

|                 |  |
|-----------------|--|
| $\alpha$        | alpha                                  |
| Å               | Angstrom ( $1 \times 10^{-10}$ meters) |
| anal.           | analysis                               |
| Ar              | aryl                                   |
| avg.            | average                                |
| ax              | axial                                  |
| $\beta$         | beta                                   |
| br              | broad or broadened (spectra)           |
| BR              | butyl rubber                           |
| <sup>n</sup> Bu | <i>n</i> -butyl                        |
| <sup>t</sup> Bu | <i>tert</i> -butyl                     |
| C               | Celsius                                |
| c               | centi ( $10^{-2}$ )                    |
| <i>ca.</i>      | circa (about)                          |
| calcd           | calculated                             |
| cf.             | compare                                |
| <i>cis</i>      | same side                              |
| CCDC            | Cambridge Crystallographic Data Centre |
| COSY            | correlation spectroscopy               |
| Cp              | cyclopentadienyl ligand                |

|              |   |
|--------------|---|
| Cp*          | pentamethylcyclopentadienyl ligand                                  |
| $\Delta$     | delta (configurational)   |
| $^{\circ}$   | degree (angle or temperature)                                       |
| $\delta$     | NMR chemical shift in parts per million (ppm)                       |
| d            | day(s); doublet (NMR spectroscopy)                                  |
| <i>d</i>     | deuterated  |
| D            | dimensional   |
| D1           | relaxation delay (NMR spectroscopy)                                 |
| d7           | inversion recovery delay (NMR spectroscopy)                         |
| DLS          | dynamic light scattering  |
| DMF          | dimethylformamide, (CH <sub>3</sub> ) <sub>2</sub> NCH              |
| DMSO         | dimethyl sulfoxide, (CH <sub>3</sub> ) <sub>2</sub> SO <sub>2</sub> |
| <i>D</i>     | dispersity  |
| <i>dn/dc</i> | refractive index increment  |
| ed.          | edition   |
| ed. eds.     | editor(s)   |
| <i>e.g.</i>  | exempli gratia (for example)  |
| elem.        | elemental   |
| ESI          | electrospray ionization   |
| eq           | equatorial  |
| equiv        | equivalent  |
| Et           | ethyl or CH <sub>3</sub> CH <sub>2</sub> –                          |

|                   |  |
|-------------------|--|
| <i>et al.</i>     | and others   |
| Et <sub>2</sub> O | diethyl ether or (C <sub>2</sub> H <sub>5</sub> ) <sub>2</sub> O |
| etc.              | and so forth   |
| eV                | electron Volt  |
| <i>fac</i>        | facial (configuration)   |
| FT                | fourier transform  |
| FW                | free weight  |
| fwhm              | full width at half maximum                                       |
| g                 | gram   |
| GOF               | goodness of fit (crystallography)                                |
| GPC               | gel permeation chromatography                                    |
| h                 | hour   |
| { <sup>1</sup> H} | proton decoupled (NMR spectroscopy)                              |
| HPLC              | high-performance liquid chromatography                           |
| HMBC              | heteronuclear multiple bond correlation                          |
| HRMS              | high resolution mass spectrometry                                |
| Hz                | Hertz (s <sup>-1</sup> )   |
| <i>i</i>          | iso (as in <i>i</i> -Pr)   |
| <i>i.e.</i>       | id est (in other words)  |
| int               | internal (X-ray)   |
| <i>in situ</i>    | in place or in the reaction                                      |
| <i>in vacuo</i>   | in a vacuum  |

|            |  |
|------------|--|
| IR         | infrared   |
| $J$        | coupling constant (NMR spectroscopy)                         |
| K          | Kelvin   |
| $K_\alpha$ | spectral line  |
| $k_i$      | rate constant of initiation                                  |
| $k_p$      | rate constant of propagation                                 |
| $k_{tr}$   | rate constant of termination                                 |
| KH         | potassium hydride  |
| $\lambda$  | wavelength   |
| $\Lambda$  | lambda (configuration)                                       |
| L          | generic ligand; liter  |
| LA         | Lewis acid   |
| LLS        | laser light scattering                                       |
| LRMS       | low resolution mass spectrometry                             |
| $\nu$      | wavenumber   |
| M          | generic metal; molarity (mol per liter)                      |
| $M^+$      | molecular ion  |
| m          | milli ( $10^{-3}$ ); multiplet (NMR spectroscopy); meter     |
| $\mu$      | micro ( $10^{-6}$ ); absorption coefficient (X-ray)          |
| MAO        | methylaluminoxane, $(-[\text{O}-\text{Al}(\text{CH}_3)]_n-)$ |
| MALDI-TOF  | matrix-assisted laser desorption ionization - time of flight |
| MALS       | multi angle light scattering                                 |

|            |   |
|------------|---|
| Me         | methyl or CH <sub>3</sub> –               |
| MeOH       | methanol                                  |
| MeOSt      | methoxystyrene                            |
| <i>mer</i> | meridional (configuration)                |
| MHz        | megahertz                                 |
| M/I        | monomer to initiator ratio                |
| min        | minute                                    |
| $M_n$      | number average molecular weight           |
| $M_w$      | weight average molecular weight           |
| MW         | molecular weight                          |
| mol        | mole                                      |
| MS         | mass spectrometry                         |
| <i>m/z</i> | mass-to-charge ratio                      |
| n          | number; normal (in <i>n</i> -butyl); nano |
| NA         | not available                             |
| $\eta$     | hapticity; intrinsic viscosity            |
| NMR        | nuclear magnetic resonance                |
| NOE        | nuclear Overhauser effect                 |
| NOESY      | nuclear Overhauser effect spectroscopy    |
| <i>o</i>   | ortho                                     |
| <i>p</i>   | para                                      |
| %          | percent (parts per hundred)               |

|                         |   |
|-------------------------|---|
| Ph                      | phenyl  |
| pH                      | negative logarithm of hydrogen ion concentration  |
| Phen                    | phenanthryl   |
| PhNH <sub>2</sub>       | aniline, C <sub>6</sub> H <sub>5</sub> NH <sub>2</sub>                                      |
| PhNMe <sub>2</sub>      | <i>N,N</i> -dimethylaniline, C <sub>6</sub> H <sub>5</sub> N(CH <sub>3</sub> ) <sub>2</sub> |
| p <i>K</i> <sub>a</sub> | p <i>K</i> for association  |
| ppm                     | parts per million   |
| py                      | pyridine  |
| <sup>i</sup> Pr         | isopropyl   |
| q                       | quartet   |
| R                       | generic substituent; residual factor (X-ray)  |
| <i>R</i>                | rectus (configuration)  |
| <i>rac</i>              | racemic mixture or racemate   |
| refln                   | reflection  |
| <i>R</i> <sub>h</sub>   | hydrodynamic radius   |
| ROESY                   | rotating-frame overhauser effect spectroscopy   |
| <i>rr</i>               | syndiotactic triad  |
| RT                      | room temperature  |
| <i>r</i> <sub>vdw</sub> | van der Waals radii   |
| s                       | second; singlet (spectra); strong (spectra)   |
| <i>S</i>                | sinister (configuration)  |
| SADABS                  | Siemens area detector absorption correction program   |

|                   |  |
|-------------------|--|
| t                 | tertiary; triplet (NMR spectroscopy); time       |
| T                 | temperature                                      |
| T <sub>c</sub>    | ceiling temperature                              |
| T <sub>g</sub>    | glass transition temperature                     |
| THF               | tetrahydrofuran, C <sub>4</sub> H <sub>8</sub> O |
| T <sub>m</sub>    | melting temperature                              |
| TMEDA             | <i>N,N,N',N'</i> -tetramethylethylenediamine     |
| <i>trans</i>      | opposite side                                    |
| trifyl            | trifluoromethanesulfonyl                         |
| TRISPHAT          | tris(tetrachlorobenzenediolato)phosphate anion   |
| UBC               | University of British Columbia                   |
| V                 | volume   |
| v                 | vibration  |
| <i>vide infra</i> | see below  |
| vol%              | volume percent                                   |
| w                 | weak (spectra)                                   |
| WCA               | weakly coordinating anion                        |
| wt %              | weight percent                                   |
| vw                | very weak (spectra)                              |
| X                 | generic halogen                                  |
| Z                 | number of units in a cell (X-ray)                |

## Acknowledgements

First, I would like to express my sincere gratitude to my PhD supervisor Prof. Derek P. Gates for his support, insight, patience and dedication to this project over the years. I appreciate and cherish our talks about science and life.

I thank my supervisory committee members Prof. Laurel L. Schafer and Prof. Chris Orvig for reviewing my thesis and their insightful advice.

My PhD journey was not a walk in a park and I am thankful for having the support of so many great people around me, who helped me get to this point.

I would like to thank Khaleda Hazin, Anna Bennett, Ben Rawe, Linus Chiang, Kerim Samedov, and Zeyu Han for proofreading parts of my thesis.

To the past and present Gates group members, who made the time in the lab enjoyable (in no particular order): Ben Rawe, Spencer Serin, Paul Siu, Anna Bennett, Harvey MacKenzie, Sonja Gerke, Andrew Priegert, Tom Hsieh, Shuai Wang, Zeyu Han, Leixing Chen, Chuantian Zhan, Jeffery Suen, Kerim Samedov, Kaoru Adachi, and Henry Walsgrove.

To Anna Bennett, Renad Al-Debasi and Ania Sergeenko for their hard work while working under my supervision.

I would like to thank the NMR, Mass Spec, and Chemistry Shops and Services for their help over the years. In particular, Dr. Maria Ezhova, Brian Ditchburn, Dr. Paul Xia, Dr. Emily Seo, Patrick Olsthoorn, and Marshall Lapawa. Further, I would like to thank Dr. Brian O. Patrick, Spencer Serin and Zeyu Han for their efforts in X-ray crystallography.

I thank my family and friends, near and far, for their encouragement. Special thanks to my husband Sal for his patience and support through the highs and lows of my PhD.

Finally, I would like to thank my sister Khaleda and especially my parents, Maliha and Amin, for believing in me and for their unconditional support in every stage of my life.

*To my family for their unconditional love and encouragement.*

## Chapter 1: Introduction

### 1.1 Butyl Rubber

Rubber is one of mankind's inimitable discoveries that has become an essential part of daily life. Natural and synthetic rubbers are elastomeric materials. Depending on the type of rubber, the additives, as well as the degree of vulcanization, widely different properties can be harvested. For instance, the degree of elasticity, hardness and strength are readily tunable.<sup>1,2</sup> Vulcanization is a process that alters the chemical structure of the rubber by forming cross-linked segments that enhance mechanical properties. This process is enabled by the reaction of the carbon double bonds (C=C) present in the rubber pre-polymer.

The microstructure of natural rubber mainly consists of high molecular weight *cis*-1,4-polyisoprene units (Figure 1.1;  $M_w = 10^6 \text{ g mol}^{-1}$ ;  $M_w$  = weight average molecular weight) and represents ca. 40% of the total global elastomer consumption. Natural rubber is commercially obtained from a fluid secretion of the rubber tree, *Hevea brasiliensis*, which is called latex. More than 90% of the cultivated *Hevea brasiliensis* trees are located in South and Southeast Asia as it must be grown in a tropical climate.<sup>3-6</sup> Natural rubber possesses ideal high-performance properties such as elasticity and heat dispersion when compared to synthetic rubber and is irreplaceable in automobile and aircraft tires, and surgical gloves.<sup>7</sup>

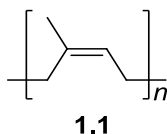
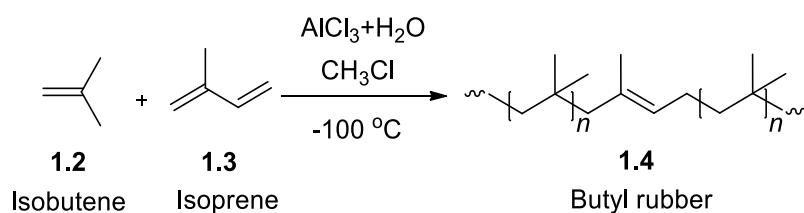


**Figure 1.1. Microstructure of natural rubber contains *cis*-1,4-polyisoprene units.**

However, the global natural rubber production is highly dependent on specific climate conditions, where the rubber tree may be grown, mainly tropical regions. Natural rubber is sensitive to ozone surface cracking and organic solvents that cause a loss in physical strength.<sup>1</sup> Therefore, synthetic rubber has been developed to replace or supplement natural rubber in many industrial applications.

Synthetic butyl rubber (**1.4**) is a copolymer of isobutene and isoprene (ca. 2 mol%) and must be produced by cationic polymerization (Scheme 1.1). Butyl rubber (BR) exhibits excellent heat, chemical and oxygen resistance.<sup>8</sup> It is susceptible to vulcanization through the residual C=C bonds that are introduced from the incorporation of isoprene moieties. The microstructure illustrates *trans*-1,4 polyisoprene units, which predominate over the 1,2- and 3,4-enchainments.<sup>9</sup> Synthetic butyl rubber is particularly intriguing for the automobile industry due to its impermeability to air. Over 70% of the BR polymer produced is incorporated into inner liners of tire and tube products.<sup>2</sup> The global market size of synthetic butyl rubber was valued at US\$ 2.9 billion in 2016 and is predicted to reach US\$ 5.2 billion by 2025.<sup>10</sup>



**Scheme 1.1. Commercial synthetic process for the production of butyl rubber.**

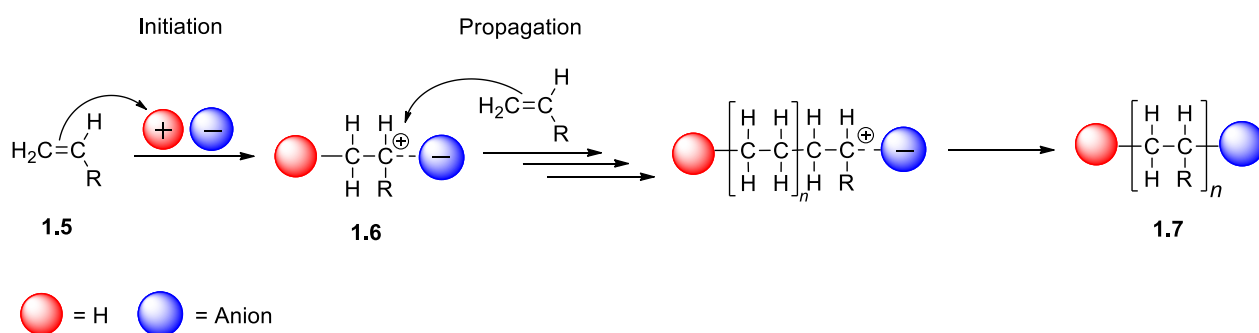
In 1844, the rubber industry was launched by Goodyear's landmark discovery of the vulcanization of natural rubber to produce a durable material with high mechanical strength.<sup>11</sup> Synthetic butyl rubber was first prepared by Otto and Müller-Cunradi, who in 1931 reported homopolymers of isobutene initiated by the Lewis acid  $\text{BF}_3$ . The polymerization of isobutene followed a cationic polymerization mechanism and afforded high molecular weight

polyisobutene ( $M_w \geq 10^6 \text{ g mol}^{-1}$ ).<sup>12,13</sup> However, the polymer was non-curable, or crosslinkable, due to the absence of unsaturated units. In 1937, the production of synthetic BR was pioneered by Thomas and Sparks at Standard Oil Development Company (Exxon Research and Engineering Company). The copolymerization of isobutene and 1,3-butadiene with  $\text{AlCl}_3$  as catalyst afforded an insoluble, colorless rubbery polymer.<sup>13</sup> Remarkably, Thomas and Sparks isolated a vulcanizable polymer by utilizing isoprene as a co-monomer in small amounts (0.5–4 mol %) with  $\text{AlCl}_3$  as catalyst in methyl chloride solution at  $-100 \text{ }^\circ\text{C}$  to produce a slurry copolymer. This process was first commercialized in 1943.<sup>14</sup> The low polymerization temperature is crucial in order to avoid side reactions during polymerization, thereby permitting access to high molecular weight BR. Notably, the introduction of halogen to synthetic butyl rubber **1.4** led to commercially available chlorinated or brominated BR with faster curing rates.<sup>1</sup> The composition of BR makes it particularly interesting for a variety of applications in industrial and household products ranging from tire products, gloves, sealants and medical stoppers to food-grade chewing gum products.<sup>6,15</sup>

The goal of this dissertation involves the development of improved synthetic methods for the isolation of single-component initiator systems for cationic polymerization of olefin monomers. In particular, the objective is to develop new initiators that will provide access to high molecular weight polymers at higher temperatures than  $-100 \text{ }^\circ\text{C}$ . The cationic polymerization of butyl rubber is a challenging and complex reaction. Current methodology necessitates low temperature ( $-100 \text{ }^\circ\text{C}$ ) for industrial scale polymerizations. In order to overcome these challenges, one needs to understand the mechanism of cationic polymerization.

## 1.2 Mechanism of Cationic Polymerization

The cationic polymerization of olefins is an ionic chain polymerization. This type of polymerization involves a positively charged carbocation at the growing polymer chain end. Cationic polymerization proceeds in three steps: initiation, propagation and termination.<sup>16</sup> The initiation step is induced via protic acids by protonation of the olefin monomer **1.5** to generate a carbocation **1.6** as illustrated in Scheme 1.2. The carbocation is charge-balanced by the counter anion. Propagation is realized by the successive addition of a monomer to the reactive carbocation chain end to form a polymer **1.7**.<sup>17</sup>



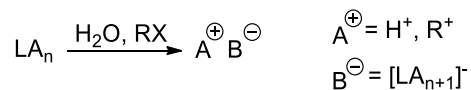
**Scheme 1.2. General mechanism of cationic chain polymerization of vinyl monomers.**

Cationic polymerization proceeds at rapid rates greater than those of radical and anionic polymerization, within a matter of seconds (typical polymerization times: anionic = minutes; radical: ~1h).<sup>18,19</sup> For comparison, the propagation rate constant in radical polymerization is  $\sim 10^2\text{-}10^4 \text{ L mol}^{-1} \text{ s}^{-1}$  and  $\sim 10^4 \text{ L mol}^{-1} \text{ s}^{-1}$  in anionic polymerization, whereas the propagation rate of cationic polymerization is several orders of magnitude higher (for styrene:  $k_p \sim 10^{4-6} \text{ L mol}^{-1} \text{ s}^{-1}$ ; isobutene:  $k_p \sim 10^8 \text{ L mol}^{-1} \text{ s}^{-1}$ ).<sup>20-24</sup> The rapid rates in cationic polymerization, with  $k_p \gg k_i$  and  $k_{tr} > k_p$ , affect the stability of the propagating carbocation and lead to uncontrolled polymerization causing side reactions including chain transfer and termination. Therefore,

cationic polymerization remains the most challenging polymerization among radical and ionic chain polymerization.<sup>25</sup>

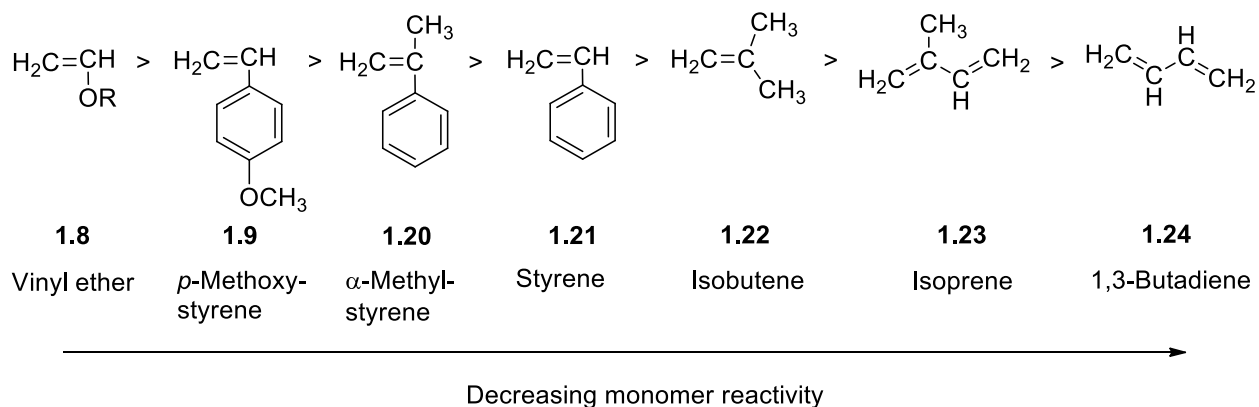
### 1.2.1 Initiation

Cationic polymerization necessitates carefully designed initiators with a cation source ( $A^{\oplus}$ ) and a charge-balancing anion ( $B^{\ominus}$ ).<sup>26,27</sup> For instance, protic acids (*e.g.*  $\text{HSO}_3\text{CF}_3$  and  $\text{HClO}_4$ ) are used as initiators in cationic polymerization.<sup>28-30</sup> Alternatively, active initiators are generated *in situ* by binary systems, in which a co-initiator is required. Binary initiators are comprised of a proton donor like water<sup>17</sup> and a neutral Lewis acid ( $\text{LA}_n$ ) (*e.g.*  $\text{AlCl}_3$ ,  $\text{BF}_3$ ,  $\text{SnCl}_4$ ,  $\text{SbCl}_5$  and  $\text{TiCl}_4$ ).<sup>22,31-34</sup> The activation of  $\text{H}_2\text{O}$  results in an  $\text{H}^+$ , whereas the activation of a cationogen ( $\text{RX}$ ) (*e.g.* alkyl and alkylaryl halides) generates a carbenium ion ( $\text{R}_3\text{C}^+$ ) as the active cationic initiator (Scheme 1.3).



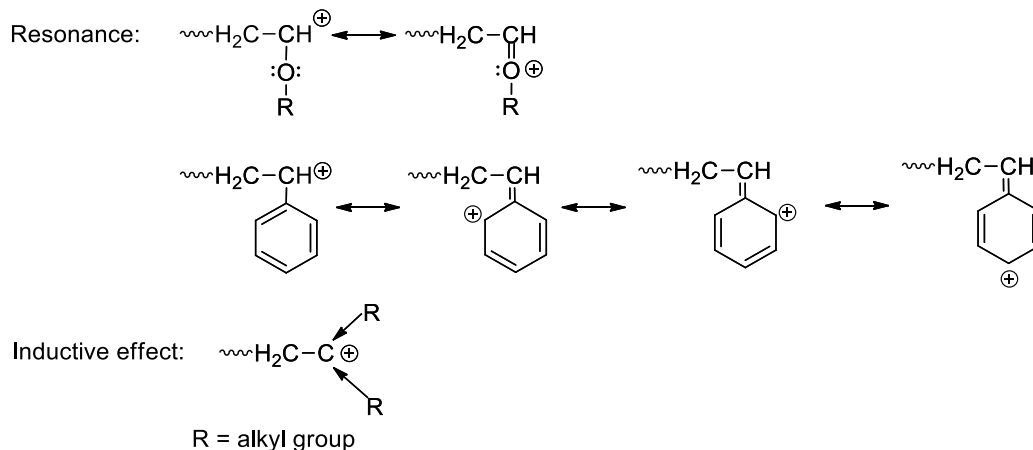
**Scheme 1.3. General formation of an active initiator ( $\text{A}^{\oplus}\text{B}^{\ominus}$ ).**

Vinyl monomers are utilized in cationic polymerization. The reactivity of the monomer depends on the electron-donating ability of the substituent. For example, vinyl ethers, **1.8**, are more reactive than styrene derivatives, **1.9**, **1.20** and **1.21**, while isobutene, **1.23**, and 1,3-butadiene, **1.24**, are less reactive monomers used in cationic polymerization (Scheme 1.4).



**Scheme 1.4. Trend in monomer reactivity in cationic polymerization.**

Vinyl monomers with substituents that possess electron donating ability can stabilize the resulting reactive carbocation **1.6**. The stability of the carbocation increases with the number of substituents on the monomer. Therefore, tertiary carbocations are more stable than secondary ( $\text{R}_3\text{C}^\oplus > \text{R}_2\text{C}^\oplus > \text{RC}^\oplus$ ). Monomers with  $\alpha$ -heteroatoms such as alkoxy groups, **1.9**, can stabilize the carbocation through resonance. Aryl monomers with electron-donating groups delocalize the positive charge through resonance as illustrated in Scheme 1.5. The carbocation is mainly stabilized by hyperconjugation.<sup>26</sup> Monomers with alkyl substituents also stabilize the carbocation via an inductive effect.



**Scheme 1.5. The carbocation can be stabilized by resonance (top) and inductive effect (bottom).**

## 1.2.2 Propagation

The rate of propagation is influenced by the temperature, solvent and counterion used. High molecular weight polymers are dependent on the formation of a stable propagating species for successive monomer addition. The application of low temperatures during polymerization lowers the rate of termination by suppressing the termination of chain growth and chain transfer, leading to the formation of a growing propagating chain.<sup>17,19</sup>

Likewise, solvent effects also influence the rate of propagation. Polar hydroxylic solvents, for example water and alcohols, most likely react with the initiator and prevent initiation. Therefore, cationic polymerization is performed in solvents with low to moderate polarity. In solvents such as tetrahydrofuran and 1,2-dichloroethane the propagating species ( $\sim\sim\sim\text{AB}$ ) can adopt different arrangements ranging from a covalent bond (**I**), contact ion pair (**II**), and the solvent-separated or so called loose ion pair (**III**) to free ions (**IV**) (Figure 1.2). The carbocation ( $\text{A}^{\oplus}$ ) has a counter anion ( $\text{B}^{\ominus}$ ) in the contact ion pair, and thus forms an inactive or dormant species. In contrast, in the solvent separated ion pair, the ions are partially separated by a solvent molecule. Increased solvent polarity favors the loose ion pair (**III**), while in solvents with lower polarity the contact ion pair (**II**) is preferred.<sup>17,18,35</sup>



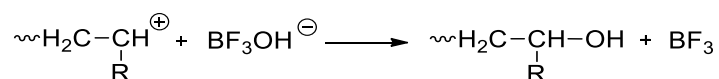
**Figure 1.2.** Solvation association of the carbocation ( $\text{A}^{\oplus}$ ) and counter anion ( $\text{B}^{\ominus}$ ).

The size of the counter anion has a significant effect on the rate of propagation. Small counterions with high charge density possess a strong electrostatic interaction with the propagating carbocation and render it unreactive. For comparison, large charge delocalized

counterions demonstrate a weaker coordination to the carbocation and facilitate the stabilization of the propagating carbocation.<sup>36</sup>

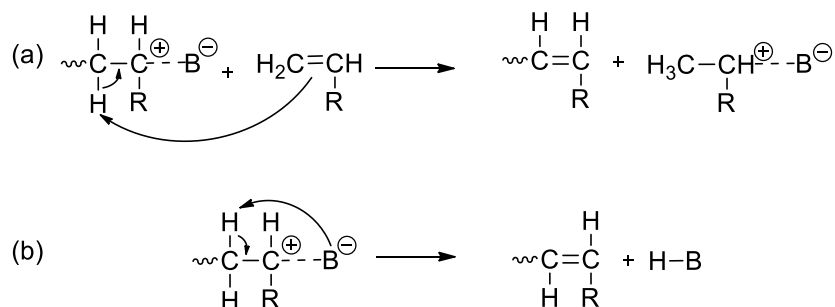
### 1.2.3 Termination and Chain Transfer

The complexity of the fast uncontrolled cationic polymerization is also indicated by termination and chain transfer reactions. One method of termination involves the combination of the propagating species with the counterion as illustrated in Scheme 1.6.<sup>13,17,37</sup>



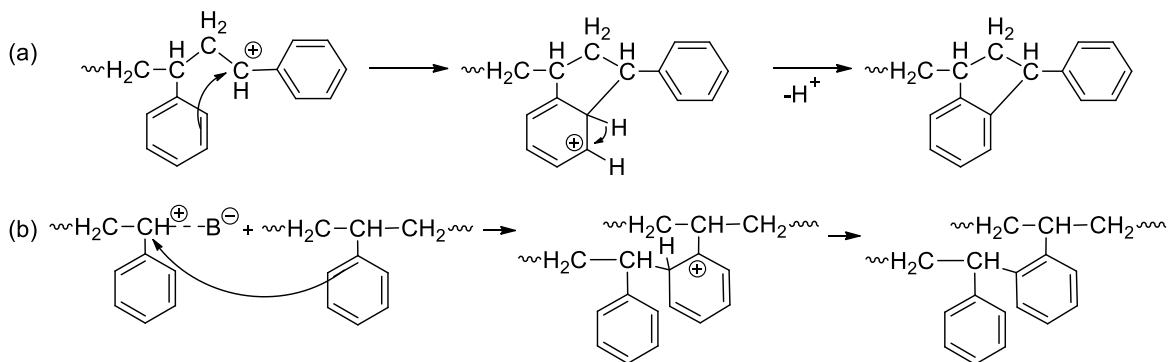
**Scheme 1.6. Combination of the propagating species with a fragment of the counterion.**

Cationic polymerization is prone to side reactions due to a faster termination rate than the propagation rate ( $k_{\text{tr}} > k_{\text{p}}$ ). Chain transfer reactions act to terminate the growing propagating species; however, they do not terminate the polymerization since a new propagating active center is generated.<sup>18</sup> Chain transfer reactions can occur by means of  $\beta$ -proton transfer to monomer, chain transfer to counterion, or chain transfer to polymer.<sup>17</sup>  $\beta$ -Proton transfer is the main side reaction in cationic polymerization. Due to the stabilization of the carbocation through hyperconjugation, the positive charge is partially delocalized onto the C-H $_{\beta}$  proton. Thus, the propagating species is prone to  $\beta$ -proton elimination by the monomer or counter anion during cationic polymerization, generating a new propagating species and resulting in the formation of an unsaturated polymer chain end (Scheme 1.7, (a)). Another possible side reaction is chain transfer to counter anion, also called spontaneous termination, which involves a  $\beta$ -proton transfer to the counterion. Subsequently, this process leads to a dormant polymer, while the initiator is regenerated (Scheme 1.7, (b)).<sup>17,38</sup>



**Scheme 1.7. Chain transfer reaction can occur via (a)  $\beta$ -proton transfer to monomer and (b) chain transfer to counterion, respectively.**

In the presence of aromatic groups, such as styrene and styrene derivatives, intramolecular electrophilic aromatic substitution (or backbiting) is often observed that results in terminal indanyl or cyclized structures as illustrated in Scheme 1.8 (a).<sup>39-41</sup> Branching or cross-linking has also been observed in the cationic polymerization of styrene through intermolecular aromatic substitution by a propagating carbocation onto the aromatic ring of another polymer chain (Scheme 1.8, (b)).<sup>42-44</sup>



**Scheme 1.8. Side reaction in styrene polymerization can occur via (a) chain transfer to growing polymer chain or (b) branching or cross-linking of styrene during cationic polymerization.**

## 1.3 Initiators Used in Cationic Polymerization

### 1.3.1 Binary Initiators

More and more studies have led to the development of initiators based on Lewis acid precursors that are suitable for the cationic polymerization of vinyl monomers. The development of binary systems bearing Lewis acids and a proton donor as active initiators for cationic polymerization was pioneered by Higashimura and Kennedy. For example, initiator systems for the polymerization of vinyl ethers (*e.g.* HI/I<sub>2</sub> and HCl/ZnCl<sub>2</sub>)<sup>45,46</sup> and isobutene (*e.g.* BCl<sub>3</sub>/acetate, 1,4-bis(1-azido-1-methylethyl)benzene/Et<sub>2</sub>AlCl, AlCl<sub>3</sub>/OBu<sub>2</sub>, AlCl<sub>3</sub>/O<sup>*i*</sup>Pr<sub>2</sub>) have been reported.<sup>47,48</sup> Styrene and styrene derivatives have been polymerized by the HI/I<sub>2</sub> and HI/ZnI<sub>2</sub> initiating system in the presence of *n*Bu<sub>4</sub>NX (X= Cl, Br, I) and other binary systems (*e.g.* 1-chloroethylbenzene/SnCl<sub>4</sub>, BF<sub>3</sub>OEt<sub>2</sub>/alcohol, cumyl acetate/BCl<sub>3</sub>).<sup>49-54</sup> In addition, isoprene and 1,3-butadiene have been polymerized by [Ph<sub>3</sub>C][B(C<sub>6</sub>F<sub>5</sub>)<sub>4</sub>] in combination with a co-initiator (C<sub>5</sub>Me<sub>5</sub>)<sub>2</sub>Ln[(*i*-Me)AlMe<sub>2</sub>(*i*-Me)]Ln(C<sub>5</sub>Me<sub>5</sub>)<sub>2</sub>/Al(<sup>*i*</sup>Bu)<sub>3</sub> (Ln = Sm, Gd) or (C<sub>5</sub>Me<sub>5</sub>)Sc(BH<sub>4</sub>)<sub>2</sub>(THF).<sup>55-57</sup> A key disadvantage of these types of two-component initiators is that the nature and concentration of the initiating species, presumably H<sup>+</sup>, is not well defined or easily studied.

### 1.3.2 Single-component Initiators

The development of single component initiators is of emergent interest. Single component initiators incorporating weakly coordinating anions (WCAs) of group 13 and 14 elements include [Al(η<sup>5</sup>-Cp)<sub>2</sub>][Al{OC(CF<sub>3</sub>)<sub>3</sub>}<sub>4</sub>],<sup>58</sup> [Al(η<sup>5</sup>-Cp)<sub>2</sub>][MeB(C<sub>6</sub>F<sub>5</sub>)<sub>3</sub>],<sup>59</sup> [Ga(C<sub>6</sub>H<sub>5</sub>F)<sub>2</sub>][Al{OC(CF<sub>3</sub>)<sub>3</sub>}<sub>4</sub>],<sup>60</sup> [EtZn(arene)<sub>2</sub>][Al{OC(CF<sub>3</sub>)<sub>3</sub>}<sub>4</sub>] (arene = toluene, mesitylene),<sup>61</sup> [Cp\*Ti(CH<sub>3</sub>)<sub>2</sub>][CH<sub>3</sub>B(C<sub>6</sub>F<sub>5</sub>)<sub>4</sub>].<sup>36,62</sup> When employed to polymerize isobutene, these

systems afford low to high molecular weight polyisobutene ( $M_n = 290 \text{ g mol}^{-1}$  to 270,000  $\text{g mol}^{-1}$ ;  $M_n$  = number average molecular weight). Further,  $[\text{Ni}(\text{C}_{12}\text{H}_{19})][\text{B}\{3,5\text{-(CF}_3)_2\text{C}_6\text{H}_3\}_4]$  has been shown to be an effective initiator in the polymerization of 1,4-butadiene.<sup>63</sup>

Single-component initiators based on Brønsted acids are less common. Although in principle  $\text{H}^+$  represents the ideal initiator, the challenge remains in the synthesis, isolation and necessity to handle these systems at lower temperatures. Examples for single component initiators for the cationic polymerization of vinyl monomers are illustrated in Figure 1.3. The Brønsted acid **1.25** has been studied in the cationic ring opening polymerization of 2-alkyl-2-oxazoline and carbocationic polymerization of isobutene, while the single component initiator **1.26** is an effective initiator for the polymerization of vinyloxazolidinones and isobutene.<sup>58,64,65</sup> The compounds **1.27** and **1.28** were shown to be effective initiators for the cationic polymerization of isobutyl vinyl ether and styrene.<sup>33,66,67</sup> The proton of the water molecule in the cation moiety of **1.27** initiates the polymerization. Single component initiators are solid and weighable and therefore give a better control over the monomer-to-initiator ratio during cationic polymerization than binary systems.

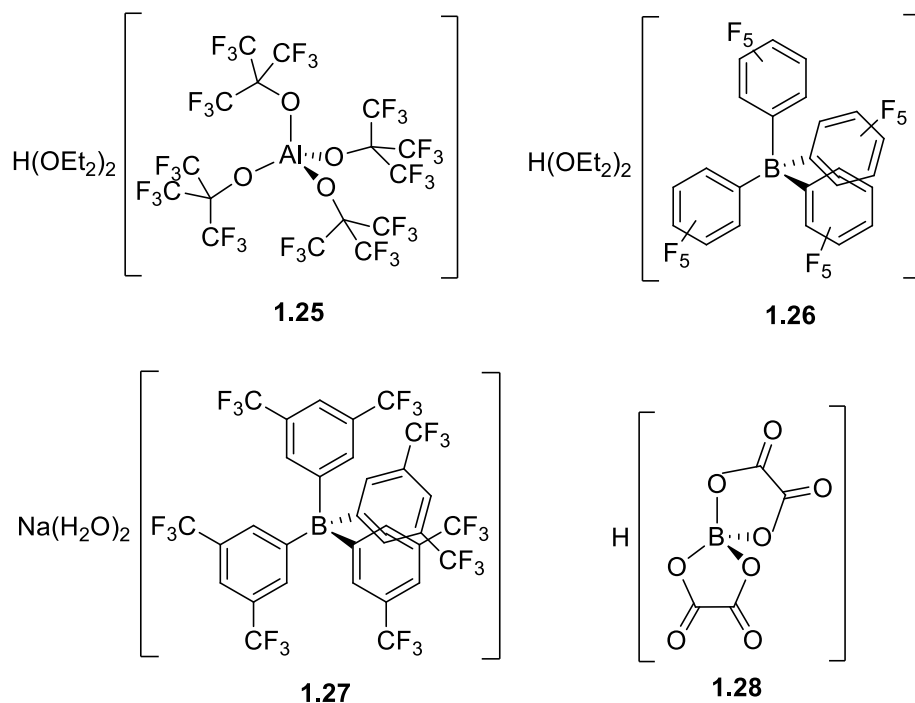


**Figure 1.3. Examples of Brønsted acids used as single-component initiators for cationic polymerization of olefins.**

#### 1.4 Weakly Coordinating Anions (WCAs)

The capability to control the interaction between the counter anion and the carbocation during cationic polymerization is challenging and critical. The objective is to retain the electrophilicity at the cation center by applying WCAs.<sup>68</sup> The development of WCAs necessitates low overall charge and charge delocalization over a large number of ligand atoms to minimize the electrostatic interaction between the cation and anion motif (**V**; Figure 1.4). Hence, the larger the anion, the more delocalized the charge will be and therefore, the more weakly coordinating the anion will be. Reducing the Coulombic interaction will facilitate the stabilization of reactive cations. WCAs should be chemically robust against oxidation, electrophilic attack and should not possess basic coordination sites.<sup>69,70</sup>

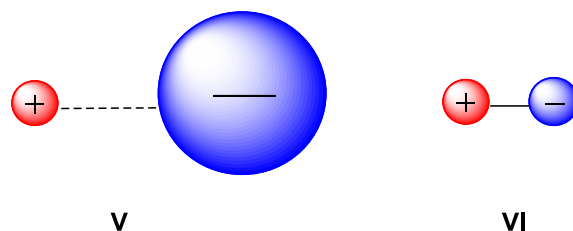
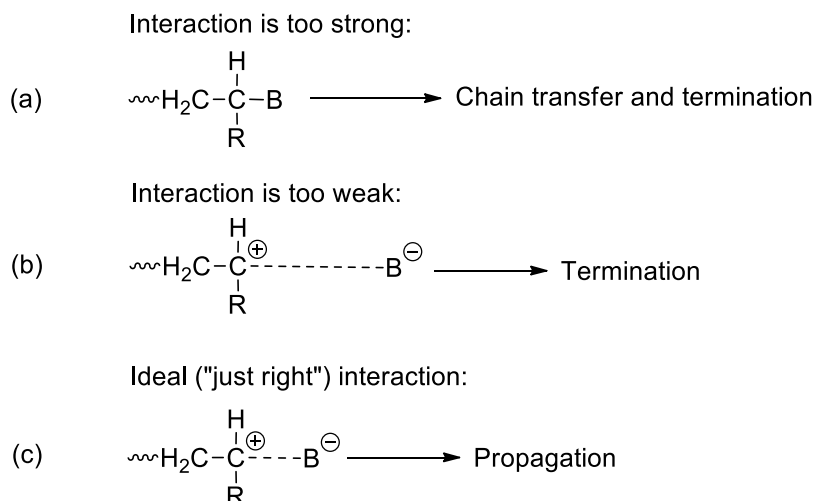


**Figure 1.4. Electrostatic interactions between a carbocation and a counterion.**

The degree of coordination of the counter anion to the carbocation has an impact on the formation of the ion-pair and therefore on the cationic polymerization step as illustrated in Scheme 1.9.<sup>71</sup> The search for the “just right” interaction between the carbocation and the counterion that is neither too strong nor too weak, refers to the Goldilocks effect derived from the fairy tale “Goldilocks and the Three Bears”. Small and nucleophilic anions such as **VI** (Figure 1.4) will coordinate to the carbocation and render it unreactive. Subsequently, this will suppress the propagation step, leading to chain transfer and termination of the polymerization (Scheme 1.9 (a)). An anion that is too weakly coordinating will not be able to stabilize the reactive carbocation during cationic polymerization and will lead to termination (Scheme 1.9 (b)). Preferably, a WCA that is charge delocalized and non-nucleophilic will stabilize the propagating carbocation during polymerization; such ideal “just right” interaction is elucidated in Scheme 1.9 (c). Therefore, high molecular-weight polymers are dependent on the formation of a stable carbocation for successive propagation.

The "Goldilocks principle":



**Scheme 1.9. Motifs of different interaction between the carbocation and counter anion during cationic polymerization.**

#### 1.4.1 Development and Application of WCAs in Cationic Olefin Polymerization

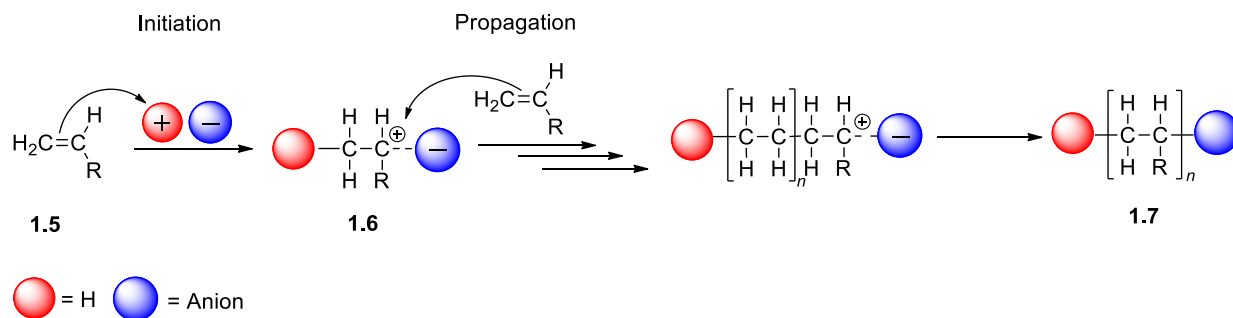
This section of Chapter 1 deals with the evolution of the “classical anion” to larger and more charge delocalizing WCAs. In addition, the application of WCAs in cationic olefin polymerization is highlighted. Therefore, a general mechanism of the different types of cationic olefin polymerization (*e.g.* cationic chain polymerization, cationic coordination polymerization, as well as cationic ring-opening polymerization) is warranted.

Cationic chain polymerization involves a protic acid as initiator to generate a positively charged carbocation **1.6** at the growing polymer chain end (Scheme 1.10 (a)) and is discussed in section 1.2. Coordination polymerization is a type of addition polymerization that involves an unsaturated metal-based complex as the active site (Scheme 1.10 (b)).<sup>72,73</sup> For example, a homogeneous metallocene catalyst [ $\text{L}_n\text{MR}_2$ ; M = metal, L = ligand, R = alkyl, aryl] is used in the presence of a Lewis or Brønsted acidic co-initiator (*e.g.*: MAO ( $-\text{[O-Al(CH}_3\text{)]}_n^-$ ),  $\text{Al(C}_2\text{H}_5\text{)}_3$ ,

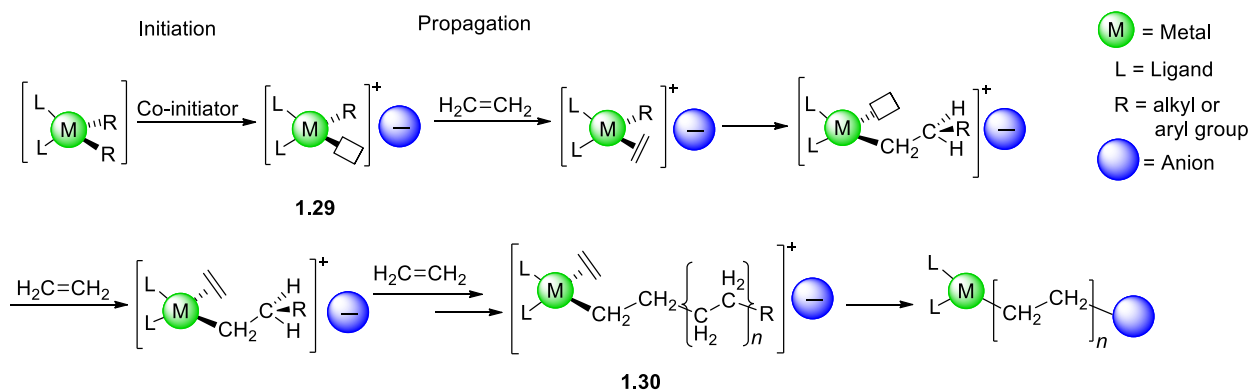
$\text{Al}(\text{C}_2\text{H}_5)_2\text{Cl}$ ,  $\text{B}(\text{C}_6\text{F}_5)_3$ ,  $\text{H}(\text{OEt}_2)_2[\text{B}(\text{C}_6\text{F}_5)_4]$ ) to generate a metal-alkyl cation with a vacant coordination site (**1.29**).<sup>68,74</sup> Propagation is realized by successive insertion of the C=C bond of  $\alpha$ -olefin monomers (*e.g.* ethylene, propene, 1-hexene, 1-octene) into the metal-alkyl bond at each active site **1.30** to form a polymer.<sup>75,76</sup> The mechanism of cationic ring-opening polymerization is illustrated in Scheme 1.10 (c). In general, initiation proceeds via activation of a heterocyclic monomer (*e.g.* oxazoline, lactone, ether) by a Brønsted acid or carbocation (**1.31**) (cation source =  $\text{H}^+$ ,  $\text{R}_3\text{C}^+$ ). Propagation is achieved by the addition of a cyclic monomer to the cationic species at the chain end **1.32**, and thereby opening the ring system resulting in a linear polymer.<sup>77</sup>

About three decades ago the term “non-coordinating anion”<sup>78,79</sup> was used when a coordinating anion such as a halide was replaced by a complex anion for example  $[\text{BF}_4]^-$ ,<sup>78</sup>  $[\text{ClO}_4]^-$ ,<sup>80</sup>  $[\text{SO}_3\text{CF}_3]^-$ ,  $[\text{SO}_3\text{F}]^-$ ,<sup>81</sup>  $[\text{PF}_6]^-$ <sup>82</sup> or  $[\text{AsF}_6]^-$ .<sup>83</sup> Their application as counter anions was fostered with the advancement of X-ray crystallographic techniques. With the help of X-ray crystallography, the structural characterization of the coordination of these anions with various metal complexes was enabled.<sup>84</sup> In the early 1990s the term “weakly coordinating anion” (WCA) was coined, which describes the interaction between the cation and anion species.<sup>69,79</sup> Since then, the research of WCAs has been widely explored with the focus to design large charge delocalized and stable counter anions with respect to oxidation.<sup>70</sup> WCAs based on group 13 elements have received considerable attention, while anions of group 15 elements are less common. In addition, WCAs are mainly used to stabilize reactive cations and are widely employed in pericyclic rearrangement and Diels-Alder reactions,<sup>85-91</sup> olefin polymerization,<sup>92-95</sup> electrochemistry<sup>96-101</sup> or lithium ion batteries.<sup>102-107</sup>

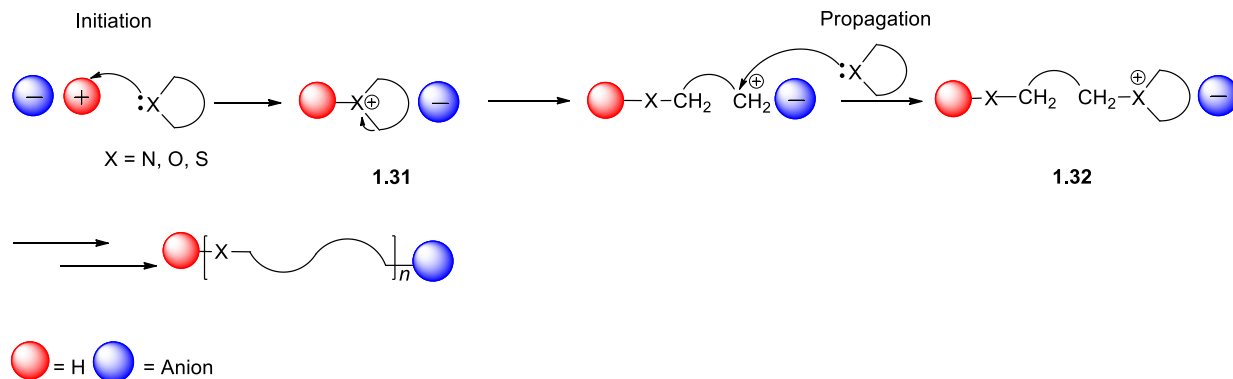
(a) Cationic Chain Polymerization



(b) Cationic Coordination Polymerization



(c) Cationic Ring-opening Polymerization



**Scheme 1.10.** Different types of cationic polymerization and their general mechanisms; (a) reveals the mechanism of cationic chain polymerization; (b) shows the mechanism of cationic coordination polymerization, and (c) illustrates the mechanism of cationic ring-opening polymerization.

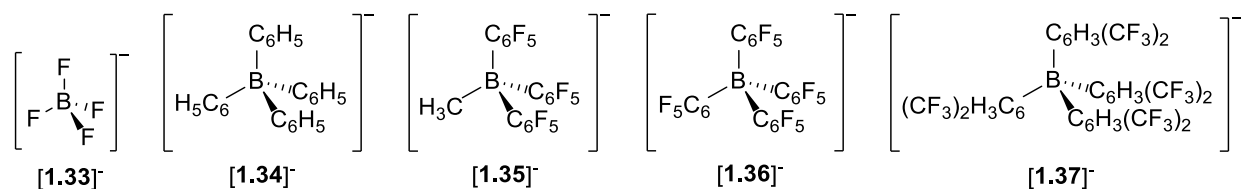
The scope of this section is confined to WCAs applied in cationic olefin polymerization including mainly coordination polymerization and a few examples in cationic chain polymerization. Rather than to separate this discussion into the two separate polymerization types (*i.e.* coordination and cationic), the progress in this field will be discussed in roughly chronological order in an effort to draw attention to the advances in WCA design.

The evolution of [1.33]<sup>-</sup> to larger WCAs began in the 1960s, when Massey and Park isolated a lithium salt containing the tetraphenylborate anion, [BPh<sub>4</sub>]<sup>-</sup>, [1.34]<sup>-</sup>.<sup>108</sup> The WCA [1.34]<sup>-</sup> is applied as a counter anion in the Ziegler-Natta catalyst for ethylene polymerization.<sup>109-111</sup> Although, the anion was resistant to hydrolysis it was found that the phenyl groups are relatively strongly coordinating. X-ray crystallography revealed that [1.34]<sup>-</sup> coordinated to the metal via  $\pi$ -interaction with one of the phenyl rings. Therefore, attempts to reduce the coordinating ability of the anion to the metal center were achieved by applying electron withdrawing groups, such as bulky fluorinated substituents (*e.g.* C<sub>6</sub>F<sub>5</sub> or C<sub>6</sub>H<sub>3</sub>-3,5-(CF<sub>3</sub>)<sub>2</sub>). The addition of fluorinated aryl moieties to the Lewis acidic boron center gave rise to bulkier and more charge delocalized WCAs [B(C<sub>6</sub>F<sub>5</sub>)<sub>4</sub>]<sup>-</sup>, [1.36]<sup>-</sup>, and [B(Ar<sup>F</sup>)<sub>4</sub>]<sup>-</sup> (Ar<sup>F</sup> = C<sub>6</sub>H<sub>3</sub>-3,5-(CF<sub>3</sub>)<sub>2</sub>), [1.37]<sup>-</sup>.<sup>112</sup>

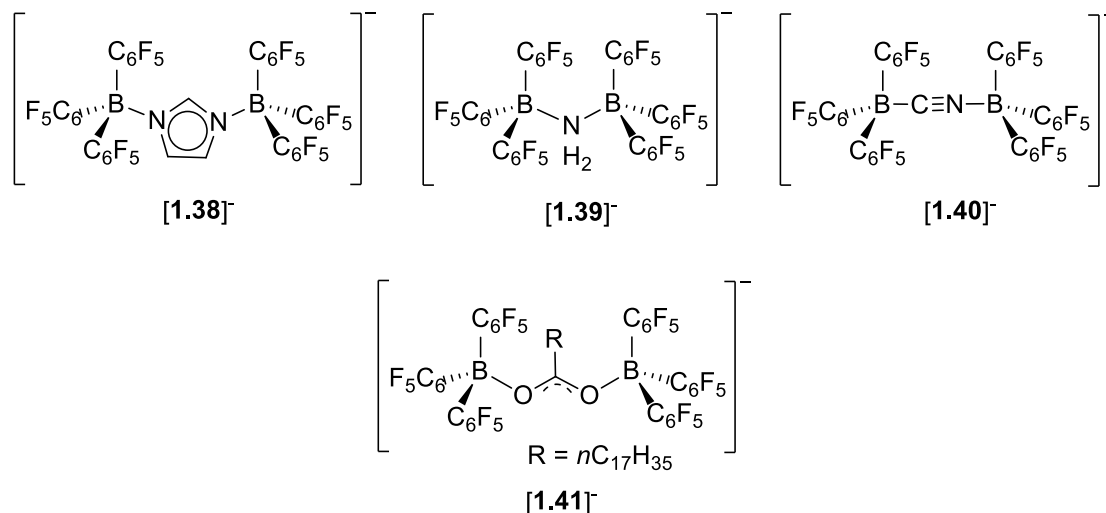
In the 1990s, Marks and co-workers studied the reactivity of the related Lewis acid B(C<sub>6</sub>F<sub>5</sub>)<sub>3</sub> and demonstrated the isolation of a “cation-like” zirconocene catalyst for propene polymerization. It was shown that B(C<sub>6</sub>F<sub>5</sub>)<sub>3</sub> abstracts a methyl group of zirconocene dimethyl complexes (L<sub>2</sub>ZrMe<sub>2</sub> with L =  $\eta^5$ -C<sub>5</sub>H<sub>5</sub>,  $\eta^5$ -1,2-(CH<sub>3</sub>)<sub>2</sub>C<sub>5</sub>H<sub>3</sub>,  $\eta^5$ -(CH<sub>3</sub>)<sub>5</sub>C<sub>5</sub>) that generated a zwitterionic complex [L<sub>2</sub>ZrMe][1.35].<sup>94,113-116</sup> The complex [Al( $\eta^5$ -C<sub>5</sub>H<sub>5</sub>)<sub>2</sub>][1.35] has been employed as an initiator for isobutene polymerization.<sup>59</sup> This sparked an interest in the application of tetrakis(pentafluorophenyl)borate, [1.36]<sup>-</sup>, as a WCA for metallocene

polymerization catalysts.<sup>117</sup> Particularly, an alkyl abstraction reagent  $[\text{Ph}_3\text{C}][\mathbf{1.36}]^-$  was synthesized and reacted with an zirconocene dimethyl complex that yielded a highly effective catalyst for propene polymerization.<sup>118</sup>

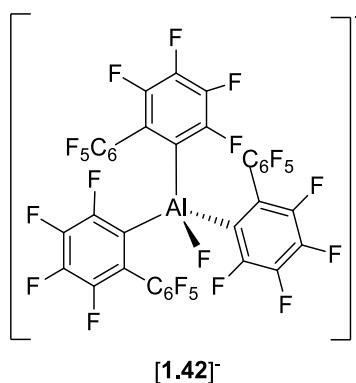
Effective metallocene catalysts for olefin polymerization are also formed through protonolysis, by reacting  $(\eta^5\text{-Me}_5\text{Cp})_2\text{ThMe}_2$  with  $[\text{HN}^t\text{Bu}_3][\mathbf{1.36}]^-$  to yield  $[(\eta^5\text{-Me}_5\text{Cp})_2\text{ThMe}][\mathbf{1.36}]^-$ .<sup>113,117</sup> Brookhart's Brønsted acid,  $\text{H}(\text{OEt}_2)_2[\mathbf{1.37}]^-$ , has proven to be a potent protic reagent for the protonolysis of  $[(\text{phen})\text{Pd}(\text{CH}_3)_2]$  to form a cationic palladium catalyst,  $[(\text{phen})\text{Pd}(\text{CH}_3)\text{NCCH}_3][\mathbf{1.37}]^-$ , that is utilized in the copolymerization of ethylene and carbon monoxide.<sup>119,120</sup> Despite the widespread use of  $[\mathbf{1.36}]^-$  as a WCA, the perfluorinated tetraphenylborate anion is prone to acid induced B–C bond cleavage.<sup>121</sup>



The quest for larger and more charge delocalized WCAs spearheaded the design of bridged borane anions to reduce the cation anion interaction. This led to the development of WCAs  $[\mathbf{1.38}]^-$ ,<sup>122</sup>  $[\mathbf{1.39}]^-$ ,<sup>123,124</sup> and  $[\mathbf{1.40}]^-$ ,<sup>125</sup> where the negative charge is distributed over two boron centers. These WCAs are utilized as activators for metallocene olefin polymerization catalysts.<sup>126-129</sup> Furthermore, Baird and co-workers were able to generate a Brønsted acid *in situ* by reacting stearic acid ( $\text{C}_{17}\text{H}_{35}\text{CO}_2\text{H}$ ) with two  $\text{B}(\text{C}_6\text{F}_5)_3$  moieties. The resulting complex,  $\text{H}[\mathbf{1.41}]$ , is a highly effective initiator for the carbocationic polymerization of isobutene and isoprene to afford butyl rubber.<sup>130,131</sup>

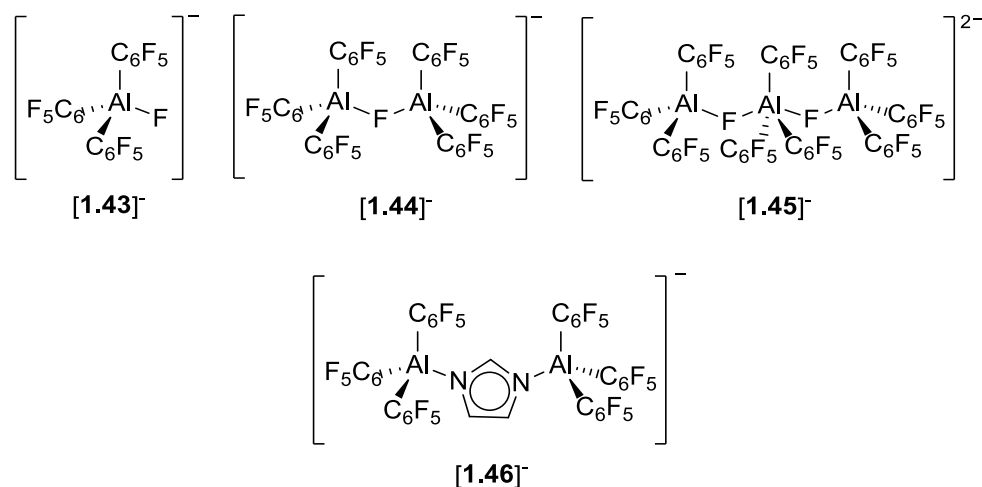


The successful application of tetrafluoroarylborates has led to the development of aluminum containing WCAs. For example, Marks and co-workers reported the complex  $[\text{Ph}_3\text{C}][\mathbf{1.42}]^-$  that is utilized as a coactivator of zirconium complexes for ethylene and propene polymerization.<sup>132-134</sup> However, studies have shown that their catalytic activities are lower than the catalysts containing  $[\mathbf{1.35}]^-$  and  $[\mathbf{1.36}]^-$ , indicating that  $[\mathbf{1.42}]^-$  might be more coordinating than the latter anions.<sup>132,135</sup>



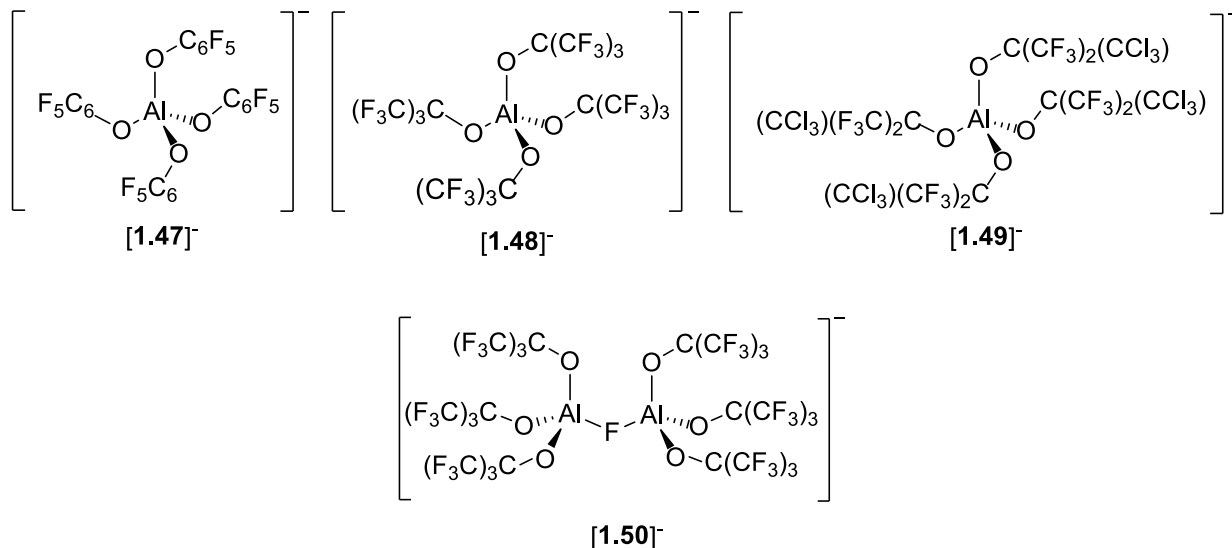
The search for weaker coordinating anions led to the design of bridged anions and the delocalization of the negative charge over multiple Lewis acid centers. Marks and co-workers isolated the fascinating perfluoroarylaluminum anions  $[\mathbf{1.43}]^-$ ,  $[\mathbf{1.44}]^-$  and  $[\mathbf{1.45}]^{2-}$  as co-catalysts for the zirconium metallocene mediated propene polymerization. Increasing the anion size from

[1.43]<sup>-</sup> to [1.44]<sup>-</sup> demonstrated an increase in activity in propene polymerization, while increasing the anion size further to three bridged aluminum centers resulted in a decrease in polymerization activity. This is due to the increase in negative charge of the dianion [1.45]<sup>2-</sup>.<sup>136-138</sup> The WCA [1.46]<sup>-</sup>, an analog of [1.38]<sup>-</sup>, with an imidazole fragment as linking group between two aluminum centers, has been employed in a titanium catalyst for the copolymerization of ethylene and 1-octene. The catalyst system with the anion [1.46]<sup>-</sup> revealed higher activity and higher molecular weight polymer than that of [1.38]<sup>-</sup>.<sup>122</sup>



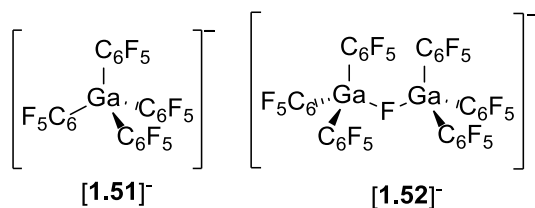
In addition, perfluoroalkoxide or perfluoroaryloxide aluminate anions were explored as effective WCAs.<sup>139-148</sup> Substantial efforts have been made to increase the stability from OC<sub>6</sub>F<sub>5</sub> to (CF<sub>3</sub>)<sub>3</sub> groups. For instance, Marks and co-workers reported zirconocene complexes of [Al(OC<sub>6</sub>F<sub>5</sub>)<sub>4</sub>]<sup>-</sup> ([1.47]<sup>-</sup>) and [Al{OC(CF<sub>3</sub>)<sub>3</sub>}<sub>4</sub>]<sup>-</sup> ([1.48]<sup>-</sup>) that are effective catalysts for ethylene polymerization.<sup>149,150</sup> The complex [Al(η<sup>5</sup>-C<sub>5</sub>H<sub>5</sub>)<sub>2</sub>][1.48] is a more effective initiator for the cationic polymerization of isobutene than [Al(η<sup>5</sup>-C<sub>5</sub>H<sub>5</sub>)<sub>2</sub>][1.35].<sup>58,59</sup> The WCA [1.48]<sup>-</sup> has been pioneered by Krossing and co-workers with the substitution of OAr<sup>F</sup> for steric OR<sup>F</sup> alkoxy ligands [e.g. OC(CF<sub>3</sub>)<sub>3</sub>], shaping a very stable and WCA due to the strong aluminum-oxygen

bonds. However, the nucleophilicity of the oxygen bonds is evaded by the incorporation of electron withdrawing fluorine groups. The electronic stabilization of **[1.48]<sup>-</sup>** was demonstrated by perfluorination resulting in an increase of acidity from non-fluorinated HO-C(CH<sub>3</sub>)<sub>3</sub> (pK<sub>a</sub> = 19.3) to partially fluorinated HO-C(H)(CF<sub>3</sub>)<sub>2</sub> (pK<sub>a</sub> = 9.5) and perfluorinated HO-C(CF<sub>3</sub>)<sub>3</sub> (pK<sub>a</sub> = 5.5) alcohol.<sup>151</sup> The WCA **[1.48]<sup>-</sup>** stabilizes several highly reactive cations {e.g. [PX<sub>4</sub>]<sup>+</sup> (X = F-I), [P<sub>2</sub>I<sub>5</sub>]<sup>+</sup>, [P<sub>5</sub>X<sub>2</sub>]<sup>+</sup> (X = Br, I), [AsBr<sub>4</sub>]<sup>+</sup>, [CX<sub>3</sub>]<sup>+</sup> (X = Cl, Br), [Cl<sub>3</sub>]<sup>+</sup>, Li<sup>+</sup>, Ag<sup>+</sup>, [M(L)]<sup>+</sup> (M = Ag, Cu; L = P<sub>4</sub>, P<sub>4</sub>S<sub>3</sub>, S<sub>8</sub>, C<sub>2</sub>H<sub>4</sub>), [Ga(C<sub>6</sub>H<sub>5</sub>F)<sub>2</sub>]<sup>+</sup>, Cs<sup>+</sup>, [Ph<sub>3</sub>C]<sup>+</sup>, [NR<sub>4</sub>]<sup>+</sup> (R = Me, Et)}.<sup>60,139,141,146,152-164</sup> Further, the anion is stable towards hydrolysis in H<sub>2</sub>O and nitric acid due to the steric shielding of the oxygen atom by the bulky C(CF<sub>3</sub>)<sub>3</sub> ligands.<sup>148</sup> The anion **[1.48]<sup>-</sup>** has been utilized in electrochemistry as a supporting electrolyte containing WCAs for the stabilization of reactive organometallic radical cations and as a WCA in ionic liquids.<sup>61,144,151,165</sup> In addition, the perhalogenated WCA **[1.49]<sup>-</sup>** has been recently reported to stabilize lithium and trityl cations.<sup>166</sup>

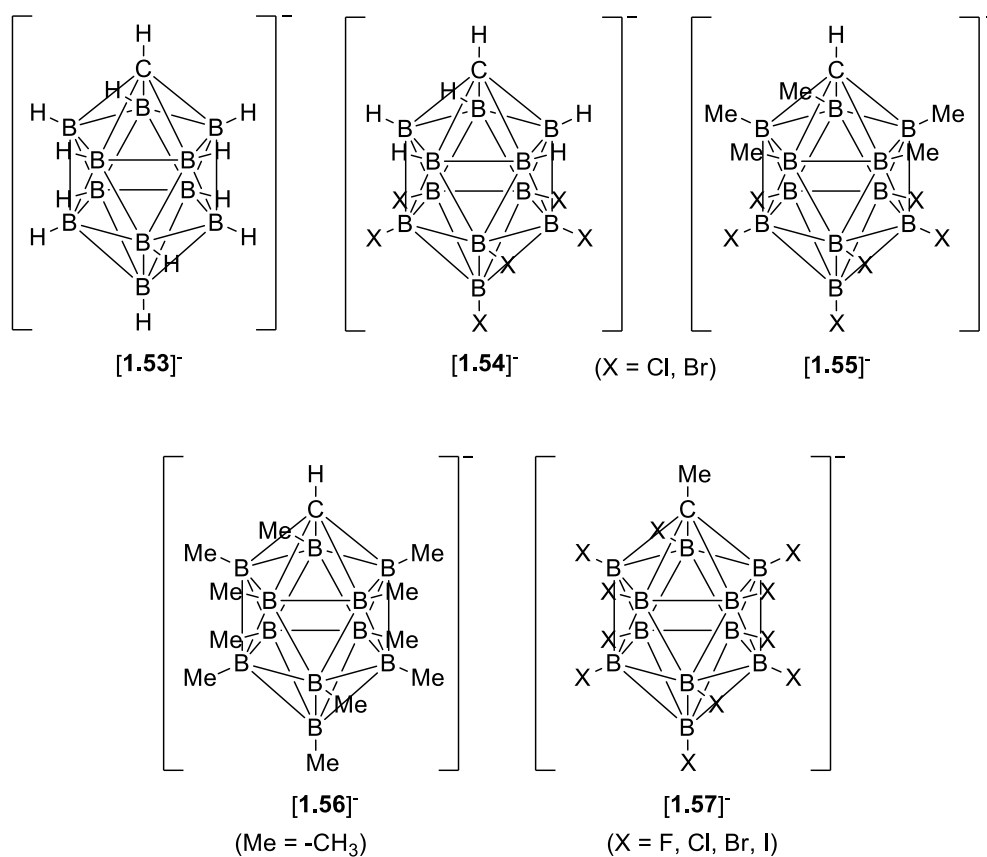


The Brønsted acid  $[\text{H}(\text{OEt})_2][\mathbf{1.48}]$  is an effective cationic single-component initiator for the ring-opening polymerization of 2-alkyl-2-oxazolines and for the carbocationic polymerization of isobutene.<sup>58,65</sup> Krossing and co-workers have applied the complex  $[\text{Ga}(\text{L})_2][\mathbf{1.48}]$  ( $\text{L} = \text{C}_6\text{H}_5\text{F}$ ,  $\text{PhC}_2\text{H}_4\text{Ph}$ ,  $1,4\text{-Me}_2\text{C}_6\text{H}_4$ ) as an efficient initiator for the polymerization of isobutene.<sup>60,167</sup> Further, the Brønsted acids  $\text{H}(\text{OEt}_2)_2[\mathbf{1.47}]$  and  $\text{H}(\text{OEt}_2)_2[\mathbf{1.48}]$ , and trityl salts of  $[\mathbf{1.48}]^-$  and  $[\mathbf{1.50}]^-$  were investigated as co-catalysts in combination with a chromium catalyst for the oligomerization of ethylene to 1-hexene and 1-octene.<sup>168</sup> The chromium complex of  $[\mathbf{1.48}]^-$  showed higher activity than the larger fluoro-bridged  $[\mathbf{1.50}]^-$ . The anion  $[\mathbf{1.50}]^-$  has been suggested as the “least coordinating anion”. However, it was found that  $[\mathbf{1.50}]^-$  was prone to dissociation in the presence of donor solvents into  $[\text{FAl}\{\text{OC}(\text{CF}_3)_3\}_3]^-$  and  $\text{Al}\{\text{OC}(\text{CF}_3)_3\}_3$ .<sup>151,155,169</sup>

Gallium-containing WCAs such as  $[\mathbf{1.51}]^-$  and  $[\mathbf{1.52}]^-$  have also been applied in polymerization. The iodonium and triphenylcyclopropenium salts of  $[\mathbf{1.51}]^-$  have been investigated as photo-initiator for the cationic polymerization of epoxides and demonstrated similar photo-activity as salts containing  $[\mathbf{1.36}]^-$  and  $[\mathbf{1.38}]^-$ .<sup>170-174</sup> The “linking” strategy of two anion motifs has been also applied for  $[\mathbf{1.52}]^-$ . This WCA has been studied as co-catalyst in combination with a zirconium metallocene for propene polymerization. The catalyst system revealed lower catalytic activity than the aluminate analog  $[\mathbf{1.44}]^-$ .<sup>136-138</sup>



Another modification of boron-based WCAs is the carborane anion. The effort to distribute the charge over a large number of atoms has led to the development of polyhedral carboranes. The cesium carborane salt of **[1.53]**<sup>−</sup> was first synthesized by Knoth in 1967.<sup>175,176</sup> However, the weakly coordinating ability of **[1.53]**<sup>−</sup> was not studied until the mid-1980s as the anion is prone to oxidation.<sup>177,178</sup> In order to overcome this limitation, partial halogenated derivatives were intensively studied that are less coordinating, chemically robust towards oxidation and acid cleavage, and thermally stable.<sup>179-181</sup> Particularly intriguing are the hexahalogenated carborane anions **[CB<sub>11</sub>R<sub>6</sub>X<sub>6</sub>]**<sup>−</sup> (R = H, Me; X = Cl, Br), **[1.54]**<sup>−</sup> and **[1.55]**<sup>−</sup>, reported by Reed and Ozerov. These WCAs delocalize the negative charge and stabilize highly electrophilic silylium cations **[R<sub>3</sub>Si]<sup>+</sup>** (e.g. **[<sup>i</sup>Pr<sub>3</sub>Si]<sup>+</sup>**, **[Et<sub>3</sub>Si]<sup>+</sup>** and **[Mes<sub>3</sub>Si]<sup>+</sup>**).<sup>182-186</sup>

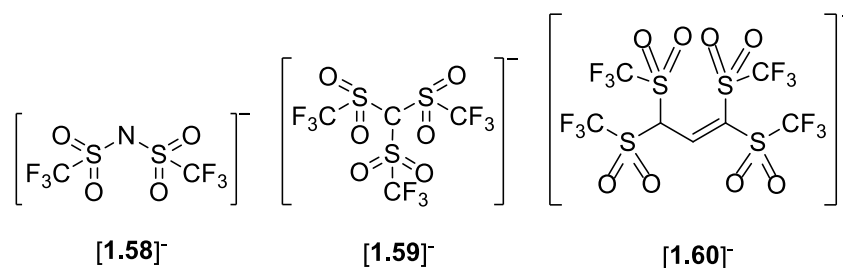


Carborane anion, **[1.54]**<sup>-</sup> (X = F, Cl, Br, I) and fully halogenated derivatives have been pioneered by Reed and co-workers and are considered “the least coordinating anions” and stabilize several highly reactive cations (*e.g.* **[HC<sub>60</sub>]**<sup>+</sup>, **C<sub>60</sub>**<sup>+</sup>, **[C<sub>6</sub>H<sub>7</sub>]**<sup>+</sup>, **H**<sup>+</sup>, **[H<sub>5</sub>O<sub>2</sub>]**<sup>+</sup>, **[H(CO<sub>2</sub>)<sub>2</sub>]**<sup>+</sup>, **[H(OEt<sub>2</sub>)<sub>2</sub>]**<sup>+</sup>, **[Ph<sub>3</sub>C]**<sup>+</sup>).<sup>187-195</sup>

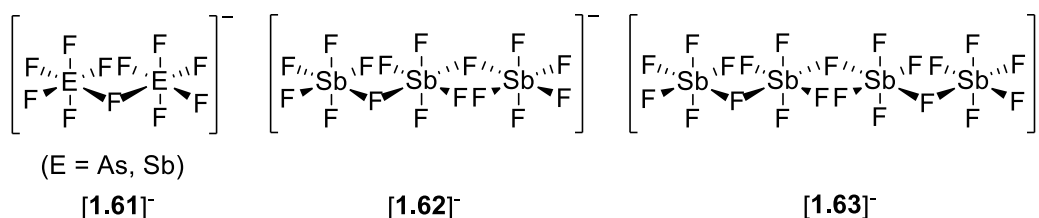
Carborane anions have been utilized as ionic liquids<sup>196</sup> and have been incorporated into transition metal frameworks as catalysts for olefin polymerization.<sup>197</sup> For instance, Exxon disclosed zirconocene complexes of **[1.53]**<sup>-</sup> as catalyst for ethylene polymerization.<sup>111,198</sup> Manners and Reed reported the trialkylsilylium salts of carborane anions **[1.54]**<sup>-</sup> and **[1.55]**<sup>-</sup> (X = Br) for the ring opening polymerization of cyclic chlorophosphazene, **[Cl<sub>2</sub>P=N]<sub>3</sub>**.<sup>199</sup> Further, Reed reported the complex **[Et<sub>2</sub>Al][1.54]** (X = Cl, Br) as catalyst for ethane and cyclohexene oxide polymerization.<sup>200</sup> The complex **Li[1.56]** catalyzes the radical polymerization of terminal alkenes.<sup>201</sup> Despite their application as WCAs, their widespread use is hindered due to the extensive synthetic procedure.

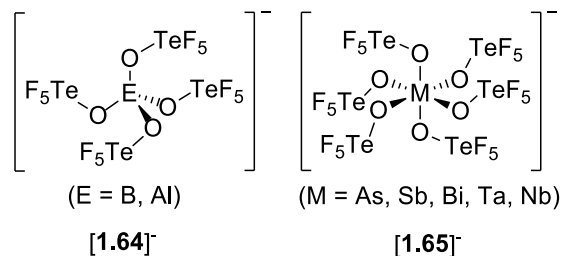
Other p-block elements such as the triflate anion analogues **[1.58]**<sup>-</sup>, **[1.59]**<sup>-</sup> and **[1.60]**<sup>-</sup> have been applied as WCAs.<sup>202-206</sup> These anions are described as highly charge delocalized.<sup>207,208</sup> The incorporation of sulfonyl groups enables the development of larger anions, **[1.58]**<sup>-</sup>, **[1.59]**<sup>-</sup> and **[1.60]**<sup>-</sup>, and facilitates the delocalization of the negative charge over the sulfonyl groups. The triflimidate anion, **[1.58]**<sup>-</sup>, was first reported in 1984<sup>209</sup> and reveals great WCA properties and has been employed as an electrolyte in batteries.<sup>210,211</sup> Salts containing **[1.58]**<sup>-</sup> have been used as ionic liquids for the copolymerization of styrene and CO.<sup>212</sup> The Brønsted acid **H[1.58]** is a highly efficient initiator for the group transfer polymerization of methyl methacrylate and a co-catalyst for the polymerization of *N,N*-dimethylacrylamide.<sup>213,214</sup> Although the Brønsted acid **H[1.59]** was first reported by Seppelt and co-workers in 1988, the application of the anion

[1.59]<sup>-</sup> as a WCA is limited to electrolytes in lithium ion batteries due to the challenging synthesis.<sup>215-217</sup> The intriguing anion [1.60]<sup>-</sup> has recently been reported as an allylic C–H acid, in which the negative charge is delocalized over four triflyl groups. The WCA [1.60]<sup>-</sup> reveals high catalytic activity in Friedel-Crafts acylation reactions.<sup>218</sup>



Larger derivatives of the “classical” anions of [EF<sub>6</sub>]<sup>-</sup> (E = As, Sb), namely [1.61]<sup>-</sup>, [1.62]<sup>-</sup> and [1.63]<sup>-</sup> were characterized in 1966 and have since been employed as WCAs.<sup>219-234</sup> However, the application of these anions has not received attention in catalysis. The anion [1.64]<sup>-</sup> that is based on pentafluoroorthotellurate groups exhibits weakly coordinating character.<sup>235</sup> The WCA [1.64]<sup>-</sup> (E = Al) has been recently reported in 2017 to promote the stabilization of reactive cations (*e.g.* H<sup>+</sup>, [Ph<sub>3</sub>C]<sup>+</sup>, [Ph<sub>4</sub>P]<sup>+</sup>, [C<sub>6</sub>H<sub>7</sub>]<sup>+</sup>, [C<sub>9</sub>H<sub>13</sub>]<sup>+</sup>).<sup>236</sup> Among the class of hexacoordinate teflate-based anion [1.65]<sup>-</sup>,<sup>237-243</sup> the anion [Sb(OTeF<sub>5</sub>)<sub>6</sub>]<sup>-241</sup> is the most promising WCA to facilitate the stabilization of reactive cations (*e.g.* [XeOTeF<sub>5</sub>]<sup>+</sup>, [Ag(S<sub>8</sub>)<sub>2</sub>]<sup>+</sup>, [Ag<sub>2</sub>(Se<sub>6</sub>)(SO<sub>2</sub>)<sub>2</sub>]<sup>+</sup>).<sup>156,244,245</sup> Catalytic application of the hexacoordinate anion [1.65]<sup>-</sup> has not been demonstrated yet.



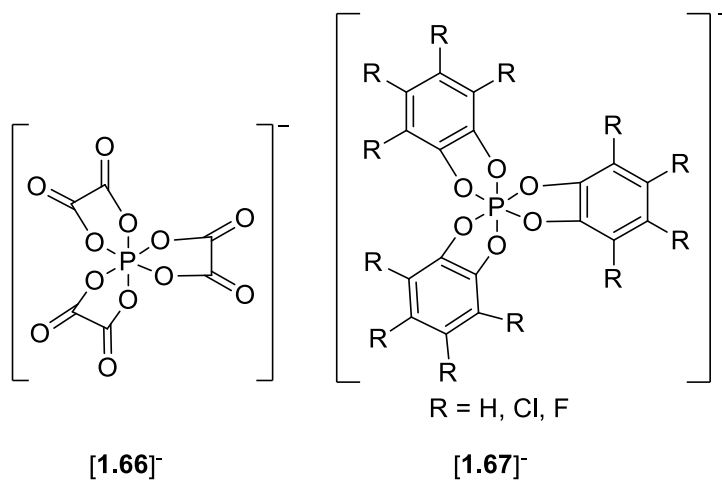


A key take-home message from this section is that there are relatively few single component initiator systems that have been developed for cationic polymerization. Namely, the only systems that have been used are  $\text{H}(\text{OEt}_2)_2[\text{Al}\{\text{OC}(\text{CF}_3)_3\}_4]$ ,  $\text{H}(\text{OEt}_2)_2[\text{B}(\text{C}_6\text{F}_5)_4]$ ,  $\text{Na}(\text{H}_2\text{O})[\text{B}\{3,5-(\text{CF}_3)_2\text{C}_6\text{H}_3\}_4]$ , and  $\text{H}[\text{B}(\text{C}_2\text{O}_4)_2]$  for the cationic ring-opening polymerization of oxalines, and cationic polymerization of isobutene, isobutyl vinyl ether, and styrene.<sup>33,64-66</sup> The potential advantages of these Brønsted acids are accurate control over monomer to initiator ratios during polymerization and polymerizations performed at higher temperatures than those typically used (*i.e.*  $-100\text{ }^\circ\text{C}$ ).<sup>246</sup>

## 1.5 Group 15 Element Based WCAs

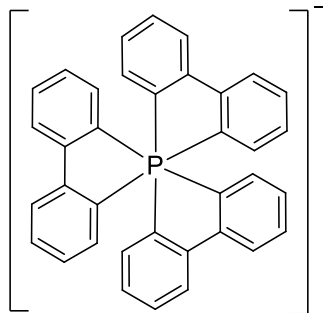
The main goal of this dissertation is the isolation of solid weighable Brønsted acids as single-component initiator systems for the cationic polymerization of olefin monomers. The initiator system requires a WCA that stabilizes the reactive carbocation during polymerization. Substantial studies have been performed in the development of WCAs based on group 13 elements that are dominated by tetracoordinate boron and aluminum anion analogues. In comparison, WCAs containing group 15 elements are less common. The investigation of hexacoordinate phosphorus compounds is of fundamental interest. Anionic species of the form  $[\text{PX}_6]^-$ , such as  $[\text{PF}_6]^-$  and  $[\text{PCl}_6]^-$ , have been employed as WCAs.<sup>247</sup> Larger derivatives of the  $[\text{PF}_6]^-$  anion are promising. The hexacoordinate phosphorus(V) anion facilitates the design of

larger WCAs that are thought to be more charge delocalized. In particular, the protic acid of the tris(oxalato)phosphate anion, **[1.66]**<sup>-</sup>, catalyzes Friedel-Crafts type alkylation reactions.<sup>248</sup> The early work of Allcock and Hellwinkel has pioneered the development of hexacoordinate phosphorus(V) anions. The anion **[1.67]**<sup>-</sup> (R = H) was accidentally discovered by Allcock in 1963 as a potential WCA.<sup>249-252</sup> At the same time Hellwinkel isolated a hexacoordinate phosphorus(V) anion with three bidentate biphenylidene ligands, **[1.68]**<sup>-</sup>.<sup>253-256</sup> Since the 1970s a library of stable and more complex phosphorus(V) anions has been generated.<sup>257-260</sup> An established example is the chiral tris(tetrachlorobenzenediolato)phosphate anion (TRISPHAT), **[1.67]**<sup>-</sup> (R = Cl), that was first reported by Schmutzler in 1992.<sup>261</sup> Lacour and co-workers shed light on **[1.67]**<sup>-</sup> (R = Cl) by resolving the anion into enantiomerically pure **[1.67]**<sup>-</sup> (R = Cl) and unveiled its numerous application.<sup>260,262-265</sup> The trityl salt of **[1.67]**<sup>-</sup> (R = Cl), in combination with a co-initiator, is an efficient initiator system for the polymerization of butyrolactone and methacrylate.<sup>266</sup>

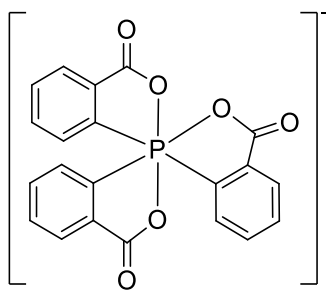


## 1.6 Outline of Thesis

The Gates group has demonstrated the weakly coordinating ability of the non-chlorinated derivative of  $[\mathbf{1.67}]^-$  to stabilize alkali metal complexes as halide abstraction agent.<sup>267</sup> Advances have led to the syntheses of Brønsted acids,  $\text{H}(\text{L})_2[\mathbf{1.67}]$  ( $\text{L} = \text{DMF}, \text{DMSO}; \text{R} = \text{H}$ ), for the protonolysis of late transition metal-carbon bonds.<sup>268</sup> Building on this prior work, we successfully isolated the strong Brønsted acid  $\text{H}(\text{OEt}_2)_2[\mathbf{1.67}]$  ( $\text{R} = \text{Cl}$ ) as a single-component initiator for the cationic polymerization of different vinyl monomers including *n*-butyl vinyl ether, styrene,  $\alpha$ -methylstyrene and isoprene.<sup>269</sup> To further explore the reactivity of single-component initiators containing the anion  $[\mathbf{1.67}]^-$  ( $\text{R} = \text{Cl}$ ), we pursued the design of new Brønsted acids. Chapter 2 describes the isolation and characterization of strong Brønsted acids,  $\text{H}(\text{L})_2[\mathbf{1.67}]$  ( $\text{L} = \text{DMF}, \text{THF}, \text{CH}_3\text{CN}; \text{R} = \text{Cl}$ ), and their application as solid and weighable single component initiators for the cationic polymerization of *n*-butyl vinyl ether and *p*-methoxystyrene. Although alkali metal salts of  $[\mathbf{1.68}]^-$  are known,<sup>253,254</sup> we sought an alternative to the WCA  $[\mathbf{1.67}]^-$ . Chapter 3 discusses the synthesis, isolation and characterization of a chiral P-C-containing spiro-compound,  $[\text{P}(\text{C}_{12}\text{H}_8)(\text{C}_{24}\text{H}_{16})][\mathbf{1.68}]$ , and the characterization of the pentavalent phosphorane  $\text{P}(\text{C}_{12}\text{H}_8)_2(\text{C}_{12}\text{H}_9)$ . Chapter 4 focuses on the weakly coordinating ability of the anion  $[\mathbf{1.69}]^-$ . In particular, the isolation and characterization of several ammonium salts and an alkali metal salt of  $[\mathbf{1.69}]^-$  are reported. Chapter 5 describes the development of two transition metal-containing WCAs and the syntheses of strong Brønsted acids for the cationic polymerization of olefin monomers. Chapter 6 gives a summary of the research findings contained within this thesis and considerations for future work are postulated.



[1.68]<sup>-</sup>



[1.69]<sup>-</sup>

## Chapter 2: [HL<sub>2</sub>][P(1,2-O<sub>2</sub>C<sub>6</sub>Cl<sub>4</sub>)<sub>3</sub>] (L = THF, DMF): Brønsted Acid Initiators for the Polymerization of *n*-Butyl Vinyl Ether and *p*-Methoxystyrene\*

### 2.1 Introduction

The carbocationic polymerization of olefins is a challenging reaction with significantly higher propagation rate constants and more termination/chain transfer pathways than related radical or anionic methods.<sup>17,37</sup> Therefore, initiators must be carefully designed with a cation source (the simplest being a proton or carbenium ion) and a weakly coordinating anion (WCA) that balances the electrophilic propagating cation.<sup>26,27,68,71,270,271</sup> The design and synthesis of large, charge delocalized and non-nucleophilic WCAs is an area of considerable current interest to generate and stabilize highly reactive cations for fundamental and applied studies.<sup>84,147,151,179,182,194,272,273</sup> Despite these efforts, only a few such systems have been employed as cationic initiators for polymerization.

Most recent developments of cationic initiators have focused on two-component initiators composed of a Lewis acid (*e.g.* B(C<sub>6</sub>F<sub>5</sub>)<sub>3</sub>, *o*-C<sub>6</sub>F<sub>4</sub>[B(C<sub>6</sub>F<sub>5</sub>)<sub>2</sub>]<sub>2</sub>, Al(C<sub>6</sub>F<sub>5</sub>)<sub>3</sub>, [η<sup>6</sup>-Ar<sub>2</sub>Ga]<sup>+</sup>) and a co-initiator (*e.g.* protic acid, water, alcohol, or carbenium source).<sup>167,274-279</sup> Even in the case of the commercial two-component systems (*e.g.* BF<sub>3</sub> or AlCl<sub>3</sub> with “adventitious” water) the exact structure of the initiating species and the mechanism of initiation is not easily studied.<sup>280</sup> The very rapid rates of propagation and sensitivity of the cationic intermediates make it very difficult to systematically study cationic polymerizations, in general. Commensurate with the rapid improvement in WCA chemistry, single-component initiators are of growing interest with examples including: [Al(η<sup>5</sup>-C<sub>5</sub>H<sub>5</sub>)<sub>2</sub>][Al{OC(CF<sub>3</sub>)<sub>3</sub>}]<sub>4</sub>,<sup>58</sup> [Ga(C<sub>6</sub>H<sub>5</sub>F)<sub>2</sub>][Al{OC(CF<sub>3</sub>)<sub>3</sub>}]<sub>4</sub>,<sup>60</sup>

---

\* This chapter has previously been published: Hazin, K.; Serin, S.C.; Patrick, B. O.; Ezhova, M. B.; Gates, D. P. *Dalton Trans.* **2017**, 46, 5901. 30

$[\text{EtZn}(\text{arene})_2][\text{Al}\{\text{OC}(\text{CF}_3)_3\}_4]$  (arene = toluene, mesitylene),<sup>61</sup>  $[\text{Cp}^*\text{Ti}(\text{CH}_3)_2][\text{CH}_3\text{B}(\text{C}_6\text{F}_5)_4]$ ,<sup>36</sup>  
 $[\text{Al}(\eta^5\text{-C}_5\text{H}_5)_2][\text{CH}_3\text{B}(\text{C}_6\text{F}_5)_4]$ ,<sup>59</sup>  $[\text{Ph}_3\text{C}][\text{B}(\text{C}_6\text{F}_5)_4]$ ,<sup>55-57,266</sup> and  $[\text{Ni}(\text{C}_{12}\text{H}_{19})][\text{B}\{3,5\text{-}(\text{CF}_3)_2\text{C}_6\text{H}_3\}_4]$ .<sup>63</sup> Single-component initiator systems based on Brønsted acids are less common with examples being shown in Figure 2.1 (A,<sup>65</sup> B,<sup>64,281</sup> C,<sup>282</sup> and D<sup>33,66</sup>). These are attractive since there is no question of the initiating species ( $\text{H}^+$ ) or the mechanism of propagation. One limitation to their widespread usage is the difficulty in synthesizing, purifying and handling highly reactive strong non-aqueous Brønsted acids with WCAs, which necessitate handling at low temperatures and/or in donor solvents.

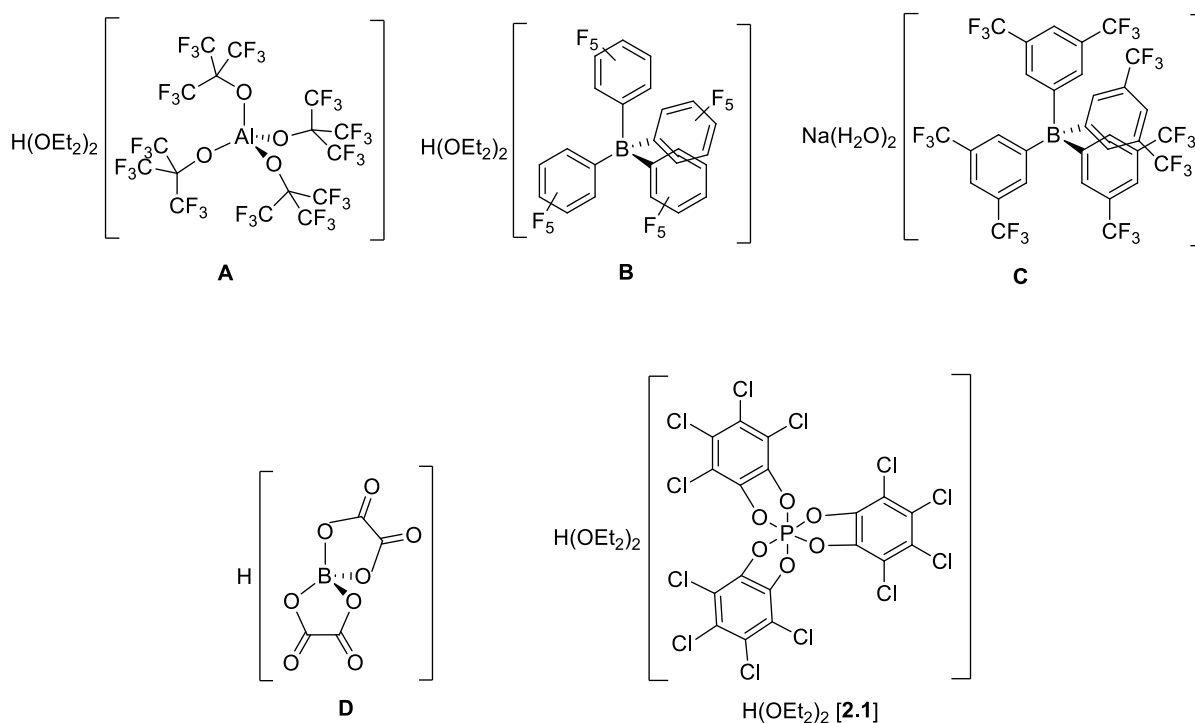


**Figure 2.1. Examples of isolable Brønsted acids that have successfully been employed as single-component initiator systems for olefins.**

The well-known charge delocalized tris(tetrachlorobenzenediolato)phosphate {TRISPHAT, **[2.1]**<sup>-</sup>}<sup>263,265,283-293</sup> exhibits ideal properties as a WCA and recently caught our attention as a potentially convenient WCA for protic acids. We have shown that the simple reaction of 1,2-C<sub>6</sub>Cl<sub>4</sub>(OH)<sub>2</sub> (3 equiv) with PCl<sub>5</sub> in CH<sub>2</sub>Cl<sub>2</sub> and a weak base (Et<sub>2</sub>O, MeCN) permits the isolation of the Brønsted acids H(OEt<sub>2</sub>)<sub>2</sub>**[2.1]** and H(OEt<sub>2</sub>)(CH<sub>3</sub>CN)**[2.1]**.<sup>269</sup> Remarkably, these solid weighable compounds show modest stability at ambient temperature and are as effective as single-component initiators for the polymerization of *n*-butyl vinyl ether,  $\alpha$ -methylstyrene, styrene and isoprene. They are rare examples of strong Brønsted acids containing P-based anions.<sup>248,268,269</sup>

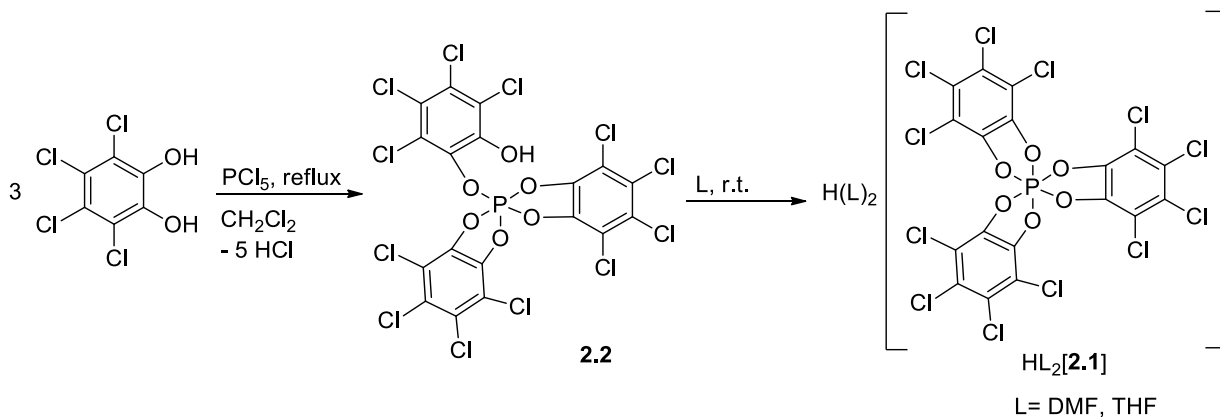
Herein, the scope of this convenient route to Brønsted acids of **[2.1]**<sup>-</sup> is expanded to the synthesis and isolation of H(DMF)<sub>2</sub>**[2.1]**, H(THF)(MeCN)**[2.1]** and H(THF)<sub>2</sub>**[2.1]** The latter is a rare example of a crystallographically characterized compound containing the [H(THF)<sub>2</sub>]<sup>+</sup> cation. Both are effective initiators for the polymerization of *n*-butyl vinyl ether and *p*-methoxystyrene. Notably, high molecular weight poly(*p*-methoxystyrene) (*M<sub>n</sub>* up to 649,000 g mol<sup>-1</sup>) in good yield (53–98%) is obtained with an unexpected branched structure.

## 2.2 Results and Discussion

### 2.2.1 Synthesis and Characterization of Initiators

It has been reported by Lacour et al. that the treatment of phosphorus pentachloride (PCl<sub>5</sub>) with tetrachlorocatechol (3 equiv) in hot toluene, followed by addition of an amine affords the ammonium salt of **[2.1]**<sup>-</sup>.<sup>262</sup> Building on this previous work, we aimed to develop H(DMF)<sub>2</sub>**[2.1]** and H(THF)<sub>2</sub>**[2.1]** as initiators for cationic olefin polymerization with the more acidic [H(DMF)<sub>2</sub>]<sup>+</sup> cation (p*K<sub>a</sub>* = -1.2 ± 0.5)<sup>294</sup> and [H(THF)<sub>2</sub>]<sup>+</sup> cation (p*K<sub>a</sub>* = -2.05).<sup>295</sup> Treating

$\text{PCl}_5$  with tetrachlorocatechol (3 equiv) in hot dichloromethane resulted in **2.2** ( $\delta = -29$  ppm). Subsequently, the weakly donating solvent (DMF or THF) was added to afford an off-white precipitate of either  $\text{H}(\text{DMF})_2[\mathbf{2.1}]$  or  $\text{H}(\text{THF})_2[\mathbf{2.1}]$  (Scheme 2.1). It is important to keep the THF concentration low to prevent its polymerization ( $< 50$  vol% in  $\text{CH}_2\text{Cl}_2$ ). The crude products,  $\text{H}(\text{DMF})_2[\mathbf{2.1}]$  or  $\text{H}(\text{THF})_2[\mathbf{2.1}]$  were recrystallized as described in the experimental section to afford colorless crystals suitable for X-ray crystallography. The molecular structures of the moisture and air-sensitive Brønsted acids  $\text{H}(\text{DMF})_2[\mathbf{2.1}]$  and  $\text{H}(\text{THF})_2[\mathbf{2.1}]$  are shown in Figures 2.4 and 2.5, respectively (*vide infra*). Although it is preferable to store  $\text{H}(\text{DMF})_2[\mathbf{2.1}]$  at low temperatures (ca.  $-30$  °C), the solid may be handled for 1 week or more at ambient temperature in an inert atmosphere without decomposition. In contrast,  $\text{H}(\text{THF})_2[\mathbf{2.1}]$  degrades in  $< 1$  h at ambient temperature.



**Scheme 2.1. Synthesis of Brønsted acid  $\text{H}(\text{L})_2[\mathbf{2.1}]$  ( $\text{L} = \text{DMF, THF}$ ).**

The  $^{31}\text{P}\{^1\text{H}\}$  NMR spectra of  $\text{H}(\text{L})_2[\mathbf{2.1}]$  ( $\text{L} = \text{DMF, THF}$ ) in  $\text{CD}_3\text{CN}$  each show a singlet resonance ( $\text{L} = \text{DMF}$ :  $\delta = -81.8$ ;  $\text{L} = \text{THF}$ :  $\delta = -80.6$ ) (see Appendix A, Figures A1 and A2), which is in the range expected for salts containing  $[\mathbf{2.1}]^-$  ( $\delta = -80.1$ ).<sup>261</sup> In addition, the isolated Brønsted acids  $\text{H}(\text{DMF})_2[\mathbf{2.1}]$  and  $\text{H}(\text{THF})_2[\mathbf{2.1}]$  were characterized by  $^1\text{H}$  and  $^{13}\text{C}\{^1\text{H}\}$  NMR

spectroscopy, X-ray crystallography and elemental analysis. At ambient temperature, the  $^1\text{H}$  NMR spectra of  $\text{H}(\text{L})_2[\mathbf{2.1}]$  ( $\text{L} = \text{THF}, \text{DMF}$ ) in  $\text{CD}_2\text{Cl}_2$  revealed signals assigned to the two coordinated DMF molecules ( $\delta = 8.07, 1\text{H}, \text{O}=\text{CH}$ ;  $3.10, 3\text{H}, \text{NCH}_3$ ;  $2.97, 3\text{H}, \text{NCH}_3$ ) or two coordinated THF moieties ( $\delta = 4.08, 4\text{H}, \text{OCH}_2$ ;  $2.04, 4\text{H}, \text{CH}_2$ ), respectively. In addition, a broad downfield signal was observed that is assigned to the acidic proton of  $\text{HL}_2[\mathbf{2.1}]$  ( $\text{L} = \text{DMF}$ :  $\delta = 16.6, 1\text{H}, \text{fwhm} = 565 \text{ Hz}$ ;  $\text{L} = \text{THF}$ :  $\delta = 13.4, 1\text{H}, \text{fwhm} = 532 \text{ Hz}$ ). For comparison, related salts containing the  $[\text{H}(\text{DMF})_2]^+$  cation show similar downfield chemical shifts in  $\text{H}_2(\text{DMF})_4[\text{TeBr}_6]$ :  $\delta = 16.8, \text{CD}_3\text{CN}$ ;  $\text{H}(\text{DMF})_2[\text{CF}_3\text{SO}_3]$ :  $\delta = 16.9, \text{CD}_3\text{CN}$ ;<sup>296</sup>  $\text{H}(\text{DMF})_2[\text{P}(1,2\text{-O}_2\text{C}_6\text{H}_4)_3]$ :  $\delta = 15.3, \text{CD}_3\text{CN}$ ;<sup>268</sup>  $\text{H}(\text{DMF})_2[\text{CF}_3\text{CO}_2]$ :  $\delta = 15.1, (\text{CD}_3)_2\text{SO}$ .<sup>297</sup> The salt  $\text{H}(\text{THF})_2[\text{CHB}_{11}\text{R}_5\text{X}_6]$  displayed a similar downfield shift for the acidic proton ( $\delta = 14.8 \text{ ppm}$ )<sup>195</sup> to that of  $\text{H}(\text{THF})_2[\mathbf{2.1}]$  whilst  $[\text{H}(\text{THF})_2][\text{Al}\{\text{OC}(\text{CF}_3)_3\}_4]$  is quite different ( $\delta = \sim 8 \text{ ppm}$ ).<sup>298</sup>

At low temperature, the  $^1\text{H}$  NMR spectra of  $\text{H}(\text{THF})_2[\mathbf{2.1}]$  (Figure 2.2) display much sharper signals for the acidic proton and are shifted downfield with respect to the ambient temperature spectra ( $T = -85 \text{ }^\circ\text{C}$ ,  $\text{CD}_2\text{Cl}_2$ :  $\text{L} = \text{DMF}$ :  $\delta = 19.2, \text{fwhm} = 102 \text{ Hz}$ ;  $\text{L} = \text{THF}$ :  $\delta = 16.9, \text{fwhm} = 15 \text{ Hz}$ ). To our knowledge, these are the furthest downfield signals detected for the acidic protons of  $[\text{H}(\text{DMF})_2]^+$  and  $[\text{H}(\text{THF})_2]^+$  cation containing salts and are comparable to that of  $\text{H}[\text{CHB}_{11}\text{Cl}_{11}]$  ( $\delta_{\text{H}} = 20.4$  in  $\text{SO}_2$  at  $-65 \text{ }^\circ\text{C}$ ).<sup>182</sup> Importantly, the integrated ratio of the signals assigned to the acidic proton and the coordinating solvent are consistent with the 2:1 ratio within the  $[\text{HL}_2]^+$  cation.

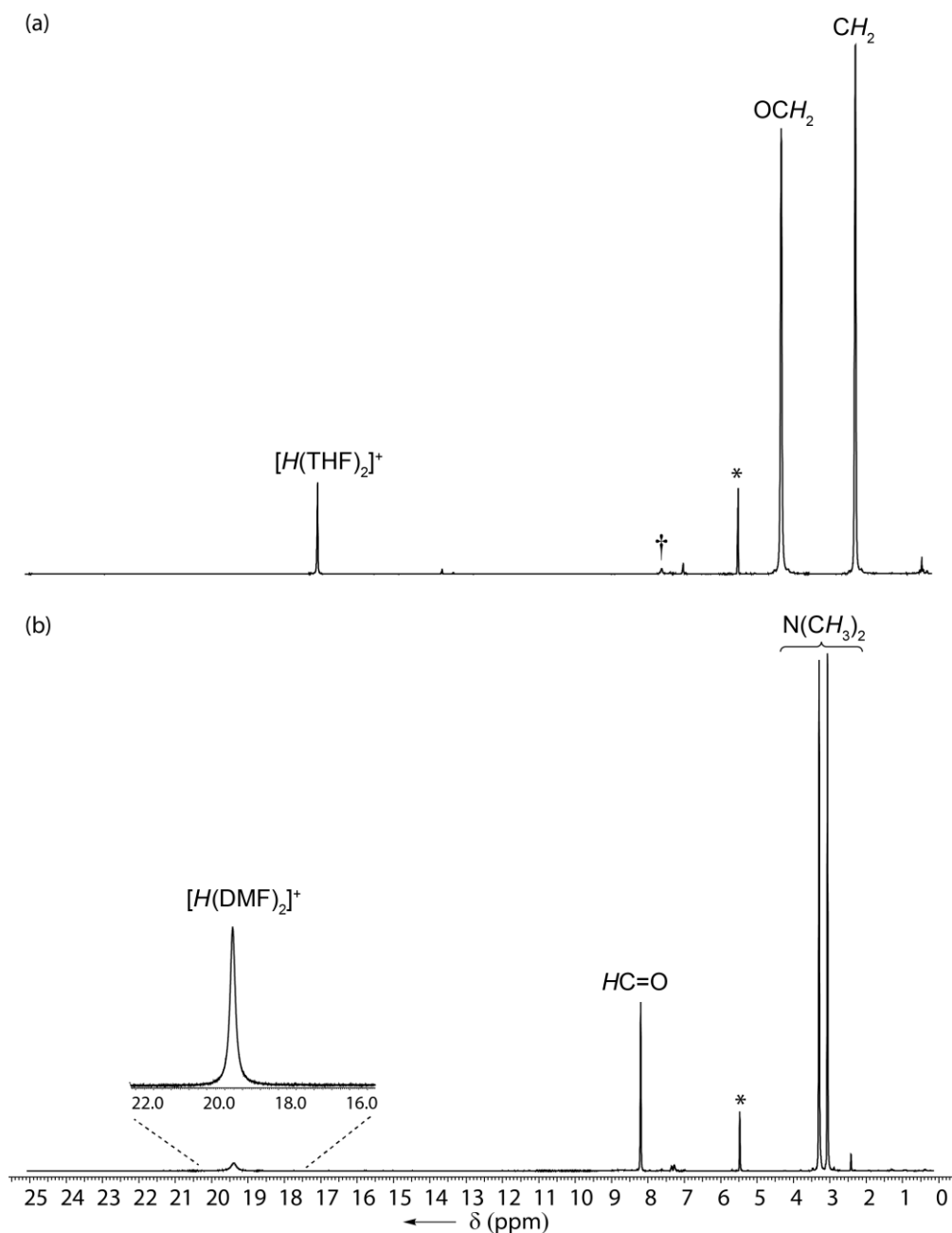


**Figure 2.2.**  $^1\text{H}$  NMR (400 MHz,  $\text{CD}_2\text{Cl}_2$ ,  $-85^\circ\text{C}$ ) spectrum of (a)  $\text{H}(\text{THF})_2[2.1]$  and (b)  $\text{H}(\text{DMF})_2[2.1]$ .

**\*** indicates residual  $\text{CHDCl}_2$ . **†** unassigned signal.

To further investigate the integrity of  $[\text{HL}_2]^+$  ( $\text{L} = \text{DMF}$ ;  $\text{L} = \text{THF}$ ) moiety in solution, low temperature  $^1\text{H}$ - $^1\text{H}$  COSY NMR experiments were performed. Given that no correlation was observed between the acidic proton and the THF  $\text{OCH}_2$  protons, the  $^1\text{H}$ - $^1\text{H}$  NOESY NMR

spectrum was recorded in  $\text{CD}_2\text{Cl}_2$  at  $-85\text{ }^\circ\text{C}$ . The spectrum of  $\text{H}(\text{THF})_2[\mathbf{2.1}]$  clearly showed an NOE between the acidic proton and the THF methylene protons, as revealed by the cross-peaks between the corresponding resonances (at 4.1 and 16.9 ppm, respectively) (Figure 2.3). These 2D NOESY NMR findings for  $\text{H}(\text{THF})_2[\mathbf{2.1}]$  were reproducible confirming the stability of the molecule. The low temperature 2D NOESY NMR spectrum of  $\text{H}(\text{DMF})_2[\mathbf{2.1}]$  (see Appendix A, Figure A5) revealed negative NOE between the acidic proton and the  $\text{HC}=\text{O}$  formyl proton as well as between the  $\text{HC}=\text{O}$  and methyl proton. This was surprising considering that  $\text{H}(\text{THF})_2[\mathbf{2.1}]$ , which is similar in size, shows positive NOE at  $-85\text{ }^\circ\text{C}$ . To confirm that negative NOE was observed in this experiment and exclude exchange, 2D ROESY data was collected for  $\text{H}(\text{DMF})_2[\mathbf{2.1}]$  in  $\text{CD}_2\text{Cl}_2$  at  $-85\text{ }^\circ\text{C}$  (see Appendix A, Figure A6). These data confirmed the NOE between the  $\text{HC}=\text{O}$  and methyl proton. No through space interactions have been observed for the acidic proton and formyl proton in the 2D ROESY experiment. Similarly, the 2D ROESY NMR spectrum of  $\text{H}(\text{THF})_2[\mathbf{2.1}]$  (see Appendix A, Figure A7) showed no interaction between the acidic proton and the THF  $\text{OCH}_2$  protons and revealed positive NOE between  $\text{CH}_2$  and  $\text{OCH}_2$  protons. In general, the tumbling rate of a molecule is responsible for the sign of NOE and is dependent on size of the molecule and solution conditions such as temperature and viscosity.<sup>299</sup> Since both  $\text{H}(\text{DMF})_2[\mathbf{2.1}]$  and  $\text{H}(\text{THF})_2[\mathbf{2.1}]$  have a similar molecular weight and both experiments were conducted under identical conditions, we tentatively attribute the difference in sign to a difference in viscosity of the solutions. Overall, these data confirmed that the  $[\text{H}(\text{THF})_2]^+$  and  $[\text{H}(\text{DMF})_2]^+$  cations are retained in  $\text{CD}_2\text{Cl}_2$  solution at  $-85\text{ }^\circ\text{C}$ .

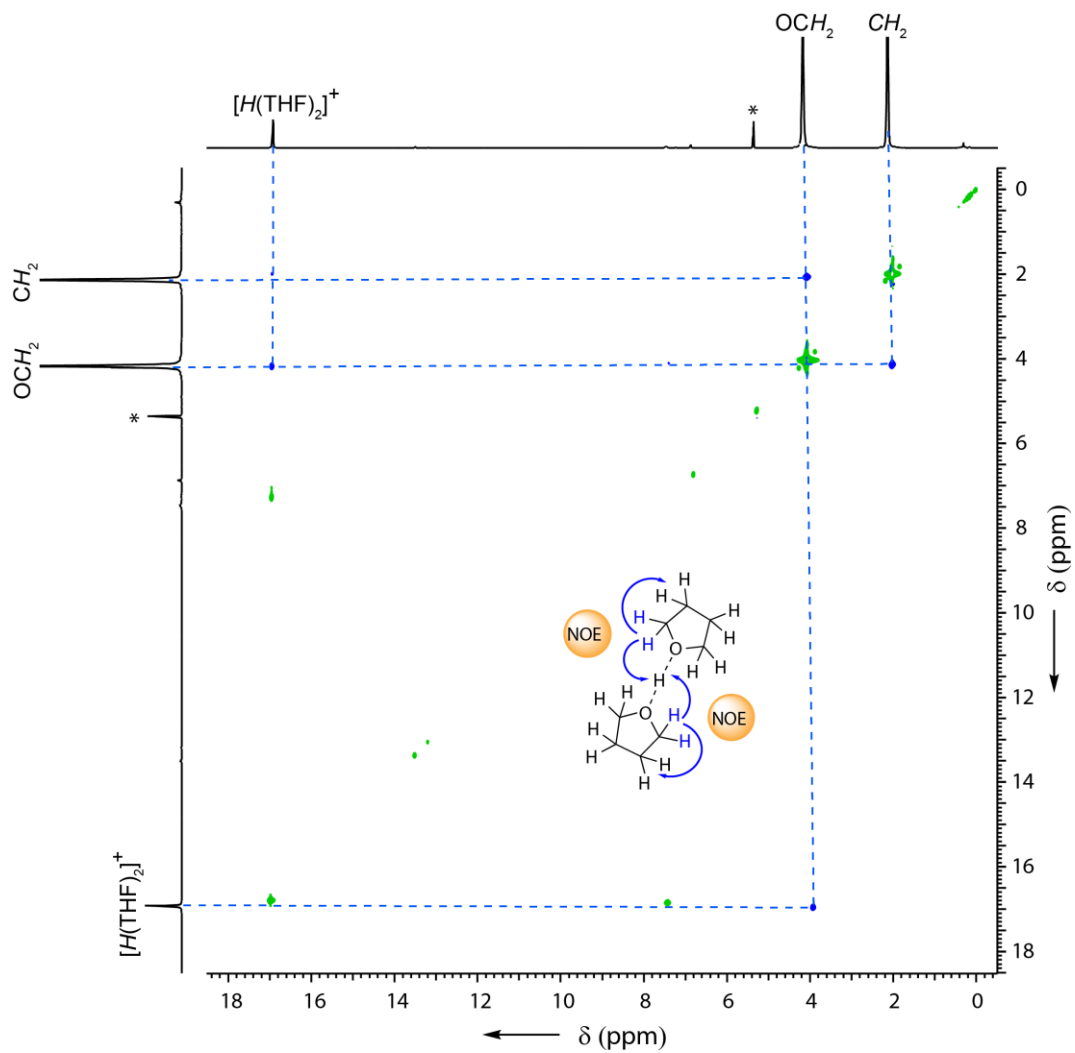
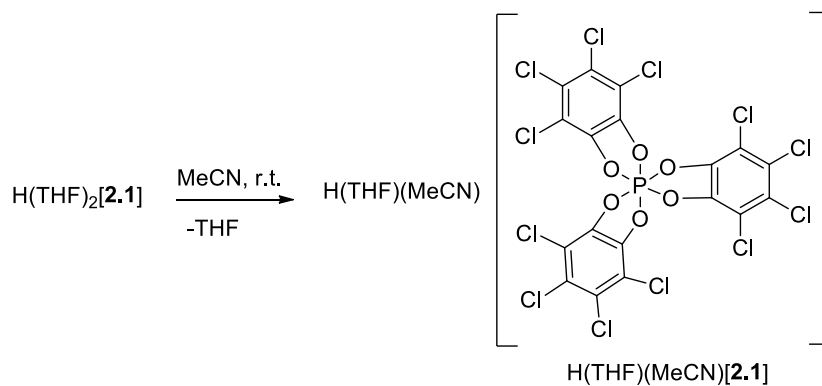


Figure 2.3. 2D  $^1\text{H}$ -NOESY (400 MHz,  $\text{CD}_2\text{Cl}_2$ ,  $-85^\circ\text{C}$ ) experiment of  $\text{H}(\text{THF})_2[2.1]$ .

A mixing time of 0.59 s was used. \* indicates residual  $\text{CHDCl}_2$ .



**Scheme 2.2. Synthesis of Brønsted acid H(THF)(MeCN)[2.1].**

We have previously shown that dissolution of H(OEt<sub>2</sub>)<sub>2</sub>[2.1] in acetonitrile results in the precipitation of single crystals of H(OEt<sub>2</sub>)(MeCN)[2.1], containing the rare [OEt<sub>2</sub>-H-NCMe]<sup>+</sup> cation. Similarly, dissolution of H(THF)<sub>2</sub>[2.1] in CD<sub>3</sub>CN affords single crystals of H(THF)(MeCN) as determined by X-ray crystallography (Figure 2.6). The <sup>31</sup>P{<sup>1</sup>H} NMR spectrum of H(THF)(MeCN)[2.1] in CD<sub>3</sub>CN recorded at 25 °C revealed a singlet resonance (δ = -80.1 ppm) suggesting that the integrity of the [TRISPHAT]<sup>-</sup> anion was preserved in solution. The <sup>1</sup>H NMR spectrum at 25 °C showed signals that were consistent with the presence of THF but the signal for the H<sup>+</sup> proton was not observed, presumably due to its breadth. Low temperature analysis in CD<sub>2</sub>Cl<sub>2</sub> was not possible due to the compound's limited stability in dichloromethane.

### 2.2.2 Metrical Parameters Determined by X-ray Crystallography

Single-crystal X-ray structures were obtained for H(DMF)<sub>2</sub>[2.1], H(THF)<sub>2</sub>[2.1] and H(THF)(MeCN)[2.1]. The molecular structures along with important metrical parameters are given in Figures 2.4, 2.5 and 2.6, respectively. Additional details are found in the supporting information. The structure of H(DMF)<sub>2</sub>[2.1] shows five crystallographically independent

complexes per asymmetric unit. For clarity, only one molecule is displayed in Figure 2.4. Compound  $\text{H}(\text{THF})_2[\mathbf{2.1}]$  (Figure 2.5) crystallizes with one tetrachlorocatechol and one THF molecule whilst  $\text{H}(\text{THF})(\text{MeCN})[\mathbf{2.1}]$  (Figure 2.6) crystallizes with large area of disordered MeCN and THF as solvate.  $\text{H}(\text{THF})_2[\mathbf{2.1}]$  displays close solvate interaction between an oxygen of the anion  $[\mathbf{2.1}]^-$  and a hydrogen of free tetrachlorocatechol [ $\text{O}(5)\cdots\text{H}(9) = 2.28(5) \text{ \AA}$ ] and between an oxygen of THF solvate and a hydrogen of the unbound tetrachlorocatechol [ $\text{O}(11)\cdots\text{H}(10) = 1.932(6) \text{ \AA}$ ]. Solvate interactions in  $\text{H}(\text{THF})(\text{MeCN})[\mathbf{2.1}]$  occur between an oxygen of the anion  $[\mathbf{2.1}]^-$  and a methyl group of the acetonitrile solvate [ $\text{O}(1)\cdots\text{H}(20a) = 2.656(2) \text{ \AA}$ ;  $\text{O}(3)\cdots\text{H}(24c) = 2.634(3) \text{ \AA}$ ].

The closest cation-anion contacts in  $\text{H}(\text{DMF})_2[\mathbf{2.1}]$  occur between an oxygen atom of the anion  $[\mathbf{2.1}]^-$  and a methyl group of DMF [ $\text{O}-\text{H}$  range:  $2.379(4)-2.717(5) \text{ \AA}$ ] and are within the sum of the van der Waals radii for oxygen and hydrogen [ $r_{\text{vdw}} = 2.72 \text{ \AA}$ ]. Similarly, the closest cation-anion contacts in  $\text{H}(\text{THF})_2[\mathbf{2.1}]$  are between an oxygen atom of the anion  $[\mathbf{2.1}]^-$  and a methylene group of THF [ $\text{O}-\text{H}$  range:  $2.620(4)-2.755(4) \text{ \AA}$ ]. In contrast,  $\text{H}(\text{THF})(\text{MeCN})[\mathbf{2.1}]$  displays close contacts between an oxygen of the anion  $[\mathbf{2.1}]^-$  and a methyl group of the  $\text{H}^+$ -coordinated acetonitrile [ $\text{O}(2)\cdots\text{H}(22c) = 2.62(18) \text{ \AA}$ ;  $\text{O}(5)\cdots\text{H}(22b) = 2.619(2) \text{ \AA}$ ] and between a chlorine of the anion  $[\mathbf{2.1}]^-$  and a methyl group of the acetonitrile solvate [ $\text{Cl}(5)\cdots\text{H}(24b) = 2.780(13)$ ].

The phosphorus(V) anion,  $[\mathbf{2.1}]^-$ , shows only minor perturbation from regular octahedral symmetry displaying metrical parameters similar to those previously reported. The average P–O bond lengths in  $\text{HLL}'[\mathbf{2.1}]$  [ $\text{L} = \text{L}' = \text{DMF}$ : avg. =  $1.71(3) \text{ \AA}$ ;  $\text{L} = \text{L}' = \text{THF}$ : avg. =  $1.715(9) \text{ \AA}$ ;  $\text{L} = \text{THF}$ ,  $\text{L}' = \text{MeCN}$ : avg. =  $1.712(4) \text{ \AA}$ ] are similar to those found in  $[\text{NEt}_2\text{H}_2][\mathbf{2.1}]$ ,<sup>261</sup>

[Et<sub>3</sub>NH][**2.1**],<sup>250</sup> H(OEt<sub>2</sub>)<sub>2</sub>[**2.1**]<sup>269</sup> and [tris(4-dimethylaminobenzene)carbenium][**2.1**]<sup>300</sup> (avg. = 1.713(8), 1.715(6), 1.715(1), 1.75(2) Å, respectively).

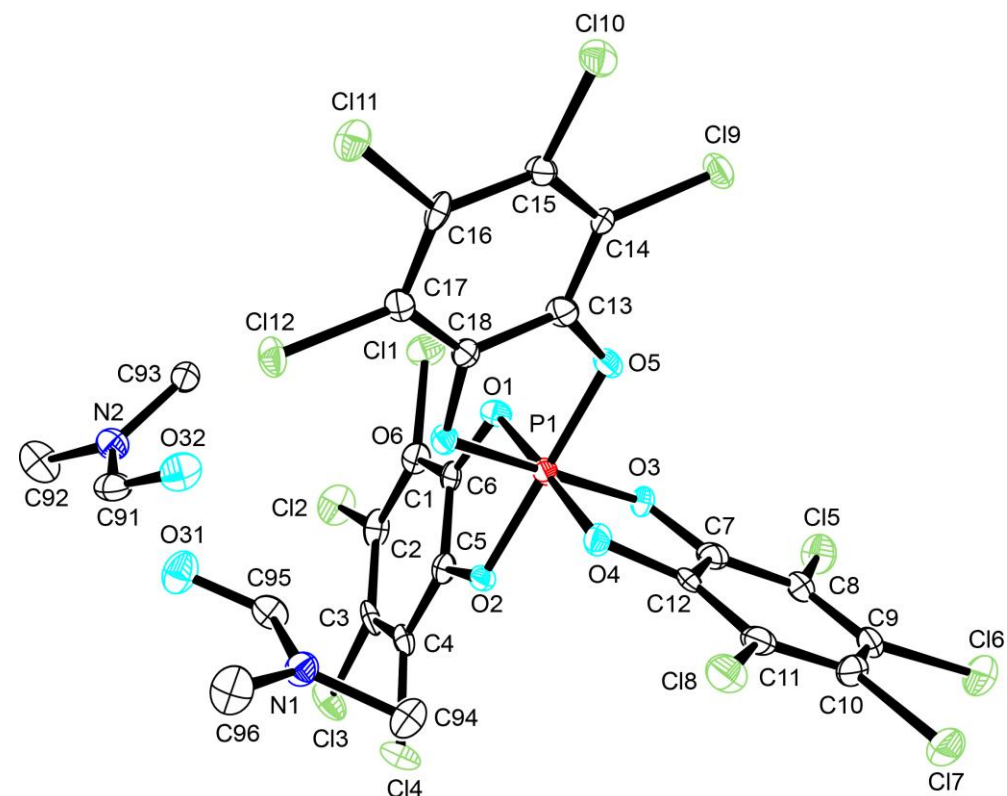


**Figure 2.4.** Molecular structure of H(DMF)<sub>2</sub>-*rac*-[**2.1**] $\cdot$ 0.2 CH<sub>2</sub>Cl<sub>2</sub> ( $\Delta$  isomer is shown; molecule 1 of 5 unique molecules). Ellipsoids are drawn at the 50% probability level. Solvents of crystallization (0.2 x CH<sub>2</sub>Cl<sub>2</sub>) and hydrogen atoms are omitted for clarity. Selected bond lengths [Å]: P(1)–O(1) = 1.719(5); P(1)–O(2) = 1.72(5); P(1)–O(3) = 1.716(5); P(1)–O(4) = 1.721(5); P(1)–O(5) = 1.709(5); P(1)–O(6) = 1.704(5); C(6)–O(2) = 1.356(8); C(94)–O(31) = 1.259(10); C(91)–O(32) = 1.261(10); C(94)–N(1) = 1.291(9); C(91)–N(2) = 1.309(10); O(31)–O(32) = 2.41(7). Selected bond angles [°]: O(1)–P(1)–O(2) = 90.8(2); O(3)–P(1)–O(4) = 91.3(3); O(5)–P(1)–O(6) = 91.1(2); C(94)–N(1)–C(96) = 121.9(7).

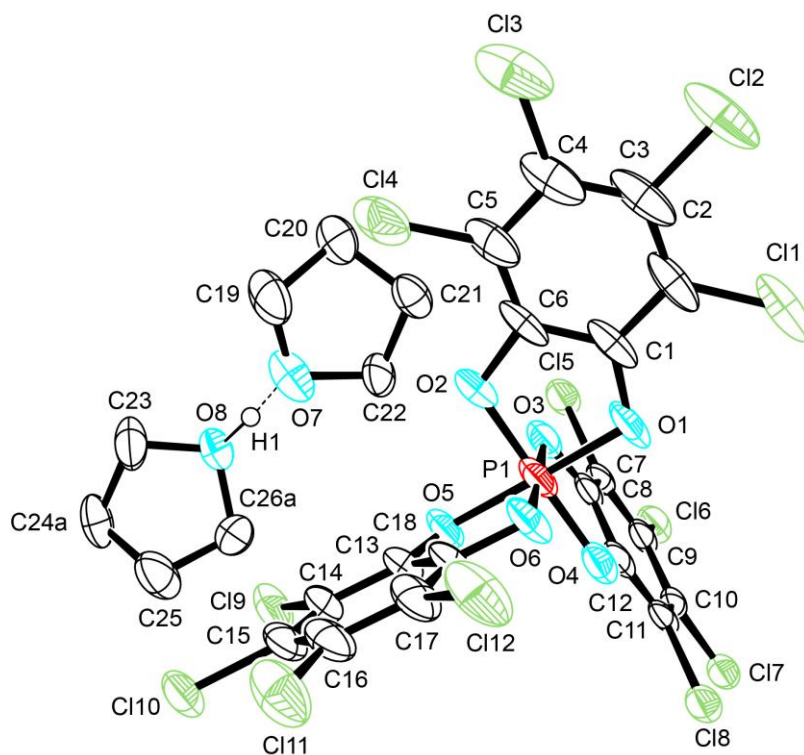


**Figure 2.5. Molecular structure of  $\text{H}(\text{THF})_2\text{-rac-[2.1]}\cdot\text{C}_6\text{H}_2\text{O}_2\text{Cl}_4\cdot\text{THF}$  ( $\Lambda$  isomer is shown).**

**Ellipsoids are drawn at the 50% probability level. Solvents of crystallization ( $1 \times \text{THF}$ ), unbound tetrachlorocatechol ( $1 \times \text{C}_6\text{H}_2\text{O}_2\text{Cl}_4$ ) and hydrogen atoms are omitted for clarity, except for H(1). Selected bond lengths [ $\text{\AA}$ ]:  $\text{P}(1)\text{-O}(1) = 1.707(3)$ ;  $\text{P}(1)\text{-O}(2) = 1.718(4)$ ;  $\text{P}(1)\text{-O}(3) = 1.714(4)$ ;  $\text{P}(1)\text{-O}(4) = 1.704(4)$ ;  $\text{P}(1)\text{-O}(5) = 1.733(3)$ ;  $\text{P}(1)\text{-O}(6) = 1.719(4)$ ;  $\text{O}(7)\text{-H}(1) = 1.35(7)$ ;  $\text{O}(8)\text{-H}(1) = 1.05(7)$ ;  $\text{C}(19)\text{-O}(7) = 1.408(16)$ ;  $\text{C}(22)\text{-O}(7) = 1.500(9)$ ;  $\text{C}(23)\text{-O}(8) = 1.465(5)$ ;  $\text{C}(26)\text{-O}(8) = 1.34(5)$ ;  $\text{O}(7)\text{-O}(8) = 2.394(5)$ . Selected bond angles [ $^\circ$ ]:  $\text{O}(2)\text{-P}(1)\text{-O}(1) = 91.1(2)$ ;  $\text{O}(3)\text{-P}(1)\text{-O}(4) = 91.2(2)$ ;  $\text{O}(5)\text{-P}(1)\text{-O}(6) = 90.2(2)$ .**

In contrast to the anion, the metrical parameters for the cation moiety provide valuable insight into the bonding within each compound. For H(THF)<sub>2</sub>[**2.1**] the acidic proton was located in the difference electron density map, whereas the acidic proton was not found for H(DMF)<sub>2</sub>[**2.1**] and H(THF)(MeCN)[**2.1**]. The acidic proton of H(THF)<sub>2</sub>[**2.1**] was refined isotropically and is coordinated asymmetrically through the oxygen atom of two THF molecules [O(7)–H(1) = 1.35(7) Å; O(8)–H(1) = 1.05(7) Å]. Asymmetric binding has been reported for related H(OEt<sub>2</sub>)<sub>2</sub>[**2.1**],<sup>269</sup> H(OEt<sub>2</sub>)<sub>2</sub>[Al{OC(CF<sub>3</sub>)<sub>3</sub>}<sub>4</sub>]<sup>298</sup> and H(OEt<sub>2</sub>)<sub>2</sub>[B(C<sub>6</sub>F<sub>5</sub>)<sub>4</sub>],<sup>301</sup> however, it has not been noted for the more rare [H(THF)<sub>2</sub>]<sup>+</sup> cation. Since the determination of the position of the central proton is generally unreliable, the more precisely determined C–O and C–C bond lengths are often used to evaluate the symmetry within the [H(OEt<sub>2</sub>)<sub>2</sub>]<sup>+</sup> cation.<sup>298</sup> These data are given in Figure 2.7 along with the previously reported H(THF)<sub>2</sub>[CHB<sub>11</sub>H<sub>5</sub>Br<sub>6</sub>],<sup>195</sup> H(THF)<sub>2</sub>[MnCl<sub>4</sub>(THF)<sub>2</sub>],<sup>302</sup> H(THF)<sub>2</sub>[TeCl<sub>5</sub>],<sup>303</sup> and H(THF)<sub>2</sub>[Al{OC(CF<sub>3</sub>)<sub>3</sub>}<sub>4</sub>].<sup>298</sup> A shortening of the C–O and C–C bonds is observed for THF<sub>B</sub> of the [THF<sub>A</sub>–H–THF<sub>B</sub>]<sup>+</sup> cation in H(THF)<sub>2</sub>[**2.1**]. This may reflect asymmetric binding within the cation. For comparison, a similar bonding situation has been observed for H(THF)<sub>2</sub>[Al{OC(CF<sub>3</sub>)<sub>3</sub>}<sub>4</sub>] whilst the binding within H(THF)<sub>2</sub>[CHBr<sub>11</sub>H<sub>5</sub>Br<sub>6</sub>] and H(THF)<sub>2</sub>[MnCl<sub>4</sub>(THF)<sub>2</sub>] appears to be more symmetric.

The C–C and C–N bonds within the acetonitrile moiety within the cation of H(THF)(MeCN)[**2.1**] [1.443(7) and 1.136(7) Å, respectively] are similar in length to those of acetonitrile (1.44 and 1.13, respectively)<sup>304</sup> and to the cation of H(OEt<sub>2</sub>)(CH<sub>3</sub>CN)[**2.1**] (1.45 and 1.14 Å, respectively).<sup>269</sup> The C–O distance in the coordinated THF molecule [C(25)–O(8a) = 1.422(18) Å; C(28a)–O(8a) = 1.42(3) Å] displays a slight lengthening from the C–O bond lengths found in THF lattice solvate [1.41(1) Å].<sup>305</sup>

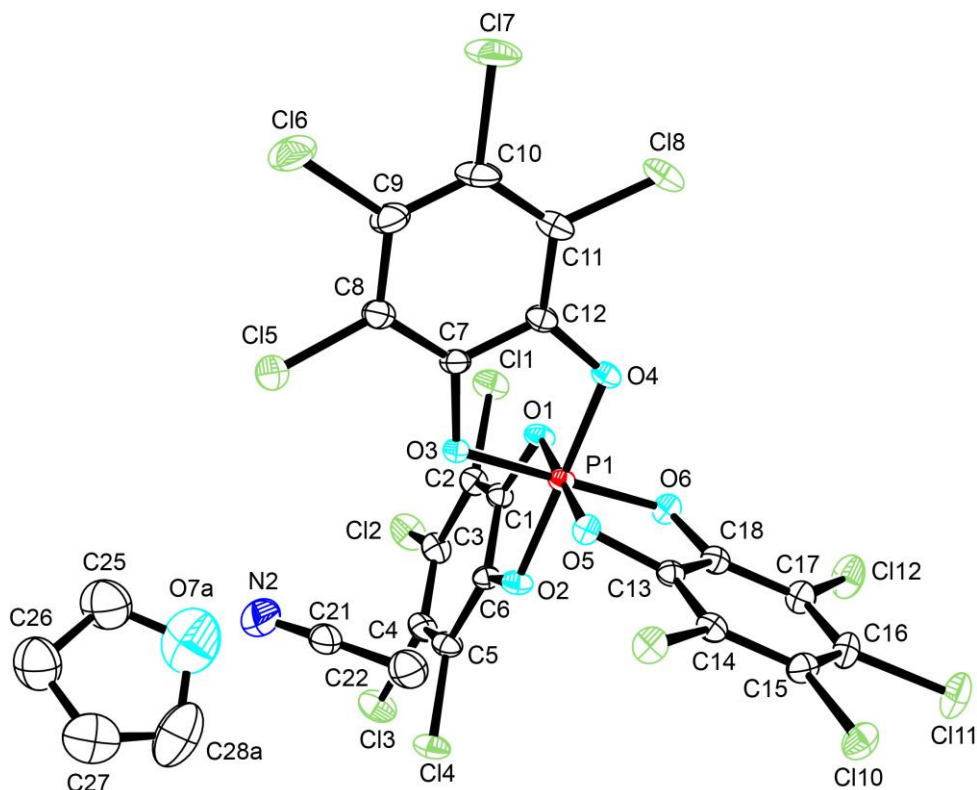


**Figure 2.6. Molecular structure of H(THF)(MeCN)-*rac*-[2.1]·3.35 MeCN·1.52 THF ( $\Delta$  isomer is shown). Ellipsoids are drawn at the 50% probability level. Solvents of crystallization and hydrogen atoms are omitted for clarity. Selected bond lengths [Å]: P(1)–O(1) = 1.714(2); P(1)–O(2) = 1.711(2); P(1)–O(3) = 1.707(2); P(1)–O(4) = 1.707(2); P(1)–O(5) = 1.714(2); P(1)–O(6) = 1.722(2); C(25)–O(8a) = 1.422(18); C(28a)–O(8a) = 1.42(3); O(8a)–N(2) = 3.15(2); C(21)–N(2) = 1.136(7). Selected bond angles [°]: O(1)–P(1)–O(2) = 91.1(10); O(5)–P(1)–O(4) = 92.9(10); O(5)–P(1)–O(6) = 90.7(10).**

The extent of hydrogen bonding within the cation of H(DMF)<sub>2</sub>[2.1] and H(THF)<sub>2</sub>[2.1] may be evaluated by considering the O...O distances. The O...O distance within the [H(DMF)<sub>2</sub>]<sup>+</sup> cation [O...O<sub>avg.</sub> = 2.41(2); range: 2.410(7)–2.431(9)] and the [H(THF)<sub>2</sub>]<sup>+</sup> cation [O(7)...O(8) = 2.394(5) Å] are significantly shorter than the sum of the van der Waals radii [*r*<sub>vdw</sub> = 3.04Å].<sup>306</sup> For comparison, these data are similar to the O...O distances for known compounds containing the [H(DMF)<sub>2</sub>]<sup>+</sup> cation [O...O<sub>avg.</sub> = 2.42(3) Å]<sup>268,296,307-309</sup> or [H(THF)<sub>2</sub>]<sup>+</sup> cation [O...O<sub>avg.</sub> =

2.40(4) Å].<sup>195,298,302,303</sup> The O...N distance within the rare [H(THF)(CH<sub>3</sub>CN)]<sup>+</sup> cation [O(8a)...N(2) = 3.15(2) Å] is significantly longer than the O...N distance found in [H(OEt<sub>2</sub>)(NCMe)]<sup>+</sup> [O(13)...N(1) = 2.536(3) Å], each with the [2.1]<sup>-</sup> anion, and slightly larger than the sum of van der Waals radii for oxygen and nitrogen [*r*<sub>vdw</sub>=3.07 Å].<sup>306</sup>

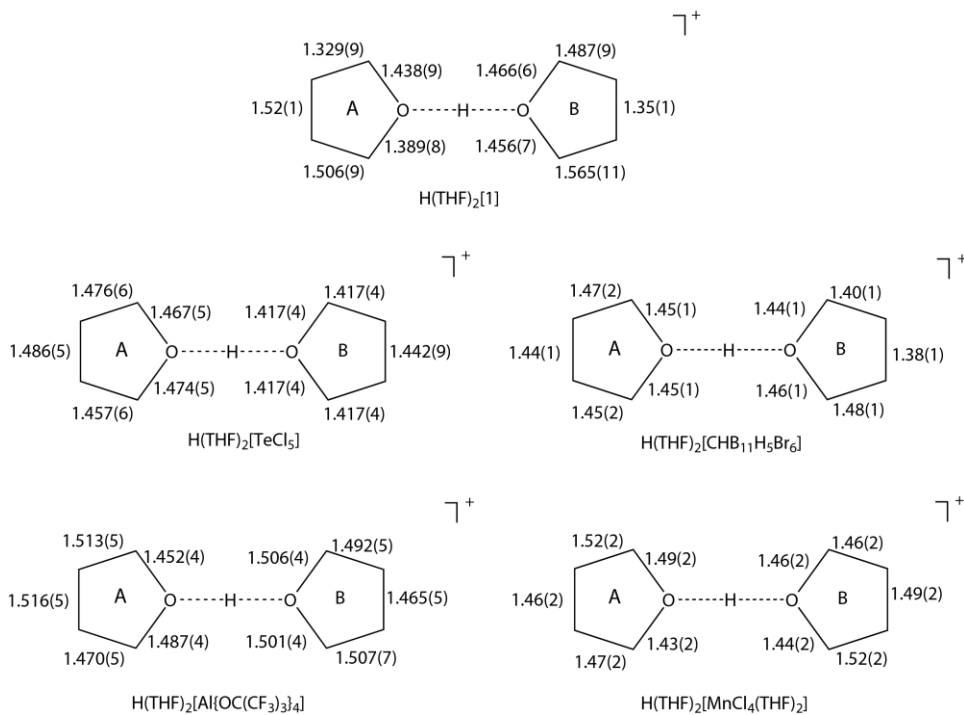


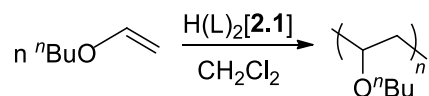
**Figure 2.7. Comparison of C–O and C–C bond length of [H(THF)<sub>2</sub>]<sup>+</sup>**

**in H(THF)<sub>2</sub>[2.1], H(THF)<sub>2</sub>[CHB<sub>11</sub>H<sub>5</sub>Br<sub>6</sub>], H(THF)<sub>2</sub>[Al(OC(CF<sub>3</sub>)<sub>3</sub>)<sub>4</sub>] and H(THF)<sub>2</sub>[MnCl<sub>4</sub>(THF)<sub>2</sub>].**

### 2.2.3 H(DMF)<sub>2</sub>[2.1] and H(THF)<sub>2</sub>[2.1]-initiated Cationic Polymerization

The complexes H(DMF)<sub>2</sub>[2.1] and H(THF)<sub>2</sub>[2.1] were investigated as initiators for the cationic polymerization of *n*-butyl vinyl ether and *p*-methoxystyrene (*p*-MeOSt) in dichloromethane at various temperatures. The results are shown in Tables 2.1 and 2.2 and each data point is representative of between two and eight repeat runs. Each polymerization was

performed utilizing freshly distilled solvent and monomers. *n*-Butyl vinyl ether was successfully polymerized by H(DMF)<sub>2</sub>[**2.1**] and H(THF)<sub>2</sub>[**2.1**] under a variety of temperatures. At ambient temperature, poly(*n*-butyl vinyl ether) was isolated as a brown viscous oil in moderate yield (47%, Table 2.1, entry 1) using H(DMF)<sub>2</sub>[**2.1**] as initiator. Although polymer is obtained in modest yield and reasonable molecular weight ( $M_n = 16,400 \text{ g mol}^{-1}$ ,  $D = 1.46$ ) at ambient temperature, the coloration suggests that terminal conjugated polyene moieties are present. Presumably, these ene functions are formed from proton elimination followed by dealcoholation.<sup>310-313</sup> Chain-transfer processes in cationic polymerizations are suppressed at lower temperatures, therefore resulting in polymers of higher molecular weight.<sup>26,27,314</sup> As the temperature was lowered, the brown color obtained at 18 °C, was not present in polymer prepared at -50 °C using H(DMF)<sub>2</sub>[**2.1**] as initiator.



**Scheme 2.3.** H(L)<sub>2</sub>[**2.1**] (L = DMF, THF) initiated cationic polymerization of *n*-butyl vinyl ether.

The <sup>1</sup>H NMR spectrum of the brown poly(*n*-butyl vinyl ether) produced at 18 °C (Figure 2.8 a) displayed signals in the vinyl region (5.0–6.0 ppm) that were not present in the colorless polymer produced at -50 °C (Figure 2.8 c). Although, H(DMF)<sub>2</sub>[**2.1**] was a competent initiator down to -50 °C, the yields averaged ca. 50% with the molecular weights ( $M_n \approx 10,000\text{--}15,000 \text{ g mol}^{-1}$ ) being much lower than those expected from the monomer-to-initiator ratio [ $M_n$  (calcd) = 45,100 g mol<sup>-1</sup>] (Table 2.1, entry 1–5). In contrast to the H(DMF)<sub>2</sub>[**2.1**] initiator, the more acidic H(THF)<sub>2</sub>[**2.1**] generally afforded higher yields of polymer at all temperatures with higher molecular weights ( $M_n \approx 17,000\text{--}41,000 \text{ g mol}^{-1}$ ) and moderate dispersity being observed. As

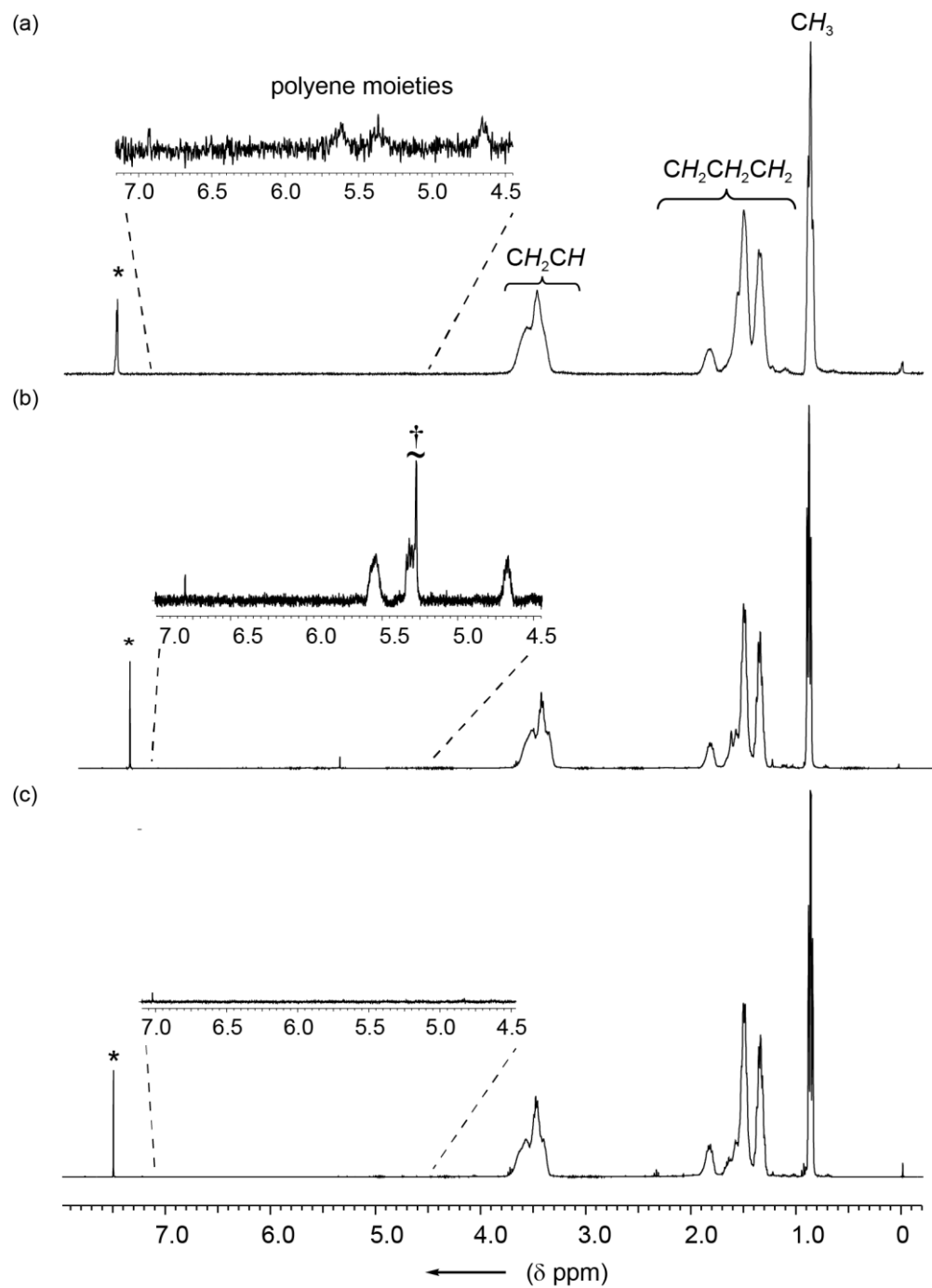
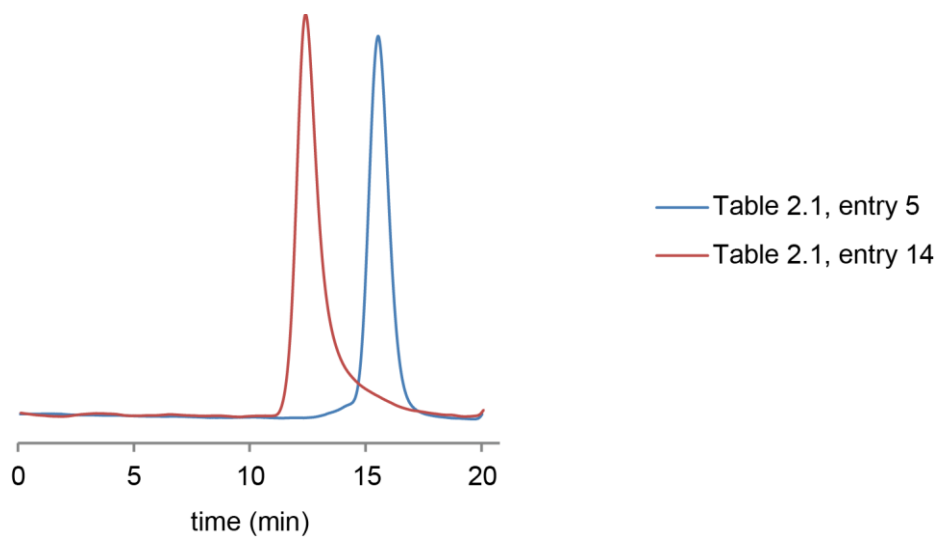


Figure 2.8.  $^1\text{H}$  NMR (400 MHz,  $\text{CDCl}_3$ ,  $25^\circ\text{C}$ ) spectra of poly(*n*-butyl vinyl ether) polymerized using (a)  $\text{H}(\text{DMF})_2[2.1]$  at  $18^\circ\text{C}$ , (b)  $\text{H}(\text{THF})_2[2.1]$  at  $18^\circ\text{C}$  and (c)  $\text{H}(\text{DMF})_2[2.1]$  at  $-50^\circ\text{C}$ .

\* indicates residual  $\text{CH}_2\text{Cl}_2$ . † indicates residual  $\text{CH}_2\text{Cl}_2$  solvent.

the polymerization temperature was lowered to  $-84\text{ }^{\circ}\text{C}$ , a colorless poly(*n*-butyl vinyl ether) was produced. The observed  $M_n$  ( $41,400\text{ g mol}^{-1}$ ) was consistent with the expected  $M_n$  ( $45,100\text{ g mol}^{-1}$ ). The GPC trace (differential refractive index) of the resultant poly(*n*-butyl vinyl ether) polymerized by  $\text{H}(\text{DMF})_2[\mathbf{2.1}]$  at  $-50\text{ }^{\circ}\text{C}$  was narrow and symmetrical (Figure 2.9 for Table 2.1, entry 5), whereas the differential refractive index trace of the resultant poly(*n*-butyl vinyl ether) polymerized using  $\text{H}(\text{THF})_2[\mathbf{2.1}]$  as initiator at  $-84\text{ }^{\circ}\text{C}$  exhibited low molecular weight tailing (Figure 2.9 for Table 2.1, entry 14). In general, the new initiators,  $\text{H}(\text{DMF})_2[\mathbf{2.1}]$  and  $\text{H}(\text{THF})_2[\mathbf{2.1}]$ , performed quite differently than the previously reported  $\text{H}(\text{OEt}_2)_2[\mathbf{2.1}]$ , which showed characteristics of a living system for *n*-butyl vinyl ether.<sup>269</sup>

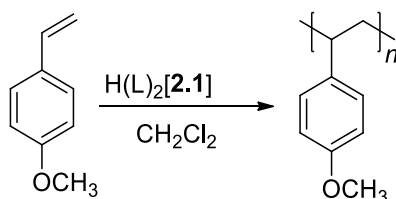


**Figure 2.9. Refractive index traces of poly(*n*-butyl vinyl ether) initiated by  $\text{H}(\text{DMF})_2[\mathbf{2.1}]$  (Table 2.1, entry 5) and  $\text{H}(\text{THF})_2[\mathbf{2.1}]$  (Table 2.1, entry 14).**

**Table 2-1. Cationic polymerization of *n*-butyl vinyl ether using H(DMF)<sub>2</sub>[2.1] and H(THF)<sub>2</sub>[2.1] as initiator.**

| Initiator                 | entry | T (°C) | t (min) | [M]:[I] <sup>a</sup> | Yield (%) | M <sub>n</sub> <sup>b</sup> (g mol <sup>-1</sup> ) | Đ <sup>c</sup>    |
|---------------------------|-------|--------|---------|----------------------|-----------|--|-------------------|
| H(DMF) <sub>2</sub> [2.1] | 1     | 18     | 15      | 450                  | 47        | 16,400   | 1.46              |
|                           | 2     | 0      | 15      | 450                  | 67        | 12,250   | 1.51              |
|                           | 3     | -15    | 15      | 450                  | 59        | 9,300  | 1.33              |
|                           | 4     | -38    | 15      | 450                  | 42        | 13,400   | 1.06              |
|                           | 5     | -50    | 15      | 450                  | 53        | 15,000   | 1.05              |
|                           | 6     | -78    | 15      | 450                  | 0         | n.d. <sup>d</sup>                                  | n.d. <sup>d</sup> |
|                           | 7     | -84    | 15      | 450                  | 0         | n.d. <sup>d</sup>                                  | n.d. <sup>d</sup> |
| H(THF) <sub>2</sub> [2.1] | 8     | 18     | 15      | 450                  | 73        | 17,200   | 1.55              |
|                           | 9     | 0      | 15      | 450                  | 86        | 21,000   | 1.49              |
|                           | 10    | -15    | 15      | 450                  | 79        | 21,000   | 1.60              |
|                           | 11    | -38    | 15      | 450                  | 72        | 21,800   | 1.84              |
|                           | 12    | -50    | 15      | 450                  | 72        | 25,600   | 1.66              |
|                           | 13    | -78    | 15      | 450                  | 82        | 21,000   | 2.07              |
|                           | 14    | -84    | 15      | 450                  | 37        | 41,400   | 1.64              |

The polymerization was carried out in 2 mL CH<sub>2</sub>Cl<sub>2</sub> solvent using 0.011 mmol of Brønsted acid as initiator.<sup>a</sup> [Monomer]/[Initiator] ratio. <sup>b</sup> Absolute molecular weights were determined using laser light scattering gel permeation chromatography (GPC–LLS); differential refractive index ( $dn/dc$ ) of poly(*n*-butyl vinyl ether) ( $dn/dc = 0.068 \text{ mL g}^{-1}$ ) in THF was calculated by assuming 100% mass recovery. <sup>c</sup> Dispersity ( $\text{Đ} = M_w/M_n$ ), where  $M_w$  is the weight–average molar mass and  $M_n$  is the number–average molar mass. <sup>d</sup> Not determined.

**Scheme 2.4. H(L)<sub>2</sub>[2.1] (L = DMF, THF) initiated cationic polymerization of *p*-methoxystyrene.**

*p*-Methoxystyrene was successfully polymerized using either H(DMF)<sub>2</sub>[2.1] or H(THF)<sub>2</sub>[2.1] as the initiator over a range of temperatures (18 °C to -84 °C) with an [M]:[I] ratio of 400:1. Employing these single-component initiators produced high molecular weight poly(*p*-methoxystyrene) in good to high isolated yield (Table 2.2). In general, the polymer obtained

from H(DMF)<sub>2</sub>[**2.1**] initiation gave higher yield but lower molecular weight than that gained for H(THF)<sub>2</sub>[**2.1**]. At ambient temperature, the molecular weight obtained using H(THF)<sub>2</sub>[**2.1**] ( $M_n = 382,000 \text{ g mol}^{-1}$ ) was much higher than that observed using H(DMF)<sub>2</sub>[**2.1**] ( $M_n = 74,900 \text{ g mol}^{-1}$ ) and both were considerably higher than that expected from the monomer-to-initiator ratio [ $M_n \text{ (calcd)} = 40,800 \text{ g mol}^{-1}$ ]. For comparison, the single component initiator [Ph<sub>3</sub>C][SbCl<sub>6</sub>] produces poly(*p*-methoxystyrene) ( $M_n = 92,500 \text{ g mol}^{-1}$ ) when polymerizations are performed in CH<sub>2</sub>Cl<sub>2</sub> solution (T = -15 to + 25 °C).<sup>315</sup> In contrast, a number of binary initiator systems have been reported to give living cationic polymerization [*e.g.* HI/ZnI<sub>2</sub> in toluene at -15 to 25 °C,<sup>54,316</sup> and HI/I<sub>2</sub> and HI/ZnI<sub>2</sub> in the presence of *n*Bu<sub>4</sub>NX (X = Cl, Br, I) in CH<sub>2</sub>Cl<sub>2</sub>].<sup>53,317</sup>

At lower temperatures, high molecular weights (>140,000 g mol<sup>-1</sup>) of poly(*p*-methoxystyrene) were obtained using either H(DMF)<sub>2</sub>[**2.1**] or H(THF)<sub>2</sub>[**2.1**] as initiators (Table 2.2). Although the H(DMF)<sub>2</sub>[**2.1**] initiator presented a decrease in dispersity as the polymerization temperature was lowered, the H(THF)<sub>2</sub>[**2.1**] did not show a significant change in dispersity as a function of polymerization temperature. Quantitative yields were observed for H(DMF)<sub>2</sub>[**2.1**] down to -50 °C. Remarkably, below this temperature, this initiator demonstrated no activity for *p*-MeOSt polymerization. In contrast, the H(THF)<sub>2</sub>[**2.1**] initiator afforded moderate (ca. 50–60%) yields of polymer regardless of temperature. Perhaps most noteworthy are the high molecular weight values observed, which are at the upper limits of the separation capability for our GPC-MALS columns (ca. 500,000 g mol<sup>-1</sup>), so may even be underestimates. Clearly, there is a considerable difference in the molecular weights observed when using H(DMF)<sub>2</sub>[**2.1**] relative to H(THF)<sub>2</sub>[**2.1**], which can only be due to the difference in the nature of

the propagating species in the presence of either DMF or THF. Further studies are needed to gain insight into this interesting observation.

**Table 2-2. Cationic polymerization of *p*-methoxystyrene using H(DMF)<sub>2</sub>[2.1] and H(THF)<sub>2</sub>[2.1] as initiator.**

| Initiator                 | entry | T<br>(°C) | t<br>(min) | [M]:[I] <sup>a</sup> | yield<br>(%) | <i>M</i> <sub>n</sub> <sup>b</sup><br>(g mol <sup>-1</sup> ) | <i>D</i> <sup>c</sup> |
|---------------------------|-------|-----------|------------|----------------------|--------------|--|-----------------------|
| H(DMF) <sub>2</sub> [2.1] | 1     | 18        | 15         | 400                  | 96           | 74,900   | 2.00                  |
|                           | 2     | 0         | 15         | 400                  | 98           | 140,000  | 1.77                  |
|                           | 3     | -15       | 15         | 400                  | 96           | 291,000  | 1.71                  |
|                           | 4     | -38       | 15         | 400                  | 96           | 351,000  | 1.42                  |
|                           | 5     | -50       | 15         | 400                  | 96           | 289,800  | 1.28                  |
|                           | 6     | -78       | 15         | 400                  | 0            | n.d. <sup>d</sup>  | n.d. <sup>d</sup>     |
|                           | 7     | -84       | 15         | 400                  | 0            | n.d. <sup>d</sup>  | n.d. <sup>d</sup>     |
| H(THF) <sub>2</sub> [2.1] | 8     | 18        | 15         | 400                  | 58           | 382,000  | 1.42                  |
|                           | 9     | 0         | 15         | 400                  | 62           | 145,200  | 1.58                  |
|                           | 10    | -15       | 15         | 400                  | 61           | 315,000  | 3.54                  |
|                           | 11    | -38       | 15         | 400                  | 58           | 375,700  | 2.28                  |
|                           | 12    | -50       | 15         | 400                  | 56           | 221,500  | 3.21                  |
|                           | 13    | -78       | 15         | 400                  | 56           | 342,800  | 3.16                  |
|                           | 14    | -84       | 15         | 400                  | 53           | 649,000  | 1.88                  |

The polymerization was carried out in 2 mL CH<sub>2</sub>Cl<sub>2</sub> solvent using 0.011 mmol of Brønsted acid as initiator.<sup>a</sup> [Monomer]/[Initiator] ratio.<sup>b</sup> Absolute molecular weights were determined using laser light scattering gel permeation chromatography (GPC-LLS); differential refractive index (*dn/dc*) of poly(*p*-methoxystyrene) used is 0.174 mL g<sup>-1</sup>.<sup>c</sup> Dispersity (*D* = *M*<sub>w</sub>/*M*<sub>n</sub>), where *M*<sub>w</sub> is the weight-average molar mass and *M*<sub>n</sub> is the number-average molar mass.<sup>d</sup> Not determined.

The cationic polymerization of *p*-MeOS<sub>t</sub> rarely affords polymer in high yield and with a higher molecular weight than that predicted from the [M]:[I] ratio. A single example has been reported with a hexafluoroisopropanol-based initiator (Yield = 95%, *M*<sub>n</sub> = 295,000 g mol<sup>-1</sup>, PDI = 3.82),<sup>318</sup> however, this work has not been elaborated upon. Rare examples also occur with styrene using stannic chloride as initiator at 0 °C (up to 97 %, *M*<sub>w</sub> up to 149,000 g mol<sup>-1</sup>).<sup>42-44,319</sup>

To account for the latter results, the authors postulated several methods of chain transfer that can lead to a branched polymer. Evidence for branching in the present study was gained by comparing the intrinsic viscosity of the sample to that of linear polystyrene. Since an authentic sample of linear poly(*p*-methoxystyrene) was unavailable, we analyzed the H(THF)<sub>2</sub>[**2.1**]-initiated *p*-MeOSt polymer against a linear polystyrene standard. For samples with identical molecular weight ( $M_w = 10^6 \text{ g mol}^{-1}$ ), a significantly lower intrinsic viscosity was observed for the *p*-methoxystyrene when compared to linear polystyrene ( $[\eta]_w = 136 \text{ mL g}^{-1}$  vs.  $250 \text{ mL g}^{-1}$ ), which is consistent with a branched polymer. The hydrodynamic radius ( $R_h$ ) determined from dynamic light scattering was significantly lower for the *p*-methoxystyrene sample when compared to linear polystyrene [ $(R_h)_z = 25 \text{ nm}$  vs  $34 \text{ nm}$ ], again suggesting a branched polymer. The final evidence for a branched polymer was obtained from the <sup>1</sup>H NMR spectrum of the poly(*p*-methoxystyrene) samples. Figure 2.10 shows a representative spectrum (Table 2.2, entry 1). Importantly, small signals were obtained in the range of 4.0 – 6.4 ppm that have previously been attributed to vinylic protons that result from branching caused by Friedel-Crafts alkylation/arylation and hydride transfer reactions during living cationic polymerization.<sup>320,321</sup> A recent study has accounted for branched structures in methoxystyrene polymers by invoking a simultaneous chain- and step-growth mechanism.<sup>322</sup>

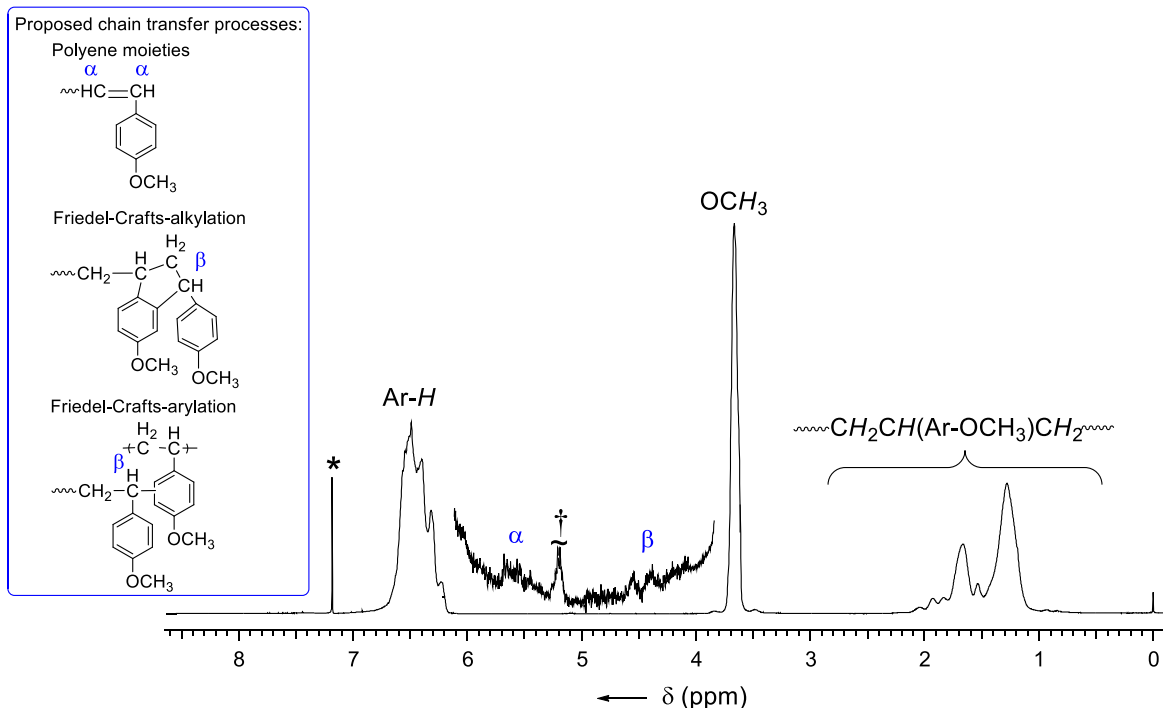


**Figure 2.10.** <sup>1</sup>H NMR (400 MHz, CDCl<sub>3</sub>, 25 °C) spectrum of poly(*p*-methoxystyrene) prepared using H(DMF)<sub>2</sub>[**2.1**] at 18 °C.

\* indicates residual CHDCl<sub>2</sub>. † indicates residual CH<sub>2</sub>Cl<sub>2</sub> solvent.

### 2.3 Summary

We have synthesized and fully characterized three new Brønsted acids containing the weakly coordinating phosphorus(V)-based [TRISPHAT]<sup>−</sup> anion. H(DMF)<sub>2</sub>[**2.1**], H(THF)<sub>2</sub>[**2.1**] and H(THF)(CH<sub>3</sub>CN)[**2.1**] are isolable and weighable proton sources. H(DMF)<sub>2</sub>[**2.1**] and H(THF)<sub>2</sub>[**2.1**] have proven to be good single-component initiators for the cationic polymerization of *n*-butyl vinyl ether and *p*-methoxystyrene. The polymerization of the olefin monomers was investigated at a variety of temperatures ranging from ambient to low temperatures keeping the monomer/initiator ratio constant. Remarkably, H(THF)<sub>2</sub>[**2.1**] afforded high molecular weight poly(*p*-methoxystyrene) with  $M_n$  up to 649,000 g mol<sup>−1</sup> in good isolated yield. This unique

combination of high molecular weight and high yield is unusual for cationic polymerization and we postulate it arises from branching of the poly(*p*-methoxystyrene) through either Friedel-Crafts alkylation/arylation or hydride transfer.

## 2.4 Experimental

### 2.4.1 General Procedures

All experiments were performed using standard Schlenk or glove box techniques under nitrogen atmosphere. CH<sub>2</sub>Cl<sub>2</sub> (Sigma Aldrich) and Et<sub>2</sub>O (Fisher Scientific) were deoxygenated with nitrogen and dried by passing the solvent through a column containing activated, basic alumina. Subsequently, the CH<sub>2</sub>Cl<sub>2</sub> and Et<sub>2</sub>O were dried over CaH<sub>2</sub>, freshly distilled, and freeze-pump-thaw (x3) degassed. Acetonitrile (Sigma Aldrich), dimethylformamide (DMF) (Fisher Scientific), *p*-methoxystyrene (TCI America) and *n*-butyl vinyl ether (Sigma Aldrich) were dried over calcium hydride, distilled and freeze-pump-thaw (x3) degassed prior to use. CH<sub>2</sub>Cl<sub>2</sub>, Et<sub>2</sub>O, acetonitrile, and DMF were stored over 3 Å molecular sieves. Tetrahydrofuran (THF) (Fisher Scientific) was dried and distilled over sodium/benzophenone ketyl immediately prior to use. Phosphorus pentachloride (Aldrich) was sublimed prior to use. Tetrachlorocatechol<sup>323</sup> was prepared following literature procedure, azeotropically distilled and recrystallized from hot toluene prior to use.

Elemental analyses, mass spectrometry and NMR spectra were performed in the Department of Chemistry Facilities. <sup>1</sup>H, <sup>13</sup>C{<sup>1</sup>H} and <sup>31</sup>P{<sup>1</sup>H} NMR spectra were recorded on Bruker Avance 300 or 400 MHz spectrometers at room temperature unless noted. H<sub>3</sub>PO<sub>4</sub> (85 %) was used as external standard for <sup>31</sup>P NMR spectra with  $\delta = 0.0$ . <sup>1</sup>H NMR and <sup>13</sup>C{<sup>1</sup>H} NMR spectra were referenced to deuterated solvents. 1D and 2D <sup>1</sup>H-<sup>1</sup>H NOESY and ROESY NMR

spectra were recorded on Bruker Avance 400 MHz spectrometer at  $-85\text{ }^{\circ}\text{C}$ . 2D NOESY spectra of complex  $\text{H}(\text{THF})_2[\mathbf{2.1}]$  were recorded by using a mixing time of 0.59 s. T1 measurements were conducted according to Bruker T1 measurement guide as a series of 1D experiments (pulse program t1ir1d) by varying d7 (inversion recovery delay). D1 (relaxation delay) was chosen to be at least 7 times longer than T1. T1 was calculated according to the formula  $T1=d7/\ln 2$  with d7 (inversion recovery delay) at which magnetization goes through null. The 2D ROESY spectra of  $\text{H}(\text{DMF})_2[\mathbf{2.1}]$  and  $\text{H}(\text{THF})_2[\mathbf{2.1}]$  (see Appendix A, Figures A6 and A7) were acquired using standard Bruker pulse program roesyetgp.2 with a continuous spin-lock during mixing (200 ms), a relaxation delay of 1.5 s and 16 scans/FID. For  $\text{H}(\text{DMF})_2[\mathbf{2.1}]$  2D ROESY spectrum was obtained with 128 increments (9.19 kHz spectral width) and for  $\text{H}(\text{THF})_2[\mathbf{2.1}]$  with 154 increments (8 kHz spectral width).

Molecular weights were determined by triple detection gel permeation chromatography (GPC-LLS) utilizing an Agilent 1260 Series standard auto sampler, an Agilent 1260 series isocratic pump, Phenomenex Phenogel 5  $\mu\text{m}$  narrowbore columns (4.6 x 300 mm)  $10^4\text{ \AA}$  (5000-500,000),  $500\text{ \AA}$  (1,000-15,000), and  $10^3\text{ \AA}$  (1,000-75,000), Wyatt Optilab rEx differential refractometer ( $\lambda = 658\text{ nm}$ ,  $25\text{ }^{\circ}\text{C}$ ), as well as a Wyatt Tristar miniDAWN (laser light scattering detector:  $\lambda = 690\text{ nm}$ ) and a Wyatt ViscoStar viscometer. Samples were dissolved in THF (ca. 2  $\text{mg mL}^{-1}$ ) and a flow rate of  $0.5\text{ mL min}^{-1}$  was applied. The differential refractive index ( $dn/dc$ ) of poly(*n*-butyl vinyl ether) ( $dn/dc = 0.068\text{ mL g}^{-1}$ ) in THF was calculated by using Wyatt ASTRA software 6.1 assuming 100 % mass recovery. The differential refractive index ( $dn/dc$ ) of poly(*p*-methoxystyrene) ( $dn/dc = 0.174\text{ mL g}^{-1}$ )<sup>324</sup> has been reported. The hydrodynamic radius  $R_h$  was measured using a DynaPro-99-E50 dynamic light scattering module with a GaAs laser

(658 nm) at 25 °C with a temperature-controlled microsampler (MSXTC 12). The sample concentration was the same as that of the GPC samples in THF (1mg/1 mL).

#### 2.4.2 Synthesis of H(DMF)<sub>2</sub>[2.1]

PCl<sub>5</sub> (0.11 g, 5.30 mmol) and tetrachlorocatechol (0.36 g, 15.8 mmol) were stirred in CH<sub>2</sub>Cl<sub>2</sub> (6 mL). The dark green suspension was slowly heated to reflux. After 2 h a colorless precipitate formed and was cooled to ambient temperature. Upon addition of DMF (1.5 mL) a clear solution was obtained. The solution was cooled in an ice bath to afford a white precipitate. The solid was collected by filtration and dried *in vacuo*. A concentrated solution of the crude product in CH<sub>2</sub>Cl<sub>2</sub> afforded colorless crystals (ambient temperature, ca. 7 d). A crystal was removed for X-ray crystallographic analysis without drying. Yield = 0.27 g, 56%. <sup>31</sup>P{<sup>1</sup>H} NMR (162 MHz, CD<sub>3</sub>CN, 25 °C): δ = -81.76; <sup>1</sup>H NMR (400 MHz, CD<sub>2</sub>Cl<sub>2</sub>, 25 °C): δ = 16.66 (s, 1H, H(DMF)<sub>2</sub>), 8.16 (s, 2H, O=CH), 3.23 (s, 6H, NCH<sub>3</sub>), 3.03 (s, 6H, NCH<sub>3</sub>); <sup>1</sup>H NMR (400 MHz, CD<sub>2</sub>Cl<sub>2</sub>, -85 °C): δ = 19.24 (s, 1H, H(DMF)<sub>2</sub>), 8.09 (s, 2H, O=CH), 3.17 (s, 6H, NCH<sub>3</sub>), 2.95 (s, 6H, NCH<sub>3</sub>); <sup>13</sup>C{<sup>1</sup>H} NMR (101 MHz, CD<sub>2</sub>Cl<sub>2</sub>, 25 °C): δ = 164.3 (s, O=CH), 141.6 (d, J<sub>CP</sub> = 6.6 Hz, Ar-C), 122.8 (s, Ar-C), 113.8 (d, J<sub>CP</sub> = 20 Hz, Ar-C), 39.2 (s, NCH<sub>3</sub>), 33.5 (s, NCH<sub>3</sub>); elem. anal. calcd for C<sub>24</sub>H<sub>15</sub>Cl<sub>12</sub>N<sub>2</sub>O<sub>8</sub>P: C, 31.48; H, 1.65; N, 3.06; found: C, 31.68; H, 1.83; N, 3.26. LRMS (ESI, negative mode) *m/z* = 768.5 ([M]<sup>-</sup>).

#### 2.4.3 Synthesis of H(THF)<sub>2</sub>[2.1]

PCl<sub>5</sub> (0.06 g, 3.20 mmol) and tetrachlorocatechol (0.25 g, 10.1 mmol) were stirred in CH<sub>2</sub>Cl<sub>2</sub> (4 mL). The dark blue suspension was slowly heated to reflux. After 2 h a colorless precipitate formed and was cooled to ambient temperature. Upon addition of THF (1.4 mL) a clear solution

was obtained. The solution was cooled at 0 °C to afford a white precipitate. The solid was collected by filtration, washed with CH<sub>2</sub>Cl<sub>2</sub> (4 mL) and dried *in vacuo*. A concentrated solution of the crude product in CH<sub>2</sub>Cl<sub>2</sub>:THF (6:1) afforded colorless crystals (−30 °C, ca. 3 d). A single crystal was removed for X-ray crystallographic analysis without drying. Yield = 0.13 g, 44%. <sup>31</sup>P{<sup>1</sup>H} NMR (162 MHz, CD<sub>3</sub>CN, 25 °C): δ = −80.6; <sup>1</sup>H NMR (400 MHz, CD<sub>3</sub>CN, 25 °C): δ = 13.42 (s, 1H, *H*(THF)<sub>2</sub>), 4.08 (s, 8H, OCH<sub>2</sub>), 2.04 (s, 8H, CH<sub>2</sub>); <sup>1</sup>H NMR (400 MHz, CD<sub>2</sub>Cl<sub>2</sub>, −85 °C): δ = 16.92 (s, 1H, *H*(THF)<sub>2</sub>), 4.17 (s, 8H, OCH<sub>2</sub>), 2.13 (s, 8H, CH<sub>2</sub>); <sup>13</sup>C{<sup>1</sup>H} NMR (101 MHz, CD<sub>3</sub>CN, 25 °C): δ = 141.6 (d, *J*<sub>CP</sub> = 6.6 Hz, Ar–C), 122.7 (s, Ar–C), 113.8 (d, *J*<sub>CP</sub> = 19 Hz, Ar–C), 70.9 (s, CH<sub>2</sub>O), 25.0 (s, CH<sub>2</sub>); elem. anal. calcd for C<sub>26</sub>H<sub>17</sub>Cl<sub>12</sub>O<sub>8</sub>P: C, 34.17; H, 1.88; found: C, 34.31; H, 2.02; LRMS (ESI, negative mode) *m/z* = 768.5 ([M]<sup>−</sup>).

#### 2.4.4 Synthesis of (CH<sub>3</sub>CN)(THF)[2.1]

H(THF)<sub>2</sub>[2.1] (0.036 g) was dissolved in CD<sub>3</sub>CN (0.5 mL) in an NMR tube. Within 7 days colorless crystals were obtained upon standing at ambient temperature. A crystal was removed for X-ray crystallographic analysis. <sup>31</sup>P{<sup>1</sup>H} NMR (162 MHz, CD<sub>3</sub>CN, 25 °C): δ = −80.1.

#### 2.4.5 Representative H(DMF)<sub>2</sub>[2.1]-initiated Polymerization of *n*-Butyl Vinyl

##### Ether

In a glovebox, freshly distilled, degassed CH<sub>2</sub>Cl<sub>2</sub> (2 mL) was added to H(DMF)<sub>2</sub>[2.1] (0.010 g, 0.011 mmol) in a 10 mL Schlenk flask. The flask was removed from the glovebox and cooled to 0 °C. Freshly distilled, *n*-butyl vinyl ether (0.49 g, 4.92 mmol) was prepared in a syringe, removed from the glovebox and added rapidly to the initiator solution. After 15 min, the

polymerization was quenched with a solution of NH<sub>4</sub>OH in MeOH (0.2 mL, 10 vol%), and all volatiles were removed *in vacuo*. The crude product was dissolved in CH<sub>2</sub>Cl<sub>2</sub> (2 mL) and added one drop at a time to stirred MeOH (40 mL) to precipitate a yellow oily residue. The polymer was collected by centrifugation and dried *in vacuo*. Yield = 0.32 g, 65%.

<sup>1</sup>H NMR spectroscopy (300 MHz, CDCl<sub>3</sub>, 25 °C): δ = 3.51-3.40 (br, CH<sub>2</sub>CH), 1.84-1.36 (br, CH<sub>2</sub>CH<sub>2</sub>CH<sub>2</sub>), 0.91 (t, CH<sub>3</sub>); GPC-LLS (THF):  $M_n = 12,250 \text{ g mol}^{-1}$ ,  $D = 1.51$ .

#### 2.4.6 Representative H(DMF)<sub>2</sub>[2.1]-initiated Polymerization of *p*-Methoxystyrene

In a glovebox, freshly distilled, degassed CH<sub>2</sub>Cl<sub>2</sub> (2 mL) was added to H(DMF)<sub>2</sub>[2.1] (0.010 g, 0.011 mmol) in a 10 mL Schlenk flask. The flask was removed from the glovebox and cooled to 0 °C. Freshly distilled, *p*-methoxystyrene (0.59 g, 4.37 mmol) was prepared in a syringe, removed from the glovebox and added rapidly to the initiator solution. After 15 min, the polymerization was quenched with a solution of NH<sub>4</sub>OH in MeOH (0.2 mL, 10 vol%) and all volatiles were removed *in vacuo*. The crude product was dissolved in CH<sub>2</sub>Cl<sub>2</sub> (2 mL) and added one drop at a time to stirred MeOH (40 mL) to precipitate a white solid. The polymer was collected by filtration and dried *in vacuo*. Yield = 0.57 g, 98%.

<sup>1</sup>H NMR spectroscopy (400 MHz, CDCl<sub>3</sub>, 25 °C): δ = 6.59-6.32 (br, Ar-H), 3.76 (br, OCH<sub>3</sub>), 2.02-1.37 (br, CH<sub>2</sub>CH(Ar-OCH<sub>3</sub>)CH<sub>2</sub>) and GPC-LLS (THF):  $M_n = 140,000 \text{ g mol}^{-1}$ ,  $D = 1.77$ .

#### 2.4.7 X-ray Structure Determination

X-ray crystallography data were collected on a Bruker X8 APEX II diffractometer with graphite-monochromated Mo K $\alpha$  radiation. A single crystal was immersed in oil and mounted on a glass fiber. Data were collected and integrated using the Bruker SAINT<sup>325</sup> software package

and corrected for absorption effect using SADABS.<sup>326</sup> All structures were solved by direct methods and subsequent Fourier difference techniques. The PLATON/SQUEEZE<sup>327</sup> program was used for H(THF)(NCMe)[**2.1**] to generate a data set free of solvent in the regions with disordered solvent. Unless noted, all non-hydrogen atoms were refined anisotropically, whereas all hydrogen atoms were included in calculated positions but not refined. All data sets were corrected for Lorentz and polarization effects. All refinements were performed using the SHELXL-2014<sup>328</sup> via the Olex2 interface.<sup>329</sup>

H(THF)<sub>2</sub>[**2.1**] co-crystallizes with one free tetrachlorocatechol molecule and one THF solvate molecule. H(1) is bound by two molecules of THF and was located using the difference map and refined isotropically. H(THF)(NCMe)[**2.1**] crystallizes with both CH<sub>3</sub>CN and THF in the lattice. CH<sub>3</sub>CN occupies four sites, two fully occupied and two partially occupied while THF occupies two sites, each only partially occupied. Restraints and constraints were employed to maintain reasonable bond lengths and angles as well as reasonable ADPs, in the case of disordered solvents. In the case of the THF molecule containing O8, the molecule resides on an inversion center. Its occupancy, as well as that of the adjacent disordered CH<sub>3</sub>CN molecules were refined such that the sum of their occupancies was 1. H(DMF)<sub>2</sub>[**2.1**] crystallizes with five crystallographically independent complexes per asymmetric unit and one CH<sub>2</sub>Cl<sub>2</sub> solvate molecule. A hydrogen atom is located between two adjacent oxygens in the DMF molecule; however the hydrogen atom could not be located or accurately modelled. Crystal data and refinement parameters are listed in Table 2.3. CIF files containing supplementary crystallographic data for the structures reported in this chapter are available from The Cambridge Crystallographic Data Centre (CCDC 1520146–1520148).

**Table 2-3. X-ray crystallographic data and refinement details for compounds H(DMF)<sub>2</sub>[2.1], H(THF)<sub>2</sub>[2.1] and H(THF)(CH<sub>3</sub>CN)[2.1].**

|   | 5 {H(DMF) <sub>2</sub> [2.1]} ·<br>0.2 CH <sub>2</sub> Cl <sub>2</sub>                           | H(THF) <sub>2</sub> [2.1] · THF<br>C <sub>6</sub> H <sub>2</sub> O <sub>2</sub> Cl <sub>4</sub> | H(THF)(CH <sub>3</sub> CN)[2.1] ·<br>3.35 MeCN · 1.52 THF.                                  |
|---|--|---|---|
| formula                                   | C <sub>121</sub> H <sub>77</sub> Cl <sub>62</sub> N <sub>10</sub> O <sub>40</sub> P <sub>5</sub> | C <sub>36</sub> H <sub>27</sub> Cl <sub>16</sub> O <sub>11</sub> P                              | C <sub>29.3</sub> H <sub>19.23</sub> Cl <sub>12</sub> N <sub>3.35</sub> O <sub>7.14</sub> P |
| Fw  | 4658.64  | 1233.74   | 988.96  |
| Cryst. syst.                              | monoclinic   | triclinic   | Triclinic   |
| space group                               | Cc   | P-1   | P-1   |
| a (Å)                                     | 40.2932(19)  | 11.5738(12)   | 11.823(3)   |
| b (Å)                                     | 26.2969(12)  | 12.1413(13)   | 12.984(3)   |
| c (Å)                                     | 16.7720(8)   | 17.4244(18)   | 14.193(3)   |
| α (deg)                                   | 90(2)  | 96.359(6)   | 66.919(5)   |
| β (deg)                                   | 104.450(2)   | 100.305(5)  | 83.382(6)   |
| γ (deg)                                   | 90(2)  | 106.108(5)  | 84.392(5)   |
| V (Å <sup>3</sup> )                       | 17209.2(14)  | 2280.9(4)   | 1987.8(7)   |
| T (K)                                     | 100(2)   | 100(2)  | 90(2)   |
| Z   | 20   | 2   | 2   |
| μ (MoKα) (mm <sup>-1</sup> )              | 1.093  | 1.056   | 0.925   |
| crystal size (mm <sup>3</sup> )           | 0.46×0.27×0.11   | 0.2×0.13×0.05   | 0.25×0.15×0.14  |
| ρ <sub>calcd.</sub> (g cm <sup>-3</sup> ) | 1.800  | 1.796   | 1.652   |
| 2θ(max) (°)                               | 55.9   | 46.5  | 60.31   |
| F(000)                                    | 9288.0   | 1236.0  | 989.0   |
| No. of total reflns.                      | 132635   | 20385   | 40254   |
| No. of unique reflns.                     | 40536  | 6470  | 11707   |
| R(int)                                    | 0.0570   | 0.0371  | 0.0337  |
| Refln./param. Ratio                       | 18.73  | 9.98  | 20.87   |
| R <sub>1</sub> [I > 2σ(I)] <sup>a</sup>   | 0.0539   | 0.0449  | 0.0546  |
| wR <sub>2</sub> [all data] <sup>b</sup>   | 0.1339   | 0.1032  | 0.1460  |
| GOF                                       | 1.050  | 1.020   | 1.041   |

<sup>a</sup>  $R_1 = \frac{\sum ||F_o| - |F_c||}{\sum |F_o|}$ . <sup>b</sup>  $wR_2(F^2[\text{all data}]) = \left\{ \frac{\sum [w(F_o^2 - F_c^2)^2]}{\sum [w(F_o^2)^2]} \right\}^{1/2}$ .

## Chapter 3: A Twist on Hellwinkel's Salt, $[\text{P}(\text{2,2}'\text{-biphenyl})_2]^+[\text{P}(\text{2,2}'\text{-biphenyl})_3]^-$ \*

### 3.1 Introduction

The development of WCAs is of particular interest as it plays a critical role in the generation and stabilization of highly reactive cations.<sup>68,69,84,147,151,187,330</sup> Many of the major advances in this area have involved the elaboration of classical group 13-element-based anions such as  $[\text{BF}_4]^-$  and  $[\text{AlCl}_4]^-$ . Particularly noteworthy are the fluorinated anions  $[\text{A}]^-$ ,<sup>64,98,121,128,266,331-337</sup>  $[\text{B}]^-$ ,<sup>119,281,338-347</sup> and  $[\text{C}]^-$ <sup>60,61,65,147,167,348,349</sup> illustrated in Figure 3.1. These anions are large and charge-delocalized and possess low nucleophilicity with electron withdrawing groups, which are ideal properties for WCAs. Each of these WCAs has been isolated as Brønsted acids and must be stored at low temperatures.

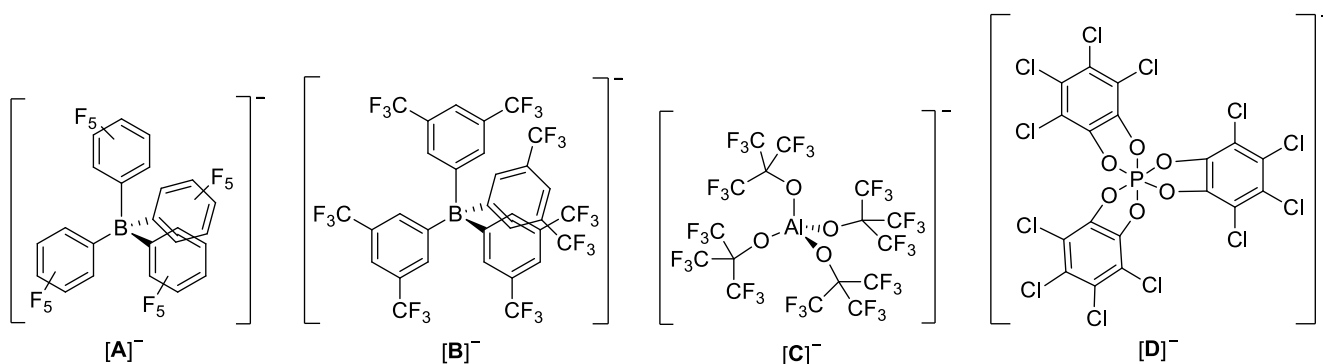
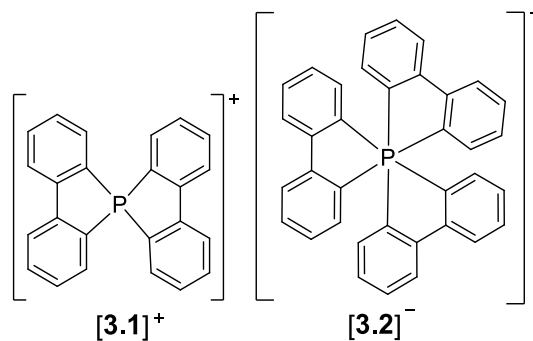


Figure 3.1. Selected examples of boron(III)-, aluminum(III)- and phosphorus(V)-containing WCAs.

We were inspired by the evolution of  $[\text{BF}_4]^-$  and  $[\text{AlCl}_4]^-$  to more complex and less donating anions (e.g.  $[\text{A}]^-$ – $[\text{C}]^-$ ). Less common are WCAs of group 15 elements. As a result, we have been exploring the WCA properties of larger derivatives of the classical WCA,  $[\text{PF}_6]^-$ . In particular, the WCA properties of the fascinating tris(tetrachlorobenzenediolato)phosphate (Figure 3.1,  $[\text{D}]^-$ ) are of

\* This chapter has previously been published: Hazin, K.; Gates, D.P. *Can. J. Chem.* **2018**, *96*, 526. 60

interest.<sup>350</sup> Hexacoordinate phosphorus(V) anions, such as  $[\mathbf{D}]^-$  and its derivatives, are large and charge delocalized. The ability of  $[\mathbf{D}]^-$  to stabilize highly reactive cations has been described in Chapter 2 and has led to the synthesis of Brønsted acids  $\text{HL}_2[\mathbf{D}]$  ( $\text{L} = \text{Et}_2\text{O}$ , THF,  $\text{CH}_3\text{CN}$ , DMF) that can be isolated as solids and used as initiators for the cationic polymerization of olefins.<sup>269,351</sup> These systems compare to the established Brønsted acid  $\text{H}(\text{OEt}_2)_2[\mathbf{A}]$  and initiator system  $\text{H}(\text{OEt}_2)_2[\mathbf{C}]$ . Attractive features of  $\text{HL}_2[\mathbf{D}]$  include: its ease of synthesis [prepared by the direct reaction of  $\text{PCl}_5$  and  $\text{C}_6\text{Cl}_4(\text{OH})_2$ ], its moderate stability at ambient temperature, and its ability to initiate polymerization at higher temperatures than are required of typical cationic initiators.<sup>246</sup> A potential concern with using  $[\mathbf{D}]^-$  in cationic polymerization applications is the lability of the P–O bonds and the donor properties of the oxygen atoms within the anion.



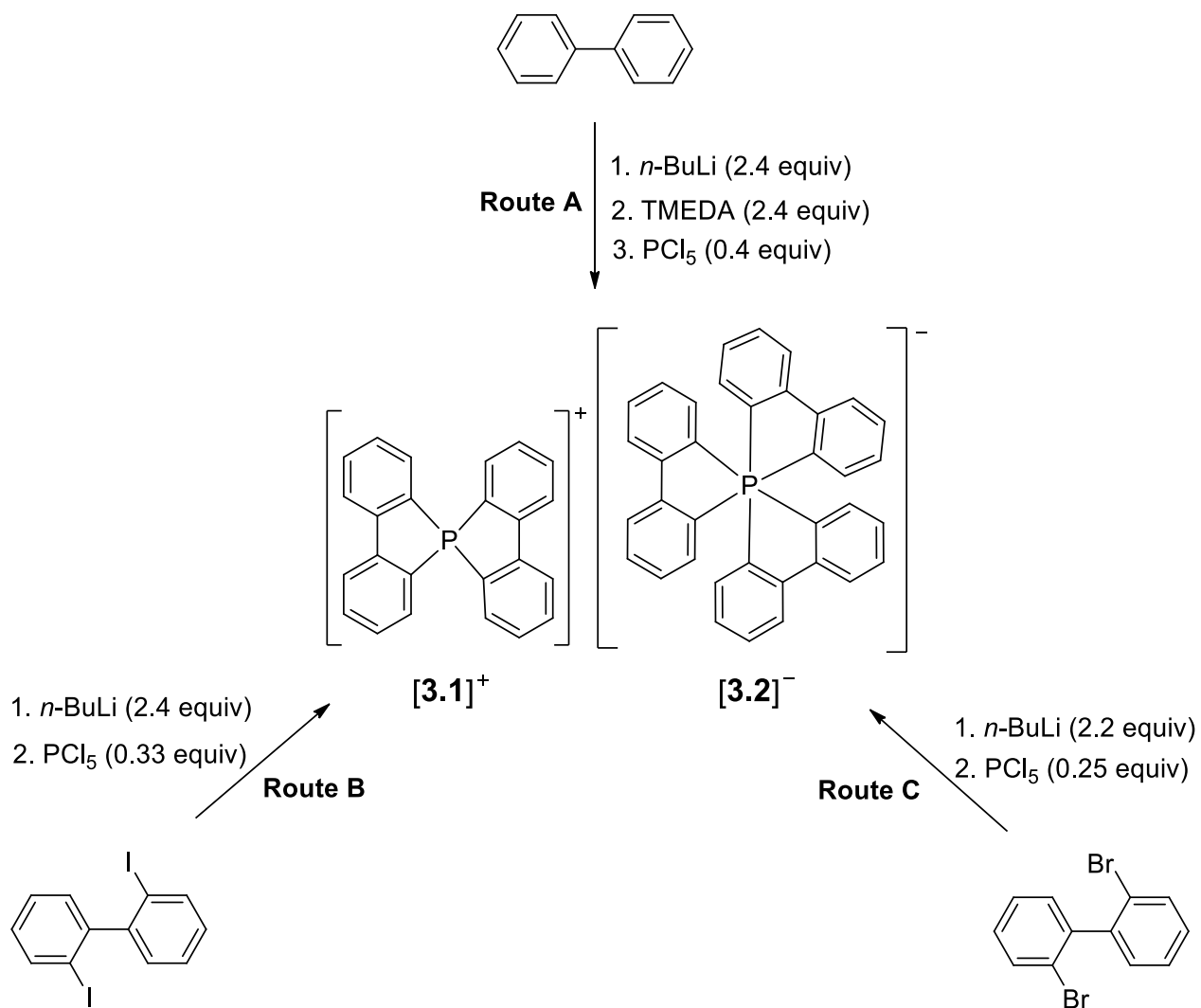
**Figure 3.2. Hellwinkel's spiro-compound [3.1][3.2].**

In order to eliminate these concerns, we sought anions featuring P–C rather than P–O bonds, analogues of the tetraarylborates. The salt  $[\mathbf{3.1}][\mathbf{3.2}]$  (Figure 3.2) featuring the P–C-containing anion  $[\mathbf{3.2}]^-$  was appealing. This compound, along with  $\text{Li}[\mathbf{3.2}]$ , was first reported in 1965 and was resolved into optically active enantiomers.<sup>253,254,352</sup> Derivatives of  $[\mathbf{3.2}]^-$  with a 4-methyl-biphenyl chelate have also been synthesized.<sup>255</sup> An ammonium salt,  $[\text{PhNMe}_2\text{H}][\text{P}(\text{C}_{12}\text{F}_8)_3]$ , has been claimed as a protic activator for metallocene catalysts for ethylene polymerization.<sup>353</sup> It should be noted that limited

synthetic and characterization details for this compound were provided. Therefore, we set out to explore the synthesis of parent **[3.1][3.2]** with the ultimate goal of accessing new Brønsted acids for the cationic polymerization of olefin monomers. Herein, the efforts to synthesize and isolate Hellwinkel's salt **[3.1][3.2]** and the unexpected discovery of the byproducts **[3.1']****[3.2]** and **3.3** are reported. Both **[3.1']****[3.2]** and **3.3** were structurally characterized by X-ray crystallography.

## 3.2 Results and Discussion

It has been shown previously that the direct metallation of biphenyl with *n*-BuLi in the presence of *N,N,N',N'*-tetramethylethylenediamine (TMEDA) leads to 2,2'-dilithiobiphenyl.<sup>354,355</sup> In order to prepare Hellwinkel's salt, biphenyl was directly lithiated with *n*-BuLi (2.4 equiv) in TMEDA (2.4 equiv) at ambient temperature (Scheme 3.1, Route A). In the present work, the dilithiation was confirmed by slowly quenching a small aliquot removed from the reaction mixture with Me<sub>3</sub>SiCl [<sup>1</sup>H NMR (THF-*d*<sub>8</sub>: δ = 0.43, 6H, Si(CH<sub>3</sub>)<sub>3</sub>; 7.24–7.89, 8H, Ar-H)]. Subsequently, a solution of PCl<sub>5</sub> in THF/Et<sub>2</sub>O (40 mL/ 6 mL) was slowly added to 2,2'-dilithiobiphenyl to afford Hellwinkel's salt **[3.1][3.2]** as the major product as estimated by <sup>31</sup>P{<sup>1</sup>H} NMR spectroscopy [Figure 3.3 (a): δ = 25.8 **[3.1]**<sup>+</sup> and –184.7 ppm **[3.2]**<sup>–</sup>]. Surprisingly, the <sup>31</sup>P{<sup>1</sup>H} NMR spectrum of the reaction mixture suggested that at least two additional products were present as evidenced by the presence of a singlet resonance at 30.6 ppm and another singlet resonance at –86.2 ppm.



**Scheme 3.1.** Synthesis of [3.1][3.2] via route A–C.

Attempts to isolate [3.1][3.2] from the aforementioned mixture were unsuccessful given the poor solubility of the products in typical organic solvents (*e.g.* CHCl<sub>3</sub>, CH<sub>2</sub>Cl<sub>2</sub>, Et<sub>2</sub>O, THF, acetone, toluene). Analysis of the crude material by electrospray mass spectrometry (ESI-MS, see Appendix B, Figures B1 and B2) was particularly informative. In the negative mode, a single ion was observed that was assigned to [3.2]<sup>−</sup> (*m/z* = 487.1). Unexpectedly, analysis in the positive mode revealed two ions, one of which was assigned to [3.1]<sup>+</sup> of Hellwinkel's salt (*m/z* = 335.2). The other cation (*m/z* = 487.2) had the same mass as the anion [3.2]<sup>−</sup>, suggesting that this cation had the formulation [P(C<sub>12</sub>H<sub>8</sub>)<sub>3</sub>]<sup>+</sup>.

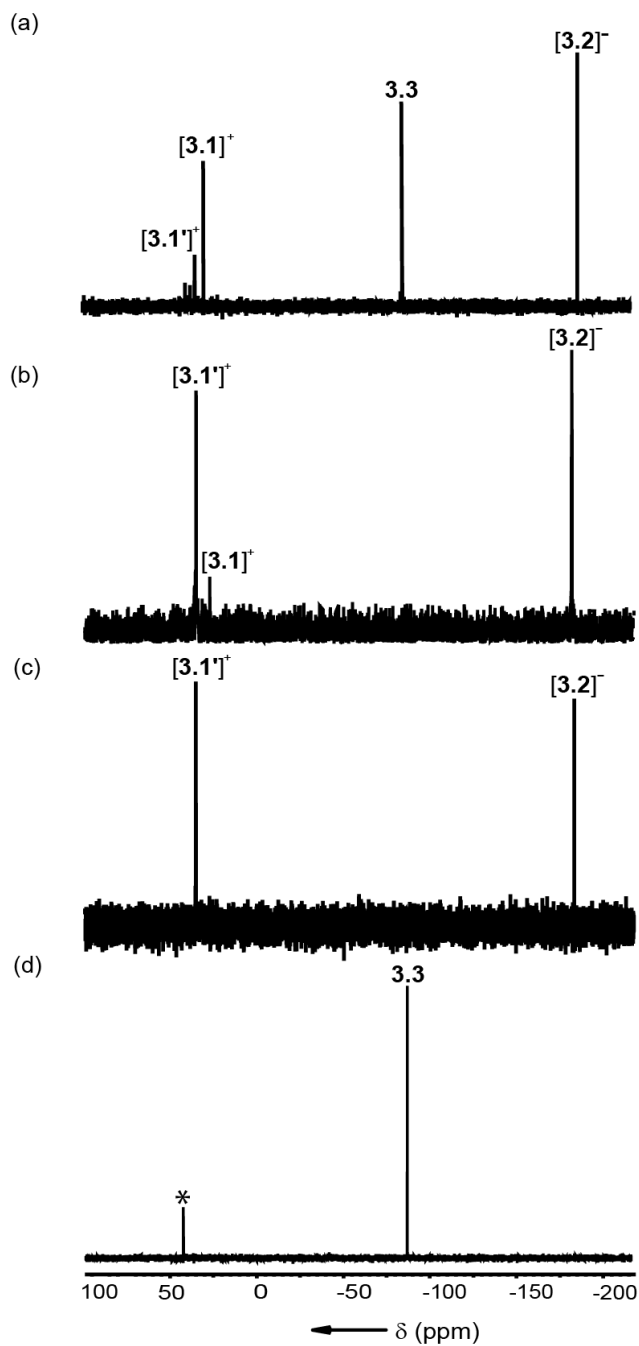


Figure 3.3.  $^{31}\text{P}\{^1\text{H}\}$  NMR (162 MHz, 25 °C) spectra of: (a) the reaction mixture obtained by reacting  $\text{PCl}_5$  with 2,2'-lithiobiphenyl [obtained from biphenyl, *n*-BuLi and TMEDA] in THF/Et<sub>2</sub>O – Route A in Scheme 3.1; (b) the reaction mixture obtained by reacting a portion of isolated reaction mixture from Route A (above) with 2,2'-dilithiobiphenyl in Et<sub>2</sub>O; (c) crystals of isolated  $[\text{3.1}]^+[\text{3.2}]^-$  dissolved in THF/Et<sub>2</sub>O solution; and (d) crystals of isolated  $3.3$  dissolved in THF/Et<sub>2</sub>O.

This was perplexing since the bond connectivity necessary to generate a P-centered cation with this molecular formula was not immediately obvious.

It has previously been reported that treating **[3.1][3.2]** with dilithiated biphenyl (1.0 equiv) affords Li**[3.2]**.<sup>253</sup> In an effort to simplify this unexpected product mixture, a portion of the isolated reaction mixture from above (Route A) was suspended in THF and treated with C<sub>12</sub>H<sub>8</sub>Li<sub>2</sub> (1 equiv) in Et<sub>2</sub>O. The 2,2'-dilithiobiphenyl was prepared from C<sub>12</sub>H<sub>8</sub>Br<sub>2</sub> and *n*-BuLi (2.0 equiv). Analysis of an aliquot of the soluble portion of the reaction mixture by <sup>31</sup>P{<sup>1</sup>H} NMR spectroscopy revealed that the major signals were at 35.2 and -183.3 ppm {see Figure 3.3 (b): major signals assigned to **[3.1']<sup>+</sup>[3.2]**} and a very small signal {<10% of the intensity of **[3.1']<sup>+</sup>**} at 27.2 ppm (assigned to **[3.1]<sup>+</sup>** of **[3.1][3.2]**). The aforementioned signal at -86.2 ppm, observed in the product mixture for Route A, was no longer observed. The reaction mixture was filtered to remove poorly soluble residual salts (*e.g.* **[3.1][3.2]**, Li**[3.2]**, LiBr, etc.). The filtrate was collected and the soluble product was isolated as a solid after solvent removal. Crystals suitable for X-ray diffraction were obtained by cooling (-30 °C) a solution of the crude product in a mixture of THF and Et<sub>2</sub>O (1:1) (Figure 3.5).

The molecular structure of the isolated compound, **[3.1']<sup>+</sup>[3.2]**, is displayed in Figure 3.5, along with selected metrical parameters. Importantly, the structure confirms the formulation obtained from mass spectrometric analysis, [P(C<sub>12</sub>H<sub>8</sub>)<sub>3</sub>][P(C<sub>12</sub>H<sub>8</sub>)<sub>3</sub>], yet the bond connectivity was totally unexpected. Particularly striking, is the structure of the cation **[3.1']<sup>+</sup>**, which contains the twisted 2,2'-bis(phenyl)biphenyl ligand (Figure 3.4). Although the neutral compound 2,2'-bis(phenyl)biphenyl is known and has been structurally characterized,<sup>356-362</sup> to our knowledge there are only three examples of complexes featuring the 2,2'-bis(phenyl)biphenyl dianionic ligand.<sup>363-365</sup> It should be noted that in the early reports of Hellwinkel, the possible coupling of the biphenyl moieties to form a byproduct was considered on the basis of IR spectra and melting point data.<sup>253,366</sup> In the present case, the structurally

characterized product **[3.1']****[3.2]** was further characterized by  $^{31}\text{P}$  NMR spectroscopy and ESI-MS (see Appendix B, Figures B1 and B2). The  $^1\text{H}$  and  $^{31}\text{C}\{^1\text{H}\}$  NMR spectra as well as the  $^1\text{H}$ - $^{31}\text{P}$  HMBC NMR spectrum were not particularly informative with many overlapping signals.

The salt **[3.1']****[3.2]** co-crystallizes with THF and diethyl ether solvent in the lattice. There are weak interactions between the cation and the anion in **[3.1']****[3.2]** (see Appendix B, Figure B3) with weak C $\cdots$ H, C $\cdots$ C and H $\cdots$ H contacts [closest contacts: C(21) $\cdots$ H(38) = 2.677(1) Å; C(15) $\cdots$ C(69) = 3.281(2) Å; H(21)  $\cdots$ H(38) = 2.361(2) Å]. In addition, there are moderate to strong interactions between the oxygen in the THF solvent and hydrogen atoms of the **[3.1']** $^+$  cation [O(1) $\cdots$ H(29) = 2.531(2) Å; O(2b) $\cdots$ H(28) = 2.553(5)]. There is also a close contact between the oxygen of THF and a methyl group of diethyl ether solvate [H(84C) $\cdots$ O(2B) = 1.639(4) Å]. For comparison, the sum of the van der Waals radii for oxygen and hydrogen is 2.72 Å, that for carbon and hydrogen is 2.90 Å<sup>367</sup> and a typical O–H bond length is 0.96 Å in water.<sup>368</sup>

The unprecedented cation **[3.1']** $^+$  adopts a highly distorted tetrahedral geometry at phosphorus. Specifically, the C(1)–P(1)–C(12) angle of the chelated 2,2'-biphenyl ligand [94.0(1) $^\circ$ ] is significantly more acute than the C(7)–P(1)–C(36) angle of the 2,2'-bis(phenyl)biphenyl ligand [121.5(5) $^\circ$ ]. In contrast, the bond lengths in the cation moiety show only minor perturbations from those expected. For example, the average P–C bond lengths [1.80(3) Å] are longer than the average P–C bond length in the previously reported **[3.1]** $^+$  [1.777(4) Å].<sup>369</sup> The C–C bond lengths connecting the four phenylene moieties of the twisted 2,2'-bis(phenyl)biphenyl ligand in **[3.1']** $^+$  [avg. 1.493(3) Å] are slightly longer than that between the phenylene of the biphenyl in **[3.1']** $^+$  [C(6)–C(7) = 1.475(2) Å]. This lengthening presumably reflects the decreased  $\pi$ -conjugation that accompanies the twisting in **[3.1']** $^+$ . For example, angles between the mean planes of the phenylene moieties in the 2,2'-bis(phenyl)biphenyl ligand

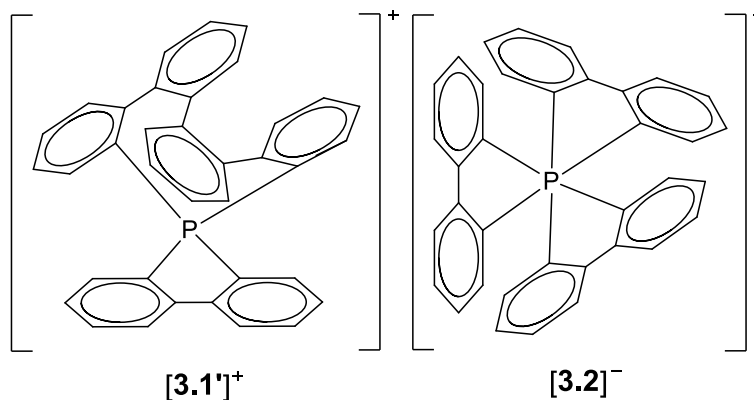


Figure 3.4. Spiro-compound  $[P(C_{12}H_8)(C_{24}H_{16})][P(C_{12}H_8)_3]$  ( $[3.1']^+[3.2]^-$ ).

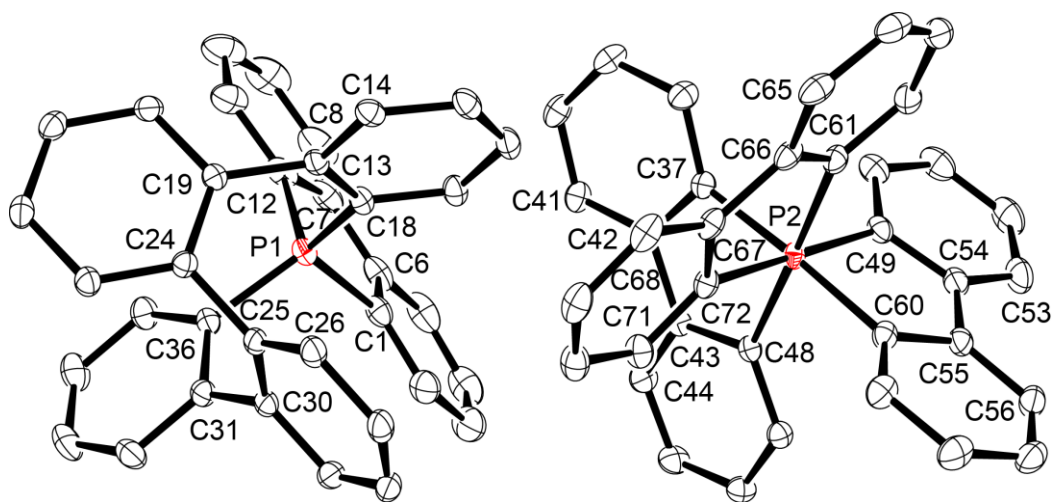


Figure 3.5. Molecular structure of the salt  $(S)\text{-}[3.1']\text{-}\Delta\text{-}[3.2]\cdot 1.73 \text{ THF}\cdot 0.27 \text{ Et}_2\text{O}$ .

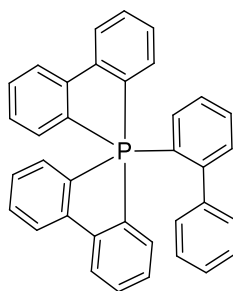
For clarity, one enantiomer of the cation  $[3.1']^+$  and one enantiomer of the anion  $[3.2]^-$  are shown. Solvents of crystallization (1.73 x THF and 0.27 x  $\text{Et}_2\text{O}$ ) and hydrogen atoms are omitted for clarity. Ellipsoids are drawn at the 50 % probability level. Selected bond lengths [Å]:  $P(1)\text{-}C(1) = 1.795(1)$ ;  $P(1)\text{-}C(12) = 1.795(1)$ ;  $P(1)\text{-}C(36) = 1.807(1)$ ;  $P(1)\text{-}C(13) = 1.797(1)$ ;  $P(2)\text{-}C(49) = 1.925(1)$ ;  $P(2)\text{-}C(61) = 1.933(1)$ ;  $P(2)\text{-}C(72) = 1.926(1)$ . Selected bond angles [°]:  $C(1)\text{-}P(1)\text{-}C(12) = 94.0(1)$ ;  $C(36)\text{-}P(1)\text{-}C(13) = 121.1(5)$ ;  $C(12)\text{-}P(1)\text{-}C(36) = 109.6(6)$ ;  $C(49)\text{-}P(2)\text{-}C(72) = 178.2(5)$ ;  $C(60)\text{-}P(2)\text{-}C(61) = 89.7(5)$ .

$[\theta_{(C13-C18)-(C19-C24)} = 80.0(4)^\circ; \theta_{(C19-C24)-(C25-C30)} = 81.9(4)^\circ; \theta_{(C25-C30)-(C31-C36)} = 73.9(4)^\circ]$  are significantly greater than that for the chelated 2,2'-biphenyl [ $\theta_{(C1-C6)-(C7-C12)} = 3.4(5)^\circ$ ]. In comparison, the angle between the mean planes of the aryl moieties in the uncomplexed 2,2'-(biphenyl)biphenyl are shorter [ $\theta = 47.3^\circ, 50.9^\circ, 43.0^\circ$ ].<sup>357</sup>

In contrast to the cation  $[3.1']^+$ , the phosphorus(V) center in  $[3.2]^-$  elucidates only minor perturbation from regular octahedral geometry displaying metrical parameters similar to those found in the previously reported salt  $[3.1][3.2]$ .<sup>369</sup> For example, the average P–C bond length in the anion of  $[P(2,2'\text{-biphenyl})_2][3.2]$  [ $d_{P-C} = 1.932(2) \text{ \AA}$ ] is similar to the average P–C bond length observed in  $[3.1']^+[3.2]$  ( $d_{P-C} = 1.929(4) \text{ \AA}$ ). The P(2)–C(48) bond length  $1.944(1) \text{ \AA}$  is slightly elongated with respect to the other P–C bonds in the anion of  $[3.1']^+[3.2]$ . The C–C bond lengths between the biphenyl moieties in the anion of  $[3.1']^+[3.2]$  [avg.  $1.478(3) \text{ \AA}$ ] are shorter than the C–C bond length in biphenyl itself [ $1.506(17) \text{ \AA}$ ].<sup>370,371</sup> Within the biphenyl ligands of  $[3.2]^-$ , the angle between the mean planes of the aryl moieties show only minor deviations from planarity [*i.e.*  $\theta_{(C49-C54)-(C55-60)} = 4.4(4)^\circ$ ,  $\theta_{(C37-C42)-(C43-C48)} = 7.2(4)^\circ$  and  $\theta_{(C61-C66)-(C67-C72)} = 5.6(5)^\circ$ ]. These angles are similar to those between the mean planes of the aryl moieties in the salt  $[3.1][3.2]$  [ $\theta = 3.0(6)^\circ, 5.1(5)^\circ, 6.3(5)^\circ$ ].<sup>369</sup>

With the identity of  $[3.1']^+[3.2]$  confirmed, it remained to identify the species responsible for the signal at  $-86.2$  ppm in the  $^{31}\text{P}$  NMR spectrum of the reaction mixture from Route A [see Figure 3.3 (a)]. Thus, a second portion of the isolated crude reaction mixture from Route A was suspended in *n*-butanol and gravity filtered. Upon standing of the filtrate at ambient temperature in air atmosphere for three weeks, crystals suitable for X-ray crystallographic analysis were isolated. The  $^{31}\text{P}\{^1\text{H}\}$  NMR spectrum of the crystals of **3.3** in THF/Et<sub>2</sub>O [see Figure 3.3 (d)] displayed a singlet resonance assigned to the product ( $\delta = -86.2$ ) and a small signal attributed to an unidentified species ( $\delta = 37.4$ ). The molecular

structure of the pentacoordinate phosphorane **3.3** is shown in Figure 3.7. The phosphorus(V) center in **3.3** adopts a distorted trigonal bipyramidal geometry with one carbon of each of the chelating



**3.3**

Figure 3.6. Pentacoordinate phosphorane **3.3**,  $[\text{P}(\text{C}_{12}\text{H}_8)_2(\text{C}_{12}\text{H}_9)]$ .

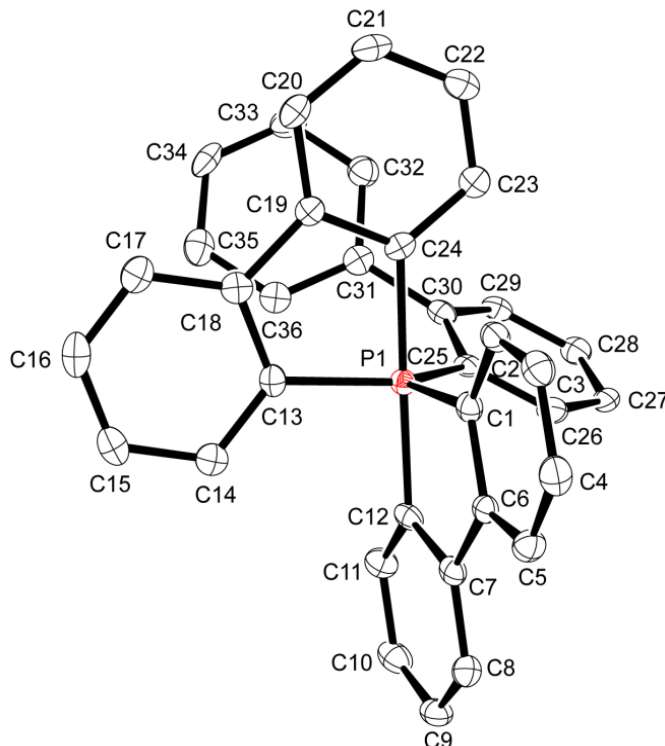


Figure 3.7. Molecular structure of **3.3**.

Ellipsoids are drawn at the 50 % probability level. Hydrogen atoms are omitted for clarity. Selected bond lengths [ $\text{\AA}$ ]:

$\text{P}(1)\text{-C}(1) = 1.868(4)$ ;  $\text{P}(1)\text{-C}(12) = 1.925(4)$ ;  $\text{P}(1)\text{-C}(13) = 1.861(4)$ ;  $\text{P}(1)\text{-C}(24) = 1.909(4)$ ;  $\text{P}(1)\text{-C}(25) = 1.874(4)$ .

Selected bond angles [ $^\circ$ ]:  $\text{C}(1)\text{-P}(1)\text{-C}(12) = 86.1(2)$ ;  $\text{C}(1)\text{-P}(1)\text{-C}(13) = 108.7(1)$ ;  $\text{C}(13)\text{-P}(1)\text{-C}(24) = 86.7(1)$ ;  $\text{C}(13)\text{-P}(1)\text{-C}(25) = 130.6(1)$ ;  $\text{C}(25)\text{-P}(1)\text{-C}(24) = 90.0(1)$ .

biphenyl ligands in the axial positions [*i.e.* C(12) and C(24)], leaving the second carbon of each of the two chelating ligands along with the carbon of the monodentate biphenyl in the equatorial plane [*i.e.* C(1), C(13) and C(25)]. As expected, the equatorial P–C bonds [avg. 1.868(7) Å] are shorter than the axial P–C bonds [avg. 1.917(6) Å].

The  $C_{ax}$ –P– $C_{eq}$  bond angles [avg. 90.0(4)°] are in the range expected for a trigonal bipyramid with the maximum deviations being C(24)–P(1)–C(1) [94.5(2)°] and C(12)–P(1)–C(1) [86.1(2)°]. The C–C bond length connecting the two phenylene moieties of the monodentate biphenyl [C(31)–C(30) = 1.491(6) Å] is slightly elongated compared to the other two chelating biphenyl ligands in **3.3** [C(6)–C(7) = 1.475(7) Å; C(18)–C(19) = 1.474(5) Å]. This lengthening is most likely due to disruption of  $\pi$ -conjugation within the twisted monodentate biphenyl ligand. Specifically, the angle between the mean planes of the phenylene moieties in the monodentate 2-biphenyl ligand [ $\theta_{(C_{25}-C_{30})-(C_{31}-C_{36})} = 51.5(2)^\circ$ ] are significantly greater than that for the two chelated 2,2'-biphenyl ligands [ $\theta_{(C_{1}-C_{6})-(C_{7}-C_{12})} = 4.9(2)^\circ$ ;  $\theta_{(C_{13}-C_{18})-(C_{19}-C_{24})} = 2.3(2)^\circ$ ].

Unfortunately, the poor solubility and limited quantity of **3.3** obtained thwarted additional characterization of this product. It should be noted that Hellwinkel previously observed **3.3** and its 4-methyl-biphenyl derivative as characterized by IR spectroscopy, elemental analysis and optical rotation studies.<sup>253,255,352</sup>

Although Hellwinkel's earlier reports mentioned the possibility that [**3.1'**][**3.2**] was a byproduct in the formation of [**3.1**][**3.2**] from 2,2'-diiodobiphenyl,<sup>253</sup> this was not shown explicitly. Thus, we followed his procedure exactly (Scheme 3.1, Route B), albeit on a smaller scale. 2,2'-Dilithiobiphenyl was prepared by treating 2,2'-diiodobenzene with *n*-BuLi (2.4 equiv) in diethyl ether at 0 °C. To this mixture was added PCl<sub>5</sub> in diethyl ether at –78 °C and the “product” was isolated according to the

reported procedure. The crude reaction mixture was dissolved in THF/Et<sub>2</sub>O and the <sup>31</sup>P{<sup>1</sup>H} NMR spectrum is shown in Figure 3.8(a). Remarkably, the major product we observed was assigned as [3.1']<sub>2</sub>[3.2] (δ = 29.8 and -183.8) with the minor product being [3.1]<sub>2</sub>[3.2] (δ = 26.8 and -183.8). The intensity of the signal for [3.2]<sup>-</sup> was very small compared to that of [3.1']<sup>+</sup> or [3.1]<sup>+</sup>, suggesting that there may be significant quantities of the Cl<sup>-</sup> or I<sup>-</sup> counterion present. These results were in contrast to those of Hellwinkel who reported only the signals attributed to [3.1]<sub>2</sub>[3.2] (δ = 26.5 and -186.5 ppm in DMF-*d*<sub>7</sub>) [the <sup>31</sup>P{<sup>1</sup>H} NMR spectrum of the reaction mixture we obtained in DMF-*d*<sub>7</sub> revealed signals at δ = 31.9, 27.0 and -183.4 ppm]. In our hands, it appeared that the insertion product

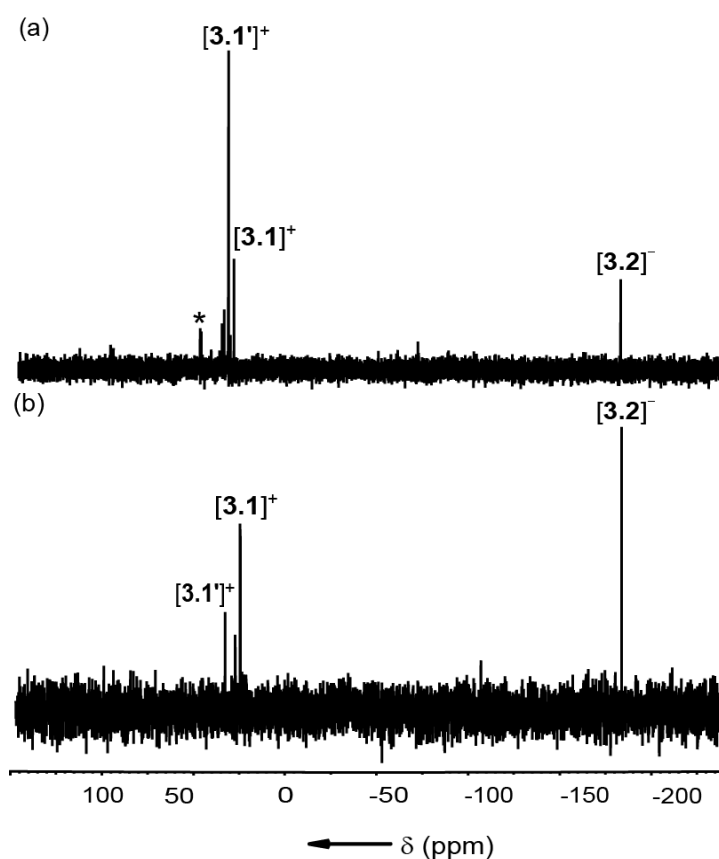


**Figure 3.8.** <sup>31</sup>P{<sup>1</sup>H} NMR (162 MHz, 25 °C) spectrum of [3.1]<sub>2</sub>[3.2] and [3.1']<sub>2</sub>[3.2] via (a) dilithiated 2,2'-diiodobiphenyl recorded in THF/Et<sub>2</sub>O solution (Route B); (b) dilithiated 2,2'-dibromobiphenyl recorded in THF/Et<sub>2</sub>O solution (Route C).

$[\mathbf{3.1}']^+$ , was the major product. Given the 3:1 stoichiometric ratio of the 2,2'-diiodobiphenyl ligand to phosphorus pentachloride, there was insufficient 2,2'-diiodobiphenyl to afford both  $[\mathbf{3.1}']^+$  and  $[\mathbf{3.2}]^-$  stoichiometrically. It was for this reason we surmise that the main products were  $[\mathbf{3.1}']\text{X}$  and  $[\mathbf{3.1}]\text{X}$  (X = Cl or Br) with minimal amounts of  $[\mathbf{3.1}'][\mathbf{3.2}]$  and  $[\mathbf{3.1}][\mathbf{3.2}]$  being formed.

Given the above results, we became interested to see whether the ratio of  $[\mathbf{3.1}]^+$  to  $[\mathbf{3.1}']^+$  could be influenced by starting with 2,2'-dibromobiphenyl instead of 2,2'-diiodobiphenyl. In this case (Scheme 3.1, Route C), 2,2'-dilithiobiphenyl was prepared by treating 2,2'-dibromobenzene with *n*-BuLi (2.2 equiv) in diethyl ether at 0 °C. To this mixture was added  $\text{PCl}_5$  in diethyl ether at -78 °C. The crude product mixture isolated from the reaction mixture was dissolved in THF/ $\text{Et}_2\text{O}$  and analyzed by  $^{31}\text{P}\{^1\text{H}\}$  NMR spectroscopy. The spectrum, shown in Figure 3.8 (b), revealed that the major product contained the cation  $[\mathbf{3.1}]^+$  with the minor product containing  $[\mathbf{3.1}']^+$ . Although the relative intensity of the signal ascribed to  $[\mathbf{3.2}]^-$  was greater than that for the iodo-precursor, the spectrum still suggested that a significant quantity of halide salt was formed.

Before closing, a comment on the mechanism of formation for  $[\mathbf{3.1}'][\mathbf{3.2}]$  is warranted. It is remarkable that the coupling of biphenyl is observed following all three routes. First, the coupling of arylene moieties during the lithiation of aryl halides [*i.e.*  $\text{Ar-X} + \text{Ar-Li} \rightarrow \text{Ar-Ar} + \text{LiX}$  (X = Br or I)] is well preceded.<sup>372,373</sup> In fact, the reaction of 1,2-diiodobenzene or 1,2-dibromobenzene with *n*-BuLi (2.4 equiv) followed by carboxylation afforded low yields of 2,2'- $\text{C}_{12}\text{H}_8(\text{COOH})_2$  (up to 17%).<sup>374-376</sup> Thus, it may be inferred that the presumptive intermediate, 1-halo-2-lithiobenzene is readily coupled to itself or to 1,2-dihalobenzene to afford 2-halo, 2'-lithiobiphenyl and 2,2'-dihalobiphenyl, respectively. These products may be further lithiated and/or coupled to the corresponding tetraphenyl derivatives. Thus, the observed formation of  $[\mathbf{3.1}']^+$  when starting with 2,2'-dihalobiphenyl derivatives (*i.e.* Routes B or C) can be rationalized.

It is considerably more difficult to explain the observed coupling of biphenyl to give  $[3.1']^+$ , which was observed following Route A. In this case, nucleophilic aromatic substitution was not possible and only an oxidative coupling of Ar–Li moieties is plausible. However, the possible oxidizing agents were limited to the phosphorus(V) of  $PCl_5$ , adventitious oxygen or perhaps solvent. Since the reactions were performed under rigorously anaerobic conditions and the results are entirely reproducible, we consider that the most likely oxidant is  $PCl_5$ . That said, we did not observe any evidence by  $^{31}P$  NMR spectroscopy of the reactions solutions for the reduced products although it is possible these species are insoluble. The coupling reaction of phosphorus(V) compounds with lithiated aryl or Grignard reagents (PhMgBr) is favoured. For example, the reaction of  $EtP(=O)(OEt)_2$  with 2PhMgBr in THF at 68 °C gives substituted phosphonates [ $Ph_2P(=O)OEt$ ,  $PhP(=O)(OEt)_2$ ,  $(EtO)_2P(=O)OEt$ ,  $EtP(=O)(OEt)_2$ , and  $(EtO)_3P(=O)$ ]<sup>377</sup> as well as the coupling of  $((C_6H_5)O)POCl_2$  with PhMgBr to afford  $(C_6H_5)_3P=O$ .<sup>378</sup> In another instance,  $(biphenyl)(Ph)P(=N-Ts)$  reacts with 2,2'-dilithiated biphenyl to give  $P(biphenyl)_2(Ph)$ .<sup>363</sup> The spirophosphorane  $(Ph(C(CF_3)_2O)_2)P-H$  reacts with RLi (R= Me, *n*-Bu, *t*-Bu, aryl) to yield  $(Ph(C(CF_3)_2O)_2)P-R$ .<sup>379</sup>

### 3.3 Summary

We have explored three potential routes to afford Hellwinkel's salt  $[3.1][3.2]$ . In addition to the desired compound, we have isolated a novel complex cation incorporating an alternative cation  $[3.1']^+$  with the formulation  $[P(C_{12}H_8)_3]^+$  that is formally derived from the insertion of an additional biphenyl unit into  $[3.1]^+$  and the phosphorus(V) containing WCA  $[3.2]^-$ . The insertion product was observed by direct lithiation of biphenyl (Route A), 2,2'-diiodobiphenyl (Route B) and 2,2'-dibromobiphenyl (Route C). This new "twist" on Hellwinkel's salt was characterized by means of mass spectrometry,  $^{31}P\{^1H\}$  NMR

spectroscopy and X-ray crystallography. Additionally, we were able to isolate and characterize the neutral species **3.3** by X-ray crystallography and  $^{31}\text{P}\{^1\text{H}\}$  NMR spectroscopy.

## 3.4 Experimental

### 3.4.1 General Procedures

All experiments were performed using standard Schlenk or glove box techniques under nitrogen atmosphere. Diethyl ether ( $\text{Et}_2\text{O}$ ) (Fisher Scientific) was deoxygenated with nitrogen and dried by passing the solvent through a column containing activated, basic alumina. Subsequently, the  $\text{Et}_2\text{O}$  was dried over calcium hydride, freshly distilled, and freeze-pump-thaw (x3) degassed and stored over 3 Å molecular sieves prior to use. Tetrahydrofuran (THF) (Fisher Scientific) was dried and distilled over sodium/benzophenone ketyl prior to use. Phosphorus pentachloride (Sigma Aldrich) was sublimed prior to use. 2,2'-Dibromobiphenyl<sup>380</sup> was prepared following literature procedure. 2,2'-Diiodobiphenyl was prepared following the analogous 2,2'-dibromobiphenyl procedure. Mass spectrometry and NMR spectra were performed in the Department of Chemistry Facilities. Low resolution electrospray ionization mass spectra {LRMS (ESI)} were recorded on Bruker Esquire LC. High resolution electrospray ionization mass spectra {HRMS (ESI)} were recorded on Micromass LCT time of flight (TOF) mass spectrometer.  $^1\text{H}$  and  $^{31}\text{P}\{^1\text{H}\}$  NMR spectra were recorded on Bruker Avance 400 MHz spectrometers at ambient temperature.  $\text{H}_3\text{PO}_4$  (85 %) was used as external standard for  $^{31}\text{P}$  NMR spectra with  $\delta = 0.0$ .  $^1\text{H}$  NMR spectra were referenced to deuterated solvents.

### 3.4.2 Synthesis of $[\text{P}(\text{C}_{12}\text{H}_8)(\text{C}_{24}\text{H}_{16})]^+$ ( $[\mathbf{3.1}']^+$ ), $[\text{P}(\text{C}_{12}\text{H}_8)_2]^+$ ( $[\mathbf{3.1}]^+$ ), $[\text{P}(\text{C}_{12}\text{H}_8)_3]^-$ ( $[\mathbf{3.2}]^-$ ) and $\text{P}(\text{C}_{12}\text{H}_8)_2(\text{C}_{12}\text{H}_9)$ ( $\mathbf{3.3}$ )

**Route A.** To a solution of biphenyl (4.73 g, 30.7 mmol) in TMEDA (11.0 mL, 8.60 g, 74.0 mmol) was added *n*-BuLi (46.0 mL, 74.0 mmol, 1.6 M in *n*-hexane). The bright orange solution was stirred at ambient temperature under  $\text{N}_2$  atmosphere for 3 d. The reaction mixture was cooled to  $-20\text{ }^\circ\text{C}$  to obtain yellow crystals. The supernatant was removed by cannula filtration and the residue washed with THF (20 mL). Subsequently a solution of  $\text{PCl}_5$  (2.51 g, 12.0 mmol) in THF/ $\text{Et}_2\text{O}$  (40 mL/ 6 mL) was slowly added at  $-78\text{ }^\circ\text{C}$ . Upon addition, a light brown precipitate was obtained and the mixture stirred overnight. The supernatant was removed via cannula filtration and the precipitate was washed with diethyl ether (30 mL), filtered and dried *in vacuo*. A beige powder was isolated (2.41 g), which was later shown to contain  $[\mathbf{3.1}][\mathbf{3.2}]$ ,  $[\mathbf{3.1}'][\mathbf{3.2}]$  and  $\mathbf{3.3}$ .

$^{31}\text{P}\{^1\text{H}\}$  NMR (162 MHz, THF/ $\text{Et}_2\text{O}$ ,  $25\text{ }^\circ\text{C}$ ):  $\delta = 30.6, 25.8, -184.7$ ; HRMS (ESI/TOF, positive mode)  $m/z = [\text{M}]^+$  calcd for  $\text{C}_{24}\text{H}_{16}\text{P}_1$  335.0990; found 335.0987 and  $[\text{M}]^+$  calcd for  $\text{C}_{36}\text{H}_{24}\text{P}_1$  487.1616; found 487.1620; LRMS (ESI, negative mode)  $m/z = 487.1$  ( $[\text{M}]^-$ ).

**Route B.** To a solution of 2,2'-diiodobiphenyl (1.01 g, 2.50 mol) in  $\text{Et}_2\text{O}$  (20 mL) was added *n*-BuLi (3.42 mL, 5.25 mol, 1.53 M in *n*-hexane) at  $0\text{ }^\circ\text{C}$ . The reaction mixture was stirred for 4 h at  $0\text{ }^\circ\text{C}$  and cooled down to  $-78\text{ }^\circ\text{C}$  for an additional 1 hour followed by the addition of a  $\text{PCl}_5$  (0.17 g, 0.83 mmol) solution in  $\text{Et}_2\text{O}$  (17 mL) at  $-78\text{ }^\circ\text{C}$  to afford a light brown precipitate. The reaction mixture was allowed to warm up to ambient temperature overnight and extracted with degassed  $\text{H}_2\text{O}$  (7 mL). The precipitate was cannula filtered, washed with  $\text{Et}_2\text{O}$  and dried *in vacuo*. A beige powder was isolated (0.66 g), which contains  $[\mathbf{3.1}][\mathbf{3.2}]$  and  $[\mathbf{3.1}'][\mathbf{3.2}]$ .

$^{31}\text{P}\{^1\text{H}\}$  NMR (162 MHz, THF/ $\text{Et}_2\text{O}$ ,  $25\text{ }^\circ\text{C}$ ):  $\delta = 29.8, 26.8, -183.8$ ;  $(\text{CD}_3)_2\text{NCOD}$   $\delta = 31.9, 27.0, -183.4$ ;  $^1\text{H}$  NMR (400 MHz,  $(\text{CD}_3)_2\text{NCOD}$ ,  $25\text{ }^\circ\text{C}$ ):  $\delta = 8.69$  (m, 1H, Ar-*H*), 8.22 (m, 1H, Ar-*H*), 7.99

(m, 2H, Ar-*H*), 7.88 (m, 1H, Ar-*H*), 7.81 (m, 1H, Ar-*H*), 7.74 (m, 1H, Ar-*H*), 7.66 (m, 1H, Ar-*H*), 7.57 (m, 2H, Ar-*H*), 7.37 (m, 1H, Ar-*H*), 7.21 (m, 2H, Ar-*H*), 7.01 (m, 1H, Ar-*H*), 6.82 (m, 1H, Ar-*H*), 6.70 (m, 1H, Ar-*H*).

**Route C.** 2,2'-dibromobiphenyl (0.73 g, 2.35 mol) was dissolved in 11 mL anhydrous Et<sub>2</sub>O. The colorless mixture was cooled at 0 °C followed by the slow addition of *n*-BuLi (2.90 mL, 4.70 mol, 1.6 M in *n*-hexane). The reaction mixture was stirred for 4 hours at 0 °C. PCl<sub>5</sub> (0.12 g, 0.59 mol) was added at -78 °C and stirred overnight to afford a light brown precipitate. The precipitate was extracted with H<sub>2</sub>O (20 mL), cannula filtered and dried *in vacuo*. A beige powder was isolated (0.64 g), which contains [3.1][3.2] and [3.1'] [3.2].

<sup>31</sup>P{<sup>1</sup>H} NMR (162 MHz, THF/Et<sub>2</sub>O, 25 °C): δ = 32.6, 24.4, -183.8.

### 3.4.3 Synthesis of [P(C<sub>12</sub>H<sub>8</sub>)(C<sub>24</sub>H<sub>16</sub>)] [3.2]

To a stirred solution of 2,2'-dibromobiphenyl (0.57 g, 1.83 mol) in diethyl ether (20 mL) at 0 °C was slowly added *n*-BuLi (2.30 mL, 3.70 mol, 1.6 M in *n*-hexane). The pale yellow solution was stirred for 4 h at 0 °C. To the reaction mixture was added a suspension of the solid from Route A described above (1.00 g, 0.56 mol) in THF (20 mL). Upon addition, an off yellow precipitate was obtained. The reaction mixture was stirred overnight at ambient temperature. The supernatant was collected by cannula filtration and dried *in vacuo*. A beige powder was isolated (0.45 g), which contains [3.1'] [3.2] and minor [3.1][3.2]. A concentrated solution of the crude product in THF/Et<sub>2</sub>O afforded colorless crystals of [3.1'] [3.2] (-30 °C, ca. 7 days). A crystal was removed for X-ray crystallographic analysis without drying.

$^{31}\text{P}\{^1\text{H}\}$  NMR (162 MHz, THF/Et<sub>2</sub>O, 25 °C):  $\delta = 35.2, -184.4$ ; HRMS (ESI/TOF, positive mode)  $m/z = [\text{M}]^+$  calcd for C<sub>36</sub>H<sub>24</sub>P<sub>1</sub> 487.1616; found 487.1615 and LRMS (ESI, negative mode)  $m/z = 487.1$  ( $[\text{M}]^-$ ).

#### 3.4.4 Synthesis of 3.3

A portion of the mixture from Route A described above (0.177 g) was dissolved in *n*-butanol (2.5 mL) and subsequently filtered to remove insoluble material. Within 3 weeks colorless crystals were obtained upon standing at ambient temperature. A crystal was removed for X-ray crystallographic analysis.

$^{31}\text{P}\{^1\text{H}\}$  NMR (162 MHz, THF/Et<sub>2</sub>O, 25 °C):  $\delta = -86.2$ .

#### 3.4.5 X-ray Structure Determination

X-ray crystallography data were collected on a Bruker X8 APEX II diffractometer with graphite-monochromated Mo K $\alpha$  radiation. A single crystal was immersed in oil and mounted on a glass fiber. Data were collected and integrated using the Bruker SAINT<sup>325</sup> software package and corrected for absorption effect using SADABS.<sup>326</sup> All structures were solved by direct methods and subsequent Fourier difference techniques. Unless noted, all non-hydrogen atoms were refined anisotropically, whereas all hydrogen atoms were included in calculated positions but not refined. All data sets were corrected for Lorentz and polarization effects. All refinements were performed using the SHELXL-2015<sup>328</sup> via the Olex2 interface.<sup>329</sup> [3.1'] [3.2] co-crystallizes with 0.27 diethyl ether and 1.73 THF solvate molecules. Crystal data and refinement parameters are listed in Table 3.1. CIF files containing supplementary crystallographic data for the structures reported in this chapter are available from The Cambridge Crystallographic Data Centre (CCDC-1573488 and CCDC-173489).

**Table 3-1. X-ray crystallographic data for [3.1'] [3.2] and 3.3.**

|  | [3.1'] [3.2] · 1.73 THF · 0.27 · Et <sub>2</sub> O               | 3.3                               |
|--|--|-----------------------------------|
| Formula  | C <sub>80</sub> H <sub>64.54</sub> O <sub>2</sub> P <sub>2</sub> | C <sub>36</sub> H <sub>25</sub> P |
| Fw   | 1119.80  | 488.53                            |
| Cryst. syst.   | Triclinic  | Trigonal                          |
| space group  | P -1   | P 3 <sub>1</sub>                  |
| Color  | Green  | Colorless                         |
| <i>a</i> (Å)   | 13.5082(17)  | 9.2847(5)                         |
| <i>b</i> (Å)   | 14.9299(19)  | 9.2847(5)                         |
| <i>c</i> (Å)   | 15.662(2)  | 24.6168(17)                       |
| <i>α</i> (deg)   | 90.349(3)  | 90                                |
| <i>β</i> (deg)   | 104.088(3)   | 90                                |
| <i>γ</i> (deg)   | 106.054(3)   | 120                               |
| <i>V</i> (Å <sup>3</sup> )   | 2935.0(6)  | 1837.8(2)                         |
| T (K)  | 90(2)  | 90(2)                             |
| Z  | 2  | 3                                 |
| $\mu$ (MoK $\alpha$ ) (mm <sup>-1</sup> )                                | 0.126  | 0.137                             |
| crystal size (mm <sup>3</sup> )  | 0.26 × 0.25 × 0.25   | 0.15 × 0.13 × 0.07                |
| $\rho_{\text{calcd.}}$ (g cm <sup>-3</sup> )                             | 1.267  | 1.327                             |
| 2 $\theta$ (max) (°)   | 60.2   | 55.8                              |
| F(000)   | 1181   | 768                               |
| No. of total reflns.   | 64238  | 13205                             |
| No. of unique reflns.  | 17187  | 5784                              |
| <i>R</i> (int)   | 0.028  | 0.042                             |
| Refln./param. Ratio  | 20.24  | 17.32                             |
| <i>R</i> <sub>1</sub> [ <i>I</i> > 2 $\sigma$ ( <i>I</i> )] <sup>a</sup> | 0.0450   | 0.052                             |
| <i>wR</i> <sub>2</sub> [all data] <sup>b</sup>                           | 0.1251   | 0.1044                            |
| GOF  | 1.033  | 1.059                             |

<sup>a</sup>  $R_1 = \sum ||F_o| - |F_c|| / \sum |F_o|$ . <sup>b</sup>  $wR_2(F^2[\text{all data}]) = \{\sum [w(F_o^2 - F_c^2)^2] / \sum [w(F_o^2)^2]\}^{1/2}$ .

## Chapter 4: Ammonium and Potassium Salts of a Hexacoordinate Phosphorus(V)

### Anion Featuring P–O and P–C Bonds

#### 4.1 Introduction

Phosphorus displays a tremendous diversity of coordination numbers in its compounds with the two extremes of one-coordinate (*e.g.* phosphalkyne, phosphinidene) and hexacoordinate (*e.g.* phosphate) systems being the rarest. Despite the fact that the simple anions  $[\text{PF}_6]^-$  and  $[\text{PCl}_6]^-$  are ubiquitous in inorganic chemistry, hexacoordinate phosphorus(V) anions featuring organic substituents are rare. Selected examples are shown in Figure 4.1 ( $[\mathbf{A}]^-$ ,<sup>264,287,381-384</sup>  $[\mathbf{B}]^-$ ,<sup>250,252,350,351,385-390</sup>  $[\mathbf{C}]^-$ ,<sup>248</sup>  $[\mathbf{D}]^-$ <sup>253,255,352</sup>). The first example of a hexacoordinate organophosphate was isolated in 1963 as a triethylammonium salt of  $[\text{P}(1,2-(\text{C}_6\text{O}_2\text{H}_4)_3)]^-$  ( $[\mathbf{B}]^-$ ).<sup>249,250,252</sup> Ideal properties for WCAs are large charge delocalized anions (*e.g.*  $[\mathbf{B}]^-$  and its derivatives) that possess low nucleophilicity. The well-known large chiral tris(tetrachlorobenzenediolato)phosphate  $[\mathbf{B}]^-$  ( $\text{R} = \text{Cl}$ ) has been widely employed as a WCA in the stabilization of unsaturated cations, as chiral solvate and resolving agent.<sup>350</sup> Chapter 2 described the isolation of Brønsted acids of  $\text{HL}_2[\mathbf{B}]$  ( $\text{L} = \text{THF}, \text{CH}_3\text{CN}, \text{DMF}$ ) as initiators for the cationic polymerization of olefins.<sup>351</sup> An advantage of  $\text{HL}_2[\mathbf{B}]$  includes the convenient one-pot reaction of  $\text{PCl}_5$  and  $\text{C}_6\text{Cl}_4(\text{OH})_2$ . However, a potential concern with employing  $[\mathbf{B}]^-$  as a WCA is the donor properties of the oxygen atoms within the anion. P–O bonds are prone to protonation and ring opening reactions. We therefore targeted P–C containing WCAs such as the famous anion  $[\mathbf{D}]^-$ . The compounds  $\text{Li}[\mathbf{D}]$  and  $[\text{P}(\text{C}_{12}\text{H}_8)_2][\mathbf{D}]$  have been previously reported.<sup>253</sup> Chapter 3 described the isolation of a salt containing the anion  $[\mathbf{D}]^-$  with the rare cation  $[\text{P}(\text{C}_{12}\text{H}_8)(\text{C}_{24}\text{H}_{16})]^+$  by reacting  $\text{PCl}_5$  with  $\text{C}_{12}\text{H}_8\text{Li}_2$  (generated from either  $\text{C}_{12}\text{H}_{10}$ ,  $\text{C}_{12}\text{H}_8\text{Br}_2$  or  $\text{C}_{12}\text{H}_8\text{I}_2$ ).<sup>391</sup>

---

\* A version of this chapter will be submitted for publication. Hazin, K. and Gates, D.P.

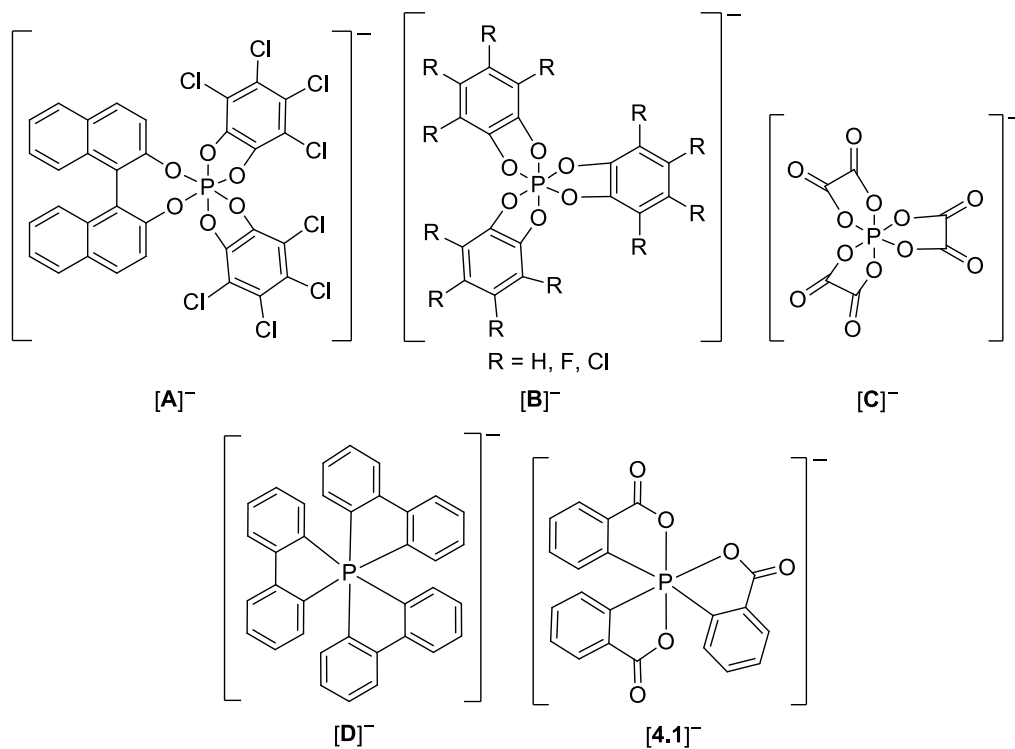


**Figure 4.1.** Examples of hexacoordinate phosphorus(V) weakly coordinating anions.

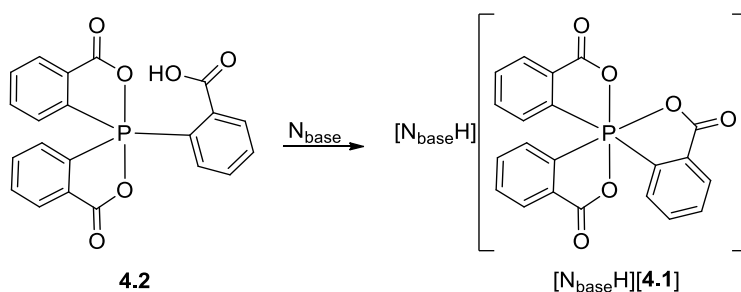
Noteworthy, less common are hybrid anions with mixed P–O and P–C bonds (*e.g.* *mer*–[**4.1**]<sup>−</sup>). Triethylammonium and diethylammonium salts of *mer*–[**4.1**]<sup>−392</sup> and their reactivity studies were reported by Holmes and inspired us to target the development of complexes featuring a potential WCA containing strong O–P–C bonds with the ultimate goal to isolate Brønsted acids containing the anion *mer*–[**4.1**]<sup>−</sup>.

Herein, we report the synthesis and crystallographic characterization of ammonium [N<sub>base</sub>H] salts featuring the anion *mer*–[**4.1**]<sup>−</sup>. The convenient preparation involves treating phosphorane P(C<sub>6</sub>H<sub>4</sub>CO<sub>2</sub>)<sub>2</sub>(C<sub>6</sub>H<sub>4</sub>COOH), **4.2**, with various amines [N<sub>base</sub> = PhNMe<sub>2</sub>, PhNH<sub>2</sub>, pyridine (py), isoquinoline, (−)-brucine, N(*n*-C<sub>8</sub>H<sub>17</sub>)<sub>3</sub>]. In addition, the synthesis and crystallographic characterization of K–*rac*–*mer*–[**4.1**] are discussed.

## 4.2 Results and Discussion

### 4.2.1 Synthesis and Characterization of Ammonium Salts of *mer*-[4.1]<sup>-</sup>

Inspired by the single report of [Et<sub>2</sub>NH<sub>2</sub>]<sup>+</sup> and [Et<sub>3</sub>NH]<sup>+</sup> salts of anion *mer*-[4.1]<sup>-</sup>,<sup>392</sup> we prepared several ammonium salts as a starting point to explore the WCA potential of *mer*-[4.1]<sup>-</sup> (Scheme 4.1). We noted that an ammonium salt, [PhNMe<sub>2</sub>H][D],<sup>353</sup> has been reported in a patent as a protic activator for metallocene catalysts for ethylene polymerization. Although very limited characterization details were provided, we were inspired to explore the synthesis of [PhNMe<sub>2</sub>H][4.1] and [PhNH<sub>3</sub>][4.1] to evaluate the prospective WCA properties of *mer*-[4.1]<sup>-</sup>. An acetone solution of acid P(C<sub>6</sub>H<sub>4</sub>CO<sub>2</sub>)<sub>2</sub>(C<sub>6</sub>H<sub>4</sub>COOH) (**4.2**) was treated with dimethylaniline (PhNMe<sub>2</sub>) or aniline (PhNH<sub>2</sub>) to afford [NPhMe<sub>2</sub>H]-*rac-mer*-[4.1] or [PhNH<sub>3</sub>]-*rac-mer*-[4.1], respectively (*vide infra*). Based on these positive results, other bases were also explored [*i.e.* pyridine (py), isoquinoline, (-)-brucine and N(*n*-C<sub>8</sub>H<sub>17</sub>)<sub>3</sub>].



**Scheme 4.1.** General synthetic route of [N<sub>base</sub>H][4.1] with N<sub>base</sub> = PhNMe<sub>2</sub>, PhNH<sub>2</sub>, py, isoquinoline, (-)-brucine and N(*n*-C<sub>8</sub>H<sub>17</sub>)<sub>3</sub>. **4.2** is phosphorane P(C<sub>6</sub>H<sub>4</sub>CO<sub>2</sub>)<sub>2</sub>(C<sub>6</sub>H<sub>4</sub>COOH).

Each crude product was recrystallized as described in the experimental section and colorless crystals suitable for X-ray crystallographic analysis were obtained for [PhNMe<sub>2</sub>H]-*rac-mer*-[4.1], [pyH]-*rac-mer*-[4.1], [isoquinolineH]-*rac-mer*-[4.1], and [(-)-brucineH]-*rac-mer*-[4.1]. The molecular structures of each ammonium salt are shown in Figure 4.3 and the metrical parameters will be

discussed in detail below. Crystallization of  $[(-)\text{-brucineH}]\text{-rac-mer-[4.1]}$  from  $\text{CD}_2\text{Cl}_2$  afforded enantiomerically pure  $[(-)\text{-brucineH}]\text{-}\Lambda\text{-mer-[4.1]}$ . Spectroscopic analysis of the isolated complexes was performed in either acetone- $d_6$  or DMSO- $d_6$  due to their solubility. The  $^{31}\text{P}\{^1\text{H}\}$  NMR spectra (see Appendix C, Figures C1 and C2) revealed signals characteristic of preservation of  $\text{mer-[4.1]}^-$  upon dissolution (range:  $-104.7$  to  $-135.2$  ppm, see Table 4.1). These signals were in the range reported for known salts containing  $\text{mer-[4.1]}^-$   $\{[\text{Et}_2\text{NH}_2][\text{P}(\text{C}_6\text{H}_4\text{CO}_2)_3]: \delta = -135.5$  and  $[\text{Et}_3\text{NH}][\text{P}(\text{C}_6\text{H}_4\text{CO}_2)_3]: \delta = -135.7$  in DMF- $d_7\}$ .<sup>392</sup> In the case of  $[\text{PhNH}_3]\text{-rac-mer-[4.1]}$ , the  $^{31}\text{P}\{^1\text{H}\}$  NMR spectrum in DMSO- $d_6$  was accompanied by a second signal at  $-55.7$  ppm (ca. 5%). The downfield signal is attributed to the formation of a small amount of  $\text{P}(\text{C}_6\text{H}_4\text{CO}_2)_2(\text{C}_6\text{H}_4\text{COOH})$ , **4.2**, from the solution protonation of  $\text{mer-[4.1]}^-$ . Spectroscopic analysis of the other salts in acetone- $d_6$  or DMSO- $d_6$  solutions showed only the signal attributed to  $\text{mer-[4.1]}^-$ , even after several weeks at ambient temperature. Whilst the  $^{31}\text{P}\{^1\text{H}\}$  NMR spectrum of  $[(-)\text{-brucineH}]\text{-rac-mer-[4.1]}$  recorded in DMSO- $d_6$  showed only a singlet resonance ( $\delta = -135.2$ ), that recorded in  $\text{CD}_2\text{Cl}_2$  displayed two resonances ( $\delta = -114.3$  and  $-114.6$ ), see Figure 4.2. We speculate that these observations suggest that there is ion-pairing in the solvent of lower polarity (*i.e.*  $\text{CD}_2\text{Cl}_2$ ) to afford the distinct diastereomers  $[(-)\text{-brucineH}]\text{-}\Delta\text{-mer-[4.1]}$  and  $[(-)\text{-brucineH}]\text{-}\Lambda\text{-mer-[4.1]}$ , which have slightly different chemical shifts.

**Table 4-1.**  $^{31}\text{P}\{^1\text{H}\}$  and  $^1\text{H}$ -NMR chemical shifts of  $[\text{N}_{\text{base}}\text{H}]\text{-rac-mer-[4.1]}$ .

| Compound  | $[\text{N}_{\text{base}}\text{H}]^+\text{-rac-mer-[4.1]}^-$ |                    |
|---|---|--------------------|
|   | $\delta^{31}\text{P}$                                       | $\delta^1\text{H}$ |
| $[\text{NPhMe}_2\text{H}]\text{-rac-mer-[4.1]}$                         | $-107.7^{(a)}$  | $9.31^{(a)}$       |
| $[\text{PhNH}_3]\text{-rac-mer-[4.1]}$                                  | $-133.6^{(b)}$  | $6.56^{(b)}$       |
| $[\text{pyH}]\text{-rac-mer-[4.1]}$                                     | $-126.8^{(a)}$  | $16.37^{(c)}$      |
| $[\text{isoquinolineH}]\text{-rac-mer-[4.1]}$                           | $-104.7^{(a)}$  | $16.34^{(c)}$      |
| $[(-)\text{-brucineH}]\text{-rac-mer-[4.1]}$                            | $-135.2^{(b)}$  | $10.60^{(b)}$      |
| $[(-)\text{-brucineH}]\text{-rac-mer-[4.1]}$                            | $-114.3, -114.6^{(c)}$                                      | $12.63^{(c)}$      |
| $[(n\text{-C}_8\text{H}_{17})_3\text{NH}]\text{-rac-mer-[4.1]}$         | $-128.9^{(a)}$  | $10.40^{(c)}$      |
| $[\text{NEt}_2\text{H}_2][\text{P}(\text{C}_6\text{H}_4\text{CO}_2)_3]$ | $-135.5^{(d) 392}$  | NA                 |
| $[\text{NEt}_3\text{H}][\text{P}(\text{C}_6\text{H}_4\text{CO}_2)_3]$   | $-135.7^{(d) 392}$  | NA                 |

<sup>(a)</sup> in  $(\text{CH}_3)_2\text{CO-}d_6$ ; <sup>(b)</sup> in  $(\text{CH}_3)_2\text{SO-}d_6$ ; <sup>(c)</sup>  $\text{CH}_2\text{Cl}_2\text{-}d_2$ ; <sup>(d)</sup> in  $\text{C}_3\text{H}_7\text{NO-}d_7$ .

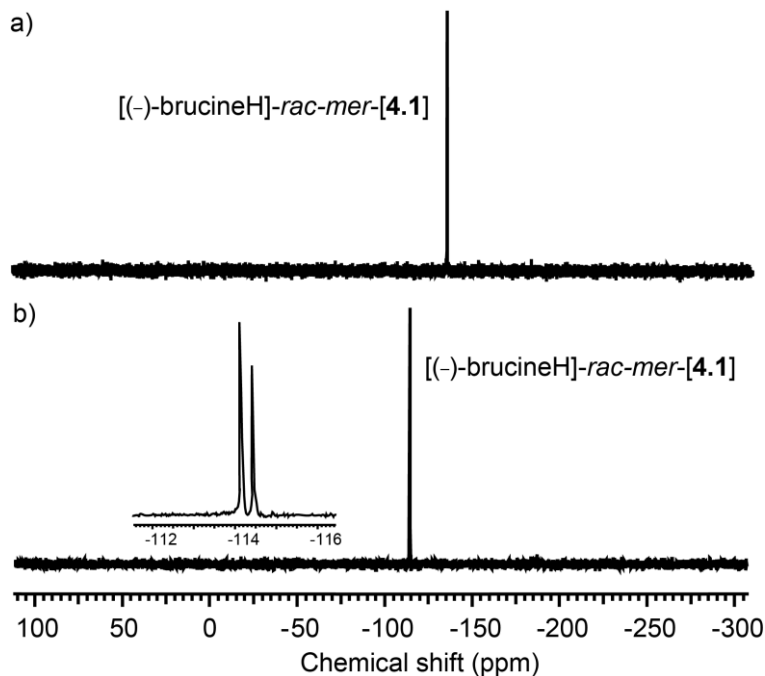


**Figure 4.2.**  $^{31}\text{P}\{^1\text{H}\}$  NMR (162 MHz, 25 °C) spectra of a)  $[(-)\text{-brucineH}]\text{-rac-mer-[4.1]}$  recorded in  $(\text{CD}_3)_2\text{SO}$  and b)  $[(-)\text{-brucineH}]\text{-rac-mer-[4.1]}$  recorded in  $\text{CD}_2\text{Cl}_2$  solvent.

The new ammonium salts were also characterized by  $^1\text{H}$  NMR spectroscopy and the spectra were consistent with the assigned formulation  $[\text{N}_{\text{base}}\text{H}]\text{-mer-}[\mathbf{4.1}]$  (see Appendix C). The acidic protons,  $[\text{N}_{\text{base}}\text{H}]\text{-mer-}[\mathbf{4.1}]$ , were detected with a wide range of chemical shifts. For instance, the signal assigned to the  $\text{N}_{\text{base}}\text{H}$  protons in the related isoquinolinium and pyridinium salts were observed at 16.34 and 16.37 ppm, respectively, in  $\text{CD}_2\text{Cl}_2$  solution. For comparison, the same proton of the pyridinium salt,  $[\text{pyH}][\text{As}(\text{N}_3)_6]$ , resonates slightly upfield [ $\delta = 13.6$  (in  $\text{CD}_2\text{Cl}_2$ )].<sup>393</sup> Although slightly upfield from the pyridinium salt, the chemical shifts of acidic protons in the tertiary ammonium salts were quite similar  $[\text{PhNMe}_2\text{H}]\text{-rac-mer-}[\mathbf{4.1}]$ :  $\delta = 9.31$  (in acetone- $d_6$ );  $[(n\text{-C}_8\text{H}_{17})_3\text{NH}]\text{-rac-mer-}[\mathbf{4.1}]$ :  $\delta = 9.76$  (in acetone- $d_6$ ), 10.40 (in  $\text{CD}_2\text{Cl}_2$ );  $[(-)\text{-brucineH}]\text{-rac-mer-}[\mathbf{4.1}]$ :  $\delta = 10.60$  (in DMSO- $d_6$ );  $[(-)\text{-brucineH}]\text{-}\Lambda\text{-mer-}[\mathbf{4.1}]$ :  $\delta = 12.63$  (in  $\text{CD}_2\text{Cl}_2$ ). The related salt featuring the weakly coordinating fluoroarylborate anion,  $[\text{PhNMe}_2\text{H}][\text{HB}(\text{C}_6\text{F}_5)_3]$ , exhibits a very similar chemical shift [ $\delta = 8.88$  ppm (in  $\text{CD}_2\text{Cl}_2$ )].<sup>394</sup> Slightly different was the anilinium salt,  $[\text{PhNH}_3]\text{-rac-mer-}[\mathbf{4.1}]$ , wherein a much higher field shift was observed [ $\delta = 6.56$  (in DMSO- $d_6$ )]. However, this behavior is quite similar to that observed for  $[\text{PhNH}_3][\text{BF}_4]$  [ $\delta = 8.20$  (in  $\text{CD}_3\text{CN}$ )].<sup>395</sup>

Additional insight into the solution behavior of the new salts was gained from their  $^{13}\text{C}\{^1\text{H}\}$  NMR spectroscopic analysis. Although the spectra (see Appendix C) displayed signals consistent with the assigned formulations, the fact that the carboxylate ligands within  $\text{mer-}[\mathbf{4.1}]^-$  were inequivalent is noteworthy. For instance, three signals were observed that were assigned to the  $\text{C}=\text{O}$  moieties (range:  $\delta = 163.9\text{--}170.7$ ), whilst eighteen signals were observed that were assigned to the aromatic carbons. In the case of  $[(-)\text{-brucineH}]\text{-rac-mer-}[\mathbf{4.1}]$ , the  $^{13}\text{C}$  NMR spectrum revealed that most signals assigned to the anion were broadened or split when compared to those of enantiomerically pure  $[(-)\text{-brucineH}]\text{-}\Lambda\text{-mer-}[\mathbf{4.1}]$ . This is most likely attributable to diastereotopism, which results from weak cation-anion interactions that differentiate  $[(-)\text{-brucineH}]\text{-}\Delta\text{-mer-}[\mathbf{4.1}]$  and  $[(-)\text{-brucineH}]\text{-}\Lambda\text{-mer-}[\mathbf{4.1}]$ .

*mer*-[4.1]. A similar phenomenon was discussed above for the  $^{31}\text{P}$  NMR analysis of this compound. Overall, the  $^{13}\text{C}\{^1\text{H}\}$  NMR spectroscopic data suggested significant asymmetry within anion *mer*-[4.1] $^-$  in solution that has not previously been observed with salts featuring the TRISPHAT anion,  $[\text{P}(\text{O}_2\text{C}_6\text{Cl}_4)_3]^-$ .<sup>265,396</sup> The asymmetry within *mer*-[4.1] $^-$  will be discussed further in the next section as this is also observed in the solid state.

## 4.2.2 Metrical Parameters Determined by X-ray Crystallography

Fortuitously, several of the new salts featuring [4.1] $^-$  afforded single-crystals suitable for X-ray crystallographic analysis. Each complex crystallizes as the *mer*-[4.1] $^-$  isomer and has been also observed by Holmes and co-workers<sup>392,434</sup> and each *mer*-[4.1] $^-$  isomer has solvent molecules of crystallization. The molecular structures of  $[\text{PhNMe}_2\text{H}]\text{-rac-mer-[4.1]}\cdot\text{Me}_2\text{C=O}$ ,  $[\text{pyH}]\text{-rac-mer-[4.1]}\cdot 0.5 \text{ Me}_2\text{C=O}$ ,  $[\text{isoquinolineH}]\text{-rac-mer-[4.1]}\cdot\text{isoquinoline}$ , and enantiomerically pure  $(-)\text{-brucineH}\text{-}\Lambda\text{-mer-[4.1]}\cdot 2 \text{ CH}_2\text{Cl}_2$  are displayed in Figure 4.3. The assignment of the  $\Lambda$ -configuration of [4.1] $^-$  in the latter structure is supported by the Flack parameter of 0.05(8).

In each salt, the closest cation-anion contact is a hydrogen-bonding interaction between the acidic N-H proton and the oxygen in the C=O moiety of anion *mer*-[4.1] $^-$ . Specifically, the  $\text{O}\cdots\text{H}$  distances are similar in  $[\text{PhNMe}_2\text{H}]\text{-rac-mer-[4.1]}$  [ $\text{O}(2)\cdots\text{H}(1) = 1.67(3) \text{ \AA}$ ],  $[\text{pyH}]\text{-rac-mer-[4.1]}$  [ $\text{O}(2)\cdots\text{H}(1) = 1.92(4) \text{ \AA}$ ],  $(-)\text{-brucineH}\text{-}\Lambda\text{-mer-[4.1]}$  [ $\text{O}(2)\cdots\text{H}(1) = 1.88(1) \text{ \AA}$ ]. In each case, these contacts are well within the sum of the van der Waals radii for oxygen and hydrogen [ $r_{\text{vdw}} = 2.72 \text{ \AA}$ ].<sup>306</sup> In contrast, the analogous  $\text{O}\cdots\text{H}$  distance in  $[\text{isoquinolineH}]\text{-rac-mer-[4.1]}$  is  $3.13(9) \text{ \AA}$  [ $\text{O}(6)\cdots\text{H}(1)$ ] suggesting little to no significant cation-anion interaction. This may be a consequence of the presence

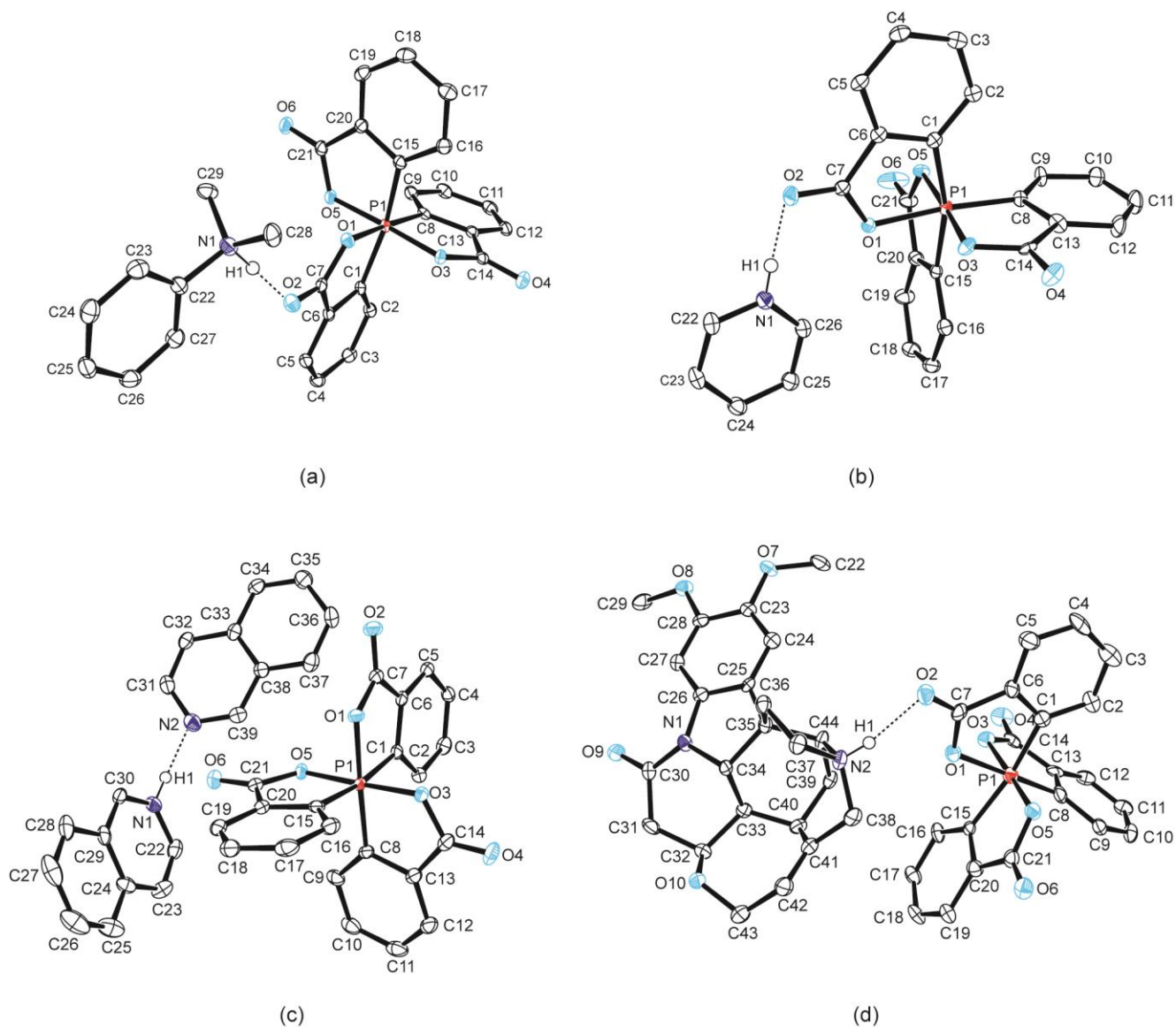


**Figure 4.3.** Molecular structures of (a) [PhNMe<sub>2</sub>H]-*rac-mer*-[4.1]·Me<sub>2</sub>C=O ( $\Delta$  isomer is shown); (b) [pyH]-*rac-mer*-[4.1]·0.5 Me<sub>2</sub>C=O ( $\Delta$  isomer is shown); (c) [isoquinolineH]-*rac-mer*-[4.1]·(C<sub>9</sub>H<sub>7</sub>N) ( $\Delta$  isomer is shown); (d) [(–)-brucineH]- $\Lambda$ -*mer*-[4.1]·2.02 CH<sub>2</sub>Cl<sub>2</sub>. Ellipsoids are drawn at the 50% probability level. Solvents of crystallization and hydrogen atoms are omitted for clarity, except for H(1). Only one enantiomer is shown in 5(a)-(c), whereas 5(d) is enantiomerically pure.

of a second hydrogen bonding interaction involving the isoquinoline solvent molecule  $[N(2)\cdots H(1) = 1.76(8) \text{ \AA}]$ , cf.  $r_{vdw} = 2.75 \text{ \AA}$ .<sup>306</sup> Similar H-bonding interactions have been reported for  $[isoquinolineH]_4 [isoquinoline]_2 [Mo_8O_{26}] [N(3)\cdots H(1A) = 1.84(1) \text{ \AA}]$ .<sup>397</sup> No such interactions between the acidic N–H proton and solvent are present in the other salts.

The ammonium salts show N–H distances within the cation that are typical of those found in related salts, especially given the difficulty determining H-positions. For instance, the *N,N'*-dimethylanilinium salt has an N–H distance of  $1.04(3) \text{ \AA}$   $[N(1)–H(1)]$ , which is at the long end of the typical range [range:  $0.84(5)–1.083(2) \text{ \AA}$ ].<sup>398–407</sup> The pyridinium salt features a slightly shorter N–H distance of  $0.85(4) \text{ \AA}$   $[N(1)–H(1)]$  that is within the range found in related salts featuring  $[pyH]^+$  [range:  $0.77(6)–0.88(2) \text{ \AA}$ ].<sup>408–413</sup> The analogous distance within  $[isoquinolineH]–rac–mer–[4.1]$  is  $0.94(7) \text{ \AA}$   $[N(1)–H(1)]$ , which fits in the middle of the normal range [range:  $0.848(8)–1.13(3) \text{ \AA}$ ].<sup>397,414–417</sup> Likewise, the N–H distance in  $[(-)-brucineH]–\Lambda–mer–[4.1]$   $[N(2)–H(1) = 0.88(9) \text{ \AA}]$  is also in the typical range [range:  $0.80(3)–0.96(5) \text{ \AA}$ ].<sup>418–425</sup> As mentioned earlier, there is significant asymmetry within the phosphorus(V) anion,  $mer–[4.1]^-$ , as concluded from solution-state NMR spectroscopic studies. In the solid state, the asymmetry is immediately apparent on consideration of the P–O bond lengths. In each case, the P–O bond of the carboxylate moiety that is H-bonded to the ammonium cation is significantly longer than the uncoordinated carboxylate moiety (see Appendix C, Table C1). For example, the P(1)–O(1) bond length in  $[PhNMe_2H]–rac–mer–[4.1]$  of  $1.92(1) \text{ \AA}$  is significantly elongated relative to P(1)–O(3) and P(1)–O(5) [ $1.778(1)$  and  $1.774(1) \text{ \AA}$ ], respectively. For comparison, the P(V)–O bond lengths found in related anions are slightly shorter than in  $mer–[4.1]^-$  {e.g.  $1.72 \text{ \AA}$  in  $[P(O_2C_6H_4)_3]^-$ ,  $1.71 \text{ \AA}$  in  $[P(O_2C_6Cl_4)_3]^-$ ,  $1.69 \text{ \AA}$  in  $[P(C_2O_4)_3]^-$ }.<sup>248,250,252,396</sup> Virtually identical metrical parameters to those described above are observed in the molecular structures of  $[pyH]–rac–mer–[4.1]$  and  $[(-)-brucineH]–\Lambda–mer–[4.1]$ . Likewise, analogous observations were made with the previously

characterized [NEt<sub>2</sub>H<sub>2</sub>][**4.1**] and [Et<sub>3</sub>NH][**4.1**] [avg.<sub>P(V)-O</sub>: 1.853(3) Å and 1.856(8) Å, respectively] with asymmetry within *mer*-[**4.1**]<sup>-</sup>.<sup>392</sup>

### 4.2.3 Placement of *mer*-[**4.1**]<sup>-</sup> on IR Scale for WCAs

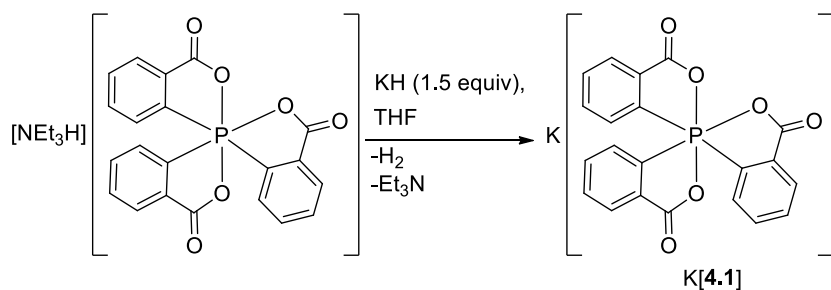
Based on the above results that suggest significant coordinating properties for *mer*-[**4.1**]<sup>-</sup>, we analyzed *mer*-[**4.1**]<sup>-</sup> in the context of the simple infrared scale proposed by Reed and co-workers to assess WCA properties.<sup>426</sup> Since there is no absolute scale to compare the WCA properties of specific anions, this analysis provides a rough idea of the donor properties of *mer*-[**4.1**]<sup>-</sup>. Specifically, the method involves comparing the N–H stretching frequencies of tri(*n*-octyl)ammonium salts in the solid-state and in solution. Solution spectra are recorded in carbon tetrachloride, where (*n*-C<sub>8</sub>H<sub>17</sub>)<sub>3</sub>N<sup>+</sup>–H···A<sup>-</sup> contact ion pairs are typically formed to varying extents dependent upon the anion. The results for *mer*-[**4.1**]<sup>-</sup> and for selected anions are presented in Table 4.2. The stretching frequency for [(*n*-C<sub>8</sub>H<sub>17</sub>)<sub>3</sub>NH]–*mer*-[**4.1**] in CCl<sub>4</sub> ( $\nu_{\text{N-H}} = 3069 \text{ cm}^{-1}$ , 0.01 M) was close to those of classical WCAs such as [ClO<sub>4</sub>]<sup>-</sup> ( $\nu_{\text{N-H}} = 3050, 2801 \text{ cm}^{-1}$ ) and [N(SO<sub>2</sub>CF<sub>3</sub>)<sub>2</sub>]<sup>-</sup> ( $\nu_{\text{N-H}} = 3086 \text{ cm}^{-1}$ ). For comparison, very weakly donating [B(C<sub>6</sub>F<sub>5</sub>)<sub>4</sub>]<sup>-</sup> and [CMeB<sub>11</sub>F<sub>11</sub>]<sup>-</sup> rank much higher ( $\nu_{\text{N-H}} = 3233$  and  $3219 \text{ cm}^{-1}$ , respectively), whereas the strongly donating Cl<sup>-</sup> ranks much lower ( $\nu_{\text{N-H}} = 2330 \text{ cm}^{-1}$ ). The results in the solid state also suggest that the WCA properties of *mer*-[**4.1**]<sup>-</sup> are comparable to perchlorate and triflamide according to this IR scale and are consistent with the moderate cation-anion interactions described for *mer*-[**4.1**]<sup>-</sup> in solution and in the solid-state.

**Table 4-2.  $\nu$ N–H frequencies for  $[(n\text{-C}_8\text{H}_{17})_3\text{NH}]^+[\text{Anion}]^-$  salts in  $\text{CCl}_4$  and solid state.**

| [Anion] <sup>−</sup>                     | $\nu$ N–H<br>in $\text{CCl}_4$ solution | $\nu$ N–H<br>solid or wax | Reference |
|--|---|---------------------------|-----------|
| $[\text{B}(\text{C}_6\text{F}_5)_4]^-$   | 3233                                    | 3241                      | 426       |
| $[\text{PF}_6]^-$                        | 3191                                    | 3219                      | 426       |
| $[\text{BF}_4]^-$                        | 3133                                    | 3156                      | 426       |
| $[\text{N}(\text{SO}_2\text{CF}_3)_2]^-$ | 3086                                    | –                         | 426       |
| <b>[4.1]<sup>−</sup></b>                 | 3069                                    | 3064                      | This work |
| $[\text{ClO}_4]^-$                       | 3050, 2801                              | 3098                      | 426       |
| $[\text{CF}_3\text{SO}_3]^-$             | 3031, 2801                              | 3056, 2815                | 426       |
| $[\text{NO}_3]^-$                        | 2451                                    | 2571                      | 426       |
| $[\text{Cl}]^-$                          | 2330                                    | 2452                      | 426       |

#### 4.2.4 Preparation of $\text{K}^+$ and $\text{H}^+$ Salts of *mer*–[4.1]<sup>−</sup>

With several ammonium salts in hand and a preliminary ranking of *mer*–[4.1]<sup>−</sup> as a WCA, we have explored the potential synthesis of alkali metal-based salts and stronger Brønsted acids. Treating a THF solution of  $[\text{NEt}_3\text{H}][4.1]$  with KH (1.5 equiv) (Scheme 4.2) resulted in the immediate evolution of a gaseous species (presumably  $\text{H}_2$ ). Over 2 h, a colorless precipitate was observed that was separated and dried. The solid was dissolved in methanol- $d_4$  and the solution was analyzed by  $^{31}\text{P}\{^1\text{H}\}$  NMR spectroscopy. A singlet resonance was observed at  $-127.6$  ppm, consistent with the preservation of the anion *mer*–[4.1]<sup>−</sup>. Additional characterization by  $^1\text{H}$  and  $^{13}\text{C}\{^1\text{H}\}$  NMR spectroscopy as well as mass spectrometry {ESI (negative mode):  $m/z = 391.0$ , *mer*–[4.1]<sup>−</sup>} supported the formulation of the product as *K-rac-mer*–[4.1].



**Scheme 4.2. Synthetic route of K-*rac-mer*-[4.1].**

Confirmation of this tentative assignment was obtained by X-ray crystallographic analysis of crystals obtained from the methanol- $d_4$  solution. The molecular structure is shown in Figure 4.4 and reveals that K-*rac-mer*-[4.1] is a coordination polymer with  $\text{K}^+$  ions bridging the anion centers. There are two crystallographically unique *mer*-[4.1] $^-$  anions and three unique  $\text{K}^+$  cations. Interestingly, K(2) is bound by two short and two long contacts to four different *mer*-[4.1] $^-$  anions [ $\text{K}(2) \cdots \text{O}(6) = 2.660(2) \text{ \AA}$ ,  $\text{K}(2) \cdots \text{O}(8) = 2.668(2) \text{ \AA}$ ,  $\text{K}(2) \cdots \text{O}(12) = 2.926(2) \text{ \AA}$ ,  $\text{K}(2) \cdots \text{O}(2) = 3.019(2) \text{ \AA}$ ] and by three methanol molecules [ $\text{K} \cdots \text{O}_{\text{avg}} = 2.762(5) \text{ \AA}$ ]. In stark contrast, K(1) and K(3) both sit on special positions and are bound by eight oxygen atoms. In each case, there are two short and two long  $\text{K} \cdots \text{O}=\text{C}$  contacts [avg. =  $2.727(3)$  and  $3.038(3) \text{ \AA}$ ], two  $\text{K} \cdots \text{O}-\text{P}$  contacts [avg.  $3.028(3) \text{ \AA}$ ] and two  $\text{K} \cdots \text{OMe}$  contacts [avg. =  $2.787(5) \text{ \AA}$ ]. The longer contacts involve binding of  $\text{K}^+$  by two chelating  $\text{CO}_2$  moieties of anion *mer*-[4.1] $^-$  (*i.e.* four  $\text{K} \cdots \text{O}$  interactions), which are related by inversion symmetry around  $\text{K}^+$ . For comparison, a survey of the Cambridge Crystallographic Database revealed  $\text{K} \cdots \text{O}=\text{C}$  contacts [between  $2.678(2)$ – $3.135(3) \text{ \AA}$ ]<sup>427-431</sup> and  $\text{K} \cdots \text{OMe}$  contacts of methanol [ $2.750(2)$ – $3.369(3) \text{ \AA}$ ].<sup>432,433</sup> Thus, the two short  $\text{K} \cdots \text{O}=\text{C}$  contacts to anion *mer*-[4.1] $^-$  and the contacts to either two or three methanol molecules are at the short end of this range. The remaining contacts are at the long end of this range.

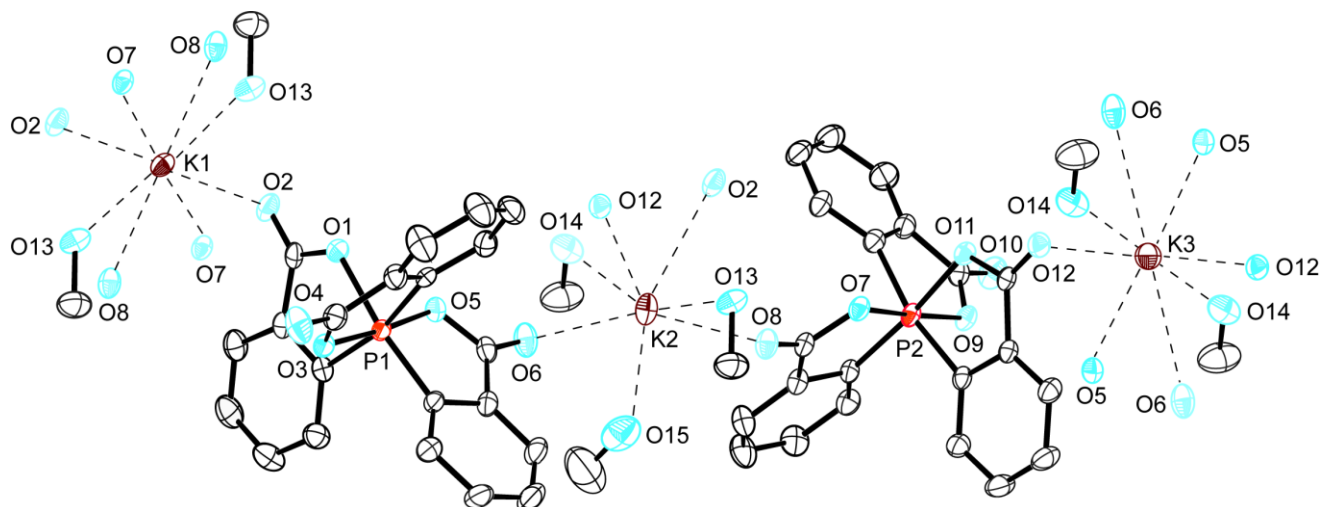
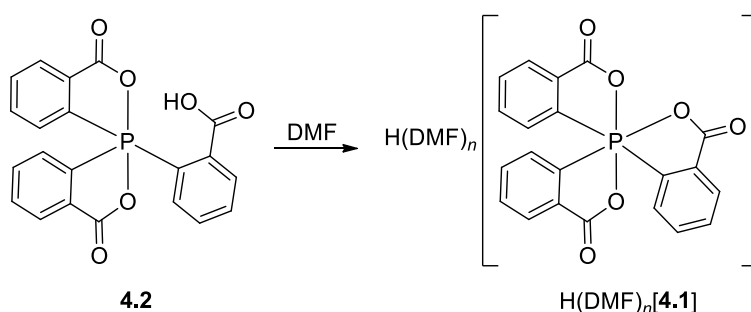


**Figure 4.4.** Extended structure showing the coordination polymer formed by  $K\text{-rac-mer-[4.1]}\cdot 3 \text{CH}_3\text{OH}$  ( $K\text{-}\Lambda,\Delta\text{-mer-[4.1]}$  is shown). Ellipsoids are drawn at the 50% probability level. Hydrogen atoms are omitted for clarity. O(13), O(14), O(15) are methanol solvate oxygen atoms. Oxygen atoms O(2), O(5), O(6), O(7), O(8), and O(12) are associated with anion  $\text{mer-[4.1]}^-$  related by inversion symmetry around  $\text{K}^+$  with O(13)\* (1-x, 1-y, 1-z), O(13) (-1+x, y, z), O(7)\* (1-x, 1-y, 1-z), O(8)\* (1-x, 1-y, 1-z), O(2)\* (-x, 1-y, 1-z), O(5)\* (2-x, 1-y, 1-z), O(6)\* (2-x, 1-y, 1-z), O(14)\* (2-x, 1-y, 1-z), O(12)\* (3-x, 1-y, 1-z), O(14) (1+x, y, z), O(6) (1+x, y, z), O(5) (1+x, y, z), O(12)\* (2-x, 1-y, 1-z), and O(2)\* (1-x, 1-y, 1-z).

Analogous to the aforementioned ammonium salts, the phosphorus(V) anion,  $\text{mer-[4.1]}^-$ , displays significant asymmetry. For instance, the P(1)–O(1) bond length [1.906(2) Å] is significantly longer than the P(1)–O(3) and P(1)–O(5) bonds [1.765(2) and 1.786(2) Å]. The situation is identical for P(2) with one long bond [P(2)–O(11) = 1.902(3) Å] and two short bonds [P(2)–O(7) = 1.785(2), P(2)–O(9) = 1.767(2) Å]. The elongated P–O bond in  $\text{mer-[4.1]}^-$  is not involved in binding to  $\text{K}^+$  in  $K\text{-rac-mer-[4.1]}$ , whereas for  $[\text{PhNMe}_2\text{H}]\text{-rac-mer-[4.1]}$ ,  $[\text{pyH}]\text{-rac-mer-[4.1]}$  and  $[(\text{-})\text{-brucineH}]\text{-}\Lambda\text{-mer-[4.1]}$  the elongated P–O moiety of  $\text{mer-[4.1]}^-$  is the one that is involved in hydrogen bonding to the cation. In all cases, the P–C bond lengths in  $\text{mer-[4.1]}^-$  do not show significant differences.

We finally explored the potential synthesis of strong Brønsted acids of  $mer\text{-}[4.1]^-$  by dissolving phosphorane **4.2** in weakly basic solvents such as DMF (Scheme 4.3). Heating the reaction mixture to 120 °C and monitoring the reaction progress by  $^{31}\text{P}\{^1\text{H}\}$  NMR spectroscopy suggested the quantitative formation of  $mer\text{-}[4.1]^-$  after one month. Namely, the signal assigned to phosphorane **4.2** ( $\delta = -55.9$ ) was replaced by two sharp singlet resonances at  $-134.6$  and  $-138.9$  ppm (ca. 9:1 ratio) (see Figure 4.5). The chemical shift of these anions is consistent with that previously observed for anion  $mer\text{-}[4.1]^-$  (Table 4.1) and the presence of two signals may suggest both  $mer\text{-}$  and  $fac\text{-}$  isomers or strong ion-pairing as observed for  $[(-)\text{-brucineH}]\text{-}mer\text{-}[4.1]$ .



**Scheme 4.3.** Proposed route to  $\text{H(DMF)}_n\text{-}mer\text{-}[4.1]$  ( $n \geq 1$ ).

Although attempts to isolate or crystallize this product were not successful, the major signal in the negative mode in the electrospray mass spectrum (ESI-MS) was consistent with the formulation of  $mer\text{-}[4.1]^-$  ( $m/z = 390.9$ ; calcd mass of  $mer\text{-}[4.1]^- = 391.0$ ). The positive mode ESI-MS showed a signal that may be consistent with the cation  $[\text{H(DMF)}]^+$  ( $m/z = 74.4$ , DMF calcd  $m/z = 73.09$ ). We hope that more definitive information about the formula of this exciting new compound can be provided in a future report.

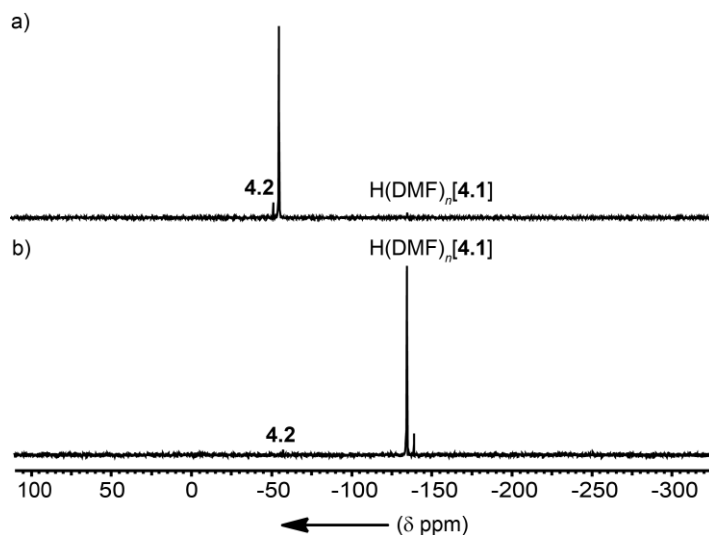


Figure 4.5.  $^{31}\text{P}\{^1\text{H}\}$  NMR (162 MHz, 25 °C) spectra of a) reaction mixture of  $\text{H}(\text{DMF})_n\text{-mer-[4.1]}$  recorded after 2 days and b) reaction mixture of  $\text{H}(\text{DMF})_n\text{-mer-[4.1]}$  recorded after ca. 4 weeks.

4.2 is phosphorane  $\text{P}(\text{C}_6\text{H}_4\text{CO}_2)_2(\text{C}_6\text{H}_4\text{COOH})$ .

### 4.3 Summary

The synthesis, isolation and characterization of a series of salts incorporating the hexacoordinate phosphorus(V) anion  $\text{mer-[4.1]}^-$  has been reported.. These compounds were conveniently obtained by treating phosphorane  $\text{P}(\text{C}_6\text{H}_4\text{CO}_2)_2(\text{C}_6\text{H}_4\text{COOH})$  with an N-containing base or KH. The complexes  $[\text{PhNMe}_2\text{H}]\text{-rac-mer-[4.1]}$ ,  $[\text{pyH}]\text{-rac-mer-[4.1]}$ ,  $[\text{isoquinolineH}]\text{-rac-mer-[4.1]}$ ,  $[(-)\text{-brucineH}]\text{-}\Lambda\text{-mer-[4.1]}$ , and  $\text{K-rac-mer-[4.1]}$  were fully characterized by spectroscopic means and X-ray crystallography.  $[\text{PhNH}_3]\text{-rac-mer-[4.1]}$  and  $[(n\text{-C}_8\text{H}_{17})_3\text{NH}]\text{-rac-mer-[4.1]}$  were characterized by NMR spectroscopy. The  $^{31}\text{P}\{^1\text{H}\}$  NMR spectrum of  $[(-)\text{-brucineH}]\text{-rac-mer-[4.1]}$  recorded in  $\text{CD}_2\text{Cl}_2$  solution revealed signals for one pair of diastereomers. The solid state structure elucidated enantiomerically pure  $[(-)\text{-brucineH}]\text{-}\Lambda\text{-mer-[4.1]}$  obtained from a  $\text{CH}_2\text{Cl}_2$  solution. The solid state structure of  $\text{K-rac-mer-[4.1]}$  revealed a coordination polymer with  $\text{K}^+$  ions bridging the anion centers. A preliminary assessment of the basicity of the  $\text{mer-[4.1]}^-$  was conducted and revealed that the

tri(*n*-octyl)ammonium salt has a similar  $\nu_{\text{N-H}}$  frequency to the salts of  $[\text{ClO}_4]^-$  and  $[\text{N}(\text{SO}_2\text{CF}_3)_2]^-$ . Finally, preliminary evidence for the potential synthesis of the Brønsted acid  $\text{H}(\text{DMF})_n\text{-mer-[4.1]}$  has been obtained. Future work will explore the potential isolation of these novel protic species and the possible applications of the  $\text{mer-[4.1]}^-$  ion as a novel WCA for application in catalysis and polymerization.

.

## 4.4 Experimental

### 4.4.1 General Procedures

All experiments were performed using standard Schlenk or glove box techniques under nitrogen atmosphere.  $\text{CH}_2\text{Cl}_2$  (Sigma Aldrich) was deoxygenated with nitrogen and dried by passing through a column containing activated alumina.  $\text{CH}_2\text{Cl}_2$  (Sigma Aldrich) was deoxygenated with nitrogen and dried by passing the solvent through a column containing activated, basic alumina. Subsequently,  $\text{CH}_2\text{Cl}_2$  was dried over  $\text{CaH}_2$ , freshly distilled, and freeze-pump-thaw (x3) degassed. Acetonitrile (Sigma Aldrich) and DMF (Fisher Scientific) were dried over calcium hydride, freshly distilled, and freeze-pump-thaw (x3) degassed. Acetone (Fisher Scientific) was dried over calcium sulfate and freshly distilled. For extended periods of storage (1 day to 2 weeks), anhydrous solvents were stored over 3 Å molecular sieves. THF (Fisher Scientific) was freshly distilled from sodium/benzophenone ketyl immediately prior to use.  $(\text{C}_6\text{H}_4\text{CO}_2)_2\text{P}(\text{C}_6\text{H}_4\text{CO}_2\text{H})$ <sup>434</sup> and  $[\text{NEt}_3\text{H}][\text{P}(\text{C}_6\text{H}_4\text{CO}_2)_3]$ <sup>392</sup> were prepared following literature procedure. Potassium hydride (30 wt% dispersion in mineral oil) was purchased from Sigma Aldrich, washed with hexanes and dried *in vacuo* prior to use. (–)-Brucine (Sigma Aldrich) was dried under vacuum at 40 °C prior use. Aniline (Sigma Aldrich) and *N,N'*-dimethylaniline (Sigma Aldrich) were dried over  $\text{CaH}_2$  and freshly distilled under partial vacuum at 40 °C. Pyridine (Fisher Scientific), trimethylamine (Fisher Scientific), and isoquinoline (Sigma Aldrich) were distilled under

partial vacuum at 30–50 °C. Tri(*n*-octyl)amine, N(*n*-C<sub>8</sub>H<sub>17</sub>)<sub>3</sub> (Sigma Aldrich) was degassed with N<sub>2</sub> gas prior to use. Elemental analyses, mass spectrometry and NMR spectra were performed in the Chemistry Department Facilities. <sup>1</sup>H, <sup>13</sup>C{<sup>1</sup>H} and <sup>31</sup>P{<sup>1</sup>H} NMR spectra were recorded on Bruker Avance 400 MHz spectrometers at ambient temperature unless noted. H<sub>3</sub>PO<sub>4</sub> (85 %) was used as external standard for <sup>31</sup>P NMR spectra with  $\delta = 0.0$ . <sup>1</sup>H NMR and <sup>13</sup>C{<sup>1</sup>H} NMR spectra were referenced to deuterated solvents. Low resolution electrospray ionization mass spectra, ESI-LRMS, were recorded on Bruker Esquire LC mass spectrometer. High resolution electrospray ionization mass spectra, ESI-HRMS, were recorded on Micromass LCT time of flight (TOF) mass spectrometer. Infrared spectra were recorded either in powder form or in CCl<sub>4</sub> solution {0.01 M for [(*n*-C<sub>8</sub>H<sub>17</sub>)<sub>3</sub>NH][**4.1**]}. on a PerkinElmer FT-IR Frontier spectrometer.

#### 4.4.2 X-ray Structure Determination

X-ray crystallography data were collected on a Bruker X8 APEX II diffractometer with graphite-monochromated Mo K $\alpha$  radiation. A single crystal was immersed in oil and mounted on a glass fiber. Data were collected and integrated using the Bruker SAINT software package<sup>325</sup> and corrected for absorption effect using SADABS.<sup>326</sup> All structures were solved by direct methods and subsequent Fourier difference techniques. All non-hydrogen atoms were refined anisotropically. The hydrogen atom of N–H was located in a difference map and refined isotropically. All other hydrogen atoms were placed in calculated positions. All data sets were corrected for Lorentz and polarization effects. All refinements were performed using the SHELXT-2015<sup>328</sup> via the Olex2 interface.<sup>329</sup>

[PhNMe<sub>2</sub>H]–*rac-mer*–[**4.1**] crystallizes with one molecule of solvent acetone in the asymmetric unit. [pyH]–*rac-mer*–[**4.1**] was solved using non-overlapped data from a major twin component. Subsequent refinements were carried out using a data set containing complete data from component one

and any overlaps from component two. [pyH]-*rac-mer*-[4.1] crystallizes with one half-molecule of acetone in the asymmetric unit. Additionally, one coordinated benzoic acid ligand is disordered and is modelled in two orientations. [isoquinolineH]-*rac-mer*-[4.1] crystallizes as a twin, with a ~9:1 ratio between the major and minor twin components. [(-)-brucineH]- $\Lambda$ -*mer*-[4.1] crystallizes with two molecules of solvent methylene chloride in the asymmetric unit. One of these solvent molecules is disordered and was modeled in three orientations, such that their combined site occupancies summed to one. K-*rac-mer*-[4.1] crystallizes with three MeOH molecules coordinated to the potassium cation. Additionally, K-*rac-mer*-[4.1] crystallizes with disordered free MeOH in the lattice. The disorder could not be reasonably modelled; therefore the PLATON/SQUEEZE<sup>435</sup> program was used to generate a data set free of disordered solvent. O—H hydrogen atoms were located in difference maps and refined isotropically. All other hydrogen atoms were placed in calculated positions.

#### 4.4.3 Synthesis of [PhNMe<sub>2</sub>H]-*mer*-[4.1]

P(C<sub>6</sub>H<sub>4</sub>CO<sub>2</sub>)<sub>2</sub>(C<sub>6</sub>H<sub>4</sub>COOH) (0.11 g, 0.28 mmol) was dissolved in anhydrous acetone (3 mL). To the clear solution was added anhydrous *N,N'*-dimethylaniline (0.16 mL, 0.15 g, 1.23 mmol). The solution was stirred overnight and concentrated *in vacuo* to give a colorless precipitate. The crude product was washed with minimal amount of acetone and dried *in vacuo*. Single crystals suitable for X-ray diffraction analysis were obtained by cooling a concentrated solution of the crude product in anhydrous acetone (-30 °C, ca. 2 weeks). Yield = 0.23 (includes acetone).

<sup>31</sup>P{<sup>1</sup>H} NMR (162 MHz, (CD<sub>3</sub>)<sub>2</sub>CO, 25 °C):  $\delta$  -107.7; <sup>1</sup>H NMR (400 MHz, (CD<sub>3</sub>)<sub>2</sub>CO, 25 °C):  $\delta$  9.31 (br s, 1H, N(CH<sub>3</sub>)<sub>2</sub>C<sub>6</sub>H<sub>5</sub>H), 8.14–8.04 (m, 5H, Ar-H), 7.89–7.81 (m, 4H, Ar-H), 7.63–7.55 (m, 2H, Ar-H), 7.34–7.29 (m, 1H, Ar-H), 7.28–7.24 (m, 2H, N(CH<sub>3</sub>)<sub>2</sub>C<sub>6</sub>H<sub>5</sub>H), 6.95–6.91 (m, 2H, N(CH<sub>3</sub>)<sub>2</sub>C<sub>6</sub>H<sub>5</sub>H), 6.84–6.80 (tt,  $J_{\text{HH}} = 7.3$  Hz, 1H, N(CH<sub>3</sub>)<sub>2</sub>C<sub>6</sub>H<sub>5</sub>H); 2.97(s, 6H, N(CH<sub>3</sub>)<sub>2</sub>C<sub>6</sub>H<sub>5</sub>H);

$^{13}\text{C}\{^1\text{H}\}$  NMR (101 MHz,  $(\text{CD}_3)_2\text{CO}$ , 25 °C):  $\delta$  168.2 (s, C=O), 168.1 (s, C=O), 165.2 (s, C=O), 149.4 (s,  $\text{N}(\text{CH}_3)_2\text{C}_6\text{H}_5\text{H}$ ), 141.2 (s, Ar-C), 140.8 (s, Ar-C), 139.7 (s, Ar-C), 138.8 (s, Ar-C), 135.1 (s, Ar-C), 134.9 (s, Ar-C), 134.3 (s, Ar-C), 134.1 (s, Ar-C), 133.6 (d,  $J_{\text{CP}} = 3.7$  Hz, Ar-C), 132.5 (s, Ar-C), 132.3 (d,  $J_{\text{CP}} = 5.1$  Hz, Ar-C), 132.2 (s, Ar-C), 130.4 (s, Ar-C), 130.3 (s, Ar-C), 130.1 (d,  $J_{\text{CP}} = 5.1$  Hz, Ar-C), 129.3 (s, Ar-C), 129.1 (s,  $\text{N}(\text{CH}_3)_2\text{C}_6\text{H}_5\text{H}$ ), 129.0 (s, Ar-C), 128.9 (s, Ar-C), 126.7 (s,  $\text{N}(\text{CH}_3)_2\text{C}_6\text{H}_5\text{H}$ ), 126.5 (s,  $\text{N}(\text{CH}_3)_2\text{C}_6\text{H}_5\text{H}$ ), 118.1 (s,  $\text{N}(\text{CH}_3)_2\text{C}_6\text{H}_5\text{H}$ ), 114.0 (s,  $\text{N}(\text{CH}_3)_2\text{C}_6\text{H}_5\text{H}$ ), 40.9 (s,  $\text{N}(\text{CH}_3)_2\text{C}_6\text{H}_5\text{H}$ ); IR (neat)  $\nu$ : 3405 (vw), 3055 (vw), 3035 (vw), 2966 (vw), 2670 (vw), 1700 (s), 1644 (m), 1633 (sh, m), 1592 (m), 1574 (m), 1511 (m), 1495 (m), 1452 (m), 1353 (m), 1299 (vw), 1277 (s), 1241 (s), 1195 (w), 1159 (w), 1125 (s), 1110 (s), 1061 (s), 1024 (w), 994 (w), 904 (m), 852 (s), 769 (m), 748 (s), 728 (sh), 700 (s), 684 (s)  $\text{cm}^{-1}$ ; LRMS (ESI, positive mode)  $m/z = 122.3$   $[\text{M}]^+$ ; HRMS (ESI/TOF, negative mode)  $m/z = [\text{M}]^-$  calcd for  $\text{C}_{21}\text{H}_{12}\text{O}_6\text{P}_1$  391.0372; found 391.0373.

#### 4.4.4 Synthesis of $[\text{PhNH}_3]\text{-mer-[4.1]}$

$\text{P}(\text{C}_6\text{H}_4\text{CO}_2)_2(\text{C}_6\text{H}_4\text{COOH})$  (0.15 g, 0.38 mmol) was dissolved in anhydrous *N,N'*-dimethylformamide (4 mL). The white suspension was stirred at ambient temperature for 40 min until fully dissolved. Upon addition of anhydrous aniline (2.00 mL, 2.05 g, 22.0 mmol) a colorless solution was obtained, which was concentrated *in vacuo* to give a colorless oil. The oily residue was washed with anhydrous *N,N'*-dimethylformamide. Yield = 0.28 g (includes *N,N'*-dimethylformamide). A ~5 mg sample was prepared for elemental analysis by drying *in vacuo* for ca. 1 day at 40 °C.

$^{31}\text{P}\{^1\text{H}\}$  NMR (162 MHz,  $(\text{CD}_3)_2\text{SO}$ , 25 °C):  $\delta$  -133.6;  $^1\text{H}$  NMR (400 MHz,  $(\text{CD}_3)_2\text{SO}$ , 25 °C):  $\delta$  7.84–7.22 (m, 11H, Ar-H), 7.17–6.78 (m, 5H,  $\text{PhNH}_3\text{-Ar-H}$ ), 6.56 (br s, 3H,  $\text{PhNH}_3$ ), 6.10 (dd,  $J_{\text{HH}} = 7.4$  Hz, 1H, Ar-H);  $^{13}\text{C}\{^1\text{H}\}$  NMR (101 MHz,  $(\text{CD}_3)_2\text{SO}$ , 25 °C):  $\delta$  168.6 (s, C=O), 167.2 (s, C=O), 167.1 (s, C=O), 156.9 (s, Ar-C), 154.0 (s, Ar-C), 145.0 (s,  $\text{PhNH}_3$ , Ar-C), 142.3 (s, Ar-C), 133.6 (s,

Ar-C), 133.4 (s, Ar-C), 132.7 (s, Ar-C), 132.4 (s, Ar-C), 131.6 (s, Ar-C), 131.4 (s, Ar-C), 129.9 (s, Ar-C), 129.5 (s, PhNH<sub>3</sub>, Ar-C), 129.4 (d,  $J_{CP} = 6.1$  Hz, Ar-C), 129.1 (d,  $J_{CP} = 3.3$  Hz, Ar-C), 126.7 (s, Ar-C), 126.3 (d,  $J_{CP} = 14.4$  Hz, Ar-C), 125.0 (s, Ar-C), 124.8 (s, Ar-C), 121.2 (s, Ar-C), 119.7 (s, Ar-C), 119.2 (s, PhNH<sub>3</sub>, Ar-C), 116.6 (s, PhNH<sub>3</sub>, Ar-C); IR (neat)  $\nu$ : 3354 (vw), 3081 (vw), 3021 (vw), 2935 (vw), 2864 (vw), 1721 (m), 1754 (s), 1653 (s), 1594 (m), 1498 (w), 1483 (w), 1458 (s), 1397 (w), 1338 (m), 1292, (s), 1276 (s), 1253 (m), 1242 (s), 1123 (s), 1108 (s), 1063 (s), 1023 (w), 967 (w), 855 (s), 816 (m), 745 (s), 729 (m), 698 (s), 687 (s)  $\text{cm}^{-1}$ ; elem. anal. calcd for C<sub>27</sub>H<sub>20</sub>N<sub>1</sub>O<sub>6</sub>P<sub>1</sub>·0.15 C<sub>3</sub>H<sub>7</sub>N<sub>1</sub>O<sub>1</sub>: C, 66.42; H, 4.27; N, 3.27; found: C, 66.57; H, 4.07; N, 3.51.

#### 4.4.5 Synthesis of [pyH]-mer-[4.1]

To a solution of P(C<sub>6</sub>H<sub>4</sub>CO<sub>2</sub>)<sub>2</sub>(C<sub>6</sub>H<sub>4</sub>COOH) (0.36 g, 0.92 mmol) in anhydrous acetone (7 mL) was added pyridine (0.10 mL, 0.10 g, 1.26 mmol) and the colorless reaction mixture was stirred for two hours at ambient temperature to afford a colorless precipitate. The precipitate was filtered, washed with cold acetone (1.2 mL), and dried *in vacuo*. Yield = 0.26 g, 60%. Single crystals suitable for X-ray crystallography were isolated by cooling a saturated solution of the crude product in CH<sub>2</sub>Cl<sub>2</sub>/hexane (1:1) to -30 °C.

<sup>31</sup>P{<sup>1</sup>H} NMR (162 MHz, (CD<sub>3</sub>)<sub>2</sub>CO, 25 °C):  $\delta$  -126.8; <sup>31</sup>P{<sup>1</sup>H} NMR (162 MHz, CD<sub>2</sub>Cl<sub>2</sub>, 25 °C):  $\delta$  -118.1; <sup>1</sup>H NMR (400 MHz, CD<sub>2</sub>Cl<sub>2</sub>, 25 °C):  $\delta$  16.37 (s, 1H, C<sub>5</sub>H<sub>5</sub>NH), 8.45 (d,  $J_{HH} = 7.3$  Hz, 2H, Ar-H), 8.11–8.02 (m, 5H, Ar-H), 7.73–7.69 (m, 4H, Ar-H), 7.54–7.48 (m, 3H, C<sub>5</sub>H<sub>5</sub>NH), 7.46–7.41(m, 1H, C<sub>5</sub>H<sub>5</sub>NH), 7.11 (d,  $J_{HH} = 6.4$  Hz, 1H, C<sub>5</sub>H<sub>5</sub>NH), 7.06 (d,  $J_{HH} = 7.3$  Hz, 1H, Ar-H); <sup>1</sup>H NMR (400 MHz, (CD<sub>3</sub>)<sub>2</sub>CO, 25 °C):  $\delta$  15.18 (br s, 1H, N-H); <sup>13</sup>C{<sup>1</sup>H} NMR (101 MHz CD<sub>2</sub>Cl<sub>2</sub>, 25 °C):  $\delta$  170.2 (s, C=O), 170.1 (s, C=O), 166.0 (s, C=O), 146.2 (s, C<sub>5</sub>H<sub>5</sub>NH), 141.2 (s, Ar-C), 140.1 (s, Ar-C), 139.8 (s, C<sub>5</sub>H<sub>5</sub>NH), 138.1 (s, Ar-C), 134.9 (s, Ar-C), 134.7 (s, Ar-C), 134.1 (s, Ar-C), 133.9 (s, Ar-C), 133.2 (d,

$J_{CP} = 2.9$  Hz, Ar-C), 132.4 (d,  $J_{CP} = 2.9$  Hz, Ar-C), 132.1 (s, Ar-C), 131.9 (s, Ar-C), 131.2 (s, Ar-C), 131.1 (s, Ar-C), 130.1 (d,  $J_{CP} = 3.7$  Hz, Ar-C), 129.3 (s, Ar-C), 129.2 (s, Ar-C), 129.0 (s, Ar-C), 128.9 (s, Ar-C), 126.8 (s,  $C_5H_5NH$ ); 126.7 (s,  $C_5H_5NH$ ); 125.0 (s,  $C_5H_5NH$ ); IR (neat)  $\nu$ : 3187 (vw), 3132 (vw), 3101 (w), 3068 (vw), 2141 (vw), 1721 (m), 1699 (s), 1638 (m), 1613 (sh, m), 1593 (sh, m), 1574 (w), 1548 (m), 1482 (m), 1455 (m), 1399 (vw), 1352 (m), 1309 (w), 1274 (s), 1239 (s), 1159 (m), 1127 (m), 1112 (s), 1065 (m), 1059 (m), 1025 (w), 1001 (w), 881 (vw), 854 (s), 819 (w), 759 (s), 730 (m), 669 (s), 661 (s)  $cm^{-1}$ ; elem. anal. calcd for  $C_{26}H_{18}NO_6P_1 \cdot 0.2 CH_2Cl_2$ : C, 64.87; H, 3.81; N, 2.89; found: C, 64.96; H, 4.06; N, 2.80.

#### 4.4.6 Synthesis of [isoquinolineH]-mer-[4.1]

To a solution of  $P(C_6H_4CO_2)_2(C_6H_4COOH)$  (0.21 g, 0.54 mmol) in anhydrous acetone (9 mL) was added isoquinoline (0.11 mL, 0.12 g, 0.93 mmol) via syringe. The reaction mixture was stirred for 2 days at ambient temperature and the solvent was removed *in vacuo*. The residue was dissolved in  $CH_2Cl_2$ /hexane (4mL/3mL) and stored at  $-30$  °C to give a colorless precipitate. The precipitate was filtered, washed with minimal amount of  $CH_2Cl_2$ , and dried *in vacuo*. Yield = 0.19 g, 68 %. The aforementioned filtrate was cooled ( $-30$  °C) to afford single crystals suitable for X-ray crystallography.

$^{31}P\{^1H\}$  NMR (162 MHz,  $(CD_3)_2CO$ , 25 °C):  $\delta$  -104.7;  $^1H$  NMR (400 MHz,  $CD_2Cl_2$ , 25 °C):  $\delta$  16.34 (s, 1H, NH), 9.19 (s, 1H, isoquinoline-Ar-H), 8.29 (d, 1H, isoquinoline-Ar-H), 8.09–8.04 (m, 5H, isoquinoline-Ar-H), 8.02–7.41 (m, 11H, Ar-H), 6.99(dd,  $J_{HH} = 7.8$  Hz, 1H, Ar-H);  $^{13}C\{^1H\}$  NMR (101 MHz,  $CD_2Cl_2$ , 25 °C):  $\delta$  170.7 (s, C=O), 170.6 (s, C=O), 166.8 (s, C=O), 148.9 (s, isoquinolineH, Ar-C), 145.0 (s, Ar-C), 144.12 (s, Ar-C), 143.44 (s, Ar-C), 142.1 (s, Ar-C), 137.4 (s, isoquinolineH, Ar-C), 136.1 (s, isoquinolineH, Ar-C), 134.0 (s, Ar-C), 133.9 (d,  $J_{CP} = 2.2$  Hz, Ar-C), 133.7 (s, Ar-C), 132.2 (d,  $J_{CP} = 2.9$  Hz, Ar-C), 132.0 (s, Ar-C), 131.0 (s, Ar-C), 130.9 (s, Ar-C), 130.8 (s, Ar-C), 129.7

(d,  $J_{CP} = 3.7$  Hz, Ar-C), 129.3 (s, isoquinolineH, Ar-C), 129.1 (s, isoquinolineH, Ar-C), 128.3 (s, Ar-C), 128.1 (s, Ar-C), 127.9 (s, Ar-C), 127.8 (s, Ar-C), 127.6 (s, Ar-C), 126.9 (s, isoquinolineH, Ar-C), 126.8 (s, isoquinolineH, Ar-C), 126.6 (s, isoquinolineH, Ar-C), 123.1 (s, isoquinolineH, Ar-C); IR (neat)  $\nu$ : 3417 (vw), 3132 (vw), 3067 (w), 3009 (vw), 2998 (vw), 2930 (vw), 2112 (vw), 1975 (vw), 1709 (s), 1651 (s), 1616 (m), 1593 (w), 1575 (w), 1494 (w), 1452 (m), 1397 (w), 1341 (m), 1278 (s), 1242 (s), 1154 (m), 1128 (s), 1114 (s), 1065 (s), 1029 (vw), 976 (w), 951 (w), 853 (s), 824 (m), 802 (m), 746 (s), 731 (s), 717 (m), 700 (s), 696 (s), 685 (s)  $\text{cm}^{-1}$ ; HRMS (ESI/TOF, positive mode)  $m/z = [M]^+$  calcd for  $\text{C}_9\text{H}_8\text{N}_1$  130.0657; found 130.0658; HRMS (ESI/TOF, negative mode)  $m/z = [M]^-$  calcd for  $\text{C}_{21}\text{H}_{12}\text{O}_6\text{P}_1$  391.0372; found 391.0376.

#### 4.4.7 Synthesis of [(-)-brucineH]-mer-[4.1]

To a solution of  $\text{P}(\text{C}_6\text{H}_4\text{CO}_2)_2(\text{C}_6\text{H}_4\text{COOH})$  (0.19 g, 0.48 mmol) in anhydrous acetone (6.5 mL) was added slowly a solution of (-)-brucine (0.22 g, 0.56 mmol) in anhydrous acetone (4 mL). The reaction mixture was stirred for an hour to afford a colorless precipitate. The precipitate was filtered, washed with minimal amount of anhydrous acetone, and dried *in vacuo*. Crude yield = 0.30 g, 79 %. Cooling a concentrated solution of the crude product (80 mg) in  $\text{CH}_2\text{Cl}_2$  (5 mL) afforded colorless crystals ( $-30$  °C, ca. 5 d). Yield = 38 mg, 48 %. A crystal was selected for X-ray crystallographic analysis without drying. In addition, a concentrated solution of the crude product was dissolved in  $(\text{CH}_3)_2\text{SO}-d_6$  solvent. Single crystals suitable for X-ray diffraction analysis were obtained upon standing for 20 min at ambient temperature.

$^{31}\text{P}\{^1\text{H}\}$  NMR (162 MHz,  $(\text{CD}_3)_2\text{SO}$ , 25 °C):  $\delta$  -135.2;  $\delta$  ( $\text{CD}_2\text{Cl}_2$ ) -114.3, -114.6;  $^1\text{H}$  NMR (300 MHz,  $\text{CD}_2\text{Cl}_2$ , 25 °C):  $\delta$  12.63 (s, 1H, NH), 8.01–7.94 (m, 3H, Ar-H), 7.79 (s, 1H, (-)-brucinium, Ar-H), 7.75–7.35 (m, 8H, Ar-H), 6.77 (s, 1H, (-)-brucinium, Ar-H), 6.45 (dd,  $J_{\text{HH}} = 7.4$  Hz, 1H, Ar-H), 6.18 (t,

$J_{\text{HH}} = 6.2$  Hz, 1H, (-)-brucinium, CH), 4.35–4.32 (m, 1H, (-)-brucinium, O–CH), 4.27–4.21 (m, 2H, (-)-brucinium, OCH<sub>2</sub>), 4.10 (dd,  $J_{\text{HH}} = 8.8$  Hz, 1H, (-)-brucinium, CH), 3.93 (s, 1H, (-)-brucinium, –N–CH–C–), 3.91 (s, 3H, (-)-brucinium, OCH<sub>3</sub>), 3.88 (s, 3H, (-)-brucinium, OCH<sub>3</sub>), 3.82 (d,  $J_{\text{HH}} = 13.7$  Hz, 1H, (-)-brucinium, –N–CH<sub>2</sub>–), 3.63–3.59 (m, 1H, brucinium, CH<sub>2</sub>), 3.14 (s, 1H, (-)-brucinium, CH), 3.09 (t,  $J_{\text{HH}} = 8.8$  Hz, 1H, (-)-brucinium, CH<sub>2</sub>), 3.02–2.94 (m, 1H, (-)-brucinium, CH), 2.87 (d,  $J_{\text{HH}} = 14.7$  Hz, 1H, (-)-brucinium, CH), 2.67 (dd,  $J_{\text{HH}} = 3.9$  Hz, 1H, (-)-brucinium, CH), 2.00–1.86 (m, 3H, (-)-brucinium, 3xCH), 1.47 (d,  $J_{\text{HH}} = 14.7$  Hz, 1H, (-)-brucinium, CH), 1.33 (dt,  $J_{\text{HH}} = 10.8$  Hz, 1H, (-)-brucinium, CH); <sup>1</sup>H NMR (400 MHz, (CD<sub>3</sub>)<sub>2</sub>SO, 25 °C): δ 10.60 (br s, 1H, N–H); <sup>13</sup>C {<sup>1</sup>H} NMR (101 MHz, CD<sub>2</sub>Cl<sub>2</sub>, 25 °C): δ 172.5 (s, (-)-brucinium, C=O), 172.2 (s, C=O), 168.3 (s, C=O), 168.1 (s, C=O), 150.5 (s, Ar–C), 148.9 (s, Ar–C), 146.9 (s, Ar–C), 136.0 (s, Ar–C), 135.5 (s, Ar–C), 133.4 (s, Ar–C), 133.2 (s, Ar–C), 133.0 (s, (-)-brucinium, Ar–C), 132.8 (s, (-)-brucinium, Ar–C), 132.5 (s, Ar–C), 132.3 (s, Ar–C), 131.7 (s, Ar–C), 131.5 (s, Ar–C), 129.9 (s, (-)-brucinium), 129.1 (s, (-)-brucinium), 127.2 (s, (-)-brucinium), 127.0 (s, Ar–C), 126.5 (s, Ar–C), 126.3 (s, Ar–C), 125.9 (s, Ar–C), 125.7 (s, Ar–C), 125.1 (s, Ar–C), 124.9 (s, Ar–C), 118.8 (s, (-)-brucinium), 105.6 (s, (-)-brucinium), 101.0 (s, (-)-brucinium), 77.3 (s, (-)-brucinium), 64.0 (s, (-)-brucinium), 61.2 (s, (-)-brucinium), 59.2 (s, (-)-brucinium), 56.6 (s, (-)-brucinium), 56.1 (s, (-)-brucinium), 52.1 (s, (-)-brucinium), 52.0 (s, (-)-brucinium), 50.2 (s, (-)-brucinium), 46.9 (s, (-)-brucinium), 42.0 (s, (-)-brucinium), 40.5 (s, (-)-brucinium), 30.4 (s, (-)-brucinium), 24.7 (s, (-)-brucinium); IR (neat)  $\nu$ : 3494 (vw), 3061 (vw), 3056 (vw), 2997 (vw), 2959 (vw), 2872 (vw), 2829 (vw), 1708 (sh, m), 1668 (s), 1648 (sh, s), 1594 (m), 1577 (w), 1502 (m), 1451 (m), 1414 (m), 1362 (w), 1331 (w), 1283 (s), 1245 (m), 1220 (m), 1198 (m), 1176 (w), 1111 (s), 1088 (w), 1071 (m), 1065 (w), 1027 (m), 1012 (w), 986 (m), 964 (w), 938 (vw), 885 (vw), 849 (s), 817 (sh, w), 790 (w), 762 (sh, w), 728 (s), 719 (m), 701 (s), 684 (m)

cm<sup>-1</sup>; elem. anal. calcd for C<sub>45</sub>H<sub>41</sub>N<sub>2</sub>O<sub>10</sub>P·0.7 CH<sub>2</sub>Cl<sub>2</sub>·0.9 C<sub>3</sub>H<sub>6</sub>O: C, 63.71; H, 5.30; N, 3.06; found: C, 63.81; H, 5.40; N, 3.10.

#### 4.4.8 Synthesis of [(*n*-C<sub>8</sub>H<sub>17</sub>)<sub>3</sub>NH]-*mer*-[4.1]

To a suspension of P(C<sub>6</sub>H<sub>4</sub>CO<sub>2</sub>)<sub>2</sub>(C<sub>6</sub>H<sub>4</sub>COOH) (0.23 g, 0.58 mmol) in anhydrous acetone (6 mL) was added degassed tri(*n*-octyl)amine, N(*n*-C<sub>8</sub>H<sub>17</sub>)<sub>3</sub> (0.50 mL, 0.40 g, 1.13 mmol). Within seconds, the reaction dissolved and was stirred overnight. Subsequently, the solvent was removed in *vacuo* to afford a pale yellow oil. The oily residue was washed with *n*-hexane, filtered and heated in *vacuo* at 140 °C for 4 h to remove residual solvent. Yield = 0.31 g, 73 %.

<sup>31</sup>P{<sup>1</sup>H} NMR (162 MHz, (CD<sub>3</sub>)<sub>2</sub>CO, 25 °C): δ -128.9; δ (CD<sub>2</sub>Cl<sub>2</sub>) -125.6; <sup>1</sup>H NMR (400 MHz, (CD<sub>3</sub>)<sub>2</sub>CO, 25 °C): δ 9.76 (br s, 1H, (CH<sub>3</sub>(CH<sub>2</sub>)<sub>5</sub>CH<sub>2</sub>CH<sub>2</sub>)<sub>3</sub>NH), 8.50–7.20 (m, 11H, Ar-H), 6.29 (dd, J<sub>HH</sub> = 7.3 Hz, 1H, Ar-H), 3.04 (t, J<sub>HH</sub> = 8.3 Hz, 6H, (CH<sub>3</sub>(CH<sub>2</sub>)<sub>5</sub>CH<sub>2</sub>CH<sub>2</sub>)<sub>3</sub>NH), 1.69 (m, 6H, (CH<sub>3</sub>(CH<sub>2</sub>)<sub>5</sub>CH<sub>2</sub>CH<sub>2</sub>)<sub>3</sub>NH), 1.31 (br s, 30H, (CH<sub>3</sub>(CH<sub>2</sub>)<sub>5</sub>CH<sub>2</sub>CH<sub>2</sub>)<sub>3</sub>NH), 0.89 (t, J<sub>HH</sub> = 6.9 Hz, 9H, (CH<sub>3</sub>(CH<sub>2</sub>)<sub>5</sub>CH<sub>2</sub>CH<sub>2</sub>)<sub>3</sub>NH); <sup>1</sup>H NMR (400 MHz, CD<sub>2</sub>Cl<sub>2</sub>, 25 °C): δ 10.40 (s, 1H, (CH<sub>3</sub>(CH<sub>2</sub>)<sub>5</sub>CH<sub>2</sub>CH<sub>2</sub>)<sub>3</sub>NH); <sup>13</sup>C{<sup>1</sup>H} NMR (101 MHz, (CD<sub>3</sub>)<sub>2</sub>CO, 25 °C): δ 169.4 (s, C=O), 169.3 (s, C=O), 163.9 (s, C=O), 156.5 (s, Ar-C), 154.3 (s, Ar-C), 135.8 (s, Ar-C), 135.7 (s, Ar-C), 134.9 (s, Ar-C), 134.8 (s, Ar-C), 132.3 (s, Ar-C), 132.1 (s, Ar-C), 131.7 (s, Ar-C), 131.5 (s, Ar-C), 130.7 (d, J<sub>CP</sub> = 3.7 Hz, Ar-C), 130.6 (s, Ar-C), 130.4 (s, Ar-C), 128.5 (d, J<sub>CP</sub> = 4.4 Hz, Ar-C), 127.2 (s, Ar-C), 127.0 (s, Ar-C), 124.8 (d, J<sub>CP</sub> = 2.2 Hz, Ar-C), 124.7 (s, Ar-C), 52.5 (s, (CH<sub>3</sub>(CH<sub>2</sub>)<sub>5</sub>CH<sub>2</sub>CH<sub>2</sub>)<sub>3</sub>NH), 31.6 (s, (CH<sub>3</sub>(CH<sub>2</sub>)<sub>5</sub>CH<sub>2</sub>CH<sub>2</sub>)<sub>3</sub>NH), 29.0 (s, (CH<sub>3</sub>(CH<sub>2</sub>)<sub>5</sub>CH<sub>2</sub>CH<sub>2</sub>)<sub>3</sub>NH), 28.9 (s, (CH<sub>3</sub>(CH<sub>2</sub>)<sub>5</sub>CH<sub>2</sub>CH<sub>2</sub>)<sub>3</sub>NH), 26.4 (s, (CH<sub>3</sub>(CH<sub>2</sub>)<sub>5</sub>CH<sub>2</sub>CH<sub>2</sub>)<sub>3</sub>NH), 23.3 (s, (CH<sub>3</sub>(CH<sub>2</sub>)<sub>5</sub>CH<sub>2</sub>CH<sub>2</sub>)<sub>3</sub>NH), 22.4 (s, (CH<sub>3</sub>(CH<sub>2</sub>)<sub>5</sub>CH<sub>2</sub>CH<sub>2</sub>)<sub>3</sub>NH), 13.5 (s, (CH<sub>3</sub>(CH<sub>2</sub>)<sub>5</sub>CH<sub>2</sub>CH<sub>2</sub>)<sub>3</sub>NH); IR (CCl<sub>4</sub>) ν: 3069 (vw), 2955 (m), 2927 (m), 2879 (w), 2857 (m), 1709 (s), 1653 (m), 1596 (m), 1579 (w), 1454 (m), 1378 (vw), 1280 (s),

1242 (s), 1127 (s), 1112(m), 1071 (m), 1061(s), 1023 (w), 984 (m), 856 (s), 809 (w), 784 (s), 757 (s), 731 (sh, m), 700(m), 686 (w); IR (neat)  $\nu$ : 3064 (vw), 3021 (vw) 2954 (m), 2925 (m), 2870 (w), 2856 (m), 1707 (s), 1653 (m), 1595 (m), 1579 (w), 1453 (m), 1378 (vw), 1277 (s), 1240 (s), 1125 (s), 1113 (s), 1071 (m), 1061(s), 1022 (w), 984 (m), 855 (s), 809 (w), 784 (s), 757 (s), 731 (sh, m), 699 (s), 686 (m)  $\text{cm}^{-1}$ .

#### 4.4.9 Synthesis of K-mer-[4.1]

To a colorless solution of  $[\text{NEt}_3\text{H}][\text{P}(\text{C}_6\text{H}_4\text{CO}_2)_3]$  (0.17 g, 0.34 mmol) in anhydrous THF (12 mL) was added slowly a suspension of potassium hydride (0.02g, 0.52 mmol) in anhydrous THF (6 mL) at ambient temperature. The immediate evolution of gas (*i.e.*  $\text{H}_2$ ) was observed and the reaction mixture was stirred for 2h at ambient temperature to afford a colorless precipitate. The precipitate was filtered and washed with minimal amount of anhydrous THF and dried *in vacuo*. Crude yield = 0.12 g, 82 %. Single crystals suitable for X-ray diffraction were obtained by cooling a concentrated solution of the crude product (44 mg) in  $\text{MeOH-}d_4$  (1.5 mL) ( $-30\text{ }^\circ\text{C}$ , ca. 9 days).

$^{31}\text{P}\{^1\text{H}\}$  NMR (162 MHz,  $\text{CD}_3\text{OD}$ ,  $25\text{ }^\circ\text{C}$ ):  $\delta$  -127.6,  $\delta$  ( $(\text{CD}_3)_2\text{CO}$ ) -136.4;  $^1\text{H}$  NMR (400 MHz,  $\text{CD}_3\text{OD}$ ,  $25\text{ }^\circ\text{C}$ ):  $\delta$  7.94–7.28 (m, 11H, Ar-H), 6.26 (dd,  $J_{\text{HH}} = 7.6\text{ Hz}$ , 1H, Ar-H);  $^{13}\text{C}\{^1\text{H}\}$  NMR (101 MHz,  $\text{CD}_3\text{OD}$ ,  $25\text{ }^\circ\text{C}$ ):  $\delta$  170.7 (s, C=O), 169.9 (s, C=O), 169.8 (s, C=O), 155.4 (s, Ar-C), 154.3 (s, Ar-C), 153.2 (s, Ar-C), 133.3 (s, Ar-C), 133.1 (s, Ar-C), 132.3 (s, Ar-C), 132.1 (d,  $J_{\text{CP}} = 2.9\text{ Hz}$ , Ar-C), 130.2 (s, Ar-C), 130.1 (s, Ar-C), 129.0 (d,  $J_{\text{CP}} = 2.9\text{ Hz}$ , Ar-C), 128.9 (s, Ar-C), 128.7 (d,  $J_{\text{CP}} = 3.7\text{ Hz}$ , Ar-C), 128.6 (s, Ar-C), 126.0 (s, Ar-C), 125.9 (s, Ar-C), 125.8 (s, Ar-C), 124.7 (s, Ar-C), 124.5 (s, Ar-C); IR (neat)  $\nu$ : 2962 (vw), 1689 (s), 1632 (sh, w), 1595 (m), 1580 (w), 1453 (m), 1391 (w), 1332 (w), 1282 (s), 1244 (s), 1120 (s), 1071 (m), 1062 (m), 1025 (w), 855 (s), 813 (w), 745 (s), 729 (s), 718 (w), 697 (s), 684 (m)  $\text{cm}^{-1}$ ; LRMS (ESI, negative mode)  $m/z = 391.0\text{ [M]}^-$ .

#### 4.4.10 Attempted Synthesis of $\text{H}(\text{DMF})_n$ [4.1]

To  $\text{P}(\text{C}_6\text{H}_4\text{CO}_2)_2(\text{C}_6\text{H}_4\text{COOH})$  (0.20 g, 0.57 mmol) was added anhydrous *N,N'*-dimethylformamide (5 mL). The initially cloudy solution cleared within a few seconds and was subsequently stirred for ca. 16 h. Despite heating to 120 °C over ca. 4 weeks, no additional changes were observed in the  $^{31}\text{P}\{^1\text{H}\}$  NMR spectrum of the reaction mixture. An aliquot was removed from the reaction mixture for mass spectrometric analysis.

$^{31}\text{P}\{^1\text{H}\}$  NMR (162 MHz,  $\text{N}(\text{CH}_3)_2\text{COH}$ , 25 °C):  $\delta$  -55.9, -134.6; -138.9; LRMS (ESI, negative mode)  $m/z = 391.0$   $[\text{M}]^-$ .

**Table 4-3. X-ray crystallographic data for [PhNMe<sub>2</sub>H]-rac-mer-[4.1], [pyH]-rac-mer-[4.1], [isoquinolineH]-rac-mer-[4.1], [(-)-brucineH]-Λ-mer-[4.1], and K-rac-mer-[4.1].**

|   | [PhNMe <sub>2</sub> H]-rac-mer-[1]·<br>Me <sub>2</sub> C=O | [pyH]-rac-mer-[1]·<br>0.5 Me <sub>2</sub> C=O         | [isoquinolineH]-rac-mer-[1]·<br>(C <sub>9</sub> H <sub>7</sub> N) | [(-)-brucineH]-Λ-mer-[1]·<br>2.02 CH <sub>2</sub> Cl <sub>2</sub>                         | K-rac-mer-[1]·<br>3 CH <sub>3</sub> OH  |
|---|--|---|---|---|---|
| Formula                                   | C <sub>32</sub> H <sub>30</sub> NO <sub>7</sub> P          | C <sub>27.5</sub> H <sub>21</sub> NO <sub>6.5</sub> P | C <sub>39</sub> H <sub>27</sub> N <sub>2</sub> O <sub>6</sub> P   | C <sub>46.01</sub> H <sub>43.03</sub> Cl <sub>4.03</sub> N <sub>2</sub> O <sub>10</sub> P | C <sub>45</sub> H <sub>36</sub> K <sub>2</sub> O <sub>15</sub> P <sub>2</sub> |
| FW  | 650.59   | 500.42  | 650.59  | 957.87  | 956.88  |
| Cryst. syst.                              | Monoclinic   | monoclinic  | Monoclinic  | Orthorhombic  | monoclinic  |
| space group                               | P2 <sub>1</sub> /n   | C2/c  | P2 <sub>1</sub> /n  | P2 <sub>1</sub> 2 <sub>1</sub> 2 <sub>1</sub>   | P2 <sub>1</sub> /n  |
| a (Å)                                     | 13.7182(6)   | 33.995(4)   | 8.3942(8)   | 14.000(2)   | 13.4404(4)  |
| b (Å)                                     | 9.6463(4)  | 7.8804(8)   | 12.9178(12)   | 14.214(3)   | 18.8521(5)  |
| c (Å)                                     | 21.0016(8)   | 18.711(2)   | 28.434(3)   | 22.114(4)   | 18.8164(5)  |
| α (deg)                                   | 90   | 90  | 90  | 90  | 90  |
| β (deg)                                   | 95.7130(10)  | 109.712(3)  | 97.682(3)   | 90  | 93.2000(10)   |
| γ (deg)                                   | 90   | 90  | 90  | 90  | 90  |
| V (Å <sup>3</sup> )                       | 2765.3(2)  | 4718.7(9)   | 3055.6(5)   | 4400.4(13)  | 4760.3(2)   |
| T (K)                                     | 90(2)  | 90(2)   | 90(2)   | 90(2)   | 100(2)  |
| Z   | 4  | 8   | 4   | 4   | 4   |
| μ (MoKα) (mm <sup>-1</sup> )              | 0.151  | 0.164   | 0.145   | 0.369   | 0.332   |
| crystal size (mm <sup>3</sup> )           | 0.20×0.11×0.10   | 0.30×0.1×0.1  | 0.18×0.15×0.08  | 0.10×0.04×0.04  | 0.13×0.12×0.08  |
| ρ <sub>calcd.</sub> (g cm <sup>-3</sup> ) | 1.373  | 1.409   | 1.414   | 1.446   | 1.335   |
| 2θ(max) (°)                               | 60.06  | 60.23   | 53.11   | 44.9  | 54.00   |
| F(000)                                    | 1200.0   | 2080.0  | 1352.0  | 1987.0  | 1976.0  |
| No. total reflns.                         | 32422  | 7158  | 38996   | 11777   | 37894   |
| No. unique reflns.                        | 8097   | 399   | 6467  | 5484  | 10359   |
| R(int)                                    | 0.0496   | 0.036   | 0.0572  | 0.0766  | 0.036   |
| Refln./param. Ratio                       | 14.7   | 17.9  | 14.7  | 9.00  | 17.5  |
| R <sub>1</sub> [I > 2σ(I)] <sup>a</sup>   | 0.0470   | 0.0654  | 0.0774  | 0.0658  | 0.0613  |
| wR <sub>2</sub> [all data] <sup>b</sup>   | 0.1181   | 0.1594  | 0.2349  | 0.1471  | 0.1782  |
| GOF                                       | 1.011  | 1.137   | 1.054   | 1.011   | 1.036   |

<sup>a</sup>  $R_1 = \frac{\sum |F_o| - |F_c|}{\sum |F_o|}$ . <sup>b</sup>  $wR_2(F^2[\text{all data}]) = \left\{ \frac{\sum [w(F_o^2 - F_c^2)^2]}{\sum w(F_o^2)^2} \right\}^{1/2}$

# Chapter 5: Brønsted Acids with Hexacoordinate Tantalum(V) Weakly Coordinating Anions as Highly Effective Initiators for the Cationic Polymerization of Vinyl Monomers

## 5.1 Introduction

The cationic polymerization of olefins is a challenging reaction due to its very fast rate of propagation and the many possible chain transfer and termination processes.<sup>17,37</sup> The polymerization necessitates initiators comprised of a cation source (a proton or carbenium ion) and a WCA that stabilizes the electrophilic propagating cation.<sup>27,68,271</sup> The nature of the coordinating anion is critical, as it affects the degree of ion-pairing and therefore has an influence over initiation, propagation, chain transfer and termination. A strong interaction between the cation and anion leads to termination, whereas a weak interaction evokes side reactions such as chain transfer. Ideally, WCAs will be able to delocalize the negative charge over a large number of atoms and will be non-nucleophilic. WCAs composed of group 13 elements, such as boron, aluminum and gallium are of particular interest and have been ubiquitously designed to stabilize highly reactive cations.<sup>33,65,66,69,74,84,119,137,138,147,148,153,155,171,174,182,186,195,298,331,436,437</sup> Only a few of these systems have been studied as potential initiators for cationic polymerization. Two-component systems comprised of a Lewis acid (*e.g.* AlCl<sub>3</sub> and BF<sub>3</sub>) in combination with a co-initiator (*e.g.* traces of water or alcohol) have been established as initiators for cationic polymerization; however, the initiating species is not well understood. Recent developments of solid and weighable single-component initiators based on Brønsted acids are of growing interest since they allow for better control over the monomer-to-initiator ratio.

---

\* A version of this chapter will be submitted for publication. Hazin, K. and Gates, D.P.

To date, they are limited to  $\text{H}(\text{OEt}_2)_2[\text{Al}\{\text{O}(\text{CF}_3)_3\}_4]$ ,  $\text{H}(\text{OEt}_2)_2[\text{B}(\text{C}_6\text{F}_5)_4]$ ,  $\text{H}[\text{B}(\text{C}_2\text{O}_4)_4]$ ,  $\text{Na}(\text{H}_2\text{O})_2[\text{B}\{3,5\text{-C}(\text{CF}_3)_2\text{C}_6\text{H}_3\}_4]$ , and  $\text{H}(\text{L})_2[\text{P}(1,2\text{-O}_2\text{C}_6\text{Cl}_4)_3]$  ( $\text{L} = \text{OEt}_2, \text{THF}, \text{DMF}$ ) due to the challenges in the synthesis and isolation of strong Brønsted acids.<sup>33,64-66,269,282,351</sup> For instance, the aforementioned systems must be stored and handled at low temperatures (*e.g.* below  $-30\text{ }^\circ\text{C}$ ). In Chapter 2 it was shown that the large charge-delocalized tris(tetrachlorocatecholato)phosphate anion can facilitate the isolation of Brønsted acids with stabilized protons such as:  $[\text{H}(\text{DMF})_2]^+$ ,  $[\text{H}(\text{THF})_2]^+$ , and  $[\text{H}(\text{THF})(\text{CH}_3\text{CN})]^+$ . Building on this previous work, we pursued the design of group 5 transition metal containing WCAs for the stabilization of protic acids.

We hypothesized that tantalum(V)-containing WCAs would possess ideal properties to isolate Brønsted acids due to the large coordination numbers possible for tantalum, which would permit the incorporation of large, charge-delocalizing ligands. The delocalization of the negative charge over a large number of atoms minimizes the potential reaction with the counter cation.

Selected examples of compounds containing tantalum(V) WCAs are illustrated in Figure 5.1. Tantalum(V)-containing WCAs with chelating oxygen ligands are limited and only a few such systems (**A–C**)<sup>438-442</sup> have been structurally characterized. Of particular importance, tantalum(V)-containing Brønsted acids are restricted to  $\text{Li}(\text{H}_2\text{O})[\text{Ta}\{\text{O}(\text{CF}_3)_3\}_6]$  (**D**),<sup>443</sup> where the proton is part of the water molecule. To our knowledge,  $[\text{Ph}_3\text{C}][\text{TaF}_6]$  (**E**)<sup>444</sup> is the only system containing a tantalum(V) WCA that has been studied as a single-component initiator. In contrast, binary initiators containing tantalum(V) anions and a co-initiator have been established in the following systems:  $[\text{Ph}_3\text{C}][\text{Ta}(\text{OC}_6\text{F}_5)_6]$  (**F**),<sup>149,150</sup>  $\text{L}[\text{TaX}_6]$  ( $\text{X} = \text{Cl}, \text{Br}, \text{I}; \text{L} = [\text{TaX}_4(\text{THF})\{\text{O}(\text{CH}_2)_4\text{O}(\text{CH}_2)_3\text{CH}_2\}]$  with  $\text{X} = \text{F}, \text{Cl}$ ),<sup>445</sup>  $\text{TaCl}_5/\text{Bu}_4\text{NCl}/\text{isobutyl vinyl ether-HCl}$ ,<sup>446</sup> and  $\text{TaF}_5$ .<sup>447</sup>

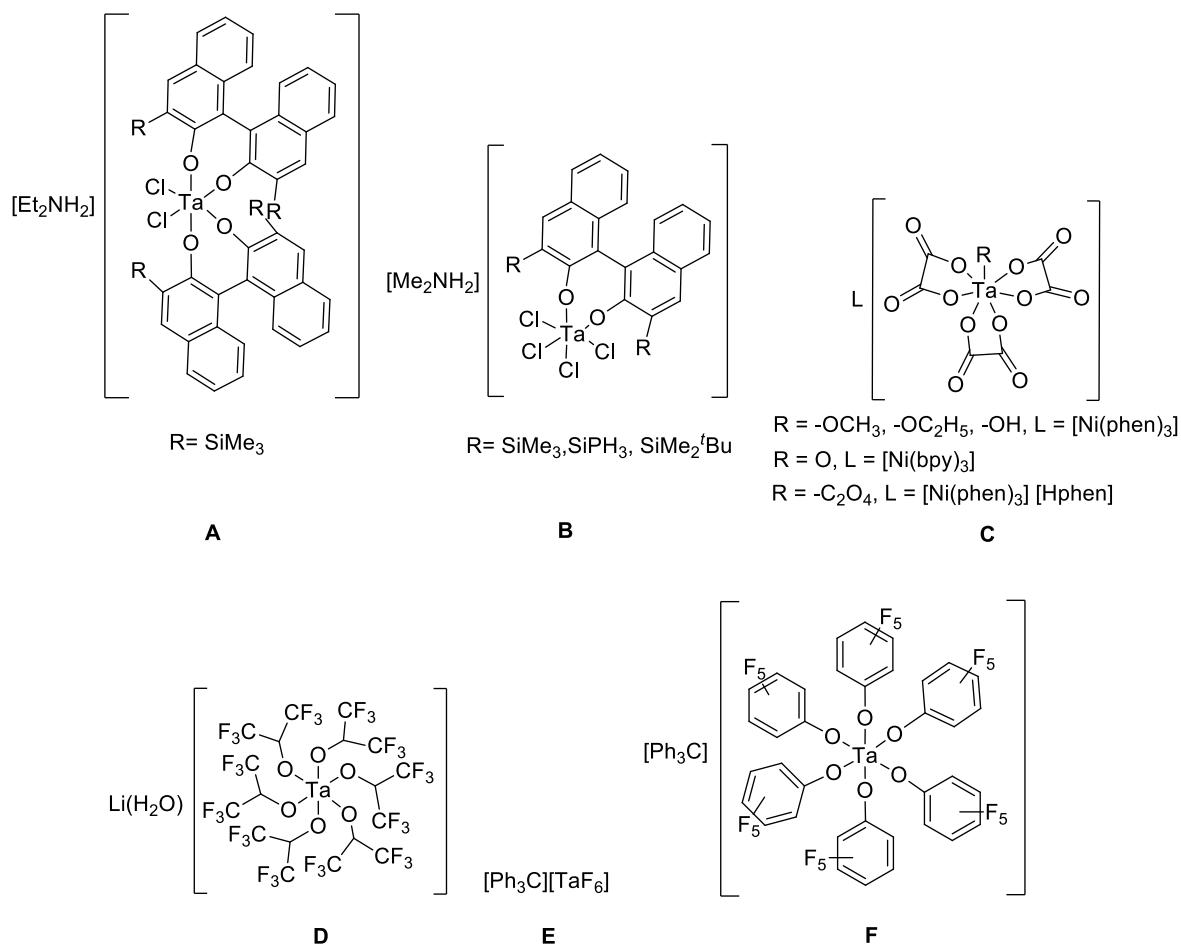


**Figure 5.1. Examples of characterized tantalum(V)-containing complexes.**

In this chapter, the synthesis and characterization of novel Brønsted acids H(OEt<sub>2</sub>)<sub>2</sub>[**5.1**] and H(OEt<sub>2</sub>)<sub>2</sub>[**5.2**] are reported. Both are highly effective single-component initiators for the cationic polymerization of olefin monomers, including *n*-butyl vinyl ether,  $\alpha$ -methylstyrene, styrene and isoprene. Remarkably, high molecular weight poly( $\alpha$ -methylstyrene) and polystyrene ( $M_n \geq 200,000 \text{ g mol}^{-1}$ ) are obtained with moderate to narrow dispersity at temperatures above  $-100 \text{ }^\circ\text{C}$ . To our knowledge, H(OEt<sub>2</sub>)<sub>2</sub>[**5.1**] and H(OEt<sub>2</sub>)<sub>2</sub>[**5.2**] are the only examples of hexacoordinate Ta(V)-bidentate oxo-complexes that have successfully been used in the cationic polymerization of olefins.

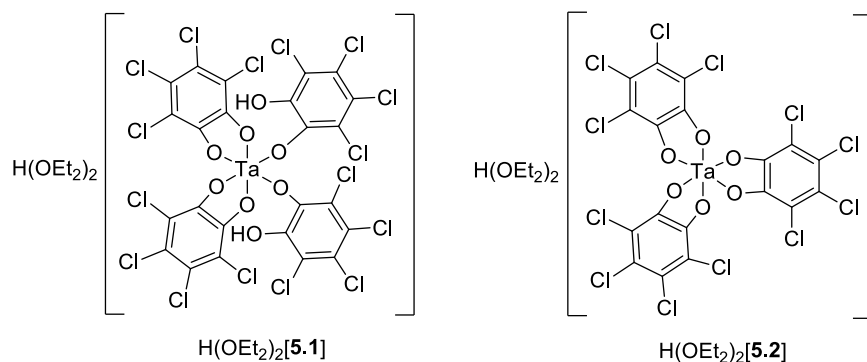
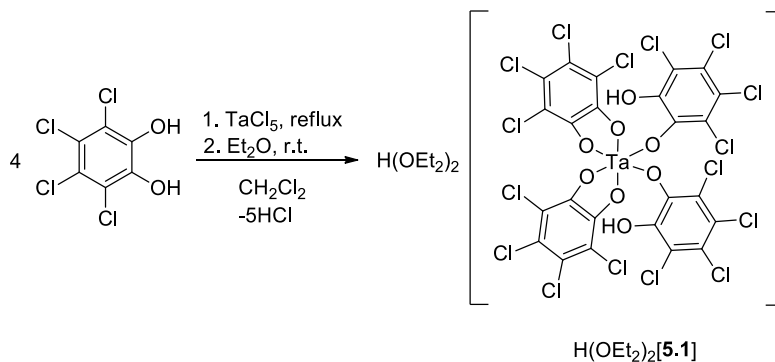


**Figure 5.2. Brønsted acids  $\text{H(OEt}_2)_2$ [5.1] and  $\text{H(OEt}_2)_2$ [5.2].**

## 5.2 Results and Discussion

### 5.2.1 Synthesis and Characterization of Initiators

Our group previously reported the convenient reaction of 1,2- $\text{C}_6\text{Cl}_4(\text{OH})_2$  with  $\text{PCl}_5$  in  $\text{CH}_2\text{Cl}_2$  and  $\text{Et}_2\text{O}$  that permitted the isolation of solid Brønsted acid  $\text{H(OEt}_2)_2[\text{P}(1,2\text{-O}_2\text{C}_6\text{Cl}_4)_3]$ .<sup>269</sup> Remarkably, this solid and weighable compound is a highly effective single-component initiator for the polymerization of *n*-butyl vinyl ether,  $\alpha$ -methylstyrene, styrene and isoprene. Based on these results, it was speculated that if  $\text{TaCl}_5$  was employed in place of  $\text{PCl}_5$ , a strong Brønsted acid with a hexacoordinate tantalum(V) anion could be isolated that may be an effective cationic initiator for olefin polymerization.



**Scheme 5.1. Synthesis of Brønsted acid  $\text{H(OEt}_2)_2$ [5.1].**

Thus, a warm solution containing an excess tetrachlorocatechol (4 equiv) in CH<sub>2</sub>Cl<sub>2</sub> was added to TaCl<sub>5</sub> in CH<sub>2</sub>Cl<sub>2</sub> that was heated to reflux. Subsequently, excess Et<sub>2</sub>O was added at ambient temperature, to give an off-white product that was presumed to be H(OEt<sub>2</sub>)<sub>2</sub>[Ta(1,2-O<sub>2</sub>C<sub>6</sub>Cl<sub>4</sub>)<sub>3</sub>]. The isolated product was characterized by <sup>1</sup>H and <sup>13</sup>C{<sup>1</sup>H} NMR spectroscopy, and elemental analysis.

At ambient temperature, the <sup>1</sup>H NMR spectrum of H(OEt<sub>2</sub>)<sub>2</sub>[**5.1**] in CD<sub>2</sub>Cl<sub>2</sub> exhibited signals assigned to the two coordinated ether molecules ( $\delta = 4.00$ , 8H, OCH<sub>2</sub>CH<sub>3</sub>; 1.40, 12H, CH<sub>2</sub>CH<sub>3</sub>). Surprisingly, the <sup>1</sup>H NMR spectrum displayed a broad undefined signal at 9.37 ppm. At low temperature, this signal became much sharper (T = -85 °C, CD<sub>2</sub>Cl<sub>2</sub>:  $\delta = 9.40$ ). In order to investigate the identity of H(OEt<sub>2</sub>)<sub>2</sub>[**5.1**], a <sup>1</sup>H-<sup>13</sup>C HMBC-NMR experiment was conducted at -85 °C that illustrated correlation between the resonance at 9.40 ppm and two aryl carbon atoms at 118.6 and 145.3 ppm (see Appendix D, Figure D1). It was assumed that the resonance at 9.40 ppm was presumably assignable to a hydroxyl proton of a tetrachlorocatechol moiety that was coordinated in a monodentate fashion. However, the identity of the compound H(OEt<sub>2</sub>)<sub>2</sub>[**5.1**] was not immediately obvious. A sharp signal assigned to the acidic proton in H(OEt<sub>2</sub>)<sub>2</sub>[**5.1**] was observed at  $\delta = 16.73$  in the low temperature spectrum (Figure 5.3) that is similar to the acidic proton in our previously reported H(OEt<sub>2</sub>)<sub>2</sub>[P(1,2-O<sub>2</sub>C<sub>6</sub>Cl<sub>4</sub>)<sub>3</sub>] (T = -85 °C, CD<sub>2</sub>Cl<sub>2</sub>:  $\delta = 16.70$ , *H*).<sup>269</sup> For comparison, related salts containing the [H(OEt<sub>2</sub>)<sub>2</sub>]<sup>+</sup> cation show similar downfield chemical shifts in H(OEt<sub>2</sub>)<sub>2</sub>[B(C<sub>6</sub>F<sub>5</sub>)<sub>4</sub>] ( $\delta = 15.5$ , CD<sub>2</sub>Cl<sub>2</sub> at 25 °C),<sup>331</sup> H(OEt<sub>2</sub>)<sub>2</sub>[B(CF<sub>3</sub>)<sub>4</sub>] ( $\delta = 16.3$ , CD<sub>2</sub>Cl<sub>2</sub> at 25 °C),<sup>448</sup> H(OEt<sub>2</sub>)<sub>2</sub>[(C<sub>3</sub>H<sub>3</sub>N<sub>2</sub>){B(C<sub>6</sub>F<sub>5</sub>)<sub>3</sub>}]<sub>2</sub>] ( $\delta = 16.3$ , CD<sub>2</sub>Cl<sub>2</sub>),<sup>449</sup> H(OEt<sub>2</sub>)<sub>2</sub>[H<sub>2</sub>N{B(C<sub>6</sub>F<sub>5</sub>)<sub>3</sub>}] ( $\delta = 16.6$ , CD<sub>2</sub>Cl<sub>2</sub>),<sup>124</sup> H(OEt<sub>2</sub>)<sub>2</sub>[C<sub>6</sub>F<sub>4</sub>-1,2-{B(C<sub>6</sub>F<sub>5</sub>)<sub>2</sub>}]<sub>2</sub>( $\mu$ -OCH<sub>3</sub>) ( $\delta = 16.4$ , CD<sub>2</sub>Cl<sub>2</sub>),<sup>450</sup> H(OEt<sub>2</sub>)<sub>2</sub>[P(C<sub>2</sub>O<sub>4</sub>)<sub>3</sub>] ( $\delta = 15.5$ , CDCl<sub>3</sub>).<sup>248</sup> The salts H(OEt<sub>2</sub>)<sub>2</sub>[B{3,5-(CF<sub>3</sub>)<sub>2</sub>C<sub>6</sub>H<sub>3</sub>}]<sub>4</sub>] ( $\delta = 11.1$ , CD<sub>2</sub>Cl<sub>2</sub>),<sup>119</sup> H(OEt<sub>2</sub>)<sub>2</sub>[CHB<sub>11</sub>Me<sub>5</sub>X<sub>6</sub>] (X = Cl,  $\delta = 13.8$ ; X = Br,  $\delta = 11.7$

ppm,  $C_6D_6$ ),<sup>195</sup> and  $H(OEt_2)_2[Al\{OC(CF_3)_3\}_4]$  ( $\delta = 14.7$ ,  $C_6D_6$ )<sup>298</sup> show a slight difference in downfield shift for the acidic proton to that of  $H(OEt_2)_2[5.1]$ . Importantly, the integrated ratio of the signals assigned to the acidic proton and the coordinating solvent are consistent with the 2:1 ratio within the  $[HL_2]^+$  cation ( $L = OEt_2$ ).

The  $^{13}C\{^1H\}$  NMR spectrum provided additional insight into the structural elucidation of  $H(OEt_2)_2[5.1]$ . Two resonances were assigned to the coordinated diethyl ether molecule ( $\delta = 70.3$ ,  $OCH_2CH_3$ ;  $13.3$ ,  $OCH_2CH_3$ ). In addition, nine resonances were observed for the aromatic carbon atoms in  $H(OEt_2)_2[5.1]$  that are consistent with three resonances for the bidentate tetrachlorocatechol aryl carbon atoms and six signals for the monodentate  $C_6Cl_4O_2H$  moieties. (see Appendix D, Figure D2).

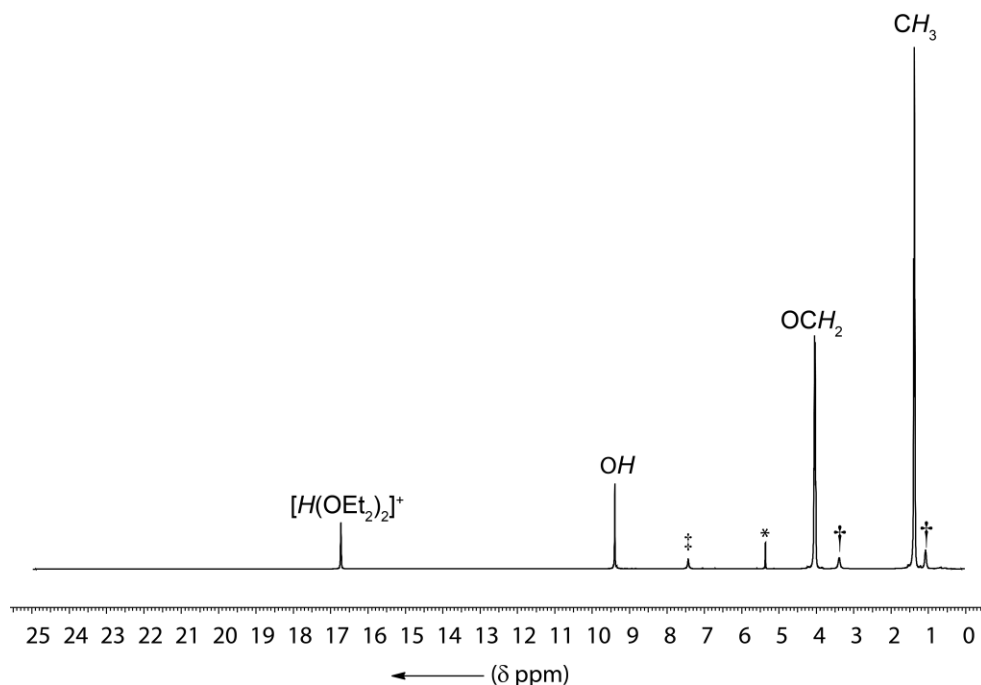


**Figure 5.3.**  $^1H$  NMR (400 MHz,  $CD_2Cl_2$ ,  $-85\text{ }^\circ C$ ) spectrum of  $H(OEt_2)_2[5.1]$ .

\* indicates residual  $CH_2Cl_2$ , † indicates free diethyl ether solvent. ‡ unassigned signal.

Crystallization from a concentrated  $CD_2Cl_2$  solution afforded a single crystal suitable for X-ray crystallography. Analysis of the crystal determined by X-ray diffraction elucidated a

product, namely  $\text{H}(\text{OEt}_2)(\text{H}_2\text{O})[\text{Ta}(1,2\text{-O}_2\text{C}_6\text{Cl}_4)_2(1,2\text{-(OH)OC}_6\text{Cl}_4)_2]$ ,  $\text{H}(\text{OEt}_2)(\text{H}_2\text{O})[\mathbf{5.1}]$ . The molecular structure of the moisture and air-sensitive Brønsted acid  $\text{H}(\text{OEt}_2)(\text{H}_2\text{O})[\mathbf{5.1}]$  and important metrical parameters are presented in Figure 5.4 and will be discussed in detail below (*vide infra*).

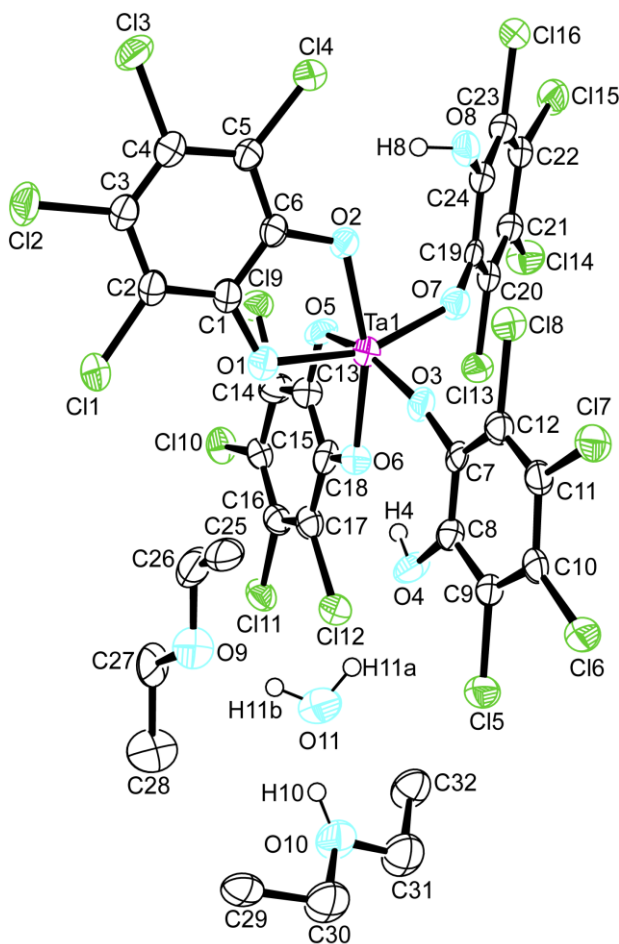
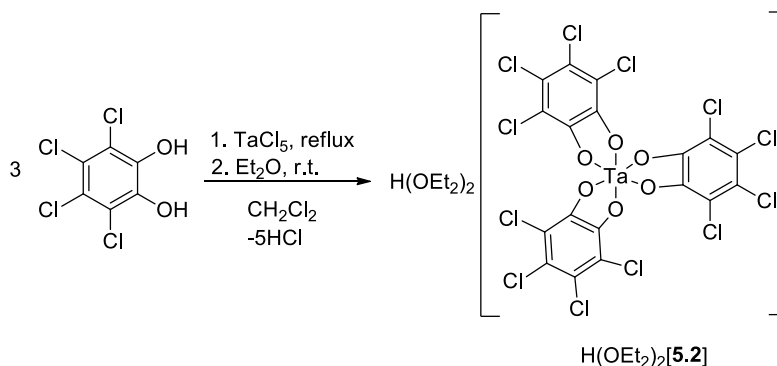


**Figure 5.4.** Molecular structure of  $\text{H}(\text{OEt}_2)(\text{H}_2\text{O})\text{-cis-}[\mathbf{5.1}]\cdot\text{OEt}_2\cdot 0.17 \text{CH}_2\text{Cl}_2$ .

Ellipsoids are drawn at the 50% probability level. Solvents of crystallization ( $0.17 \times \text{CH}_2\text{Cl}_2$ ) and hydrogen atoms are omitted for clarity, except for H(4), H(8), H(10), H(11a) and H(11b). Selected bond lengths [ $\text{\AA}$ ]: Ta(1)–O(1) = 2.011(18); Ta(1)–O(2) = 2.027(17); Ta(1)–O(3) = 1.879(18); Ta(1)–O(5) = 1.967(19); Ta(1)–O(6) = 2.074(18); Ta(1)–O(7) = 1.932(18); C(8)–O(4) = 1.360(3); C(13)–O(5) = 1.31(3); C(24)–O(8) = 1.340(3); C(26)–O(9) = 1.41(3); C(30)–O(10) = 1.49(5); O(9)–O(11) = 2.43(3); O(10)–O(11) = 2.46(3); O(4)–H(4) = 0.84(2); O(10)–H(10) = 1.10(4); O(11)–H(11a) = 0.87(2). Selected bond angles [ $^\circ$ ]: O(1)–Ta(1)–O(2) = 77.1(7); O(3)–Ta(1)–O(6) = 83.5(8); O(2)–Ta(1)–O(7) = 82.2(7); O(2)–Ta(1)–O(6) = 163.4(7); O(3)–Ta(1)–O(5) = 159.4(7); C(31)–O(10)–C(32) = 107.0(3).

Although it is preferable to store  $\text{H}(\text{OEt}_2)_2[\mathbf{5.1}]$  at low temperatures (*ca.*  $-30\text{ }^\circ\text{C}$ ), the integrity of the  $[\text{H}(\text{OEt}_2)_2]^+$  moiety in solution was investigated. A concentrated sample of  $\text{H}(\text{OEt}_2)_2[\mathbf{5.1}]$  in  $\text{CD}_2\text{Cl}_2$  was stored at ambient temperature under an inert atmosphere. The stability of the complex in solution was monitored by recording low temperature  $^1\text{H}$ -NMR spectra at  $-85\text{ }^\circ\text{C}$  over a period of 15 days (see Appendix D, Figure D3). The spectra showed no change for a period of *ca.* one week. After one week an additional signal was observed at around 13.1 ppm suggestive of degradation. Elemental analysis of the crude product was consistent with the assigned formulation of  $\text{H}(\text{OEt}_2)_2[\mathbf{5.1}]$  with  $\text{CH}_2\text{Cl}_2$  (1.4 equiv) solvate of reaction.

Inspired by the successful synthesis and isolation of  $\text{H}(\text{OEt}_2)_2[\mathbf{5.1}]$ , we set out to isolate a Brønsted acid containing a hexacoordinate tantalum(V) anion with three chelated tetrachlorocatechol moieties. The reaction of  $\text{TaCl}_5$  and tetrachlorocatechol (3 equiv) in  $\text{CH}_2\text{Cl}_2$  afforded the Brønsted acid  $\text{H}(\text{OEt}_2)_2[\mathbf{5.2}]$  in moderate yield (Scheme 5.2).



**Scheme 5.2. Synthesis of Brønsted acid  $\text{H}(\text{OEt}_2)_2[\mathbf{5.2}]$ .**

$\text{H}(\text{OEt}_2)_2[\mathbf{5.2}]$  was characterized by  $^1\text{H}$  and  $^{13}\text{C}\{^1\text{H}\}$  NMR spectroscopy, elemental analysis and mass spectrometry. At ambient temperature, the  $^1\text{H}$  NMR spectrum of  $\text{H}(\text{OEt}_2)_2[\mathbf{5.2}]$  in  $\text{CD}_2\text{Cl}_2$  exhibited signals assigned to the two coordinated diethyl ether molecules ( $\delta = 4.00$ ,

8H,  $\text{OCH}_2\text{CH}_3$ ; 1.40, 12H,  $\text{OCH}_2\text{CH}_3$ ). At low temperature, the  $^1\text{H}$  NMR spectrum of  $\text{H}(\text{OEt}_2)_2[\mathbf{5.2}]$  (Figure 5.5) displayed a much sharper signal for the acidic proton in  $\text{H}(\text{OEt}_2)_2[\mathbf{5.2}]$  ( $\delta = 16.74$ ). This chemical shift is similar to that observed for the acidic proton in our previously reported  $\text{H}(\text{OEt}_2)_2[\text{P}(1,2\text{-O}_2\text{C}_6\text{Cl}_4)_3]$  ( $T = -85\text{ }^\circ\text{C}$ ,  $\text{CD}_2\text{Cl}_2$ :  $\delta = 16.70$ ,  $H$ ).<sup>269</sup> The  $^1\text{H}$  NMR spectrum did not reveal a signal in the range 9.0 to 10.0 ppm, attributable to a hydroxyl group of a tetrachlorocatechol moiety in  $\text{H}(\text{OEt}_2)_2[\mathbf{5.2}]$ . The  $^{13}\text{C}\{^1\text{H}\}$  NMR spectrum (Figure 5.6) exhibited only three aromatic resonances confirming the symmetry and equivalence of the three chelated tetrachlorocatechol moieties. In addition, elemental analysis and mass spectrometry were consistent with a tris(tetrachlorobenzenediolato)tantalate(V) anion species.

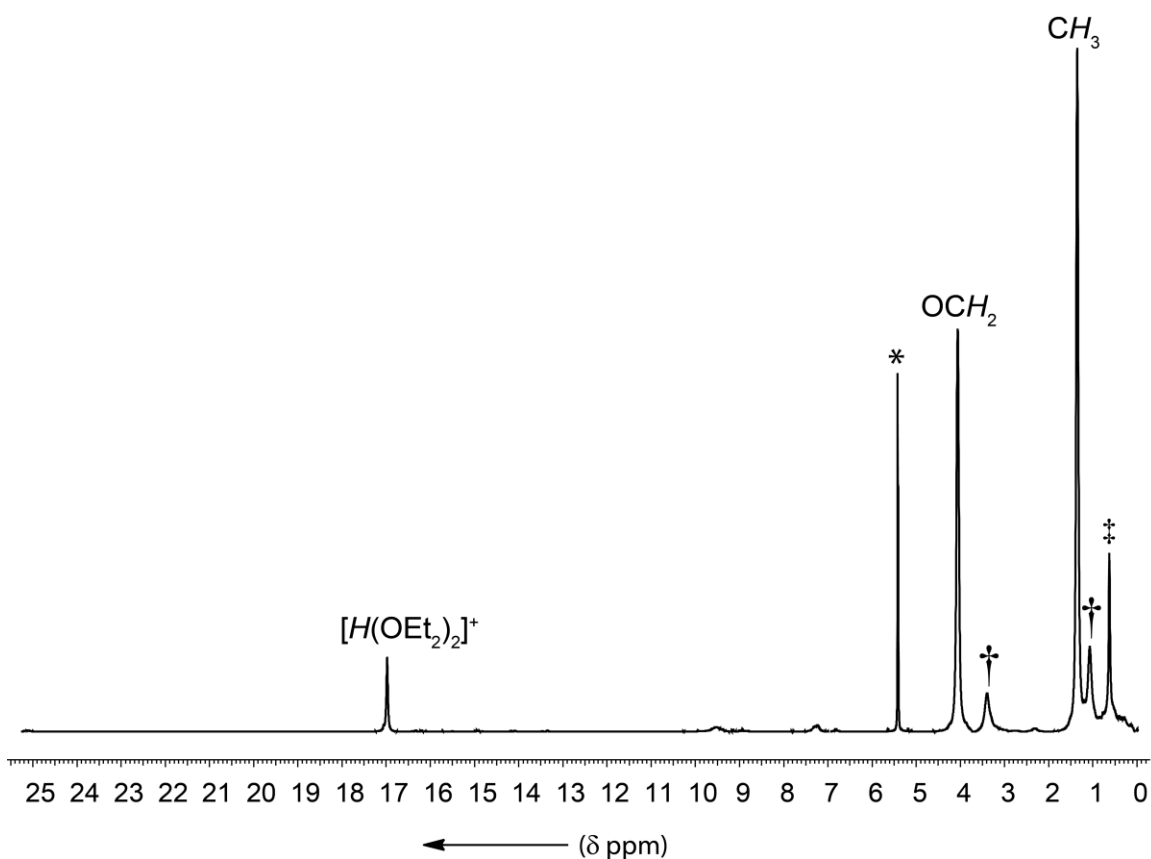


Figure 5.5.  $^1\text{H}$  NMR (400 MHz,  $\text{CD}_2\text{Cl}_2$ ,  $-85\text{ }^\circ\text{C}$ ) spectrum of  $\text{H}(\text{OEt}_2)_2[\mathbf{5.2}]$ .

\* indicates residual  $\text{CH}_2\text{Cl}_2$ , † indicates free diethyl ether solvent. ‡ grease.

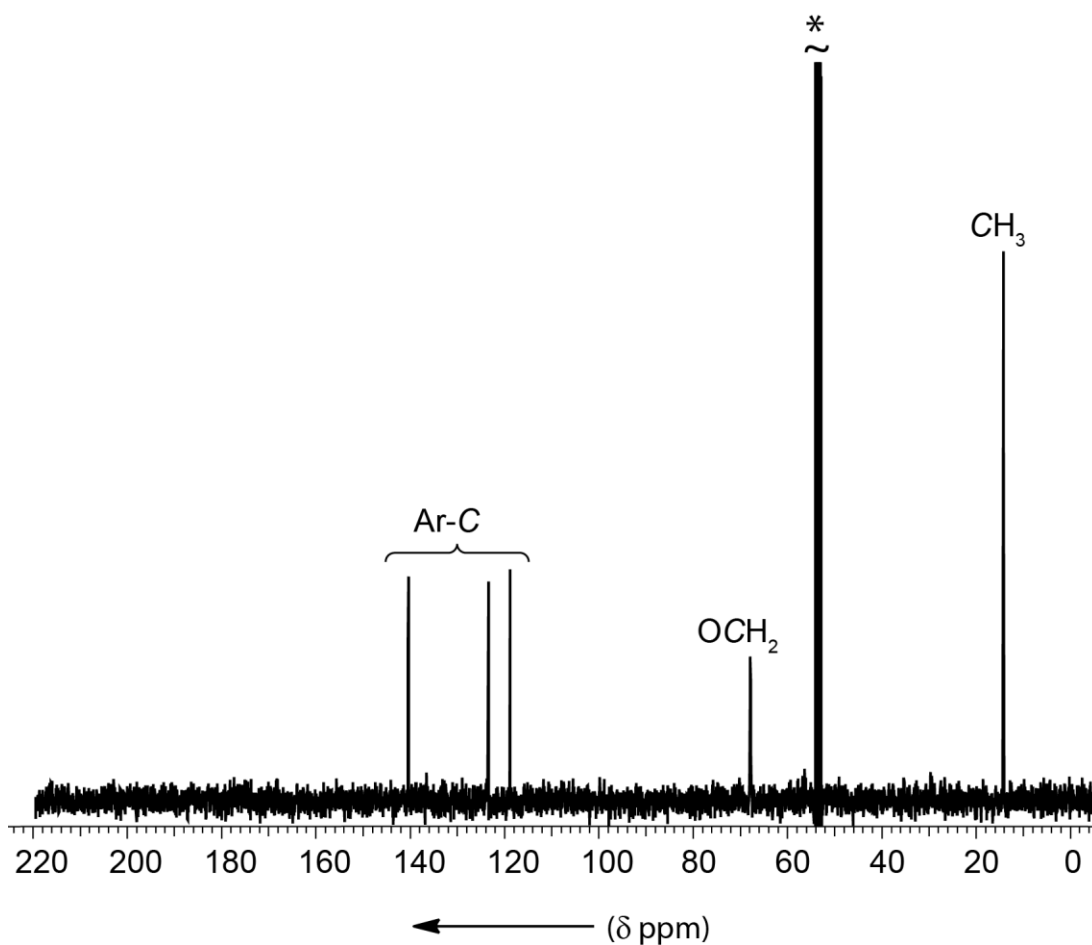


Figure 5.6.  $^{13}\text{C}\{^1\text{H}\}$  NMR (400 MHz,  $\text{CD}_2\text{Cl}_2$ , 25 °C) spectrum of  $\text{H}(\text{OEt}_2)_2[5.2]$ .

\* indicates residual NMR solvent.

### 5.2.2 Metrical Parameters Determined by X-ray Crystallography

The crude Brønsted acid  $\text{H}(\text{OEt}_2)_2[5.1]$  was crystallized from a concentrated solution of the crude product in  $\text{CD}_2\text{Cl}_2$  at  $-30\text{ °C}$  under inert atmosphere to afford colorless crystals within *ca.* 3 days. The solid state structure exhibits one water molecule and one diethyl ether molecule within the cation moiety in  $[\text{H}(\text{OEt}_2)(\text{H}_2\text{O})]^+$ . Presumably, adventitious water in the solvent for crystallization led to the unexpected growth of a single crystal of  $[\text{H}(\text{OEt}_2)(\text{H}_2\text{O})][5.1] \cdot \text{OEt}_2 \cdot 0.17 \text{ CH}_2\text{Cl}_2$ .

Particularly intriguing is the structure of the anion with two chelated tetrachlorocatechol moieties [Ta(1)–O(1) and Ta(1)–O(2); Ta(1)–O(5) and Ta(1)–O(6)] and two monodentate tetrachlorocatechol ligands coordinated in the *cis* position. The molecular structure of H(OEt<sub>2</sub>)(H<sub>2</sub>O)[**5.1**] displays close interaction between an oxygen of the bidentate tetrachlorocatechol of the anion [**5.1**]<sup>–</sup> and a hydrogen of the hydroxyl group of the monodentate tetrachlorocatechol of the anion [**5.1**]<sup>–</sup> [O(6)···H(4) = 1.91(2) Å; O(2)···H(8) = 2.23(2) Å].

The closest cation–anion contact in H(OEt<sub>2</sub>)(H<sub>2</sub>O)[**5.1**] occurs between an oxygen atom of the anion [**5.1**]<sup>–</sup> and a hydrogen atom of H<sub>2</sub>O solvate [O(4)···H(11a) = 2.00(2) Å] and is within the sum of the van der Waals radii for oxygen and hydrogen [ $r_{\text{vdw}} = 2.72 \text{ Å}$ ].<sup>306</sup> Notably striking is the coordination environment around the Ta(V) center. Specifically, the hydroxyl groups of the two monodentate C<sub>6</sub>Cl<sub>4</sub>O(OH)–ligand moieties are bent toward the oxygen atoms of the chelated tetrachlorocatechol ligands. The tantalum(V) center in the anion [**5.1**]<sup>–</sup> exhibits a distorted octahedral geometry. The two monodentate coordinated tetrachlorocatechol moieties are *cis* disposed and demonstrate a deviation from octahedral angles for the anion in H(OEt<sub>2</sub>)(H<sub>2</sub>O)[**5.1**] [O(3)–Ta(1)–O(7) = 93.0(8)°; O(1)–Ta(1)–O(3) = 95.4(8)°; O(2)–Ta(1)–O(7) = 82.2(7)°; O(5)–Ta(1)–O(7) = 86.7(8)°; O(3)–Ta(1)–O(6) = 86.6(7)°], likely due to steric repulsion or short intermolecular contacts. The chelated tetrachlorocatechol ligands occupy positions through the oxygen atoms [Ta(1)–O(2) and Ta(1)–O(6); Ta(1)–O(1) and Ta(1)–O(5)] and display perturbation from regular octahedral angles [O(2)–Ta(1)–O(6) = 163.4(7)°; O(3)–Ta(1)–O(5) = 159.4(7)°]. In comparison, a *pseudo*–octahedral geometry around the tantalum(V) center has been observed in [NEt<sub>2</sub>H<sub>2</sub>][Ta–(O<sub>2</sub>C<sub>20</sub>H<sub>10</sub>{SiMe<sub>3</sub>}<sub>2–3,3'</sub>)<sub>2</sub>Cl<sub>2</sub>] with two binaphthoxide ligands bound to the metal center in a bidentate fashion and two chlorine atoms bound in a *cis*–arrangement [O–Ta–O, 92.7°; Cl–Ta–Cl, 84.6°].<sup>438</sup> Furthermore, a *pseudo*–

octahedral geometry around each metal center has been reported in  $[\text{Ta}(\text{OCH}_3)_4\{(\text{Me})_3\text{CCOCH}_2\text{CO}(\text{Me})_3\}]$  [O–Ta–O range from  $79.3(2)^\circ$  to  $92.7(3)^\circ$ ] and  $[\text{Ta}(\text{OCH}_3)_4\{(\text{CH}_3\text{C}(\text{O})\text{CH}_2\text{C}(\text{O})\text{CH}_3\}]$  [O–Ta–O range from  $78.9(2)^\circ$  to  $92.5(5)^\circ$ ].<sup>451</sup>

The Ta–O bond distances in  $\text{H}(\text{OEt}_2)(\text{H}_2\text{O})[\mathbf{5.1}]$  range from  $1.879(12)$  Å to  $2.074(16)$  Å. The average Ta–O bond lengths in  $\text{H}(\text{OEt}_2)(\text{H}_2\text{O})[\mathbf{5.1}]$  [avg. Ta–O  $2.019(34)$  Å and  $1.906(21)$  Å] is at the shorter end of the typical range found in  $[\text{Ta}(\text{C}_6\text{H}_4\text{O}_2)_3\text{py}]$  [avg.  $2.025(12)$  Å],<sup>452</sup>  $[\text{Ph}_3\text{C}][\text{Ta}(\text{OC}_6\text{F}_5)_6]$  [avg.  $1.952(3)$  Å],<sup>150</sup> and other tantalum-oxygen containing bidentate and mono-dentate systems [avg. range:  $2.032(2)$ – $2.16(1)$  and  $1.863(3)$ – $1.976(1)$ ].<sup>441,451,453-457</sup>

In addition to the anion, the metrical parameters for the cation moiety provide valuable insight into the bonding within the compound. The  $[\text{H}(\text{OEt}_2)(\text{H}_2\text{O})]^+$  moiety in  $\text{H}(\text{OEt}_2)(\text{H}_2\text{O})[\mathbf{5.1}]$  crystallizes out with one  $\text{H}_2\text{O}$  molecule. The acidic proton in  $[\text{H}(\text{OEt}_2)(\text{H}_2\text{O})]^+$  was located in the difference electron density map and refined isotropically. It appears that the acidic proton is coordinated asymmetrically through the oxygen atom of one diethyl ether molecule and an oxygen atom of the  $\text{H}_2\text{O}$  group [O(10)–H(10) =  $1.10(4)$  Å; O(11)–H(10) =  $1.50(4)$  Å] (Figure 5.7). Further, a close contact is observed in the cation moiety in  $[\text{H}(\text{OEt}_2)(\text{H}_2\text{O})]^+$  between an oxygen atom of diethyl ether solvate molecule and a hydrogen of the  $\text{H}_2\text{O}$  molecule [O(9)–H(11b) =  $1.57(2)$  Å] and is within the sum of the van der Waals radii for oxygen and hydrogen [ $r_{\text{vdw}} = 2.72$  Å].<sup>306</sup>

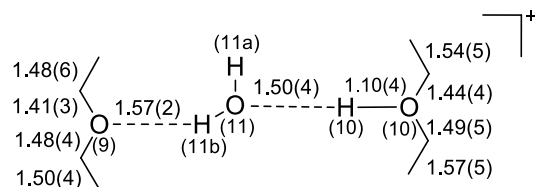


**Figure 5.7.** Metrical parameters [Å] for the cation in  $\text{H}(\text{OEt}_2)(\text{H}_2\text{O})[\mathbf{5.1}] \cdot \text{OEt}_2 \cdot 0.17 \text{CH}_2\text{Cl}_2$ .

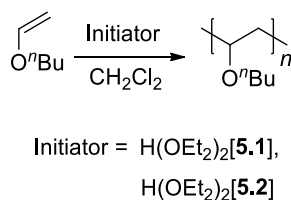
Asymmetric binding has been reported for related systems containing the cation moiety  $[\text{H}(\text{OEt}_2)_2]^+$  in  $\text{H}(\text{OEt}_2)_2[\text{P}(\text{1,2-O}_2\text{C}_6\text{Cl}_4)_3]$  [1.09(4) Å and 1.34(4) Å],<sup>269</sup>  $\text{H}(\text{OEt}_2)_2[\text{Al}\{\text{OC}(\text{CF}_3)_3\}_4]$  [0.75(5) Å and 1.76(5) Å]<sup>298</sup>,  $\text{H}(\text{OEt}_2)_2[\text{B}(\text{C}_6\text{F}_5)_4]$  [0.93(1) Å and 1.52(1) Å],<sup>331</sup>  $\text{H}(\text{OEt}_2)_2[\text{CHB}_{11}\text{Me}_5\text{Cl}_6]$  [1.08(3) Å and 1.59(3) Å; 0.80(3) Å and 1.45(3) Å]<sup>195</sup> and  $\text{H}(\text{OEt}_2)_2[(\text{C}_3\text{H}_3\text{N}_2)\{\text{B}(\text{C}_6\text{F}_5)_3\}_2]$  [1.11(1) Å and 1.34(9) Å].<sup>449</sup> Though, it has not been extensively noted for the more rare  $[\text{H}(\text{OEt}_2)(\text{H}_2\text{O})]^+$  cation. Reed and co-workers reported the mixed  $[\text{H}(\text{OEt}_2)(\text{H}_2\text{O})]^+$  cation and concluded that the position of the acidic proton is located closer to the ether molecule.<sup>195</sup> In addition, theoretical calculations of the gas-phase structure of  $[\text{H}(\text{MeOH})(\text{H}_2\text{O})]^+$  suggest an asymmetric binding of  $\text{H}^+-\text{O}-\text{H}$  in protonated methanol.<sup>458</sup> Since the determination of the position of the central proton is generally unreliable, the more precisely determined C–O and C–C bond lengths are often used to evaluate the symmetry within the  $[\text{H}(\text{OEt}_2)(\text{H}_2\text{O})]^+$  cation. The C–O distances in the coordinated ether molecules [C(30)–O(10) = 1.49(5) Å and C(31)–O(10) = 1.44(4) Å; C(26)–O(9) = 1.41(3) Å and C(27)–O(9) = 1.48(4) Å] display a slight lengthening from the C–O bond lengths found in ether lattice solvate [1.416 Å].<sup>459</sup> This may reflect asymmetric binding within the  $[\text{H}(\text{OEt}_2)(\text{H}_2\text{O})]^+$  cation. For comparison, a similar bonding situation has been observed for  $\text{H}(\text{OEt}_2)(\text{H}_2\text{O})[\text{CHB}_{11}\text{H}_5\text{Cl}_6]$  [avg. 1.445(9) Å and 1.471(1) Å],<sup>195</sup>  $\text{H}(\text{OEt}_2)_2[\text{B}(\text{C}_6\text{F}_5)_4]$  [1.443(14) Å and 1.429(13) Å; 1.542(12) Å and 1.466(15) Å],<sup>331</sup>  $\text{H}(\text{OEt}_2)_2[\text{Al}\{\text{OC}(\text{CF}_3)_3\}_4]$  [1.440(6) Å and 1.508(5) Å; 1.412(5) Å and 1.470(6) Å],<sup>298</sup> as well as  $\text{H}(\text{OEt}_2)_2[(\text{C}_3\text{H}_3\text{N}_2)\{\text{B}(\text{C}_6\text{F}_5)_3\}_2]$  [1.44(1)(12) Å and 1.52(2) Å; 1.456(9) Å and 1.448(10) Å].<sup>449</sup>

The extent of hydrogen bonding within the cation of  $[\text{H}(\text{OEt}_2)_2(\text{H}_2\text{O})][\mathbf{5.1}]$  may be evaluated by considering the  $\text{O}\cdots\text{O}$  distances. The  $\text{O}\cdots\text{O}$  distance within the  $[\text{H}(\text{OEt}_2)_2(\text{H}_2\text{O})]^+$  cation between one diethyl ether molecule and water [O(9) $\cdots$ O(11) = 2.43(3) Å; O(10) $\cdots$ O(11)

= 2.46(3) Å] is significantly shorter than the sum of the van der Waals radii [ $r_{\text{vdw}} = 3.04 \text{ Å}$ ].<sup>306</sup> For comparison, this data is similar to the O...O distances for the known compounds containing the  $[\text{H}(\text{OEt}_2)_2]^+$  cation in  $\text{H}(\text{OEt}_2)(\text{H}_2\text{O})[\text{CHB}_{11}\text{H}_5\text{Cl}_6]$  [avg. 2.441(6) Å] and  $\text{H}(\text{OEt}_2)_2[\text{CHB}_{11}\text{Me}_5\text{Cl}_6]$  [avg. 2.40(1) Å],<sup>195</sup>  $\text{H}(\text{OEt}_2)_2[\text{B}(\text{C}_6\text{F}_5)_4]$  [2.446(9) Å],<sup>331</sup>  $\text{H}(\text{OEt}_2)_2[\text{P}(1,2\text{-O}_2\text{C}_6\text{Cl}_4)_3]$  [2.429(2) Å],<sup>269</sup>  $\text{H}(\text{OEt}_2)_2[\text{Zn}_2\text{Cl}_6]$  [2.396(4) Å],<sup>460</sup>  $\text{H}(\text{OEt}_2)_2[\text{Al}\{\text{OC}(\text{CF}_3)_3\}_4]$  [2.424(5) Å],<sup>298</sup> whilst the O...O distances in  $\text{H}(\text{OEt}_2)_2[(\text{C}_3\text{H}_3\text{N}_2)\{\text{B}(\text{C}_6\text{F}_5)_3\}_2]$  [2.395(8) Å],<sup>449</sup> and  $\text{H}(\text{OEt}_2)_2[\text{P}(\text{C}_2\text{O}_4)_3]$  [avg. 2.37(3) Å]<sup>248</sup> are slightly shorter.

### 5.2.3 $\text{H}(\text{OEt}_2)_2[\mathbf{5.1}]$ and $\text{H}(\text{OEt}_2)_2[\mathbf{5.2}]$ -initiated Cationic Polymerization

The complexes  $\text{H}(\text{OEt}_2)_2[\mathbf{5.1}]$  and  $\text{H}(\text{OEt}_2)_2[\mathbf{5.2}]$  were investigated as initiators for the cationic polymerization of olefins at a variety of temperatures (between 18 °C to -78 °C). Chain transfer processes are suppressed in cationic polymerization by applying low temperatures resulting in higher molecular weight polymers.<sup>26,27,314</sup> The results of the polymerization studies are given in Tables 5.1 and 5.2 and each data point is representative of two or more repeat runs. Each polymerization was performed utilizing freshly distilled solvents and monomers. The polymerization results demonstrated that the Brønsted acids  $\text{H}(\text{OEt}_2)_2[\mathbf{5.1}]$  and  $\text{H}(\text{OEt}_2)_2[\mathbf{5.2}]$  were effective initiators for the carbocationic polymerization of *n*-butyl vinyl ether (Scheme 5.3) and  $\alpha$ -methylstyrene (Scheme 5.4).  $\text{H}(\text{OEt}_2)_2[\mathbf{5.1}]$  was investigated as a single-component initiator for the cationic polymerization of styrene (Scheme 5.5) and isoprene (Scheme 5.6).



**Scheme 5.3. H(OEt<sub>2</sub>)<sub>2</sub>[5.1] and H(OEt<sub>2</sub>)<sub>2</sub>[5.2]-initiated cationic polymerization of *n*-butyl vinyl ether.**

Vinyl ethers are ideal monomers for cationic polymerization studies since they form more stable carbocations during polymerization than many other monomers. This is due to the ether group that effectively stabilizes the propagating carbocation with strong electron donating ability. *n*-Butyl vinyl ether was successfully polymerized by H(OEt<sub>2</sub>)<sub>2</sub>[**5.1**] and H(OEt<sub>2</sub>)<sub>2</sub>[**5.2**]. The ambient temperature polymerization resulted in poly(*n*-butyl vinyl ether) as a brown viscous oil in moderate yield and reasonable molecular weight (yield: 38%,  $M_n = 19,800 \text{ g mol}^{-1}$ ,  $D = 1.69$ , Table 5.1, entry 1; yield: 33%,  $M_n = 16,300 \text{ g mol}^{-1}$ ,  $D = 1.54$ , Table 5.2, entry 1). For comparison, other binary initiator systems [*e.g.* EtAlCl<sub>2</sub>/H<sub>3</sub>C(CH<sub>2</sub>)<sub>3</sub>(O)CH(CH<sub>2</sub>)COOCH<sub>3</sub> ( $M_n = 19,500 \text{ g mol}^{-1}$ ,  $D = 1.14$ ,  $T = 20 \text{ }^\circ\text{C}$ )] afford poly(*n*-butyl vinyl ether) with comparable moderate molecular weight.<sup>461</sup> Although the polymers obtained at 18 °C and 19.3 °C were colored, the polymerizations at lower temperatures gave colorless poly(*n*-butyl vinyl ether). The brown color of the isolated poly(*n*-butyl vinyl ether) suggested that terminal conjugated polyene moieties were present. It has previously been reported that these ene functionalities were formed from proton elimination followed by dealcoholation.<sup>310-313</sup> The <sup>1</sup>H NMR spectra of poly(*n*-butyl vinyl ether) with a brown coloration produced at 18 °C and 19.3 °C using initiators H(OEt<sub>2</sub>)<sub>2</sub>[**5.1**] and H(OEt<sub>2</sub>)<sub>2</sub>[**5.2**], respectively, displayed signals in the vinyl region (5.0–6.0 ppm) that were not present in the colorless polymer produced at –84 °C (Figure 5.8).

At lower temperatures, the isolated yields and molecular weights of poly(*n*-butyl vinyl ether) each increased when similar monomer-to-initiator ratios were employed (yield: 65–71%,  $M_n = 25,300\text{--}39,100 \text{ g mol}^{-1}$ ,  $D = 2.07\text{--}1.12$ , Table 5.1, entries 3–7; yield: 31–77%,  $M_n = 19,400\text{--}53,100 \text{ g mol}^{-1}$ ,  $D = 1.69\text{--}1.14$  Table 5.2, entries 2–5). Remarkably, the initiators, H(OEt<sub>2</sub>)<sub>2</sub>[**5.1**] and H(OEt<sub>2</sub>)<sub>2</sub>[**5.2**], were able to initiate *n*-butyl vinyl ether at temperatures as low as –84 °C and gave similar results producing poly(*n*-butyl vinyl ether) with moderate isolated yield, high molecular weight and narrow dispersity ( $M_n = 39,100 \text{ g mol}^{-1}$ ,  $D = 1.12$  and  $M_n = 53,100 \text{ g mol}^{-1}$ ,  $D = 1.14$ , respectively). It should be noted that the molecular weights observed were close to that predicted from the monomer-to-initiator ratio [ $M_n = 40,100 \text{ g mol}^{-1}$  and  $M_n = 40,900 \text{ g mol}^{-1}$ , respectively] and may indicate characteristics of a living polymerization for *n*-butyl vinyl ether, similar to our findings with the previously reported single-component initiator H(OEt<sub>2</sub>)<sub>2</sub>[P(1,2-O<sub>2</sub>C<sub>6</sub>Cl<sub>4</sub>)<sub>3</sub>] (–78 °C: 88%;  $M_n = 41,600 \text{ g mol}^{-1}$ ,  $D = 1.11$ ).<sup>269</sup> Confirming the living character of *n*-butyl vinyl ether polymerization is beyond the scope of the present study. Living cationic polymerization of vinyl ethers has been investigated with binary initiator systems (*e.g.* HCl/ZnCl<sub>2</sub> in toluene at –30 °C; HCl/ZnCl<sub>2</sub> in CH<sub>2</sub>Cl<sub>2</sub> at –15 °C; C<sub>9</sub>H<sub>12</sub>N<sub>6</sub>Cl<sub>6</sub>/ZnCl<sub>2</sub> in CH<sub>2</sub>Cl<sub>2</sub> at –45 °C).<sup>177,462,463</sup> In contrast, the cationic polymerization of isobutyl vinyl ether and *tert*-butyl vinyl ether with two-component systems comprised of Lewis acids (*e.g.* ZnCl<sub>2</sub>, TiCl<sub>4</sub>, SnCl<sub>4</sub>, EtAlCl<sub>2</sub>) and a proton donor (*e.g.* CF<sub>3</sub>COOH, HCl) give low to moderate molecular weight poly(vinyl ethers) at –78 °C.<sup>464,465</sup> Notably, these initiators afford polymers with lower molecular weights and broader dispersity than those obtained using H(OEt<sub>2</sub>)<sub>2</sub>[**5.1**] as initiator.

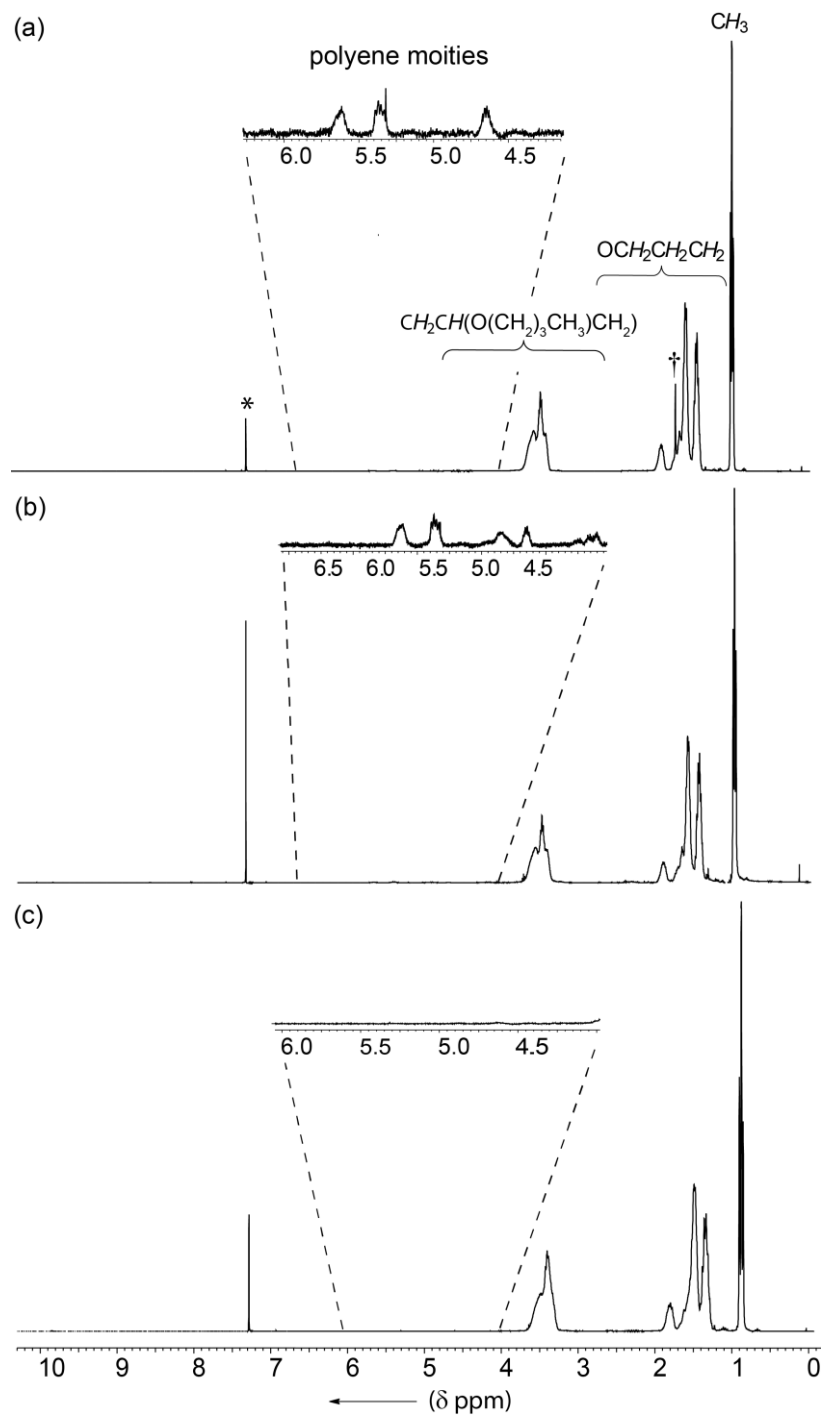


**Figure 5.8.**  $^1\text{H}$  NMR (400 MHz,  $\text{CDCl}_3$ , 25  $^\circ\text{C}$ ) spectrum of poly(*n*-butyl vinyl ether); polymerization performed (a) with initiator  $\text{H}(\text{OEt}_2)_2[5.1]$  at 18  $^\circ\text{C}$ , (b) with initiator  $\text{H}(\text{OEt}_2)_2[5.2]$  at 19.3  $^\circ\text{C}$ , (c) with initiator  $\text{H}(\text{OEt}_2)_2[5.1]$  at -84  $^\circ\text{C}$ .

\* indicates residual  $\text{CHCl}_3$ , † indicates  $\text{H}_2\text{O}$  residue.

**Table 5-1. Temperature dependencies of H(OEt)<sub>2</sub>[5.1]-initiated cationic polymerizations of *n*-butyl vinyl ether,  $\alpha$ -methylstyrene, styrene, and isoprene in CH<sub>2</sub>Cl<sub>2</sub>. The results shown are representative of multiple repeat runs.**

| Entry | monomer                     | <i>T</i><br>(°C) | <i>t</i><br>(min) | [M]:[I] <sup>a</sup> | yield<br>(%) | <i>M</i> <sub>n</sub> <sup>b</sup><br>(g mol <sup>-1</sup> ) | <i>D</i> <sup>c</sup> |
|-------|-----------------------------|------------------|-------------------|----------------------|--------------|--|-----------------------|
| 1     | <i>n</i> -butyl vinyl ether | 18               | 15                | 492                  | 38           | 19,800   | 1.69                  |
| 2     | <i>n</i> -butyl vinyl ether | 0                | 15                | 492                  | 40           | 17,000   | 1.21                  |
| 3     | <i>n</i> -butyl vinyl ether | -15              | 15                | 492                  | 65           | 25,300   | 1.89                  |
| 4     | <i>n</i> -butyl vinyl ether | -38              | 15                | 492                  | 62           | 30,600   | 1.96                  |
| 5     | <i>n</i> -butyl vinyl ether | -50              | 15                | 492                  | 68           | 29,400   | 2.07                  |
| 6     | <i>n</i> -butyl vinyl ether | -78              | 15                | 492                  | 71           | 32,200   | 1.58                  |
| 7     | <i>n</i> -butyl vinyl ether | -84              | 15                | 492                  | 57           | 39,100   | 1.12                  |
| 8     | styrene                     | 18               | 15                | 492                  | 67           | 6,100  | 2.16                  |
| 9     | styrene                     | 0                | 15                | 492                  | 82           | 9,500  | 2.94                  |
| 10    | styrene                     | -15              | 15                | 492                  | 85           | 12,800   | 3.51                  |
| 11    | styrene                     | -38              | 15                | 492                  | 72           | 131,500  | 1.34                  |
| 12    | styrene                     | -50              | 15                | 492                  | 78           | 147,100  | 1.43                  |
| 13    | styrene                     | -78              | 15                | 492                  | 5            | 205,600  | 1.29                  |
| 14    | $\alpha$ -methylstyrene     | 19               | 15                | 400                  | 0            | n.d. <sup>d</sup>  | n.d. <sup>d</sup>     |
| 15    | $\alpha$ -methylstyrene     | 0                | 15                | 400                  | 3            | 5,100  | 1.63                  |
| 16    | $\alpha$ -methylstyrene     | -15              | 15                | 400                  | 45           | 4,800  | 2.37                  |
| 17    | $\alpha$ -methylstyrene     | -38              | 15                | 400                  | 63           | 10,100   | 1.87                  |
| 18    | $\alpha$ -methylstyrene     | -50              | 15                | 400                  | 84           | 66,400   | 1.81                  |
| 19    | $\alpha$ -methylstyrene     | -78              | 15                | 400                  | 75           | 279,500  | 1.21                  |
| 20    | isoprene                    | 18               | 15                | 400                  | 70           | 3,000  | 2.13                  |
| 21    | isoprene                    | 0                | 15                | 400                  | 52           | 3,200  | 4.84                  |
| 22    | isoprene                    | -15              | 15                | 400                  | 65           | 2,100  | 5.01                  |
| 23    | isoprene                    | -38              | 15                | 400                  | 55           | 2,900  | 1.52                  |
| 24    | isoprene                    | -50              | 15                | 400                  | 40           | 2,600  | 1.73                  |
| 25    | isoprene                    | -78              | 15                | 400                  | 4            | n.d. <sup>d</sup>  | n.d. <sup>d</sup>     |

The polymerization was carried out in 2 mL CH<sub>2</sub>Cl<sub>2</sub> solvent using 0.0075 mmol of Brønsted acid as initiator.

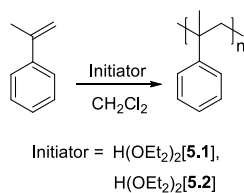
<sup>a</sup> [Monomer]/[Initiator] ratio. <sup>b</sup> Absolute molecular weights were determined using laser light scattering gel permeation chromatography (GPC-LLS); differential refractive index (*dn/dc*) of poly(*n*-butyl vinyl ether) (*dn/dc* = 0.068 mL g<sup>-1</sup>) in THF was calculated by assuming 100% mass recovery; (*dn/dc*) of poly( $\alpha$ -methylstyrene) used is 0.174 mL g<sup>-1</sup>; (*dn/dc*) of polystyrene used is 0.185 mL g<sup>-1</sup> and (*dn/dc*) of polyisoprene used is 0.129 mL g<sup>-1</sup>. <sup>c</sup> Dispersity (*D* = *M*<sub>w</sub>/*M*<sub>n</sub>), where *M*<sub>w</sub> is the weight-average molar mass and *M*<sub>n</sub> is the number-average molar mass. <sup>d</sup> Not determined.

**Table 5-2. Temperature dependencies of H(OEt)<sub>2</sub>[5.2]-initiated cationic polymerizations of *n*-butyl vinyl ether and  $\alpha$ -methylstyrene in CH<sub>2</sub>Cl<sub>2</sub>.**

| Entry | monomer                     | <i>T</i><br>(°C) | <i>t</i><br>(min) | [M]:[I] <sup>a</sup> | yield<br>(%) | <i>M<sub>n</sub></i> <sup>b</sup><br>(g mol <sup>-1</sup> ) | <i>D</i> <sup>c</sup> |
|-------|-----------------------------|------------------|-------------------|----------------------|--------------|---|-----------------------|
| 1     | <i>n</i> -butyl vinyl ether | 19.3             | 15                | 400                  | 33           | 16,300  | 1.54                  |
| 2     | <i>n</i> -butyl vinyl ether | 0                | 15                | 400                  | 31           | 19,400  | 1.69                  |
| 3     | <i>n</i> -butyl vinyl ether | -50              | 15                | 400                  | 61           | 18,200  | 1.57                  |
| 4     | <i>n</i> -butyl vinyl ether | -78              | 15                | 400                  | 72           | 34,100  | 1.45                  |
| 5     | <i>n</i> -butyl vinyl ether | -84              | 15                | 400                  | 77           | 53,100  | 1.14                  |
| 6     | $\alpha$ -methylstyrene     | 19               | 15                | 400                  | 0            | n.d. <sup>d</sup>   | n.d. <sup>d</sup>     |
| 7     | $\alpha$ -methylstyrene     | 0                | 15                | 400                  | 38           | 3,500   | 1.67                  |
| 8     | $\alpha$ -methylstyrene     | -38              | 15                | 400                  | 75           | 10,100  | 1.86                  |
| 9     | $\alpha$ -methylstyrene     | -50              | 15                | 400                  | 65           | 17,000  | 1.59                  |
| 10    | $\alpha$ -methylstyrene     | -78              | 15                | 400                  | 53           | 205,000   | 1.28                  |

The polymerization was carried out in 2 mL CH<sub>2</sub>Cl<sub>2</sub> solvent using 0.010 mmol of Brønsted acid as initiator.

<sup>a</sup> [Monomer]/[Initiator] ratio. <sup>b</sup> Absolute molecular weights were determined using laser light scattering gel permeation chromatography (GPC-LLS); differential refractive index (*dn/dc*) of poly(*n*-butyl vinyl ether) (*dn/dc* = 0.068 mL g<sup>-1</sup>.) in THF was calculated by assuming 100% mass recovery; (*dn/dc*) of poly( $\alpha$ -methylstyrene) used is 0.174 mL g<sup>-1</sup>. <sup>c</sup> Dispersity (*D* = *M<sub>w</sub>*/*M<sub>n</sub>*), where *M<sub>w</sub>* is the weight-average molar mass and *M<sub>n</sub>* is the number-average molar mass. <sup>d</sup> Not determined.



**Scheme 5.4. H(OEt<sub>2</sub>)<sub>2</sub>[5.1] and H(OEt<sub>2</sub>)<sub>2</sub>[5.2]-initiated cationic polymerization of  $\alpha$ -methylstyrene.**

$\alpha$ -Methylstyrene was successfully polymerized by using either H(OEt<sub>2</sub>)<sub>2</sub>[5.1] or H(OEt<sub>2</sub>)<sub>2</sub>[5.2] as the initiator over a range of temperatures (0 °C to –78 °C; Table 5.1, entries 15–19; Table 5.2, entries 7–10). The ceiling temperature ( $T_c$ ) of  $\alpha$ -methylstyrene is around ambient temperature at which the rate of polymerization and depolymerization are equal.<sup>466,467</sup> Thus, the ambient temperature polymerization of  $\alpha$ -methylstyrene initiated by H(OEt<sub>2</sub>)<sub>2</sub>[5.1] and H(OEt<sub>2</sub>)<sub>2</sub>[5.2] gave no polymer. This effect has also been observed using H(OEt<sub>2</sub>)<sub>2</sub>[P(1,2–O<sub>2</sub>C<sub>6</sub>Cl<sub>4</sub>)<sub>3</sub>] as initiating system<sup>269</sup> and other binary initiators.<sup>466, 467</sup> In particular, lowering the polymerization temperature ranging from 0 °C to –50 °C resulted in moderate to high molecular weight poly( $\alpha$ -methylstyrene) ( $M_n = 5,100$ – $66,400$  g mol<sup>-1</sup>, Table 5.1, entry 15–18;  $M_n = 3,500$ – $17,000$  g mol<sup>-1</sup>, Table 5.2, entry 6–8) in low to good yield. The low molecular weight of poly( $\alpha$ -methylstyrene) obtained using H(OEt<sub>2</sub>)<sub>2</sub>[5.1] and H(OEt<sub>2</sub>)<sub>2</sub>[5.2] at temperatures ranging from 0 °C to –38 °C were indicative of chain transfer and/or termination reactions. Above all, lowering the polymerization temperature to –78 °C afforded very high molecular weight polymer ( $M_n = 279,500$  g mol<sup>-1</sup>,  $D = 1.21$ , yield: 75%, Table 5.1, entry 19;  $M_n = 205,000$  g mol<sup>-1</sup>,  $D = 1.28$ , yield: 53%, Table 5.2, entry 10) with narrow dispersity in a moderate to good yield.

Integration of the triad signal ( $rr$ ) of the <sup>1</sup>H NMR spectra of the poly( $\alpha$ -methylstyrene) produced at –78 °C using either H(OEt<sub>2</sub>)<sub>2</sub>[5.1] or H(OEt<sub>2</sub>)<sub>2</sub>[5.2] as initiator (Figure 5.9 and Appendix D, Figure D4) suggested a predominantly syndiotactic rich polymer (% $rr = 90$  and

%*rr* = 86, respectively). Similarly, syndiotactic rich poly( $\alpha$ -methylstyrene) has been isolated with single-component initiators (*e.g.* H(OEt<sub>2</sub>)<sub>2</sub>[P(1,2-O<sub>2</sub>C<sub>6</sub>Cl<sub>4</sub>)<sub>3</sub>] (%*rr* = 87); [Ph<sub>3</sub>C][BF<sub>4</sub>] %*rr* = 86 and [Ph<sub>3</sub>C][SnCl<sub>6</sub>] %*rr* = 87)<sup>269,468</sup> and binary initiator systems (*e.g.* FeCl<sub>3</sub>/[*n*Bu<sub>4</sub>NBr] %*rr* = 84; BI<sub>3</sub>/[(CH<sub>3</sub>)<sub>3</sub>C]<sub>2</sub>C<sub>5</sub>H<sub>3</sub>N %*rr* = 90; C<sub>8</sub>H<sub>17</sub>Cl/TiCl<sub>4</sub>/Et<sub>3</sub>N %*rr* = 94; BCl<sub>3</sub>/[(CH<sub>3</sub>)<sub>3</sub>C]<sub>2</sub>C<sub>5</sub>H<sub>3</sub>N %*rr* = 87).<sup>41,469-472</sup>

The cationic polymerization of  $\alpha$ -methylstyrene initiated by either H(OEt<sub>2</sub>)<sub>2</sub>[**5.1**] or H(OEt<sub>2</sub>)<sub>2</sub>[**5.2**] afforded polymer with a higher molecular weight compared to the calculated [M]:[I] ratio that suggested the presence of side reactions during polymerization. The <sup>1</sup>H NMR spectra of poly( $\alpha$ -methylstyrene) (Figure 5.9 and Appendix D4) displayed small signals in the vinyl region in the range between 4.0 to 6.0 ppm. These signals have previously been ascribed to vinylic protons that may result from branching caused by Friedel-Crafts alkylation/arylation and hydride transfer reactions during living cationic polymerization of styrene.<sup>320,321</sup> In order to investigate branching in the high molecular weight polymer obtained by either H(OEt<sub>2</sub>)<sub>2</sub>[**5.1**] or H(OEt<sub>2</sub>)<sub>2</sub>[**5.2**] as initiator, the intrinsic viscosity of the samples were compared to that of a linear polystyrene standard with identical molecular weight ( $M_w = 10^5 \text{ g mol}^{-1}$ ), as a bona fide sample of linear poly( $\alpha$ -methylstyrene) was unavailable. The intrinsic viscosity for poly( $\alpha$ -methylstyrene) was lower than that for linear polystyrene ( $[\eta]_w = 67 \text{ mL g}^{-1}$  vs.  $76 \text{ mL g}^{-1}$ ) that may indicate branching in the polymer. Branched polymers possess unique physical properties including viscosity and elasticity, when compared to linear polymers. The physical property of the branched polymer was not studied further.

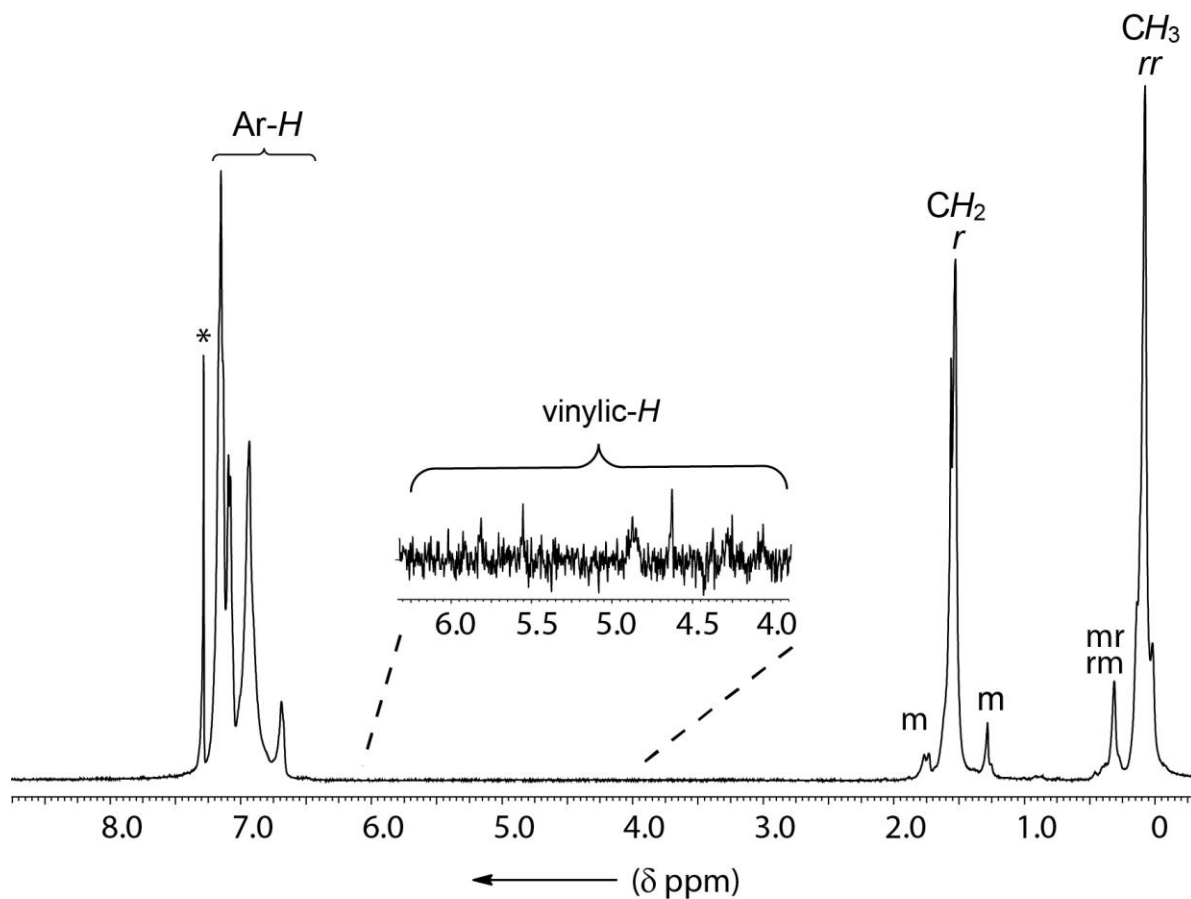
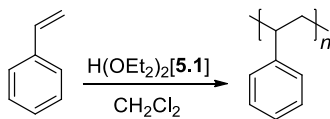


Figure 5.9.  $^1\text{H}$  NMR (400 MHz,  $\text{CDCl}_3$ ,  $25^\circ\text{C}$ ) spectrum of syndiotactic-rich poly( $\alpha$ -methylstyrene) ( $rr = 90\%$ ); polymerization performed with initiator  $\text{H}(\text{OEt}_2)_2[5.1]$  at  $-78^\circ\text{C}$ . \* indicates residual  $\text{CHCl}_3$ .



Scheme 5.5.  $\text{H}(\text{OEt}_2)_2[5.1]$ -initiated cationic polymerization of styrene.

Controlled cationic polymerization of styrene is challenging due to chain transfer reaction and termination.<sup>37</sup> Unlike vinyl ethers, styrene forms a relatively unstable growing carbocation during polymerization due to weaker electron donating properties of the aryl substituent.<sup>473</sup> Uncontrolled polymerization with broad dispersity and low molecular weight polymer has been observed with binary cationic initiators [e.g.  $\text{AlCl}_3/\text{CH}_2\text{Cl}_2$  ( $M_n = 4,400 \text{ g mol}^{-1}$ ,  $D = 3.6$ ,  $T =$

0 °C); C<sub>6</sub>H<sub>5</sub>(C<sub>2</sub>H<sub>4</sub>)Cl/SnCl<sub>4</sub> CH<sub>2</sub>Cl<sub>2</sub> ( $M_n = 5,000 \text{ g mol}^{-1}$ ,  $D = 3.6$ ,  $T = 20 \text{ °C}$ )].<sup>66,474</sup> Styrene was successfully polymerized by H(OEt<sub>2</sub>)<sub>2</sub>[**5.1**] over a range of temperatures (18 °C to –78 °C; Table 5.1, entries 8–13). The ambient temperature polymerization afforded an off-white polymer in moderate yield with low molecular weight (18 °C: 67%;  $M_n = 6,100 \text{ g mol}^{-1}$ ,  $D = 2.16$ ; Table 5.2, entry 8). These data are typical of styrene polymers obtained when prepared at higher temperatures. Notably, at lower temperatures (–38 °C to –50 °C) high molecular weight polystyrene was obtained ( $M_n = 131,500\text{--}147,100 \text{ g mol}^{-1}$ ,  $D = 1.34\text{--}1.43$ ; Table 5.1, entries 11–12) as a colorless solid in high yield (ca. 72–78%). The single-component system H(OEt<sub>2</sub>)<sub>2</sub>[P(1,2-O<sub>2</sub>C<sub>6</sub>Cl<sub>4</sub>)<sub>3</sub>] afforded polystyrene with lower molecular weight ( $M_n = 37,800 \text{ g mol}^{-1}$ ,  $D = 1.88$ , [M]:[I] = 493)<sup>269</sup> opposed to H(OEt<sub>2</sub>)<sub>2</sub>[**5.1**] at –50 °C with the same monomer-to-initiator ratio.

The <sup>1</sup>H NMR spectrum of polystyrene produced at –50 °C displayed small signals in the vinyl region between 4.0–6.2 ppm (Figure 5.10). These signals have previously been attributed to vinylic protons that may result from branching caused by Friedel-Crafts alkylation/arylation and hydride transfer reactions during living cationic polymerization of styrene.<sup>320, 321</sup> Branching due to chain transfer in polystyrene has been reported when using stannic chloride as the initiator at 0 °C and higher molecular weights were obtained than that calculated from the [M]:[I] ratio ( $M_w$  up to 149,000 g mol<sup>-1</sup>).<sup>42-44,319</sup> A lower intrinsic viscosity was obtained for polystyrene afforded by H(OEt<sub>2</sub>)<sub>2</sub>[**5.1**] compared to that of a linear polystyrene standard ( $[\eta]_w = 63 \text{ mL g}^{-1}$  vs. 76 mL g<sup>-1</sup>) that may indicate branching in the polymer. It should be noted that samples with the same molecular weight ( $M_w = 10^5 \text{ g mol}^{-1}$ ) were used. The tacticity of polystyrene produced at –50 °C was investigated by <sup>13</sup>C{<sup>1</sup>H} NMR spectroscopy. The analysis of the resonances for the aromatic and methylene carbon regions was consistent with that of atactic polystyrene.

Remarkably, the polymerization at  $-78\text{ }^{\circ}\text{C}$  afforded the highest molecular weight polymer with a narrow dispersity ( $M_n = 205,600\text{ g mol}^{-1}$ ,  $D = 1.29$ , Table 5.1, entry 13), albeit in low yield (5%). At this temperature, the initiator,  $\text{H}(\text{OEt}_2)_2[\mathbf{5.1}]$ , shows limited capability to polymerize styrene. Similarly, this effect has been noticed with the single component initiator  $\text{H}(\text{OEt}_2)_2[\text{P}(1,2\text{-O}_2\text{C}_6\text{Cl}_4)_3]$ .<sup>269</sup> Lower molecular weight polystyrene in higher dispersity has been observed with other cationic initiators at  $-80\text{ }^{\circ}\text{C}$  (e.g.  $(\text{C}_6\text{H}_5\text{C}(\text{CH}_3)_3\text{OH}/\text{AlCl}_3\text{OBu}_2/\text{Py}$ ,  $M_n = 82,000\text{ g mol}^{-1}$ ,  $D = 1.80$ ; yield: ca. 35%). However, the polymer revealed a broader dispersity compared to the  $\text{H}(\text{OEt}_2)_2[\mathbf{5.1}]$ -initiated polystyrene.<sup>475</sup>

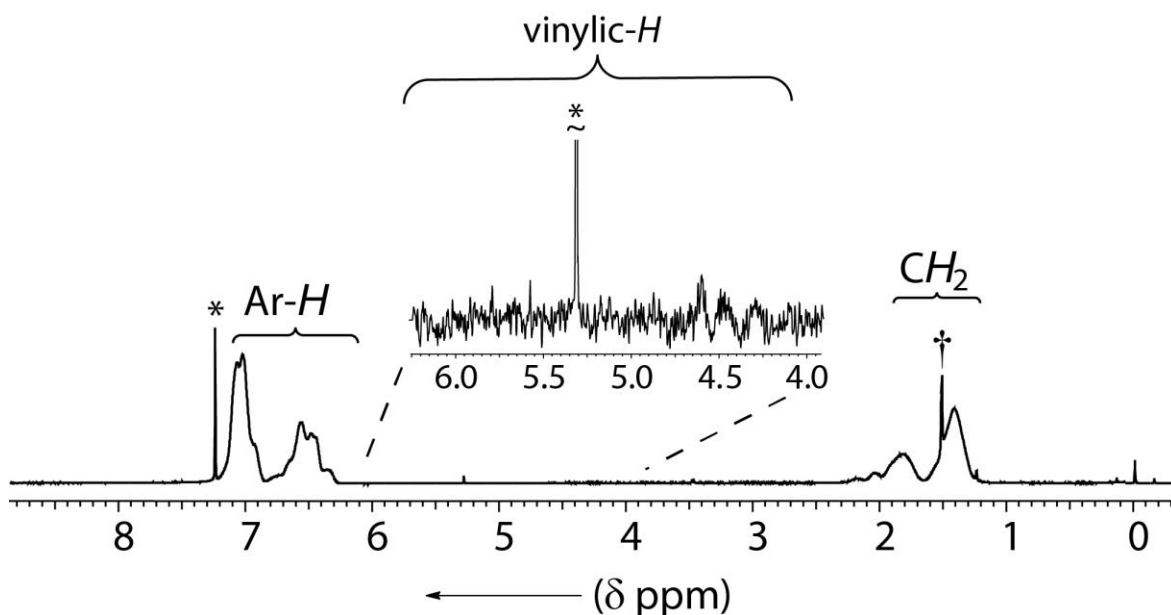
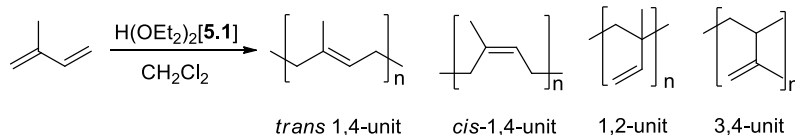


**Figure 5.10.**  $^1\text{H}$  NMR (400 MHz,  $\text{CDCl}_3$ ,  $25\text{ }^{\circ}\text{C}$ ) spectrum of polystyrene; polymerization performed with initiator  $\text{H}(\text{OEt}_2)_2[\mathbf{5.1}]$  at  $-50\text{ }^{\circ}\text{C}$ . \* indicates residual  $\text{CHCl}_3$  and  $\text{CH}_2\text{Cl}_2$ . † indicates  $\text{H}_2\text{O}$  residue.



**Scheme 5.6. H(OEt<sub>2</sub>)<sub>2</sub>[5.1]-initiated cationic polymerization of isoprene.**

The cationic polymerization of isoprene is a challenging reaction and the polymerization mechanism has not been fully elucidated. Controlled or living cationic polymerization of isoprene is demanding due to side reactions, including chain transfer, cyclization, and cross-linking reactions.<sup>476,477</sup> Low molecular weight polyisoprene or oligomeric polymer have been observed with the single-component initiator H(OEt<sub>2</sub>)<sub>2</sub>[P(1,2-O<sub>2</sub>C<sub>6</sub>Cl<sub>4</sub>)<sub>3</sub>] ( $M_n = 5,500 \text{ g mol}^{-1}$ )<sup>269</sup> and other binary systems (*e.g.* BF<sub>3</sub>OEt<sub>2</sub>/CCl<sub>3</sub>COOH, TiCl<sub>4</sub>/CCl<sub>3</sub>COOH, ZnBr/CCl<sub>3</sub>COOH, B(C<sub>6</sub>F<sub>5</sub>)<sub>3</sub>/CH<sub>3</sub>OC<sub>6</sub>H<sub>4</sub>CH<sub>2</sub>CH<sub>2</sub>OH, B(C<sub>6</sub>F<sub>5</sub>)<sub>3</sub>/C<sub>6</sub>H<sub>10</sub>CHCH<sub>2</sub>OH, B(C<sub>6</sub>F<sub>5</sub>)<sub>3</sub>/CH<sub>2</sub>Cl<sub>2</sub> with  $M_n = 680$  to  $8,800 \text{ g mol}^{-1}$ ).<sup>275,478,479</sup> Similarly, the polymerization of isoprene initiated by H(OEt<sub>2</sub>)<sub>2</sub>[5.1] at 18 °C afforded low molecular weight polyisoprene as a pale yellow solid with broad dispersity ( $M_n = 3,000 \text{ g mol}^{-1}$ ,  $D = 2.13$ , Table 5.1, entry 20). It should be noted that a small fraction of the polymer sample was soluble in THF solution and only the soluble fraction was utilized for GPC analysis.

At lower temperatures (−38 °C to −50 °C), side reactions were reduced and resulted in polymer with narrower dispersity. However, chain transfer processes were not fully suppressed, thereby compromising molecular weight and yield of oligoisoprene. Only traces of polymer were isolated when the polymerization was performed at −78 °C (Table 5.1, entry 25), likely a consequence of the limited initiation capability of H(OEt<sub>2</sub>)<sub>2</sub>[5.1]. For comparison, the single-component initiator H(OEt<sub>2</sub>)<sub>2</sub>[P(1,2-O<sub>2</sub>C<sub>6</sub>Cl<sub>4</sub>)<sub>3</sub>] gave polyisoprene of moderate molecular weight and yield at −38 °C ( $M_n = 11,600$  to  $\text{g mol}^{-1}$ ; yield 56%). At lower polymerization temperatures the initiator was not active.<sup>269</sup> In contrast, other binary initiators (*e.g.* TiCl<sub>4</sub>/<sup>*t*</sup>BuCl

and  $\text{TiCl}_4/\text{CCl}_3\text{COOH}$ ) afford low to moderate molecular weight polyisoprene at  $-78\text{ }^\circ\text{C}$ , albeit with broader dispersity ( $M_n = 6,400\text{--}16,200\text{ g mol}^{-1}$ ,  $D = 3.6$  to  $21.5$ ; yield: 35 to 37%).<sup>480,481</sup>

Analysis of the  $\text{H}(\text{OEt}_2)_2[\mathbf{5.1}]$ -initiated oligoisoprene at  $-50\text{ }^\circ\text{C}$  by  $^1\text{H-NMR}$  spectroscopy revealed signals associated with 1,4-unit [ $\delta$  (CH) = 5.0–5.1;  $\delta$  (CH<sub>2</sub>) = 2.1–2.2;  $\delta$  (CH<sub>3</sub>) = 1.6], 3,4-unit [ $\delta$  (CH<sub>2</sub>) = 4.6–4.8] and 1,2-unit [ $\delta$  (CH<sub>2</sub>) = 4.8–5.0]. In addition, a broad signal detected between 0.7 and 0.9 ppm was presumably assignable to cyclized or branched units that have been commonly observed for cationic polymerized polyisoprene.<sup>275,482-</sup>

<sup>485</sup> Analysis of the  $^{13}\text{C}\{^1\text{H}\}$  NMR spectrum (Figure 5.11) elucidated methyl carbon atom signals attributed to predominantly *trans*-1,4 unit ( $\delta = 15.6$ ) and minor signals were detected for the *cis*-1,4 unit ( $\delta = 23.4$ ), 3,4-unit ( $\delta = 18.3$ ) and 1,2-unit ( $\delta = 22.2$ ). A signal was observed at 13.6 ppm that has also been detected in polyisoprene obtained from two-component systems and is associated with the signal for the methyl group of the cyclic or branched structure.<sup>483</sup>

### **$\text{H}(\text{OEt}_2)_2[\mathbf{5.1}]$ -initiated cationic polymerization at varying monomer-to-initiator ratios:**

The effect of monomer-to-initiator ratio on the performance of the initiator  $\text{H}(\text{OEt}_2)_2[\mathbf{5.1}]$  was investigated. The cationic polymerizations of *n*-butyl vinyl ether and styrene were conducted at temperatures that gave the highest molecular weight polymer. Increasing the monomer-to-initiator ratio remarkably afforded poly(*n*-butyl vinyl ether) with increased molecular weight and low dispersity (Table 5.3, entries 1–3). The refractive index traces displayed unimodal distribution. In contrast, increasing the monomer-to-initiator ratio for the polymerization of styrene at  $-50\text{ }^\circ\text{C}$  did not result in an increase in molecular weight and may indicate a chain transfer to monomer process.

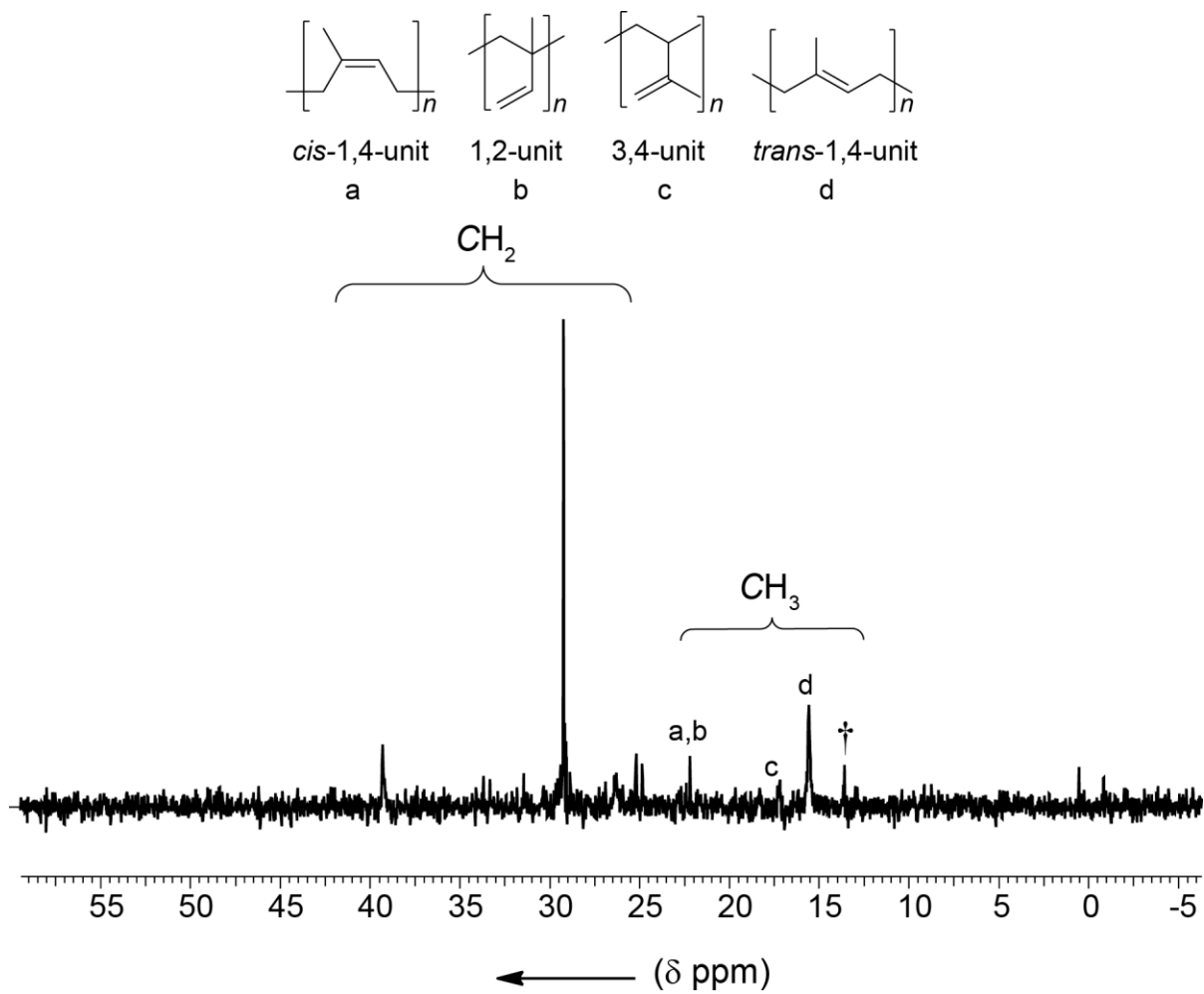


**Figure 5.11.**  $^{13}\text{C}\{^1\text{H}\}$  NMR (101 MHz,  $\text{CDCl}_3$ , 45 °C) spectrum of oligoisoprene; polymerization performed with initiator  $\text{H}(\text{OEt})_2[5.1]$  at 18 °C.  $\dagger$  Methyl group of cyclic or branched structure.

**Table 5-3. H(OEt<sub>2</sub>)<sub>2</sub>[5.1]-initiated cationic polymerizations of *n*-butyl vinyl ether and styrene in CH<sub>2</sub>Cl<sub>2</sub> with varying monomer-to-initiator ratio.**

| entry | Monomer                     | <i>T</i><br>(°C) | <i>t</i><br>(min) | [M]:[I] <sup>a</sup> | yield<br>(%) | <i>M<sub>n</sub></i> <sup>b</sup><br>(g mol <sup>-1</sup> ) | <i>D</i> <sup>c</sup> |
|-------|-----------------------------|------------------|-------------------|----------------------|--------------|---|-----------------------|
| 1     | <i>n</i> -butyl vinyl ether | -84              | 15                | 200                  | 29           | 34,200  | 1.24                  |
| 2     | <i>n</i> -butyl vinyl ether | -84              | 15                | 492                  | 57           | 39,100  | 1.12                  |
| 3     | <i>n</i> -butyl vinyl ether | -84              | 15                | 800                  | 44           | 73,300  | 1.13                  |
| 4     | Styrene                     | -50              | 15                | 200                  | 72           | 147,100   | 1.37                  |
| 5     | Styrene                     | -50              | 15                | 492                  | 78           | 147,100   | 1.43                  |
| 6     | Styrene                     | -50              | 15                | 800                  | 72           | 106,000   | 1.76                  |

The polymerization was carried out in 2 mL CH<sub>2</sub>Cl<sub>2</sub> solvent using 0.0075 mmol of Brønsted acid as initiator. <sup>a</sup> [Monomer]/[Initiator] ratio. <sup>b</sup> Absolute molecular weights were determined using laser light scattering gel permeation chromatography (GPC-LLS); differential refractive index (*dn/dc*) of poly(*n*-butyl vinyl ether) (*dn/dc* = 0.068 mL g<sup>-1</sup>) in THF was calculated by assuming 100% mass recovery; (*dn/dc*) of polystyrene used is 0.185 mL g<sup>-1</sup>. <sup>c</sup> Dispersity (*D* = *M<sub>w</sub>*/*M<sub>n</sub>*), where *M<sub>w</sub>* is the weight-average molar mass and *M<sub>n</sub>* is the number-average molar mass.

#### **Effect of H<sub>2</sub>O addition on the H(OEt<sub>2</sub>)<sub>2</sub>[5.1]-initiated cationic polymerization of styrene:**

The stability of the single component initiator H(OEt<sub>2</sub>)<sub>2</sub>[5.1] during the cationic polymerization of styrene was investigated under the influence of traces of water. Various amounts of distilled H<sub>2</sub>O were added to a CH<sub>2</sub>Cl<sub>2</sub> solution containing the initiator H(OEt<sub>2</sub>)<sub>2</sub>[5.1] at -50 °C. The results are demonstrated in Table 5.4 (entries 1–5). As the amount of added H<sub>2</sub>O was increased, the molecular weight and yield of polystyrene were significantly reduced and an increase in the dispersity was observed. The nature and stability of the initiator is highly influenced by the amount of H<sub>2</sub>O and has a significant effect on the cationic polymerization of styrene, leading to chain transfer and termination process. Therefore, it is of utmost importance to carry out the cationic polymerization of olefin monomers, initiated by single-component systems, under an inert atmosphere with dry solvent.

**Table 5-4. H(OEt<sub>2</sub>)<sub>2</sub>[5.1]-initiated cationic polymerizations of styrene in CH<sub>2</sub>Cl<sub>2</sub> with varying amounts of added H<sub>2</sub>O (μL).**

| Entry | monomer | <i>T</i><br>(°C) | H <sub>2</sub> O (μL) | [M]:[I] <sup>a</sup> | yield<br>(%) | <i>M<sub>n</sub></i> <sup>b</sup><br>(g mol <sup>-1</sup> ) | <i>D</i> |
|-------|---------|------------------|-----------------------|----------------------|--------------|---|----------|
| 1     | styrene | -50              | 0                     | 492                  | 78           | 145,000   | 1.43     |
| 2     | styrene | -50              | 1                     | 492                  | 1.6          | 54,800  | 1.42     |
| 3     | styrene | -50              | 5                     | 492                  | 0.9          | 67,700  | 1.58     |
| 4     | styrene | -50              | 10                    | 492                  | 0.8          | 59,900  | 1.62     |
| 5     | styrene | -50              | 100                   | 492                  | 0.6          | 47,110  | 1.84     |

The polymerization was carried out in 2 mL CH<sub>2</sub>Cl<sub>2</sub> solvent using 0.0075 mmol of Brønsted acid as initiator. <sup>a</sup> [Monomer]/[Initiator] ratio. <sup>b</sup> Absolute molecular weights were determined using laser light scattering gel permeation chromatography (GPC-LLS); differential refractive index (*dn/dc*) of polystyrene used is 0.185 mL g<sup>-1</sup>. <sup>c</sup> Dispersity (*D* = *M<sub>w</sub>*/*M<sub>n</sub>*), where *M<sub>w</sub>* is the weight-average molar mass and *M<sub>n</sub>* is the number-average molar mass.

### 5.3 Summary

In this chapter, the synthesis and characterization of unprecedented solid and weighable Brønsted acids, H(OEt<sub>2</sub>)<sub>2</sub>[5.1] and H(OEt<sub>2</sub>)<sub>2</sub>[5.2], comprised of weakly coordinating Ta(V)-containing anions were presented. Particularly intriguing is the reaction of TaCl<sub>5</sub> with tetrachlorocatechol (4 equiv) that resulted in the product H(OEt<sub>2</sub>)<sub>2</sub>[5.1]. X-ray crystallographic analysis, however, elucidated the formation of H(OEt<sub>2</sub>)(H<sub>2</sub>O)[5.1]. The compound H(OEt<sub>2</sub>)<sub>2</sub>[5.2] was isolated by treating TaCl<sub>5</sub> with tetrachlorocatechol (3 equiv). The complexes H(OEt<sub>2</sub>)<sub>2</sub>[5.1] and H(OEt<sub>2</sub>)<sub>2</sub>[5.2] were characterized by NMR spectroscopy and elemental analysis. The Brønsted acids have proven to be highly effective single-component initiators for the cationic polymerization of vinyl monomers at various temperatures. The H(OEt<sub>2</sub>)<sub>2</sub>[5.1] and H(OEt<sub>2</sub>)<sub>2</sub>[5.2]-initiated polymerization of *n*-butyl vinyl ether at low temperatures revealed moderate molecular weight poly(*n*-butyl vinyl ether) with low dispersity that is close to the calculated molecular weight. The polymerization of  $\alpha$ -methylstyrene initiated by H(OEt<sub>2</sub>)<sub>2</sub>[5.1] and H(OEt<sub>2</sub>)<sub>2</sub>[5.2] gave high molecular weight syndiotactic rich poly( $\alpha$ -methylstyrene) in good

yield. The Brønsted acid  $\text{H}(\text{OEt}_2)_2[\mathbf{5.1}]$  is an effective single-component initiator for the polymerization of styrene to give polystyrene of high molecular weight at  $-50\text{ }^\circ\text{C}$  with moderate yield and dispersity. Remarkably, the same initiator,  $\text{H}(\text{OEt}_2)_2[\mathbf{5.1}]$ , was able to polymerize isoprene at various temperatures and generated oligoisoprene in moderate yield.

## 5.4 Experimental

### 5.4.1 General Procedures

All experiments were performed using standard Schlenk or glove box techniques under nitrogen atmosphere.  $\text{CH}_2\text{Cl}_2$  (Sigma Aldrich) and  $\text{Et}_2\text{O}$  (Fisher Scientific) were deoxygenated with nitrogen and dried by passing the solvents through a column containing activated, basic alumina. Subsequently,  $\text{CH}_2\text{Cl}_2$  and  $\text{Et}_2\text{O}$  were dried over  $\text{CaH}_2$ , freshly distilled, and freeze-pump-thaw (x3) degassed. For extended periods of storage (1 day to 2 weeks), anhydrous solvents were stored over  $3\text{ \AA}$  molecular sieves. THF (Fisher Scientific) was freshly distilled from sodium/benzophenone ketyl immediately prior to use. Styrene (Sigma Aldrich) and *n*-butyl vinyl ether (Sigma Aldrich) were dried over calcium hydride, distilled and freeze-pump-thaw (x3) degassed prior to use. Tantalum pentachloride (Sigma Aldrich) was used without further purification. Tetrachlorocatechol was prepared following a literature procedure<sup>486</sup> and azeotropically distilled and recrystallized from hot toluene prior to use.

Mass spectrometry, NMR spectra, X-ray crystallography, elemental analysis and GPC analysis were performed in the Chemistry Department Facilities.  $^1\text{H}$  and  $^{13}\text{C}\{^1\text{H}\}$  NMR spectra were recorded on Bruker Avance 400 MHz spectrometers at ambient temperature unless noted.  $^1\text{H}$  NMR and  $^{13}\text{C}\{^1\text{H}\}$  NMR spectra were referenced to deuterated solvents. Molecular weight of poly(*n*-butyl vinyl ether) was determined by triple detection gel permeation chromatography

(GPC-LLS) utilizing an Agilent 1260 Series standard auto sampler, an Agilent 1260 series isocratic pump, Phenomenex Phenogel 5  $\mu\text{m}$  narrowbore columns (4.6 x 300 mm)  $10^4$  Å (5000-500,000), 500 Å (1,000-15,000), and  $10^3$  Å (1,000-75,000), Wyatt Optilab rEx differential refractometer ( $\lambda = 658$  nm, 25 °C), as well as Wyatt tristar miniDAWN (laser light scattering detector ( $\lambda = 690$  nm)) and a Wyatt ViscoStar viscometer. Samples were dissolved in THF (*ca.* 2 mg mL<sup>-1</sup>) and a flow rate of 0.5 mL min<sup>-1</sup> was applied. The differential refractive index ( $dn/dc$ ) of poly(*n*-butyl vinyl ether) ( $dn/dc = 0.068$  mL g<sup>-1</sup>) in THF was calculated by using Wyatt ASTRA software 6.1 assuming 100 % mass recovery. The differential refractive indices ( $dn/dc$ ) of polystyrene ( $dn/dc = 0.185$  mL g<sup>-1</sup>), poly( $\alpha$ -methylstyrene) ( $dn/dc = 0.204$  mL g<sup>-1</sup>)<sup>487</sup> and of polyisoprene ( $dn/dc = 0.129$  mL g<sup>-1</sup>)<sup>488</sup> have been reported.

#### 5.4.2 Synthesis of H(OEt<sub>2</sub>)<sub>2</sub>[5.1]

TaCl<sub>5</sub> (0.53 g, 1.48 mmol) was stirred in anhydrous CH<sub>2</sub>Cl<sub>2</sub> (10 mL) and the white suspension was slowly heated to reflux under N<sub>2</sub> atmosphere. In another Schlenk flask, tetrachlorocatechol (1.48 g, 5.99 mmol) was prepared in warm anhydrous CH<sub>2</sub>Cl<sub>2</sub> (14 mL) and the bright orange-red solution was added via cannula to the refluxing TaCl<sub>5</sub> solution at 90 °C to afford a dark green reaction mixture. After 10 min, a faint green precipitate was obtained. The reaction mixture was refluxed for 80 min and cooled to ambient temperature. Upon addition of Et<sub>2</sub>O (25 mL), a green clear solution formed. The solution was cooled in an ice bath to afford a colorless precipitate within 15 min. The solid was collected by filtration, washed with CH<sub>2</sub>Cl<sub>2</sub> (5 mL) and dried *in vacuo*. Yield = 1.13 g, 0.85 mmol, 57 % based on TaCl<sub>5</sub>. A concentrated solution of the crude product in CH<sub>2</sub>Cl<sub>2</sub> afforded colorless crystals of H(OEt<sub>2</sub>)<sub>2</sub>(H<sub>2</sub>O)[Ta(1,2-O<sub>2</sub>C<sub>6</sub>Cl<sub>4</sub>)<sub>2</sub>(1,2-

O(OH)C<sub>6</sub>Cl<sub>4</sub>)] (-30 °C, ca. 3 d). A crystal was removed for X-ray crystallographic analysis without drying.

<sup>1</sup>H NMR (400 MHz, CD<sub>2</sub>Cl<sub>2</sub>, 25 °C): δ = 9.37 (br, OH), 4.00 (q, <sup>3</sup>J<sub>HH</sub> = 7.1 Hz, 8H, OCH<sub>2</sub>CH<sub>3</sub>), 1.40 ppm (t, <sup>3</sup>J<sub>HH</sub> = 7.1 Hz, 12H, OCH<sub>2</sub>CH<sub>3</sub>); <sup>1</sup>H NMR (400 MHz, CD<sub>2</sub>Cl<sub>2</sub>, -85 °C): δ = 16.73 (s, 1H, H(OEt<sub>2</sub>)<sub>2</sub>), 9.40 (s, 1H, OH), 4.03 (q, <sup>3</sup>J<sub>HH</sub> = 7.0 Hz, 8H, OCH<sub>2</sub>CH<sub>3</sub>), 1.38 (t, <sup>3</sup>J<sub>HH</sub> = 7.1 Hz, 12H, OCH<sub>2</sub>CH<sub>3</sub>); <sup>13</sup>C{<sup>1</sup>H} NMR (75 MHz, CD<sub>2</sub>Cl<sub>2</sub>, -85 °C): δ = 149.9 (s, Ar-C), 145.3 (s, Ar-C), 144.3 (s, Ar-C), 139.8 (s, Ar-C), 124.9 (s, Ar-C), 121.6 (s, Ar-C), 121.1 (s, Ar-C), 118.6 (s, Ar-C), 116.7 (s, Ar-C), 70.3 (s, OCH<sub>2</sub>CH<sub>3</sub>), 13.3 (s, OCH<sub>2</sub>CH<sub>3</sub>) ppm; elem. anal. calcd for C<sub>33</sub>H<sub>26</sub>Cl<sub>16</sub>O<sub>10</sub>Ta·1.4 CH<sub>2</sub>Cl<sub>2</sub>: C, 28.50; H, 2.00; found: C, 28.30; H, 1.80.

### 5.4.3 Synthesis of H(OEt<sub>2</sub>)<sub>2</sub>[5.2]

TaCl<sub>5</sub> (0.48 g, 13.4 mmol) was stirred in anhydrous CH<sub>2</sub>Cl<sub>2</sub> (6 mL) and the white suspension was slowly heated to reflux under N<sub>2</sub> atmosphere. In another Schlenk flask, tetrachlorocatechol (1.00 g, 40.3 mmol) was prepared in warm anhydrous CH<sub>2</sub>Cl<sub>2</sub> (6 mL) and the bright orange-red solution was added via cannula to the refluxing TaCl<sub>5</sub> solution at 90 °C to afford a dark green reaction mixture. After 10 min, a faint green precipitate was obtained. The reaction mixture was refluxed for 100 min and cooled to ambient temperature. Upon addition of Et<sub>2</sub>O (22 mL), a green clear solution formed. The solution was cooled in an ice bath to afford a colorless precipitate within 20 min. The solid was collected by filtration, washed with CH<sub>2</sub>Cl<sub>2</sub> (3 mL) and dried *in vacuo*. Yield = 1.28 g, 11.9 mmol, 89 % based on TaCl<sub>5</sub>.

<sup>1</sup>H NMR (400 MHz, CD<sub>2</sub>Cl<sub>2</sub>, 25 °C): δ = 7.54 (br, 1H, H(OEt<sub>2</sub>)<sub>2</sub>), 4.00 (br, 8H, OCH<sub>2</sub>CH<sub>3</sub>), 1.40 ppm (br, 12H, OCH<sub>2</sub>CH<sub>3</sub>); <sup>1</sup>H NMR (400 MHz, CD<sub>2</sub>Cl<sub>2</sub>, -85 °C): δ = 16.74 (s, 1H, H(OEt<sub>2</sub>)<sub>2</sub>),

4.04 (br, 8H, OCH<sub>2</sub>CH<sub>3</sub>), 1.38 (br, 12H, OCH<sub>2</sub>CH<sub>3</sub>); <sup>13</sup>C {<sup>1</sup>H} NMR (75 MHz, CD<sub>2</sub>Cl<sub>2</sub>, 25 °C): δ = 140.4 (s, Ar–C), 123.4 (s, Ar–C), 118.9 (s, Ar–C), 67.9 (s, OCH<sub>2</sub>CH<sub>3</sub>), 14.2 (s, OCH<sub>2</sub>CH<sub>3</sub>) ppm; elem. anal. calcd for C<sub>26</sub>H<sub>21</sub>Cl<sub>12</sub>O<sub>8</sub>Ta·1.35 CH<sub>2</sub>Cl<sub>2</sub>: C, 27.78; H, 2.02; found: C, 27.51; H, 1.74.; MALDI–TOF MS (355 nm) *m/z* = 918.6 [M]<sup>–</sup>.

#### 5.4.4 Representative H(OEt)<sub>2</sub>[5.1]-initiated Polymerization of *n*-Butyl Vinyl Ether

In a glovebox, freshly distilled, degassed CH<sub>2</sub>Cl<sub>2</sub> (2 mL) was added to H(OEt)<sub>2</sub>[5.1] (0.010 g, 0.008 mmol) in a 10 mL Schlenk flask. The flask was removed from the glovebox and cooled to –78 °C. Freshly distilled, *n*-butyl vinyl ether (0.37 g, 3.70 mmol, 0.49 mL) was prepared in a syringe, removed from the glovebox and added rapidly to the initiator solution. After 15 min, the polymerization was quenched with a solution of NH<sub>4</sub>OH in MeOH (0.2 mL, 10 vol%) and all volatiles were removed *in vacuo*. The crude product was dissolved in CH<sub>2</sub>Cl<sub>2</sub> (2 mL) and added one drop at a time to stirred MeOH (40 mL) to precipitate a yellow oily residue. The polymer was collected by centrifugation and dried *in vacuo*. Yield = 0.27 g, 71 %. The isolated material was analyzed by <sup>1</sup>H NMR spectroscopy (400 MHz, CDCl<sub>3</sub>, 25 °C): δ = 3.52–3.36 (br, CH<sub>2</sub>CH(O(CH<sub>2</sub>)<sub>3</sub>CH<sub>3</sub>)CH<sub>2</sub>), 1.86–1.39 (br, OCH<sub>2</sub>CH<sub>2</sub>CH<sub>2</sub>), 0.93 (t, CH<sub>3</sub>). GPC–MALS (THF): *M<sub>n</sub>* = 32,200 g mol<sup>–1</sup>, Đ = 1.58.

#### 5.4.5 Representative H(OEt)<sub>2</sub>[5.1]-initiated Polymerization of Styrene

In a glovebox, freshly distilled, degassed CH<sub>2</sub>Cl<sub>2</sub> (2 mL) was added to H(OEt)<sub>2</sub>[5.1] (0.010 g, 0.008 mmol) in a 10 mL Schlenk flask. The flask was removed from the glovebox and cooled to –15 °C. Freshly distilled styrene (0.38 g, 3.70 mmol, 0.34 mL) was prepared in a syringe, removed from the glovebox and added rapidly to the initiator solution. After 15 min, the

polymerization was quenched with a solution of  $\text{NH}_4\text{OH}$  in  $\text{MeOH}$  (0.2 mL, 10 vol%) and all volatiles were removed *in vacuo*. The crude product was dissolved in  $\text{CH}_2\text{Cl}_2$  (2 mL) and added one drop at a time to stirred  $\text{MeOH}$  (40 mL) to precipitate a colorless residue. The polymer was collected by centrifugation and dried *in vacuo*. Yield = 0.33 g, 85 %. The isolated material was analyzed by  $^1\text{H}$  NMR spectroscopy (400 MHz,  $\text{CDCl}_3$ , 25 °C):  $\delta$  = 7.11–6.39 (br, Ar-H), 2.22–1.46 (br,  $\text{CH}_2\text{CH}(\text{Ar-H})\text{CH}_2\text{CH}_2$ ). GPC–MALS (THF):  $M_n$  = 12,800  $\text{g mol}^{-1}$ ,  $D$  = 3.51.

#### 5.4.6 Representative $\text{H}(\text{OEt}_2)_2[5.1]$ -initiated Polymerization of $\alpha$ -Methylstyrene

In a glovebox, freshly distilled, degassed  $\text{CH}_2\text{Cl}_2$  (2 mL) was added to  $\text{H}(\text{OEt}_2)_2[5.1]$  (0.010 g, 0.008 mmol) in a 10 mL Schlenk flask. The flask was removed from the glovebox and cooled to –50 °C. Freshly distilled,  $\alpha$ -methylstyrene (0.35 g, 3.00 mmol, 0.39 mL) was prepared in a syringe, removed from the glovebox and added rapidly to the initiator solution. After 15 min, the polymerization was quenched with a solution of  $\text{NH}_4\text{OH}$  in  $\text{MeOH}$  (0.2 mL, 10 vol%), and all volatiles were removed *in vacuo*. The crude product was dissolved in  $\text{CH}_2\text{Cl}_2$  (2 mL) and added one drop at a time to stirred  $\text{MeOH}$  (40 mL) to precipitate a colorless residue. The polymer was collected by centrifugation and dried *in vacuo*. Yield = 0.30 g, 84%. The isolated material was analyzed by  $^1\text{H}$  NMR spectroscopy (400 MHz,  $\text{CDCl}_3$ , 25 °C):  $\delta$  = 7.15–6.69 (br, Ar-H), 1.56–1.53 (br,  $\text{CH}_2\text{CH}_2\text{CH}(\text{Ar-H})\text{CH}_3$ ), 0.91 (t,  $\text{CH}_3\text{CH}(\text{Ar-H})\text{CH}_2\text{CH}_2$ ). GPC–MALS (THF):  $M_n$  = 66,400  $\text{g mol}^{-1}$ ,  $D$  = 1.81.

#### 5.4.7 Representative $\text{H}(\text{OEt}_2)_2[5.1]$ -initiated Polymerization of Isoprene

In a glovebox, freshly distilled, degassed  $\text{CH}_2\text{Cl}_2$  (2 mL) was added to  $\text{H}(\text{OEt}_2)_2[5.1]$  (0.010 g, 0.008 mmol) in a 10 mL Schlenk flask. The flask was removed from the glovebox and cooled to

0 °C. Freshly distilled, isoprene (0.20 g, 3.00 mmol, 0.31 mL) was prepared in a syringe, removed from the glovebox and added rapidly to the initiator solution. After 15 min, the polymerization was quenched with a solution of NH<sub>4</sub>OH in MeOH (0.2 mL, 10 vol%), and all volatiles were removed *in vacuo*. The crude product was dissolved in CH<sub>2</sub>Cl<sub>2</sub> (2 mL) and added one drop at a time to stirred MeOH (40 mL) to precipitate a light brown residue. The polymer was collected by centrifugation and dried *in vacuo*. Yield = 0.11 g, 52 %. The isolated material was analyzed by <sup>1</sup>H NMR and <sup>13</sup>C-NMR spectroscopy. The isolated material was analyzed by GPC-MALS (THF):  $M_n = 3,200 \text{ g mol}^{-1}$ ,  $D = 4.84$ .

#### 5.4.8 Representative H(OEt)<sub>2</sub>[5.2]-initiated Polymerization of *n*-Butyl Vinyl Ether

In a glovebox, freshly distilled, degassed CH<sub>2</sub>Cl<sub>2</sub> (2 mL) was added to H(OEt)<sub>2</sub>[5.2] (0.011 g, 0.010 mmol) in a 10 mL Schlenk flask. The flask was removed from the glovebox and cooled to -78 °C. Freshly distilled, *n*-butyl vinyl ether (0.41 g, 4.10 mmol, 0.54 mL) was prepared in a syringe, removed from the glovebox and added rapidly to the initiator solution. After 15 min, the polymerization was quenched with a solution of NH<sub>4</sub>OH in MeOH (0.2 mL, 10 vol%) and all volatiles were removed *in vacuo*. The crude product was dissolved in CH<sub>2</sub>Cl<sub>2</sub> (2 mL) and added one drop at a time to stirred MeOH (40 mL) to precipitate a colorless oily residue. The polymer was collected by centrifugation and dried *in vacuo*. Yield = 0.29 g, 72 %. The isolated material was analyzed by <sup>1</sup>H NMR spectroscopy (400 MHz, CDCl<sub>3</sub>, 25 °C):  $\delta = 3.53\text{--}3.37$  (br, CH<sub>2</sub>CH(O(CH<sub>2</sub>)<sub>3</sub>CH<sub>3</sub>)CH<sub>2</sub>), 1.87–1.39 (br, OCH<sub>2</sub>CH<sub>2</sub>CH<sub>2</sub>), 0.93 (t, CH<sub>3</sub>). GPC-MALS (THF):  $M_n = 34,100 \text{ g mol}^{-1}$ ,  $D = 1.45$ .

#### 5.4.9 Representative H(OEt)<sub>2</sub>[5.2]-initiated Polymerization of $\alpha$ -Methylstyrene

In a glovebox, freshly distilled, degassed CH<sub>2</sub>Cl<sub>2</sub> (2 mL) was added to H(OEt)<sub>2</sub>[5.2] (0.011 g, 0.010 mmol) in a 10 mL Schlenk flask. The flask was removed from the glovebox and cooled to -78 °C. Freshly distilled,  $\alpha$ -methylstyrene (0.48 g, 4.10 mmol, 0.54 mL) was prepared in a syringe, removed from the glovebox and added rapidly to the initiator solution. After 15 min, the polymerization was quenched with a solution of NH<sub>4</sub>OH in MeOH (0.2 mL, 10 vol%) and all volatiles were removed *in vacuo*. The crude product was dissolved in CH<sub>2</sub>Cl<sub>2</sub> (2 mL) and added one drop at a time to stirred MeOH (40 mL) to precipitate a colorless residue. The polymer was collected by centrifugation and dried *in vacuo*. Yield = 0.26 g, 53%. The isolated material was analyzed by <sup>1</sup>H NMR spectroscopy (400 MHz, CDCl<sub>3</sub>, 25 °C):  $\delta$  = 7.17–6.67 (br, Ar-H), 1.61–1.53 (br, CH<sub>2</sub>CH<sub>2</sub>CH(Ar-H)CH<sub>3</sub>), 0.07 (t, CH<sub>3</sub>CH(Ar-H)CH<sub>2</sub>CH<sub>2</sub>). GPC-MALS (THF):  $M_n$  = 205,000 g mol<sup>-1</sup>,  $D$  = 1.28.

#### 5.4.10 X-ray Structure Determination of H(OEt)<sub>2</sub>(H<sub>2</sub>O)[5.1]

X-ray crystallography data were collected on a Bruker X8 APEX II diffractometer with graphite-monochromated Mo K $\alpha$  radiation. A single marginal crystal was immersed in oil and mounted on a glass fiber. Data were collected with 120 s exposure and integrated using the Bruker SAINT software package and corrected for absorption effect using SADABS.<sup>325,326</sup> All structures were solved by direct methods and subsequent Fourier difference techniques. The material crystallizes with one molecule of water and two molecules of diethyl ether in the asymmetric unit. A hydrogen atom situated between a water molecule and an ether molecule was located in a difference map and refined isotropically. All other O—H hydrogen atoms were placed in calculated positions. All C—H hydrogen atoms were placed in calculated positions. All

non-hydrogen atoms were refined anisotropically. All refinements were performed using the SHELXL-2015<sup>328</sup> via the Olex2 interface.<sup>329</sup>

**Table 5-5. X-ray crystallographic parameters for H(OEt<sub>2</sub>)(H<sub>2</sub>O)[5.1].**

| H(OEt <sub>2</sub> )(H <sub>2</sub> O)[5.1]·OEt <sub>2</sub> ·0.17 CH <sub>2</sub> Cl <sub>2</sub> |   |
|--|---|
| formula  | C <sub>32</sub> H <sub>25</sub> O <sub>11</sub> Cl <sub>16</sub> Ta |
| Fw   | 1333.67   |
| crystal size (mm)  | 0.12 x 0.15 x 0.25  |
| colour   | Colorless   |
| cell setting   | Monoclinic  |
| space group  | <i>P</i> 2 <sub>1</sub> / <i>c</i>                                  |
| <i>a</i> (Å)   | 10.3993(9)  |
| <i>b</i> (Å)   | 29.634(3)   |
| <i>c</i> (Å)   | 15.4817(14)   |
| <i>α</i> (°)   | 90  |
| <i>β</i> (°)   | 108.100(2)  |
| <i>γ</i> (°)   | 90  |
| <i>V</i> (Å <sup>3</sup> )   | 3708.8(10)  |
| <i>Z</i>   | 4   |
| <i>ρ</i> calcd ( <i>g cm</i> -3)   | 1.953   |
| <i>F</i> (000)   | 2600.00   |
| <i>μ</i> (MoK $\alpha$ ) (mm-1)  | 34.21   |
| 2 $\theta$ max (°)   | 45.6  |
| total no. of reflns  | 32468   |
| no. of unique reflns   | 6060  |
| no. of reflns  | 15262   |
| no. of variables   | 667   |
| <i>R</i> 1 ( <i>F</i> , <i>I</i> > 2 $\sigma$ ( <i>I</i> ))  | 0.116   |
| <i>wR</i> 2 ( <i>F</i> 2, all data)  | 0.286   |
| goodness of fit  | 1.24  |

$$^a R_1 = \frac{\sum |F_o| - |F_c|}{\sum |F_o|}, \quad ^b wR_2(F^2[\text{all data}]) = \left\{ \frac{\sum [w(F_o^2 - F_c^2)^2]}{\sum [w(F_o^2)^2]} \right\}^{1/2}.$$

## Chapter 6: Conclusion and Future Work

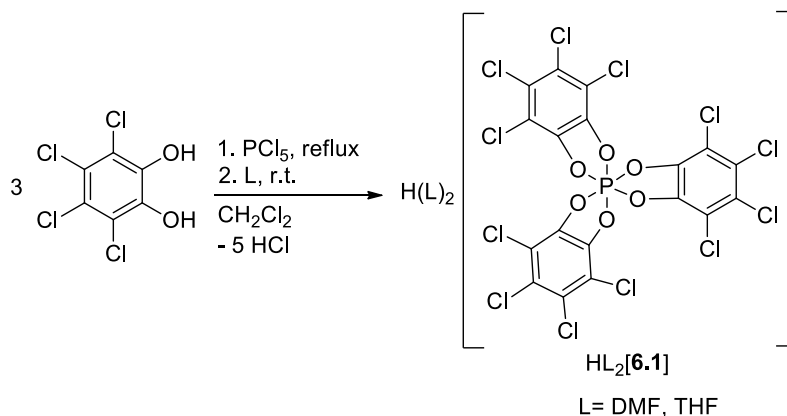
### 6.1 Introduction

The main goal of this dissertation was the isolation of solid weighable Brønsted acids as single-component initiator systems for the cationic polymerization of olefin monomers. In addition, the aim was to obtain high molecular weight polymers at higher temperatures than  $-100\text{ }^{\circ}\text{C}$ . The initiator system requires a WCA that stabilizes the reactive carbocation during cationic polymerization. Substantial studies have been performed in the development of WCAs based on group 13 elements, dominated by tetracoordinate boron and aluminum anion analogues.<sup>68-70,84,151</sup> Therefore, it was postulated that hexacoordinate phosphorus(V) anions facilitate the design of large and more charge-delocalized anions and thus, sought to be weakly coordinating.

### 6.2 Hexacoordinate WCAs

Chapter 2 described the one-pot reaction of  $\text{PCl}_5$  with tetrachlorocatechol to afford the compound  $\text{H(L)}_2[\mathbf{6.1}]$  ( $\text{L} = \text{DMF}, \text{THF}, \text{CH}_3\text{CN}$ ) in the presence of weak donor solvents (Scheme 6.1). The Brønsted acids  $\text{H(L)}_2[\mathbf{6.1}]$  incorporated the weakly coordinating phosphorus(V)-based  $[\text{TRISPHAT}]^-$  anion,  $[\mathbf{6.1}]^-$ . The integrity of the  $[\text{H(L)}_2]^+$  moiety ( $\text{L} = \text{DMF}, \text{THF}$ ) in solution was investigated. The low temperature  $^1\text{H}$ - $^1\text{H}$ -NOESY NMR spectrum elucidated positive NOE for  $\text{H(THF)}_2[\mathbf{6.1}]$  and negative NOE for  $\text{H(DMF)}_2[\mathbf{6.1}]$ . The compounds  $\text{H(DMF)}_2[\mathbf{6.1}]$ ,  $\text{H(THF)}_2[\mathbf{6.1}]$  and  $\text{H(THF)(CH}_3\text{CN)[6.1]}$  are isolable and weighable Brønsted acids. In particular,  $\text{H(DMF)}_2[\mathbf{6.1}]$  and  $\text{H(THF)}_2[\mathbf{6.1}]$  were employed as effective single-component initiators for the cationic polymerization of *n*-butyl vinyl ether and

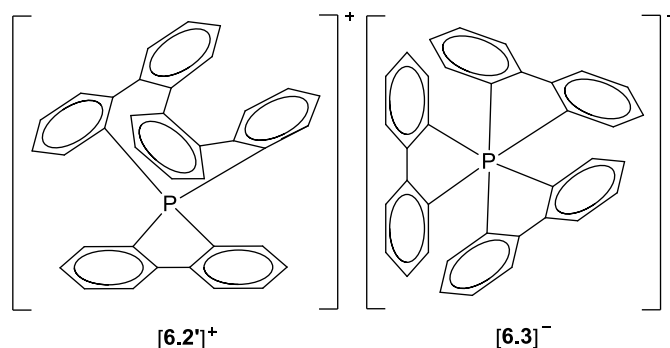
*p*-methoxystyrene at various temperatures. Remarkably, H(THF)<sub>2</sub>[**6.1**] afforded high molecular weight poly(*p*-methoxystyrene) with  $M_n$  up to 649,000 g mol<sup>-1</sup> at -78 °C. The unexpected high molecular weight might arise from branching of the poly(*p*-methoxystyrene) through either Friedel-Crafts alkylation/arylation or hydride transfer. The physical properties (for example  $T_g$  or  $T_m$ ) of the branched polymer were not studied and are of interest and may be investigated further.



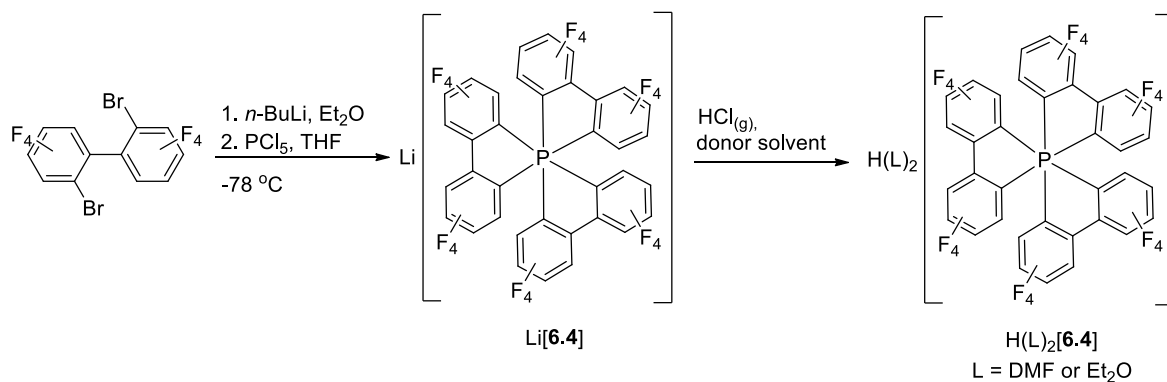
**Scheme 6.1.** Synthesis of Brønsted acid H(L)<sub>2</sub>[**6.1**] (L = DMF, THF).

The main objective of Chapter 3 was the search of an alternative for the WCA [**6.1**]<sup>-</sup> to ultimately access new Brønsted acids for the cationic polymerization of olefin monomers. Despite that Brønsted acids containing the anion [**6.3**]<sup>-</sup> were not isolated, intriguing research findings have been harvested in exploring the WCA potential of [**6.3**]<sup>-</sup>. Chapter 3 outlined three potential routes to afford Hellwinkel's salt, [**6.2**][**6.3**], that features a P-C-containing anion. In addition to the desired compound, an unexpected complex cation was isolated incorporating an alternative cation [**6.2'**]<sup>+</sup>, with a “twist”, that was formally derived from the insertion of an additional biphenyl unit into [**6.2**]<sup>+</sup> and the phosphorus(V)-containing WCA [**6.3**]<sup>-</sup>. The insertion product was observed by direct lithiation of biphenyl, 2,2'-diidobiphenyl and

2,2'-dibromobiphenyl. A pentavalent phosphorane  $P(C_{12}H_8)_2(C_{24}H_9)$  was isolated and characterized.

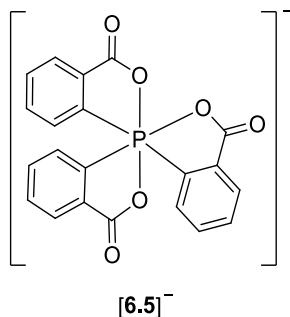


The application of the WCA  $[6.3]^-$  in the stabilization of highly reactive cations is of interest. In order to decrease the nucleophilicity of the anion  $[6.3]^-$ , it may be possible to introduce halogenated biphenyls and investigate the development of halogenated P–C containing WCAs. The incorporation of electron withdrawing fluorinated aryl groups to afford anions of type  $[6.4]^-$  with a charge-balancing  $[PhNMe_2H]^+$  cation has been mentioned in a patent application and these systems have been employed as activators in metallocene-based coordination polymerization. Detailed characterization of the activator was not reported.<sup>353</sup> As an extension to the work reported in this thesis, future work might be aimed at generating Brønsted acids of anion  $[6.4]^-$  as outlined in Scheme 6.2.



**Scheme 6.2.** Proposed synthetic route of compound  $\text{Li}[6.4]$  and  $\text{H(L)}_2[6.4]$  (L = DMF or  $\text{Et}_2\text{O}$ ).

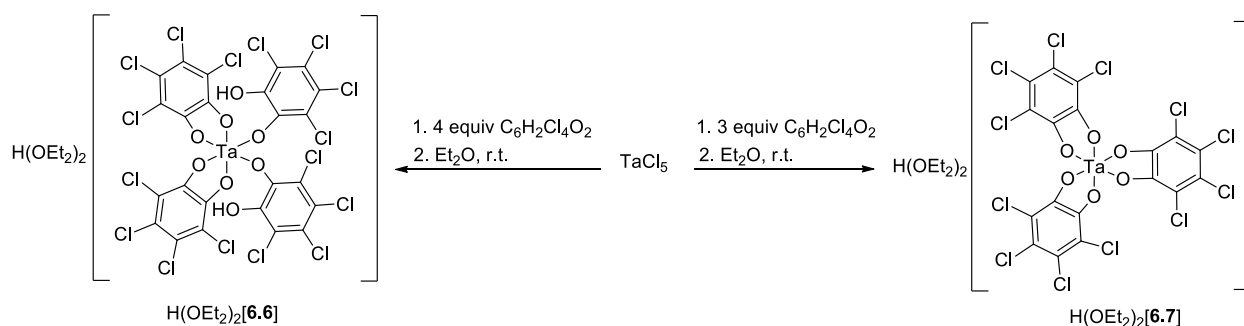
Chapter 4 described the synthesis and characterization of  $[\text{N}_{\text{base}}\text{H}]\text{-mer-[6.5]}$  ( $\text{N}_{\text{base}} = \text{PhNMe}_2, \text{PhNH}_2, \text{py}, \text{isoquinoline}, (-)\text{-brucine}, \text{N}(n\text{-C}_8\text{H}_{17})_3$ ) and  $\text{K-rac-mer-[6.5]}$  featuring the hexacoordinate phosphorus(V) anion  $\text{mer-[6.5]}^-$ . The molecular structure of  $\text{K-rac-mer-[6.5]}$  elucidated a coordination polymer. The  $^{31}\text{P}\{^1\text{H}\}$  NMR spectrum of  $[(-)\text{-brucineH}]\text{-rac-mer-[6.5]}$  recorded in  $\text{CD}_2\text{Cl}_2$  solution revealed signals for one pair of diastereomers. Further, the development towards Brønsted acids containing the anion  $\text{mer-[6.5]}^-$  have been alluded to in Chapter 4. The weakly coordinating character of  $\text{mer-[6.5]}^-$  was investigated. The basicity of  $\text{mer-[6.5]}^-$  was determined by comparing the  $\nu\text{N-H}$  stretching vibration of  $[(n\text{-C}_8\text{H}_{17})_3\text{NH}]\text{-mer-[6.5]}$  in  $\text{CCl}_4$  solution with the  $\text{N-H}$  stretching frequency of tri(*n*-octyl)ammonium salts of several weakly basic anions utilizing IR spectroscopy. The basicity of the anion  $\text{mer-[6.5]}^-$  in  $[(n\text{-C}_8\text{H}_{17})_3\text{NH}]\text{-mer-[6.5]}$  was found to be similar to the anions  $[\text{ClO}_4]^-$  and  $[\text{N}(\text{SO}_2\text{CF}_3)_2]^-$ , respectively.



A potential future direction in this area involves the incorporation of halogenated substituents to provide additional delocalization properties to the anion, thereby significantly lowering the donor ability of the halogenated version of  $[\text{6.5}]^-$ .

Chapter 5 described the synthesis and characterization of solid and weighable Brønsted acids,  $\text{H}(\text{OEt}_2)_2[\text{6.6}]$  and  $\text{H}(\text{OEt}_2)_2[\text{6.7}]$ , comprised of unprecedented weakly coordinating Ta(V)-containing anions. Particularly intriguing was the reaction of  $\text{TaCl}_5$  with different

amounts of tetrachlorocatechol that resulted in the products  $\text{H}(\text{OEt}_2)_2[\mathbf{6.6}]$  and  $\text{H}(\text{OEt}_2)_2[\mathbf{6.7}]$ , respectively, (Scheme 6.3). The Brønsted acids have proven to be highly effective single-component initiators for the cationic polymerization of vinyl monomers at various temperatures. The  $\text{H}(\text{OEt}_2)_2[\mathbf{6.6}]$  and  $\text{H}(\text{OEt}_2)_2[\mathbf{6.7}]$ -initiated polymerization of *n*-butyl vinyl ether at low temperatures revealed moderate molecular weight poly(*n*-butyl vinyl ether) with narrow dispersity that is close to the calculated molecular weight. The living cationic polymerization was not explored further within the research contained in this thesis and might be of interest. The living cationic polymerization study of vinyl ethers might allow for the synthesis of block copolymers with intriguing physical properties.



**Scheme 6.3.** Synthesis of Brønsted acids  $\text{H}(\text{OEt}_2)_2[\mathbf{6.6}]$  and  $\text{H}(\text{OEt}_2)_2[\mathbf{6.7}]$ .

The polymerization of  $\alpha$ -methylstyrene initiated by  $\text{H}(\text{OEt}_2)_2[\mathbf{6.6}]$  and  $\text{H}(\text{OEt}_2)_2[\mathbf{6.7}]$  gave high molecular weight syndiotactic rich poly( $\alpha$ -methylstyrene) ( $M_n$  up to 279,000  $\text{g mol}^{-1}$ , *rr* up to 90%). The Brønsted acid  $\text{H}(\text{OEt}_2)_2[\mathbf{6.6}]$  was an effective single-component initiator for the polymerization of styrene to give polystyrene of high molecular weight ( $M_n$  up to 147,000  $\text{g mol}^{-1}$ ) at  $-50$  °C. Remarkably,  $\text{H}(\text{OEt}_2)_2[\mathbf{6.6}]$  was able to polymerize isoprene at various temperatures. In conclusion, the strong Brønsted acids  $\text{H}(\text{OEt}_2)_2[\mathbf{6.6}]$  and  $\text{H}(\text{OEt}_2)_2[\mathbf{6.7}]$  have provided access to high molecular weight polymers at higher temperatures than  $-100$ ° C. The development of tantalum(V)-containing WCAs,  $[\mathbf{6.6}]^-$  and  $[\mathbf{6.7}]^-$ , has opened a new avenue in

exploring the design of large charge delocalized WCAs. The investigation of the basicity of the unprecedented anions [6.6]<sup>-</sup> and [6.7]<sup>-</sup> is of importance. Future work should consider the isolation of the salts [(*n*-C<sub>8</sub>H<sub>17</sub>)<sub>3</sub>NH][6.6] and [(*n*-C<sub>8</sub>H<sub>17</sub>)<sub>3</sub>NH][6.7] to determine the basicity of the anions [6.6]<sup>-</sup> and [6.7]<sup>-</sup> on the IR scale that can be compared to existing WCAs. The acidity of the Brønsted acids H(OEt<sub>2</sub>)<sub>2</sub>[6.6] and H(OEt<sub>2</sub>)<sub>2</sub>[6.7] could be determined by applying Krossing's recently reported unified Brønsted acidity scale.<sup>489</sup> Further, the reactivity of the Brønsted acids H(L)<sub>2</sub>[6.6] and H(L)<sub>2</sub>[6.7] as single-component initiators for the cationic polymerization of olefin monomers may be investigated with different ethers.

### 6.3 Concluding Remarks

By this point, the reader will acknowledge that crafting an ideal WCA for the stabilization of reactive cations is challenging. The research work contained within this dissertation has made an impact in the development of WCAs.

## References

- (1) Morton, M. *Rubber Technology*, 3rd ed.; Van Nostrand Reinhold: New York, 1987.
- (2) Mark, J. E.; Erman, B.; Eirich, F. R. *Science and Technology of Rubber*, 3rd ed.; Elsevier Inc.: Boston, 2005.
- (3) Kush, A.; Goyvaerts, E.; Chye, M.-L.; Chua, N.-H. *Proc. Natl. Acad. Sci. U.S.A.* **1990**, *87*, 1787.
- (4) Van Beilen, J. B.; Poirier, Y. *Plant J.* **2008**, *54*, 684.
- (5) Hausmann, T.; Broer, I. Renewable Polymers in Transgenic Crop Plants. In *Renewable Polymers*, Mittal, V., Ed.; John Wiley & Sons, Inc. and Scrivener Publishing LLC: Salem, Massachusetts, 2011; pp 247.
- (6) Waddell, W.H.; Tsou, A.H. Butyl Rubbers. In *Rubber Compounding, Chemistry and Applications*, 2nd ed.; Rodgers, B. Ed.; CRC Press: Boca Raton, 2016.
- (7) Cornish, K. *Phytochem.* **2001**, *57*, 1123.
- (8) Haworth, J. P.; Baldwin, F. P. *Ind. Eng. Chem.* **1942**, *34*, 1301.
- (9) Rehner, J. *Ind. Eng. Chem.* **1944**, *36*, 46.
- (10) Grand View Research, Inc. Available <https://www.grandviewresearch.com/press-release/global-butyl-rubber-market> (access on January 10, 2018)
- (11) Goodyear, C. Improvement in India-Rubber Fabrics, US Patent 3633, 1844.
- (12) Thomas, R. M.; Sparks, W. J.; Frolich, P. K.; Otto, M.; Mueller-Cunradi, M. *J. Am. Chem. Soc.* **1940**, *62*, 276.
- (13) Kennedy, J. P. *Cationic Polymerization of Olefins: A critical Inventory*, Wiley-Interscience: New York, 1975.
- (14) R.M. Thomas; R.W. Sparks, Standard Oil Development Company, US Patent 2,356,128, 1944.
- (15) Puskas, J. E.; Chen, Y. *Biomacromolecules* **2004**, *5*, 1141.
- (16) Szwarc, M.; Van Beylen, M. *Ionic Polymerization and Living Polymers*, Springer Science and Business Media, B. V.: Dordrecht, 1993.
- (17) Odian, G. Ionic Chain Polymerization. In *Principles of Polymerization*, 4th ed.; John Wiley & Sons, Inc.: Hoboken, New Jersey, 2004; pp 372.
- (18) Matyjaszewski, K.; Pugh, C. *Cationic Polymerizations: Mechanisms, Synthesis and Applications*, Matyjaszewski, K. Ed.; Marcel Dekker, Inc.: New York, 1996; Chapter 1.
- (19) Plesch, P. H. The propagation rate-constants in cationic polymerisations. In *Advances in Polymer Science*, Springer Berlin Heidelberg: 1971; p 137.
- (20) Puskas, J. E.; Chan, S. W. P.; McAuley, K. B.; Shaikh, S.; Kaszas, G. *J. Polym.Sci. Part A: Polym. Chem.* **2005**, *43*, 5394.
- (21) Sigwalt, P.; Moreau, M. *Prog. Polym. Sci.* **2006**, *31*, 44.
- (22) De, P.; Faust, R.; Schimmel, H.; Ofial, A. R.; Mayr, H. *Macromolecules* **2004**, *37*, 4422.
- (23) Roth, M.; Mayr, H. *Macromolecules* **1996**, *29*, 6104.
- (24) Schlaad, H.; Kwon, Y.; Sipos, L.; Faust, R.; Charleux, B. *Macromolecules* **2000**, *33*, 8225.
- (25) Sigwalt, P. *Macromol. Chem. Phys.* **1974**, *175*, 1017.
- (26) Goethals, E. J.; Du Prez, F. *Prog. Polym. Sci.* **2007**, *32*, 220.
- (27) Aoshima, S.; Kanaoka, S. *Chem. Rev.* **2009**, *109*, 5245.
- (28) De Sorgo, M.; Pepper, D. C.; Szwarc, M. *J. Chem. Soc. Chem. Commun.* **1973**, 419.

- (29) Matyjaszewski, K.; Sigwalt, P. *Macromol. Chem. Phys.* **1986**, *187*, 2299.
- (30) Gandini, A.; Plesch, P. H. *J. Chem. Soc.* **1965**, 4826.
- (31) Subira, F.; Sauvet, G.; Vairon, J. P.; Sigwalt, P. *J. Polym.Sci. Polym. Symp.* **1976**, *56*, 221.
- (32) Li, D.; Hadjikyriacou, S.; Faust, R. *Macromolecules* **1996**, *29*, 6061.
- (33) Vijayaraghavan, R.; MacFarlane, D. R. *Macromolecules* **2007**, *40*, 6515.
- (34) Kukhta, N. A.; Vasilenko, I. V.; Kostjuk, S. V. *Green Chem.* **2011**, *13*, 2362.
- (35) Winstein, S.; Clippinger, E.; Fainberg, A. H.; Robinson, G. C. *J. Am. Chem. Soc.* **1954**, *76*, 2597.
- (36) Kumar, K. R.; Hall, C.; Penciu, A.; Drewitt, M. J.; McInenly, P. J.; Baird, M. C. *J. Polym. Sci. A Polym. Chem.* **2002**, *40*, 3302.
- (37) De, P.; Faust, R. Carbocationic Polymerization. In *Controlled and Living Polymerizations*, Muller, A.H.E.; Matyjaszewski, K. Eds.; Wiley-VCH Verlag GmbH & Co. KGaA: 2009; pp 57.
- (38) Higashimura, T.; Sawamoto, M. Living polymerization and selective dimerization: Two extremes of the polymer synthesis by cationic polymerization. In *Advances in Polymer Science*, Springer Berlin Heidelberg: 1984; pp 49.
- (39) Barton, J. M.; Pepper, D. C. *J. Chem. Soc.* **1964**, 1573.
- (40) Higashimura, T.; Hiza, M.; Hasegawa, H. *Macromolecules* **1979**, *12*, 1058.
- (41) Tsunogae, Y.; Kennedy, J. P. *J. Polym. Sci. Part A: Polym. Chem.* **1994**, *32*, 403.
- (42) Atkins, J. T.; Billmeyer, F. W. *J. Phys. Chem.* **1959**, *63*, 1966.
- (43) Endres, G. F.; Kamath, V. G.; Overberger, C. G. *J. Am. Chem. Soc.* **1962**, *84*, 4813.
- (44) Endres, G. F.; Overberger, C. G. *J. Am. Chem. Soc.* **1955**, *77*, 2201.
- (45) Miyamoto, M.; Sawamoto, M.; Higashimura, T. *Macromolecules* **1984**, *17*, 265.
- (46) Namikoshi, T.; Hashimoto, T.; Kodaira, T. *J. Polym. Sci. Part A: Polym. Chem.* **2004**, *42*, 2960.
- (47) Shiman, D. I.; Vasilenko, I. V.; Kostjuk, S. V. *Polymer* **2013**, *54*, 2235.
- (48) Rajabalitabar, B.; Nguyen, H. A.; Cheradame, H. *Macromolecules* **1996**, *29*, 514.
- (49) Faust, R.; Kennedy, J. P. *Polym. Bull.* **1988**, *19*, 21.
- (50) Kwon, O.-S.; Kim, Y.-B.; Kwon, S.-K.; Choi, B.-S.; Choi, S.-K. *Macromol. Chem. Phys.* **1993**, *194*, 251.
- (51) Satoh, K.; Nakashima, J.; Kamigaito, M.; Sawamoto, M. *Macromolecules* **2001**, *34*, 396.
- (52) Kojima, K.; Sawamoto, M.; Higashimura, T. *J. Polym. Sci. Part A: Polym. Chem.* **1990**, *28*, 3007.
- (53) Kojima, K.; Sawamoto, M.; Higashimura, T. *Macromolecules* **1990**, *23*, 948.
- (54) Higashimura, T.; Kojima, K.; Sawamoto, M. *Polym. Bull.* **1988**, *19*, 7.
- (55) Kaita, S.; Doi, Y.; Kaneko, K.; Horiuchi, A. C.; Wakatsuki, Y. *Macromolecules* **2004**, *37*, 5860.
- (56) Kaita, S.; Yamanaka, M.; Horiuchi, A. C.; Wakatsuki, Y. *Macromolecules* **2006**, *39*, 1359.
- (57) Bonnet, F.; Da Costa Violante, C.; Roussel, P.; Mortreux, A.; Visseaux, M. *Chem. Commun.* **2009**, 3380.
- (58) Huber, M.; Kurek, A.; Krossing, I.; Mulhaupt, R.; Schnoekel, H. *Z. Anorg. Allg. Chem.* **2009**, *635*, 1787.
- (59) Bochmann, M.; Dawson, D. M. *Angew. Chem. Int. Ed.* **1996**, *35*, 2226.

- (60) Lichtenthaler, M. R.; Higelin, A.; Kraft, A.; Hughes, S.; Steffani, A.; Plattner, D. A.; Slattery, J. M.; Krossing, I. *Organometallics* **2013**, *32*, 6725.
- (61) Petersen, T. O.; Simone, D.; Krossing, I. *Chem. Eur. J.* **2016**, *22*, 15847.
- (62) Barsan, F.; Karam, A. R.; Parent, M. A.; Baird, M. C. *Macromolecules* **1998**, *31*, 8439.
- (63) Taube, R.; Wache, S. *J. Organomet. Chem.* **1992**, *428*, 431.
- (64) Miyake, G. M.; DiRocco, D. A.; Liu, Q.; Oberg, K. M.; Bayram, E.; Finke, R. G.; Rovis, T.; Chen, E. Y. X. *Macromolecules* **2010**, *43*, 7504.
- (65) Rudolph, T.; Kempe, K.; Crotty, S.; Paulus, R. M.; Schubert, U. S.; Krossing, I.; Schacher, F. H. *Polym. Chem.* **2013**, *4*, 495.
- (66) Vijayaraghavan, R.; MacFarlane, D. R. *Chem. Commun.* **2004**, 700.
- (67) Chang, C.-T.; Chen, C.-L.; Liu, Y.-H.; Peng, S.-M.; Chou, P.-T.; Liu, S.-T. *Inorg. Chem.* **2006**, *45*, 7590.
- (68) Bochmann, M. *Acc. Chem. Res.* **2010**, *43*, 1267.
- (69) Strauss, S. H. *Chem. Rev.* **1993**, *93*, 927.
- (70) Riddlestone, I. M.; Kraft, A.; Schaefer, J.; Krossing, I. *Angew. Chem. Int. Ed.* **2018**, 10.1002/anie.201710782, In press.
- (71) Shaffer, T. D.; Ashbaugh, J. R. *J. Polym. Sci. Part A: Polym. Chem.* **1997**, *35*, 329.
- (72) Chen, E. Y. X. *Chem. Rev.* **2009**, *109*, 5157.
- (73) Odian, G. Stereochemistry of Polymerization. In *Principles of Polymerization*, 4th ed.; John Wiley & Sons, Inc.: Hoboken, New Jersey, 2004; pp 619.
- (74) Chen, E. Y.-X.; Marks, T. J. *Chem. Rev.* **2000**, *100*, 1391.
- (75) Kaminsky, W. *J. Chem. Soc. Dalton Trans.* **1998**, 1413.
- (76) Alt, H. G.; Köppl, A. *Chem. Rev.* **2000**, *100*, 1205.
- (77) Nuyken, O.; Pask, S. *Polymers* **2013**, *5*, 361.
- (78) Rosenthal, M. R. *J. Chem. Educ.* **1973**, *50*, 331.
- (79) Beck, W.; Suenkel, K. *Chem. Rev.* **1988**, *88*, 1405.
- (80) Gowda, N. M. N.; Naikar, S. B.; Reddy, G. K. N. Perchlorate Ion Complexes. In *Advances in Inorganic Chemistry*, Emeleus, H. J., Sharpe, A. G., Eds.; Academic Press: 1984; Vol. 28, pp 255.
- (81) Lawrance, G. A. *Chem. Rev.* **1986**, *86*, 17.
- (82) Dartiguenave, M.; Dartiguenave, Y.; Mari, A.; Guitard, A.; Olivier, M. J.; Beauchamp, A. L. *Can. J. Chem.* **1988**, *66*, 2386.
- (83) Buss, B.; Clegg, W.; Hartmann, G.; Jones, P. G.; Mews, R.; Noltemeyer, M.; Sheldrick, G. M. *J. Chem. Soc. Dalton Trans.* **1981**, 61.
- (84) Krossing, I.; Raabe, I. *Angew. Chem. Int. Ed.* **2004**, *43*, 2066.
- (85) Barbarich, T. J.; Handy, S. T.; Miller, S. M.; Anderson, O. P.; Grieco, P. A.; Strauss, S. H. *Organometallics* **1996**, *15*, 3776.
- (86) Grieco, P. A.; Nunes, J. J.; Gaul, M. D. *J. Am. Chem. Soc.* **1990**, *112*, 4595.
- (87) Grieco, P. A.; Cooke, R. J.; Henry, K. J.; VanderRoest, J. M. *Tetrahedron Lett.* **1991**, *32*, 4665.
- (88) Kanji, F.; Shin-ya, I.; Hiroshi, K.; Akira, M.; Akihisa, N.; Jin, N.; Takaaki, S.; Yurii, Y. *Chem. Lett.* **2000**, *29*, 62.
- (89) Moss, S.; King, B. T.; de Meijere, A.; Kozhushkov, S. I.; Eaton, P. E.; Michl, J. *Organic Letters* **2001**, *3*, 2375.

- (90) Rockwell, J. J.; Kloster, G. M.; DuBay, W. J.; Grieco, P. A.; Shriver, D. F.; Strauss, S. H. *Inorganica Chim. Acta* **1997**, 263, 195.
- (91) Patmore, N. J.; Hague, C.; Cotgreave, J. H.; Mahon, M. F.; Frost, C. G.; Weller, A. S. *Chem. Eur. J.* **2002**, 8, 2088.
- (92) Brintzinger, H. H.; Fischer, D.; Mülhaupt, R.; Rieger, B.; Waymouth, R. M. *Angew. Chem. Int. Ed.* **1995**, 34, 1143.
- (93) Piers, W. E. *Chem. Eur. J.* **1998**, 4, 13.
- (94) Piers, W. E.; Chivers, T. *Chem. Soc. Rev.* **1997**, 26, 345.
- (95) Piers, Warren E.; Irvine, Geoffrey J.; Williams, V. C. *Eur. J. Inorg. Chem.* **2000**, 2000, 2131.
- (96) LeSuer, R. J.; Geiger, W. E. *Angew. Chem. Int. Ed.* **2000**, 39, 248.
- (97) Barrière, F.; Camire, N.; Geiger, W. E.; Mueller-Westerhoff, U. T.; Sanders, R. *J. Am. Chem. Soc.* **2002**, 124, 7262.
- (98) Camire, N.; Nafady, A.; Geiger, W. E. *J. Am. Chem. Soc.* **2002**, 124, 7260.
- (99) Camire, N.; Mueller-Westerhoff, U. T.; Geiger, W. E. *J. Organomet. Chem.* **2001**, 637-639, 823.
- (100) Hill, M. G.; Lamanna, W. M.; Mann, K. R. *Inorg. Chem.* **1991**, 30, 4687.
- (101) Pospíšil, L. r.; King, B. T.; Michl, J. *Electrochim. Acta* **1998**, 44, 103.
- (102) Armand, M.; Johansson, P. *J. Power Sources* **2008**, 178, 821.
- (103) Yu, B.-T.; Qiu, W.-H.; Li, F.-S.; Xu, G.-X. *Electrochem. Solid State Lett.* **2006**, 9, A1.
- (104) Xu, W.; Angell, C. A. *Electrochem. Solid State Lett.* **2000**, 3, 366.
- (105) Nanbu, N.; Tsuchiya, K.; Shibazaki, T.; Sasaki, Y. *Electrochem. Solid State Lett.* **2002**, 5, A202.
- (106) Xu, W.; Angell, C. A. *Electrochem. Solid State Lett.* **2001**, 4, E1.
- (107) Kita, F.; Sakata, H.; Sinomoto, S.; Kawakami, A.; Kamizori, H.; Sonoda, T.; Nagashima, H.; Nie, J.; Pavlenko, N. V.; Yagupolskii, Y. L. *J. Power Sources* **2000**, 90, 27.
- (108) Massey, A. G.; Park, A. J. *J. Organomet. Chem.* **1964**, 2, 461.
- (109) Bochmann, M. *Angew. Chem. Int. Ed.* **1992**, 31, 1181.
- (110) Jordan, R. F.; Bajgur, C. S.; Willett, R.; Scott, B. *J. Am. Chem. Soc.* **1986**, 108, 7410.
- (111) Hlatky, G. G.; Turner, H. W.; Eckman, R. R. *J. Am. Chem. Soc.* **1989**, 111, 2728.
- (112) Seppelt, K. *Angew. Chem. Int. Ed.* **1993**, 32, 1025.
- (113) Yang, X.; Stern, C. L.; Marks, T. J. *J. Am. Chem. Soc.* **1991**, 113, 3623.
- (114) Bochmann, M.; Lancaster, S. J. *J. Organomet. Chem.* **1995**, 497, 55.
- (115) Yang, X.; Stern, C. L.; Marks, T. J. *J. Am. Chem. Soc.* **1994**, 116, 10015.
- (116) Chien, J. C. W.; Song, W.; Rausch, M. D. *Macromolecules* **1993**, 26, 3239.
- (117) Jia, L.; Yang, X.; Stern, C. L.; Marks, T. J. *Organometallics* **1997**, 16, 842.
- (118) Chien, J. C. W.; Tsai, W. M.; Rausch, M. D. *J. Am. Chem. Soc.* **1991**, 113, 8570.
- (119) Brookhart, M.; Grant, B.; Volpe, A. F. *Organometallics* **1992**, 11, 3920.
- (120) Brookhart, M.; Rix, F. C.; DeSimone, J. M.; Barborak, J. C. *J. Am. Chem. Soc.* **1992**, 114, 5894.
- (121) Bochmann; Sarsfield, M. J. *Organometallics* **1998**, 17, 5908.
- (122) LaPointe, R. E.; Roof, G. R.; Abboud, K. A.; Klosin, J. *J. Am. Chem. Soc.* **2000**, 122, 9560.
- (123) Sarazin, Y.; Hughes, D. L.; Kaltsoyannis, N.; Wright, J. A.; Bochmann, M. *J. Am. Chem. Soc.* **2007**, 129, 881.

- (124) Lancaster, S. J.; Rodriguez, A.; Lara-Sanchez, A.; Hannant, M. D.; Walker, D. A.; Hughes, D. H.; Bochmann, M. *Organometallics* **2002**, *21*, 451.
- (125) J. Lancaster, S.; A. Walker, D.; Thornton-Pett, M.; Bochmann, M. *Chem. Commun.* **1999**, 1533.
- (126) Hijazi, A. K.; Radhakrishnan, N.; Jain, K. R.; Herdtweck, E.; Nuyken, O.; Walter, H.-M.; Hanefeld, P.; Voit, B.; Kühn, F. E. *Angew. Chem. Int. Ed.* **2007**, *46*, 7290.
- (127) Garratt, S.; Carr, A. G.; Langstein, G.; Bochmann, M. *Macromolecules* **2003**, *36*, 4276.
- (128) Zhou, J.; Lancaster, S. J.; Walker, D. A.; Beck, S.; Thornton-Pett, M.; Bochmann, M. *J. Am. Chem. Soc.* **2001**, *123*, 223.
- (129) Bochmann, M. *Organometallics* **2010**, *29*, 4711.
- (130) McInenly, P. J.; Drewitt, M. J.; Baird, M. C. *Macromol. Chem. Phys.* **2004**, *205*, 1707.
- (131) Tse, C. K. W.; Penciu, A.; McInenly, P. J.; Kumar, K. R.; Drewitt, M. J.; Baird, M. C. *Eur. Polym. J.* **2004**, *40*, 2653.
- (132) Chen, M.-C.; Marks, T. J. *J. Am. Chem. Soc.* **2001**, *123*, 11803.
- (133) Chen, Y.-X.; Stern, C. L.; Marks, T. J. *J. Am. Chem. Soc.* **1997**, *119*, 2582.
- (134) Chen, Y.-X.; Metz, M. V.; Li, L.; Stern, C. L.; Marks, T. J. *J. Am. Chem. Soc.* **1998**, *120*, 6287.
- (135) Chen, M.-C.; Roberts, J. A. S.; Marks, T. J. *J. Am. Chem. Soc.* **2004**, *126*, 4605.
- (136) Chen, M.-C.; Roberts, J. A. S.; Seyam, A. M.; Li, L.; Zuccaccia, C.; Stahl, N. G.; Marks, T. J. *Organometallics* **2006**, *25*, 2833.
- (137) Chen, M.-C.; Roberts, J. A. S.; Marks, T. J. *Organometallics* **2004**, *23*, 932.
- (138) Roberts, J. A. S.; Chen, M.-C.; Seyam, A. M.; Li, L.; Zuccaccia, C.; Stahl, N. G.; Marks, T. J. *J. Am. Chem. Soc.* **2007**, *129*, 12713.
- (139) Krossing, I.; van Wüllen, L. *Chem. Eur. J.* **2002**, *8*, 700.
- (140) Stewart, M. P.; Paradee, L. M.; Raabe, I.; Trapp, N.; Slattery, J. S.; Krossing, I.; Geiger, W. E. *J. Fluorine Chem.* **2010**, *131*, 1091.
- (141) Krossing, I.; Brands, H.; Feuerhake, R.; Koenig, S. *J. Fluorine Chem.* **2001**, *112*, 83.
- (142) Barbarich, T. J.; Miller, S. M.; Anderson, O. P.; Strauss, S. H. *J. Mol. Catal. A: Chem.* **1998**, *128*, 289.
- (143) Lund, H.; Harloff, J.; Schulz, A.; Villinger, A. *Z. Anorg. Allg. Chem.* **2013**, *639*, 754.
- (144) Bulut, S.; Klose, P.; Huang, M.-M.; Weingärtner, H.; Dyson, P. J.; Laurency, G.; Friedrich, C.; Menz, J.; Kümmerer, K.; Krossing, I. *Chem. Eur. J.* **2010**, *16*, 13139.
- (145) Himmel, D.; Scherer, H.; Kratzert, D.; Krossing, I. *Z. Anorg. Allg. Chem.* **2015**, *641*, 655.
- (146) Raabe, I.; Antonijevic, S.; Krossing, I. *Chem. Eur. J.* **2007**, *13*, 7510.
- (147) Engesser, T. A.; Lichtenthaler, M. R.; Schleep, M.; Krossing, I. *Chem. Soc. Rev.* **2016**, *45*, 789.
- (148) Krossing, I. *Chem. Eur. J.* **2001**, *7*, 490.
- (149) Metz, M. V.; Sun, Y.; Stern, C. L.; Marks, T. J. *Organometallics* **2002**, *21*, 3691.
- (150) Sun, Y.; Metz, M. V.; Stern, C. L.; Marks, T. J. *Organometallics* **2000**, *19*, 1625.
- (151) Krossing, I.; Reisinger, A. *Coord. Chem. Rev.* **2006**, *250*, 2721.
- (152) Santiso-Quiñones, G.; Higelin, A.; Schaefer, J.; Brückner, R.; Knapp, C.; Krossing, I. *Chem. Eur. J.* **2009**, *15*, 6663.
- (153) Krossing, I.; Bihlmeier, A.; Raabe, I.; Trapp, N. *Angew. Chem. Int. Ed.* **2003**, *42*, 1531.
- (154) Raabe, I.; Himmel, D.; Müller, S.; Trapp, N.; Kaupp, M.; Krossing, I. *Dalton Trans.* **2008**, 946.

- (155) Lehner, A. J.; Trapp, N.; Scherer, H.; Krossing, I. *Dalton Trans.* **2011**, *40*, 1448.
- (156) Cameron, T. S.; Decken, A.; Dionne, I.; Fang, M.; Krossing, I.; Passmore, J. *Chem. Eur. J.* **2002**, *8*, 3386.
- (157) Krossing, I. *J. Am. Chem. Soc.* **2001**, *123*, 4603.
- (158) Gonsior, M.; Krossing, I.; Müller, L.; Raabe, I.; Jansen, M.; van Wüllen, L. *Chem. Eur. J.* **2002**, *8*, 4475.
- (159) Reisinger, A.; Trapp, N.; Knapp, C.; Himmel, D.; Breher, F.; Rügger, H.; Krossing, I. *Chem. Eur. J.* **2009**, *15*, 9505.
- (160) Santiso-Quiñones, G.; Brückner, R.; Knapp, C.; Dionne, I.; Passmore, J.; Krossing, I. *Angew. Chem. Int. Ed.* **2009**, *48*, 1133.
- (161) Krossing, I.; Reisinger, A. *Angew. Chem.* **2003**, *115*, 5903.
- (162) Gonsior, M.; Krossing, I. *Dalton Trans.* **2005**, *0*, 1203.
- (163) Lichtenthaler, M. R.; Stahl, F.; Kratzert, D.; Heidinger, L.; Schleicher, E.; Hamann, J.; Himmel, D.; Weber, S.; Krossing, I. *Nat. Commun.* **2015**, *6*, 8288.
- (164) Malinowski, P. J.; Himmel, D.; Krossing, I. *Angew. Chem. Int. Ed.* **2016**, *55*, 9259.
- (165) Rupp, A. B. A.; Krossing, I. *Acc. Chem. Res.* **2015**, *48*, 2537.
- (166) Zheng, X.; Zhang, Z.; Tan, G.; Wang, X. *Inorg. Chem.* **2016**, *55*, 1008.
- (167) Lichtenthaler, M. R.; Maurer, S.; Mangan, R. J.; Stahl, F.; Mönkemeyer, F.; Hamann, J.; Krossing, I. *Chem. Eur. J.* **2015**, *21*, 157.
- (168) McGuinness, D. S.; Rucklidge, A. J.; Tooze, R. P.; Slawin, A. M. Z. *Organometallics* **2007**, *26*, 2561.
- (169) Bihlmeier, A.; Gonsior, M.; Raabe, I.; Trapp, N.; Krossing, I. *Chem. Eur. J.* **2004**, *10*, 5041.
- (170) Ren, K.; Serguievski, P.; Gu, H.; Grinevich, O.; Malpert, J. H.; Neckers, D. C. *Macromolecules* **2002**, *35*, 898.
- (171) Ren, K.; Malpert, J. H.; Li, H.; Gu, H.; Neckers, D. C. *Macromolecules* **2002**, *35*, 1632.
- (172) Li, H.; Ren, K.; Zhang, W.; Malpert, J. H.; Neckers, D. C. *Macromolecules* **2001**, *34*, 2019.
- (173) Li, H.; Ren, K.; Neckers, D. C. *Macromolecules* **2001**, *34*, 8637.
- (174) Ren, K.; Mejiritski, A.; Malpert, J. H.; Grinevich, O.; Gu, H.; Neckers, D. C. *Tetrahedron Lett.* **2000**, *41*, 8669.
- (175) Knoth, W. H. *J. Am. Chem. Soc.* **1967**, *89*, 1274.
- (176) Knoth, W. H. *Inorg. Chem.* **1971**, *10*, 598.
- (177) Namikoshi, T.; Hashimoto, T.; Kodaira, T. *J. Polym. Sci., Part A: Polym. Chem.* **2004**, *42*, 3649.
- (178) Jelínek, T.; Plešek, J.; Mareš, F.; Heřmánek, S.; Štůbr, B. *Polyhedron* **1987**, *6*, 1981.
- (179) Körbe, S.; Schreiber, P. J.; Michl, J. *Chem. Rev.* **2006**, *106*, 5208.
- (180) Jelinek, T.; Baldwin, P.; Scheidt, W. R.; Reed, C. A. *Inorg. Chem.* **1993**, *32*, 1982.
- (181) Shelly, K.; Finster, D. C.; Lee, Y. J.; Scheidt, W. R.; Reed, C. A. *J. Am. Chem. Soc.* **1985**, *107*, 5955.
- (182) Reed, C. A. *Acc. Chem. Res.* **2010**, *43*, 121.
- (183) Reed, C. A.; Xie, Z.; Bau, R.; Benesi, A. *Science* **1993**, *262*, 402.
- (184) Xie, Z.; Manning, J.; Reed, R. W.; Mathur, R.; Boyd, P. D. W.; Benesi, A.; Reed, C. A. *J. Am. Chem. Soc.* **1996**, *118*, 2922.

- (185) Kim, K.-C.; Reed, C. A.; Elliott, D. W.; Mueller, L. I.; Tham, F.; Lin, L.; Lambert, J. B. *Science* **2002**, 297, 825.
- (186) Reed, C. A. *Acc. Chem. Res.* **1998**, 31, 133.
- (187) Reed, C. A.; Kim, K. C.; Bolskar, R. D.; Mueller, L. J. *Science* **2000**, 289, 101.
- (188) Stasko, D.; Reed, C. A. *J. Am. Chem. Soc.* **2002**, 124, 1148.
- (189) Ivanov, S. V.; Miller, S. M.; Anderson, O. P.; Strauss, S. H. *Cryst. Growth Des.* **2004**, 4, 249.
- (190) Stoyanov, E. S.; Hoffmann, S. P.; Juhasz, M.; Reed, C. A. *J. Am. Chem. Soc.* **2006**, 128, 3160.
- (191) Reed, C. A. *Chem. Commun.* **2005**, 0, 1669.
- (192) Cummings, S.; Hratchian, H. P.; Reed, C. A. *Angew. Chem. Int. Ed.* **2016**, 55, 1382.
- (193) Nava, M.; Stoyanova, I. V.; Cummings, S.; Stoyanov, E. S.; Reed, C. A. *Angew. Chem.* **2014**, 126, 1149.
- (194) Reed, C. A. *Acc. Chem. Res.* **2013**, 46, 2567.
- (195) Stasko, D.; Hoffmann, S. P.; Kim, K.-C.; Fackler, N. L. P.; Larsen, A. S.; Drovetskaya, T.; Tham, F. S.; Reed, C. A.; Rickard, C. E. F.; Boyd, P. D. W.; Stoyanov, E. S. *J. Am. Chem. Soc.* **2002**, 124, 13869.
- (196) Larsen, A. S.; Holbrey, J. D.; Tham, F. S.; Reed, C. A. *J. Am. Chem. Soc.* **2000**, 122, 7264.
- (197) Crowther, D. J.; Borkowsky, S. L.; Swenson, D.; Meyer, T. Y.; Jordan, R. F. *Organometallics* **1993**, 12, 2897.
- (198) Hlatky, G. G.; Eckman, R. R.; Turner, H. W. *Organometallics* **1992**, 11, 1413.
- (199) Zhang, Y.; Huynh, K.; Manners, I.; Reed, C. A. *Chem. Commun.* **2008**, 494.
- (200) Kim, K.-C.; Reed, C. A.; Long, G. S.; Sen, A. *J. Am. Chem. Soc.* **2002**, 124, 7662.
- (201) Vyakaranam, K.; Barbour, J. B.; Michl, J. *J. Am. Chem. Soc.* **2009**, 131, 5359.
- (202) Foropoulos, J.; DesMarteau, D. D. *J. Am. Chem. Soc.* **1982**, 104, 4260.
- (203) Vij, A.; Kirchmeier, R. L.; Shreeve, J. n. M.; Verma, R. D. *Coord. Chem. Rev.* **1997**, 158, 413.
- (204) Antoniotti, S.; Dalla, V.; Duñach, E. *Angew. Chem. Int. Ed.* **2010**, 49, 7860.
- (205) Hasani, M.; Yarger, J. L.; Angell, C. A. *Chem. Eur. J.* **2016**, 22, 13312.
- (206) Shainyan, B. A.; Tolstikova, L. L. *Chem. Rev.* **2013**, 113, 699.
- (207) Haas, A.; Klare, C.; Betz, P.; Bruckmann, J.; Krüger, C.; Tsay, Y. H.; Aubke, F. *Inorg. Chem.* **1996**, 35, 1918.
- (208) Williams, D. B.; Stoll, M. E.; Scott, B. L.; Costa, D. A.; Oldham, J. W. *J. Chem. Commun.* **2005**, 1438.
- (209) Foropoulos, J.; DesMarteau, D. D. *Inorg. Chem.* **1984**, 23, 3720.
- (210) Broussely, M.; Biensan, P.; Simon, B. *Electrochim. Acta* **1999**, 45, 3.
- (211) Wang, X.; Yasukawa, E.; Kasuya, S. *J. Electrochem. Soc.* **2000**, 147, 2421.
- (212) Klingshirn, M. A.; Broker, G. A.; Holbrey, J. D.; Shaughnessy, K. H.; Rogers, R. D. *Chem. Commun.* **2002**, 1394.
- (213) Kakuchi, R.; Chiba, K.; Fuchise, K.; Sakai, R.; Satoh, T.; Kakuchi, T. *Macromolecules* **2009**, 42, 8747.
- (214) Fuchise, K.; Sakai, R.; Satoh, T.; Sato, S.-i.; Narumi, A.; Kawaguchi, S.; Kakuchi, T. *Macromolecules* **2010**, 43, 5589.
- (215) Turowsky, L.; Seppelt, K. *Inorg. Chem.* **1988**, 27, 2135.

- (216) Murmann, P.; Schmitz, R.; Nowak, S.; Ignatiev, N.; Sartori, P.; Cekic-Laskovic, I.; Winter, M. *J. Electrochem. Soc.* **2015**, *162*, A1738.
- (217) Aravindan, V.; Gnanaraj, J.; Madhavi, S.; Liu, H.-K. *Chem. Eur. J.* **2011**, *17*, 14326.
- (218) Höfler, D.; van Gemmeren, M.; Wedemann, P.; Kaupmees, K.; Leito, I.; Leutzsch, M.; Lingnau, J. B.; List, B. *Angew. Chem.* **2017**, *129*, 1433.
- (219) Gillespie, R. J.; Moss, K. C. *J. Chem. Soc. A* **1966**, 1170.
- (220) Bacon, J.; Dean, P. A. W.; Gillespie, R. J. *Can. J. Chem.* **1970**, *48*, 3413.
- (221) Bacon, J.; Dean, P. A. W.; Gillespie, R. J. *Can. J. Chem.* **1969**, *47*, 1655.
- (222) Dean, P. A. W.; Gillespie, R. J.; Hulme, R. *J. Chem. Soc. D* **1969**, 990.
- (223) Brownstein, S. *Can. J. Chem.* **1969**, *47*, 605.
- (224) Minkwitz, R.; Neikes, F. *Inorg. Chem.* **1999**, *38*, 5960.
- (225) Christe, K. O.; Maya, W. *Inorg. Chem.* **1969**, *8*, 1253.
- (226) Christe, K. O.; Zhang, X.; Bau, R.; Hegge, J.; Olah, G. A.; Prakash, G. K. S.; Sheehy, J. A. *J. Am. Chem. Soc.* **2000**, *122*, 481.
- (227) Dean, P. A. W.; Gillespie, R. J.; Hulme, R.; Humphreys, D. A. *J. Chem. Soc. A* **1971**, 341.
- (228) Drews, T.; Koch, W.; Seppelt, K. *J. Am. Chem. Soc.* **1999**, *121*, 4379.
- (229) Elliott, H. S. A.; Lehmann, J. F.; Mercier, H. P. A.; Jenkins, H. D. B.; Schrobilgen, G. J. *Inorg. Chem.* **2010**, *49*, 8504.
- (230) Hughes, M. J.; Mercier, H. P. A.; Schrobilgen, G. J. *Inorg. Chem.* **2010**, *49*, 271.
- (231) Drews, T.; Seppelt, K. *Angew. Chem. Int. Ed.* **1997**, *36*, 273.
- (232) Hollenstein, S.; Laube, T. *J. Am. Chem. Soc.* **1993**, *115*, 7240.
- (233) Stein, L.; Norris, J. R.; Downs, A. J.; Minihan, A. R. *J. Chem. Soc. Chem. Commun.* **1978**, 502.
- (234) Lehmann, J. F.; Riedel, S.; Schrobilgen, G. J. *Inorg. Chem.* **2008**, *47*, 8343.
- (235) Noirot, M. D.; Anderson, O. P.; Strauss, S. H. *Inorg. Chem.* **1987**, *26*, 2216.
- (236) Wiesner, A.; Gries, T. W.; Steinhauer, S.; Beckers, H.; Riedel, S. *Angew. Chem. Int. Ed.* **2017**, *56*, 8263.
- (237) Mercier, H. P. A.; Sanders, J. C. P.; Schrobilgen, G. J. *J. Am. Chem. Soc.* **1994**, *116*, 2921.
- (238) Collins, M. J.; Schrobilgen, G. J. *Inorg. Chem.* **1985**, *24*, 2608.
- (239) Moock, K.; Seppelt, K. *Z. Anorg. Allg. Chem.* **1988**, *561*, 132.
- (240) Cameron, T. S.; Krossing, I.; Passmore, J. *Inorg. Chem.* **2001**, *40*, 4488.
- (241) Van Seggen, D. M.; Hurlburt, P. K.; Anderson, O. P.; Strauss, S. H. *Inorg. Chem.* **1995**, *34*, 3453.
- (242) Mercier, H. P. A.; Moran, M. D.; Schrobilgen, G. J.; Steinberg, C.; Suontamo, R. J. *J. Am. Chem. Soc.* **2004**, *126*, 5533.
- (243) Aris, D.; Beck, J.; Decken, A.; Dionne, I.; Schmedt auf der Gunne, J.; Hoffbauer, W.; Kochner, T.; Krossing, I.; Passmore, J.; Rivard, E.; Steden, F.; Wang, X. *Dalton Trans.* **2011**, *40*, 5865.
- (244) Mercier, H. P. A.; Moran, M. D.; Sanders, J. C. P.; Schrobilgen, G. J.; Suontamo, R. J. *Inorg. Chem.* **2005**, *44*, 49.
- (245) Aris, D.; Beck, J.; Decken, A.; Dionne, I.; Krossing, I.; Passmore, J.; Rivard, E.; Steden, F.; Wang, X. *Phosphorus Sulfur Silicon Relat. Elem.* **2004**, *179*, 859.

- (246) It should be noted that butyl rubber is produced commercially using cationic polymerization conducted in CH<sub>3</sub>Cl at -100 °C.
- (247) Macchioni, A. *Eur. J. Inorg. Chem.* **2003**, 2003, 195.
- (248) Wietelmann, U.; Bonrath, W.; Netscher, T.; Nöth, H.; Panitz, J.-C.; Wohlfahrt-Mehrens, M. *Chem. Eur. J.* **2004**, 10, 2451.
- (249) Allcock, H. R. *J. Am. Chem. Soc.* **1963**, 85, 4050.
- (250) Allcock, H. R.; Bissell, E. C. *J. Am. Chem. Soc.* **1973**, 95, 3154.
- (251) Allcock, H. R. *J. Am. Chem. Soc.* **1964**, 86, 2591.
- (252) Allcock, H. R.; Bissell, E. C. *J. Chem. Soc. Chem. Commun.* **1972**, 676.
- (253) Hellwinkel, D. *Chem. Ber.* **1965**, 98, 576.
- (254) Hellwinkel, D. *Angew. Chem. Int. Ed. Eng.* **1965**, 4, 356.
- (255) Hellwinkel, D. *Chem. Ber.* **1966**, 99, 3642.
- (256) Hellwinkel, D.; Wilfinger, H.-J. *Chem. Ber.* **1970**, 103, 1056.
- (257) Holmes, R. R. *Chem. Rev.* **1996**, 96, 927.
- (258) Holmes, R. R. *Acc. Chem. Res.* **1998**, 31, 535.
- (259) Wong, C. Y.; Kennepohl, D. K.; Cavell, R. G. *Chem. Rev.* **1996**, 96, 1917.
- (260) Constant, S.; Lacour, J. New Trends in Hexacoordinated Phosphorus Chemistry. In *New Aspects in Phosphorus Chemistry V*, Majoral, J.-P., Ed. ; Springer Berlin Heidelberg: 2005; pp 1.
- (261) Shevchenko, I. V.; Fischer, A.; Jones, P. G.; Schmutzler, R. *Chem. Ber.* **1992**, 125, 1325.
- (262) Lacour, J.; Ginglinger, C.; Grivet, C.; Bernardinelli, G. *Angew. Chem. Int. Ed.* **1997**, 36, 608.
- (263) Lacour, J.; Moraleda, D. *Chem. Commun.* **2009**, 7073.
- (264) Lacour, J.; Londez, A.; Goujon-Ginglinger, C.; Buss, V.; Bernardinelli, G. *Org. Lett.* **2000**, 2, 4185.
- (265) Favarger, F.; Goujon-Ginglinger, C.; Monchaud, D.; Lacour, J. *J. Org. Chem.* **2004**, 69, 8521.
- (266) Zhang, Y.; Gustafson, L. O.; Chen, E. Y. X. *J. Am. Chem. Soc.* **2011**, 133, 13674.
- (267) Siu, P. W.; Gates, D. P. *Can. J. Chem.* **2012**, 90, 574.
- (268) Siu, P. W.; Gates, D. P. *Organometallics* **2009**, 28, 4491.
- (269) Siu, P. W.; Hazin, K.; Gates, D. P. *Chem. Eur. J.* **2013**, 19, 9005.
- (270) Baird, M. C. *Chem. Rev.* **2000**, 100, 1471.
- (271) Kennedy, J. P. *J. Polym. Sci., Part A: Polym. Chem.* **1999**, 37, 2285.
- (272) Sarazin, Y.; Carpentier, J.-F. *Chem. Rev.* **2015**, 115, 3564.
- (273) Reed, C. A. *Chem. Commun.* **2005**, 1669.
- (274) Ouardad, S.; Deffieux, A.; Peruch, F. *Polym. Chem.* **2013**, 4, 1874.
- (275) Kostjuk, S. V.; Ouardad, S.; Peruch, F.; Deffieux, A.; Absalon, C.; Puskas, J. E.; Ganachaud, F. *Macromolecules* **2011**, 44, 1372.
- (276) Radchenko, A. V.; Kostjuk, S. V.; Vasilenko, I. V.; Ganachaud, F.; Kaputsky, F. N.; Guillaneuf, Y. *J. Polym. Sci. Part A: Polym. Chem.* **2008**, 46, 6928.
- (277) Kostjuk, S. V.; Ganachaud, F. *Macromolecules* **2006**, 39, 3110.
- (278) Tse, C. K. W.; Kumar, K. R.; Drewitt, M. J.; Baird, M. C. *Macromol. Chem. Phys.* **2004**, 205, 1439.
- (279) Bergquist, C.; Bridgewater, B. M.; Harlan, C. J.; Norton, J. R.; Friesner, R. A.; Parkin, G. *J. Am. Chem. Soc.* **2000**, 122, 10581.

- (280) It is generally accepted that cationic polymerizations, due in part to the nature of the initiating species, are not as well understood as radical or ionic polymerizations. See, for example: G. Odian, *Principles of Polymerization*, John Wiley & Sons, Inc.: Hoboken, New Jersey, 2004; p. 373.
- (281) Hijazi, A. K.; Taha, Z. A.; Ajlouni, A.; Radhakrishnan, N.; Voit, B.; Kühn, F. E. *J. Organomet. Chem.* **2014**, 763–764, 65.
- (282) Chang, C. T.; Chen, C. L.; Liu, Y. H.; Peng, S. M.; Chou, P. T.; Liu, S. T. *Inorg. Chem.* **2006**, 45, 7590.
- (283) Reddy G. N, M.; Ballesteros-Garrido, R.; Lacour, J.; Caldarelli, S. *Angew. Chem. Int. Ed.* **2013**, 52, 3255.
- (284) Bonnot, C.; Aubert, E.; Banerji, N.; Lacour, J.; Espinosa, E.; Chambron, J.-C. *Chem. Eur. J.* **2010**, 16, 5706.
- (285) Frantz, R.; Grange, C. S.; Al-Rasbi, N. K.; Ward, M. D.; Lacour, J. *Chem. Commun.* **2007**, 1459.
- (286) Gaillard, S.; Rix, D.; Slawin, A. M. Z.; Lacour, J.; Nolan, S. P. *Dalton Trans.* **2012**, 41, 8235.
- (287) Lacour, J.; Hebbe-Viton, V. *Chem. Soc. Rev.* **2003**, 32, 373.
- (288) Tortoreto, C.; Achard, T.; Zeghida, W.; Austeri, M.; Guénée, L.; Lacour, J. *Angew. Chem. Int. Ed.* **2012**, 51, 5847.
- (289) Vachon, J.; Bernardinelli, G.; Lacour, J. *Chem. Eur. J.* **2010**, 16, 2797.
- (290) Zalubovskis, R.; Bouet, A.; Fjellander, E.; Constant, S.; Linder, D.; Fischer, A.; Lacour, J.; Privalov, T.; Moberg, C. *J. Am. Chem. Soc.* **2008**, 130, 1845.
- (291) Andersen, S. S.; Jensen, M.; Sorensen, A.; Miyazaki, E.; Takimiya, K.; Laursen, B. W.; Flood, A. H.; Jeppesen, J. O. *Chem. Commun.* **2012**, 48, 5157.
- (292) Bouit, P.-A.; Aronica, C.; Toupet, L.; Le Guennic, B.; Andraud, C.; Maury, O. *J. Am. Chem. Soc.* **2010**, 132, 4328.
- (293) Sharma, S.; Lombeck, F.; Eriksson, L.; Johansson, O. *Chem. Eur. J.* **2010**, 16, 7078.
- (294) Grant, H.; Mctigue, P.; Ward, D. *Aust. J. Chem.* **1983**, 36, 2211.
- (295) Ripin, D.; Evans, D. [http://evans.rc.fas.harvard.edu/pdf/evans\\_pKa\\_table.pdf](http://evans.rc.fas.harvard.edu/pdf/evans_pKa_table.pdf) (accessed October 25, 2016).
- (296) Behmel, P.; Jones, P. G.; Sheldrick, G. M.; Ziegler, M. *J. Mol. Struct.* **1980**, 69, 41.
- (297) Jiang, B.; Yang, H.; Zhang, L.; Zhang, R.; Sun, Y.; Huang, Y. *Chem. Eng. J.* **2016**, 283, 89.
- (298) Krossing, I.; Reisinger, A. *Eur. J. Inorg. Chem.* **2005**, 2005, 1979.
- (299) The sign of NOE is dependent on the size of a molecule and solution conditions. See, for example: T.D.W. Claridge, *High-Resolution NMR Techniques in Organic Chemistry*, Tetrahedron Organic Chemistry Series, Pergamon: Oxford, 1999, p. 299-300.
- (300) Lacour, J.; Bernardinelli, G.; Russell, V.; Dance, I. *CrystEngComm* **2002**, 4, 165.
- (301) Jutzi, P.; Müller, C.; Stämmler, A.; Stämmler, H.-G. *Organometallics* **2000**, 19, 1442.
- (302) Nachtigall, O.; Pataki, A.; Molski, M.; Lentz, D.; Spandl, J. *Z. Anorg. Allg. Chem.* **2015**, 641, 1164.
- (303) Pietikäinen, J.; Maaninen, A.; Laitinen, R. S.; Oilunkaniemi, R.; Valkonen, J. *Polyhedron* **2002**, 21, 1089.
- (304) Barrow, M. *Acta Crystallogr. Sect. B: Struct. Sci.* **1981**, 37, 2239.
- (305) Cotton, F. A.; Ilsley, W. H. *Inorg. Chem.* **1981**, 20, 572.

- (306) Bondi, A. *J. Phys. Chem.* **1964**, *68*, 441.
- (307) Adonin, S. A.; Udalova, L. I.; Smolentsev, A. I.; Sokolov, M. N.; Fedin, V. P. *Russ. J. Coord. Chem.* **2015**, *41*, 633.
- (308) Krill, J.; Shevehenko, I. V.; Fischer, A.; Jones, P. G.; Schmutzler, R. *Chem. Ber.* **1997**, *130*, 1479.
- (309) Frydrych, R.; Muschter, T.; Brudgam, I.; Hartl, H. *Z Naturforsch B* **1990**, *45*, 679.
- (310) Kanazawa, A.; Kanaoka, S.; Aoshima, S. *Macromolecules* **2010**, *43*, 3682.
- (311) Bae, Y. C.; Faust, R. *Macromolecules* **1998**, *31*, 2480.
- (312) Pernecker, T.; Kennedy, J. P.; Ivan, B. *Macromolecules* **1992**, *25*, 1642.
- (313) Kanaoka, S.; Sawamoto, M.; Higashimura, T. *Macromolecules* **1991**, *24*, 2309.
- (314) Kostjuk, S. V.; Ganachaud, F. *Acc. Chem. Res.* **2010**, *43*, 357.
- (315) Cotrel, R.; Sauvet, G.; Vairon, J. P.; Sigwalt, P. *Macromolecules* **1976**, *9*, 931.
- (316) Higashimura, T.; Aoshima, S.; Sawamoto, M. *Makromol. Chem. Macromol. Symp.* **1988**, *13-14*, 457.
- (317) Kojima, K.; Sawamoto, M.; Higashimura, T. *Polym. Bull.* **1990**, *23*, 149.
- (318) Kuznetsov, D. M.; Tumanov, V. V.; Smit, W. A. *J. Polym. Res.* **2013**, *20*, 1.
- (319) Fontana, C. M.; Kidder, G. A.; Herold, R. J. *Ind. Eng. Chem.* **1952**, *44*, 1688.
- (320) Kanazawa, A.; Shibutani, S.; Yoshinari, N.; Konno, T.; Kanaoka, S.; Aoshima, S. *Macromolecules* **2012**, *45*, 7749.
- (321) Yoshizaki, T.; Kanazawa, A.; Kanaoka, S.; Aoshima, S. *Macromolecules* **2016**, *49*, 71.
- (322) Shi, X.; Nishiura, M.; Hou, Z. *Angew. Chem. Int. Ed. Engl.* **2016**, *55*, 14812.
- (323) Lübbecke, H.; Boldt, P. *Tetrahedron* **1978**, *34*, 1577.
- (324) Liu, Q.; Huang, Y.-k.; Zhou, X.-d.; Zhao, Y.-l. *Chin. J. Polym. Sci.* **2010**, *28*, 819.
- (325) SAINT, Version 8.34 A, Bruker AXS Inc., Madisoc, WI, **1997-2013**.
- (326) SADABS, V2014/5, Krause, L.; Herbst-Irmer, R.; Sheldrick, G. M.; Stalke, D. *J. Appl. Crystallogr.* **2015**, *48*, 3.
- (327) SQUEEZE, Spek, A.L. *Acta Cryst. C* **2015**, *71*, 9-18.
- (328) SHELXT, Sheldrick, G. M. *Acta Cryst. A* **2015**, *71*, 3-8.
- (329) G. M. Sheldrick, *SHELXL-97*, University of Göttingen, Germany, **1997**.
- (330) Geiger, W. E.; Barrière, F. *Acc. Chem. Res.* **2010**, *43*, 1030.
- (331) Jutzi, P.; Müller, C.; Stammler, A.; Stammler, H.-G. *Organometallics* **2000**, *19*, 1442.
- (332) Williams, V. C.; Irvine, G. J.; Piers, W. E.; Li, Z.; Collins, S.; Clegg, W.; Elsegood, M. R. J.; Marder, T. B. *Organometallics* **2000**, *19*, 1619.
- (333) Liang, H.-C.; Kim, E.; Incarvito, C. D.; Rheingold, A. L.; Karlin, K. D. *Inorg. Chem.* **2002**, *41*, 2209.
- (334) Ewart, S. W.; Sarsfield, M. J.; Williams, E. F.; Baird, M. C. *J. Organomet. Chem.* **1999**, *579*, 106.
- (335) Pan, B.; Gabbai, F. P. *J. Am. Chem. Soc.* **2014**, *136*, 9564.
- (336) Holthausen, M. H.; Mehta, M.; Stephan, D. W. *Angew. Chem. Int. Ed.* **2014**, *53*, 6538.
- (337) Grumbine, S. K.; Tilley, T. D.; Arnold, F. P.; Rheingold, A. L. *J. Am. Chem. Soc.* **1994**, *116*, 5495.
- (338) Huang, D.; Huffman, J. C.; Bollinger, J. C.; Eisenstein, O.; Caulton, K. G. *J. Am. Chem. Soc.* **1997**, *119*, 7398.
- (339) Reger, D. L.; Collins, J. E.; Rheingold, A. L.; Liable-Sands, L. M. *Inorg. Chem.* **1999**, *38*, 3235.

- (340) Reger, D. L.; Wright, T. D.; Little, C. A.; Lamba, J. J. S.; Smith, M. D. *Inorg. Chem.* **2001**, *40*, 3810.
- (341) Yakelis, N. A.; Bergman, R. G. *Organometallics* **2005**, *24*, 3579.
- (342) Kolychev, E. L.; Bannenberg, T.; Freytag, M.; Daniliuc, C. G.; Jones, P. G.; Tamm, M. *Chem. Eur. J.* **2012**, *18*, 16938.
- (343) Kawano, Y.; Hashiva, M.; Shimoi, M. *Organometallics* **2006**, *25*, 4420.
- (344) Bahr, S. R.; Boudjouk, P. *J. Org. Chem.* **1992**, *57*, 5545.
- (345) Zhang, J.; Barakat, K. A.; Cundari, T. R.; Gunnoe, T. B.; Boyle, P. D.; Petersen, J. L.; Day, C. S. *Inorg. Chem.* **2005**, *44*, 8379.
- (346) Stoccoro, S.; Alesso, G.; Cinellu, M. A.; Minghetti, G.; Zucca, A.; Bastero, A.; Claver, C.; Manassero, M. *J. Organomet. Chem.* **2002**, *664*, 77.
- (347) Huang, D.; Bollinger, J. C.; Streib, W. E.; Folting, K.; Young, V.; Eisenstein, O.; Caulton, K. G. *Organometallics* **2000**, *19*, 2281.
- (348) Huber, M.; Kurek, A.; Krossing, I.; Mülhaupt, R.; Schnöckel, H. *Z. Anorg. Allg. Chem.* **2009**, *635*, 1787.
- (349) Li, Y.; Yeong, H. Y.; Herdtweck, E.; Voit, B.; Kühn, F. E. *Eur. J. Inorg. Chem.* **2010**, *2010*, 4587.
- (350) For applications of the TRISPHAT anion, see: (a) Reddy, M.; Ballesteros-Garrido, R.; Lacour, J.; Caldarelli, . *Angew. Chem. Int. Ed.* **2013**, *52*, 3255; (b) Tortoreto, C.; Achard, T.; Zeghida, W.; Austeri, M.; Guénée, L.; Lacour, J. *Angew. Chem. Int. Ed.* **2012**, *51*, 5847; (c) Gaillard, S.; Rix, D.; Slawin, A. M. Z.; Lacour, J.; Nolan, S. P. *Dalton Trans.* **2012**, *41*, 8235; (d) Phipps, R. J.; Hamilton, G. L.; Toste, F. D. *Nat. Chem.* **2012**, *4*, 603; (e) Andersen, S. S.; Jensen, M.; Sorensen, A.; Miyazaki, E.; Takimiya, K.; Laursen, B. W.; Flood, A. H.; Jeppesen, J. O. *Chem. Commun.* **2012**, *48*, 5157; (f) Siu, P. W.; Gates, D. P. *Can. J. Chem.* **2012**, *90*, 574; (g) Bouit, P.-A.; Aronica, C.; Toupet, L.; Le Guennic, B.; Andraud, C.; Maury, O. *J. Am. Chem. Soc.* **2010**, *132*, 4328; (h) Sharma, S.; Lombeck, F.; Eriksson, L.; Johansson, O. *Chem. Eur. J.* **2010**, *16*, 7078; (i) Bonnot, C.; Aubert, E.; Banerji, N.; Lacour, J.; Espinosa, E.; Chambron, J.-C. *Chem. Eur. J.* **2010**, *16*, 5706; (j) Vachon, J.; Bernardinelli, G.; Lacour, J.; *Chem. Eur. J.* **2010**, *16*, 2797; (k) Lacour, J.; Moraleda, D.; *Chem. Commun.* **2009**, 7073; (l) Constable, E. C.; Housecroft, C. E.; Neuburger, M.; Rösel, P. J.; Schaffner, S.; Zampese, J. A. *Chem. Eur. J.* **2009**, *15*, 11746; (m) Zalubovskis, R.; Bouet, A.; Fjellander, E.; Constant, S.; Linder, D.; Fischer, A.; Lacour, J.; Privalov, T.; Moberg, C. *J. Am. Chem. Soc.* **2008**, *130*, 1845; (n) Frantz, R.; Grange, C. S.; Al-Rasbi, N. K.; Ward, M. D.; Lacour, J. *Chem. Commun.* **2007**, 1459; (o) Favarger, F.; Goujon-Ginglinger, C.; Monchaud, D.; Lacour, J. *J. Org. Chem.* **2004**, *69*, 8521; (p) Lacour, J.; Hebbe-Viton, V. *Chem. Soc. Rev.* **2003**, *32*, 373.
- (351) Hazin, K.; Serin, S. C.; Patrick, B. O.; Ezhova, M. B.; Gates, D. P. *Dalton Trans.* **2017**, *46*, 5901.
- (352) Hellwinkel, D. *Chem. Ber.* **1966**, *99*, 3628.
- (353) The patent application claims the synthesis and characterization and the use of ammonium salts of  $[P(C_{12}F_8)_3]^-$  as initiators for olefin polymerization. However, it should be noted, that the anion system was only characterized by  $^{19}F$  NMR spectroscopy. Bohnen, H.; Fritze, C.; Kueber, F. *Compounds having an ionic structure used as constituent of an olefin polymerisation catalyst*; WO 99/43685, September 2, 1999.

- (354) Schubert, U.; Neugebauer, W.; von Rague Schleyer, P. *J. Chem. Soc. Chem. Commun.* **1982**, 1184.
- (355) Neugebauer, W.; Kos, A. J.; von Ragué Schleyer, P. *J. Organomet. Chem.* **1982**, 228, 107.
- (356) Toussaint, C. *Acta. Crystallogr.* **1966**, 21, 1002.
- (357) Toussaint, C.; Vos, G. *J. Chem. Soc. B* **1966**, 813.
- (358) Bowden, S. T. *J. Chem. Soc.* **1931**, 1111.
- (359) Rapson, W. S.; Schwartz, H. M.; Stewart, E. T. *J. Chem. Soc.* **1944**, 73.
- (360) Hertel, E.; Roemer, G.H. *Z. Phys. Chem.*, **1933**, 21B, 292.
- (361) Zhang, Y.; Han, J.; Liu, Z.-J. *J. Org. Chem.* **2016**, 81, 1317.
- (362) Mathew, S. M.; Hartley, C. S. *Macromolecules* **2011**, 44, 8425.
- (363) Wittig, G.; Maercker, A. *Chem. Ber.* **1964**, 97, 747.
- (364) Hellwinkel, D. *Phosphorus Relat. Group V Elem.* **1973**, 2, 167.
- (365) Eisch, J. J.; Shah, J. H.; Boleslawski, M. P. *J. Organomet. Chem.* **1994**, 464, 11.
- (366) Hellwinkel, D. *Ann. N. Y. Acad. Sci.* **1972**, 192, 158.
- (367) Batsanov, S. *Inorg. Mater.* **2001**, 37, 871.
- (368) Stillinger, F. H. Theory and Molecular Models for Water. In *Advances in Chemical Physics*, John Wiley & Sons, Inc.: Hoboken, New Jersey, 1975; pp 1.
- (369) Jee, B.; Zank, J.; Dance, I.; Bruce Wild, S.; Klufers, P.; Willis, A. *CrystEngComm* **2000**, 2, 191.
- (370) Hargreaves, A.; Rizvi, S. H. *Acta. Crystallogr.* **1962**, 15, 365.
- (371) Trotter, J. *Acta. Crystallogr.* **1961**, 14, 1135.
- (372) Wittig, G.; Pieper, G.; Fuhrmann, G. *Ber. Dtsch. Chem. Ges.* **1940**, 73, 1193.
- (373) Wittig, G. *Sci. Nat.* **1942**, 30, 696.
- (374) Heaney, H.; Mann, F. G.; Millar, I. T. *J. Chem. Soc.* **1956**, 1.
- (375) Heaney, H.; Mann, F. G.; Millar, I. T. *J. Chem. Soc.* **1957**, 3930.
- (376) Chen, L. S.; Chen, G. J.; Tamborski, C. *J. Organomet. Chem.* **1980**, 193, 283.
- (377) Hays, H. R. *J. Org. Chem.* **1971**, 36, 98.
- (378) Gilman, H.; Vernon, C. C. *J. Am. Chem. Soc.* **1926**, 48, 1063.
- (379) Kajiyama, K.; Yoshimune, M.; Nakamoto, M.; Matsukawa, S.; Kojima, S.; Akiba, K.-y. *Org. Lett.* **2001**, 3, 1873.
- (380) Liang, Y.; Zhang, S.; Xi, Z. *J. Am. Chem. Soc.* **2011**, 133, 9204.
- (381) Lacour, J.; Vial, L.; Herse, C. *Org. Lett.* **2002**, 4, 1351.
- (382) Hebbe, V.; Londez, A.; Goujon-Ginglinger, C.; Meyer, F.; Uziel, J.; Jugé, S.; Lacour, J. *Tetrahedron Lett.* **2003**, 44, 2467.
- (383) Vial, L.; Lacour, J. *Org. Lett.* **2002**, 4, 3939.
- (384) Pasquato, L.; Herse, C.; Lacour, J. *Tetrahedron Lett.* **2002**, 43, 5517.
- (385) Gloede, J.; Gross, H. *Tetrahedron Lett.* **1976**, 17, 917.
- (386) Cavezzan, J.; Etemad-Moghadam, G.; Koenig, M.; Klaebe, A. *Tetrahedron Lett.* **1979**, 20, 795.
- (387) Schmidpeter, A.; von Criegern, T.; Sheldrick, W. S.; Schomburg, D. *Tetrahedron Lett.* **1978**, 19, 2857.
- (388) Koenig, M.; Klaebe, A.; Munoz, A.; Wolf, R. *J. Chem. Soc. Perkin Trans. 2* **1979**, 40.
- (389) Gallagher, M.; Munoz, A.; Gence, G.; Koenig, M. *J. Chem. Soc. Chem. Commun.* **1976**, 321.

- (390) Eberwein, M.; Schmid, A.; Schmidt, M.; Zabel, M.; Burgemeister, T.; Barthel, J.; Kunz, W.; Gores, H. J. *J. Electrochem. Soc.* **2003**, *150*, A994.
- (391) Hazin, K.; Gates, D. P. *Can. J. Chem.* **2018**, *0*, 1.
- (392) Chandrasekaran, A.; Day, R. O.; Holmes, R. R. *Inorg. Chem.* **2002**, *41*, 1645.
- (393) Karaghiosoff, K.; Klapötke, T. M.; Krumm, B.; Nöth, H.; Schütt, T.; Suter, M. *Inorg. Chem.* **2002**, *41*, 170.
- (394) Voss, T.; Mahdi, T.; Otten, E.; Fröhlich, R.; Kehr, G.; Stephan, D. W.; Erker, G. *Organometallics* **2012**, *31*, 2367.
- (395) Naudin, E.; Gouérec, P.; Bélanger, D. *J. Electroanal. Chem.* **1998**, *459*, 1.
- (396) Lacour, J.; me; Ginglinger, C.; Grivet, C.; Bernardinelli, G. *Angew. Chem. Int. Ed.* **1997**, *36*, 608.
- (397) Fu, L.; Zhao, D.; Li, F.-F.; Zhang, R.; Wang, C.-P.; Zhang, D.-D. *Synth. React. Inorg. Met.-Org. Chem., Nano-Met. Chem.* **2016**, *46*, 370.
- (398) Kaul, F. A. R.; Puchta, G. T.; Schneider, H.; Grosche, M.; Mihalios, D.; Herrmann, W. A. *J. Organomet. Chem.* **2001**, *621*, 177.
- (399) Rodriguez, G.; Brant, P. *Organometallics* **2001**, *20*, 2417.
- (400) Ryan, J. M.; Xu, Z. *Inorg. Chem.* **2004**, *43*, 4106.
- (401) Tafenko, V. A.; Gurskiy, S. I. *Cryst. Growth Des.* **2016**, *16*, 940.
- (402) Wang, P.; Yue, Z.; Zhang, J.; Feng, S. *Inorg. Chem. Commun.* **2011**, *14*, 1027.
- (403) Chouaib, H.; Kamoun, S.; Ayedi, H. F. *Acta Crystallogr. E* **2013**, *69*, m311.
- (404) Chouaib, H.; Kamoun, S.; Costa, L. C.; Graça, M. P. F. *J. Mol. Struct.* **2015**, *1102*, 71.
- (405) Chouaib, H.; Elfaleh, N.; Karoui, S.; Kamoun, S.; Graça, M. P. F. *Synth. Met.* **2016**, *217*, 129.
- (406) Chu, K.-T.; Liu, Y.-C.; Huang, Y.-L.; Hsu, C.-H.; Lee, G.-H.; Chiang, M.-H. *Chem. Eur. J.* **2015**, *21*, 10978.
- (407) Vembu, N.; Fronczek, F. R. *Acta Crystallogr. E* **2009**, *65*, o111.
- (408) Asaji, T.; Fujimori, H.; Ishida, H.; Eda, K.; Hashimoto, M. *J. Phys. Chem. Solids* **2005**, *66*, 869.
- (409) Jain, S. L.; Bhattacharyya, P.; Milton, H. L.; Slawin, A. M. Z.; Woollins, D. J. *Inorg. Chem. Commun.* **2004**, *7*, 423.
- (410) Duggirala, N. K.; Wood, G. P. F.; Fischer, A.; Wojtas, Ł.; Perry, M. L.; Zaworotko, M. J. *Cryst. Growth Des.* **2015**, *15*, 4341.
- (411) Goettel, J. T.; Kostiuk, N.; Gerken, M. *Inorg. Chem.* **2016**, *55*, 7126.
- (412) Yamada, T.; Nankawa, T. *Inorg. Chem.* **2016**, *55*, 8267.
- (413) Goldberg, I. *Acta Crystallogr., Sect. C* **2009**, *65*, o509.
- (414) Daly, J. J.; Pinkerton, A. A.; Schwarzenbach, D. *Acta Crystallogr., Sect. C* **1987**, *43*, 1818.
- (415) James, B. D.; Mrozinski, J.; Klak, J.; Skelton, B. W.; White, A. H. *Z. Anorg. Allg. Chem.* **2009**, *635*, 317.
- (416) Gotoh, K.; Ishida, H. *Acta Crystallogr., Sect. E* **2015**, *71*, 31.
- (417) Norihito, K.; Toshio, N.; Tamotsu, I. *Bull. Chem. Soc. Jpn.* **2003**, *76*, 1351.
- (418) Tsuyoshi, W.; Ichiro, H.; Norimitsu, T.; Mikiji, M. *Chem. Lett.* **2007**, *36*, 234.
- (419) Smith, G.; Wermuth, U. D.; Healy, P. C.; Young, D. J.; White, J. M. *Acta Crystallogr., Sect. E* **2005**, *61*, o2646.
- (420) Bialonska, A.; Ciunik, Z. *CrystEngComm* **2013**, *15*, 5681.

- (421) Moreno, A.; Pregosin, P. S.; Veiros, L. F.; Albinati, A.; Rizzato, S. *Chem. Eur. J.* **2009**, *15*, 6848.
- (422) Smith, G.; Wermuth, U. D.; Young, D. J. *J. Chem. Crystallogr.* **2010**, *40*, 520.
- (423) Polavarapu, P. L.; Petrovic, A. G.; Vick, S. E.; Wulff, W. D.; Ren, H.; Ding, Z.; Staples, R. J. *J. Org. Chem.* **2009**, *74*, 5451.
- (424) Bialonska, A.; Ciunik, Z. *Acta Crystallogr., Sect. C* **2006**, *62*, o450.
- (425) Białońska, A.; Ciunik, Z. *J. Mol. Struct.* **2006**, *791*, 144.
- (426) Stoyanov, E. S.; Kim, K.-C.; Reed, C. A. *J. Am. Chem. Soc.* **2006**, *128*, 8500.
- (427) Lv, Z. P.; Chen, B.; Wang, H. Y.; Wu, Y.; Zuo, J. L. *Small* **2015**, *11*, 3597.
- (428) Wu, W.; Xie, J. M.; Xuan, Y. W. *Z. Anorg. Allg. Chem.* **2009**, *635*, 351.
- (429) Benedict, J. B.; Bullard, T.; Kaminsky, W.; Kahr, B. *Acta Cryst. C* **2004**, *60*, m551.
- (430) Karpov, S. V.; Kaukov, Y. S.; Grigor'ev, A. A.; Nasakin, O. E.; Kaukova, O. V.; Tafenko, V. A. *Org. Biomol. Chem.* **2016**, *14*, 3758.
- (431) Clegg, W.; Holcroft, J. M. *Cryst. Growth Des.* **2014**, *14*, 6282.
- (432) Sah, A. K.; Rao, C. P.; Saarenketo, P. K.; Wegelius, E. K.; Rissanen, K.; Kolehmainen, E. *J. Chem. Soc. Dalton Trans.* **2000**, 3681.
- (433) Krivec, M.; Perdih, F.; Košmrlj, J.; Kočevar, M. *J. Org. Chem.* **2016**, *81*, 5732.
- (434) Chandrasekaran, A.; Day, R. O.; Holmes, R. R. *Inorg. Chem.* **2001**, *40*, 6229.
- (435) SQUEEZE: A. L. Spek, *Acta Crystallogr., Sect. C: Cryst. Struct. Commun.*, **2015**, *71*, 9.
- (436) Krossing, I. *J. Chem. Soc. Dalton Trans.* **2002**, 500.
- (437) Straus, D. A.; Zhang, C.; Tilley, T. D. *J. Organomet. Chem.* **1989**, *369*, C13.
- (438) Weinert, C. S.; Fanwick, P. E.; Rothwell, I. P. *Organometallics* **2002**, *21*, 484.
- (439) Thorn, M. G.; Moses, J. E.; Fanwick, P. E.; Rothwell, I. P. *J. Chem. Soc. Dalton Trans.* **2000**, 2659.
- (440) Andros, L.; Juric, M.; Popovic, J.; Planinic, P. *RSC Adv.* **2014**, *4*, 37051.
- (441) Andros, L.; Matkovic-Calogovic, D.; Planinic, P. *CrystEngComm* **2013**, *15*, 533.
- (442) Dubraja, L. A.; Matkovic-Calogovic, D.; Planinic, P. *CrystEngComm* **2015**, *17*, 2021.
- (443) Preiss, U. P.; Steinfeld, G.; Scherer, H.; Erle, A. M. T.; Benkmil, B.; Kraft, A.; Krossing, I. *Z. Anorg. Allg. Chem.* **2013**, *639*, 714.
- (444) Kunitake, T.; Takarabe, K.; Tsugawa, S.-i. *Polymer J.* **1976**, *8*, 363.
- (445) Marchetti, F.; Pampaloni, G.; Zacchini, S. *Inorg. Chem.* **2008**, *47*, 365.
- (446) Kanazawa, A.; Kanaoka, S.; Aoshima, S. *Macromolecules* **2009**, *42*, 3965.
- (447) Hayatifar, M.; Marchetti, F.; Pampaloni, G.; Patil, Y.; Galletti, A. M. R. *Catal. Today* **2012**, *192*, 177.
- (448) Finze, M.; Bernhardt, E.; Berkei, M.; Willner, H.; Hung, J.; Waymouth, R. M. *Organometallics* **2005**, *24*, 5103.
- (449) Vagedes, D.; Erker, G.; Fröhlich, R. *J. Organomet. Chem.* **2002**, *641*, 148.
- (450) Henderson, L. D.; Piers, W. E.; Irvine, G. J.; McDonald, R. *Organometallics* **2002**, *21*, 340.
- (451) Davies, H. O.; Leedham, T. J.; Jones, A. C.; O'Brien, P.; White, A. J. P.; Williams, D. J. *Polyhedron* **1999**, *18*, 3165.
- (452) Boyle, T. J.; Tribby, L. J.; Alam, T. M.; Bunge, S. D.; Holland, G. P. *Polyhedron* **2005**, *24*, 1143.
- (453) Petrykin, V.; Kakihana, M.; Yoshioka, K.; Sasaki, S.; Ueda, Y.; Tomita, K.; Nakamura, Y.; Shiro, M.; Kudo, A. *Inorg. Chem.* **2006**, *45*, 9251.

- (454) Perić, B.; Brničević, N.; Jurić, M.; Planinić, P.; Matković-Čalogović, D. *Struct. Chem.* **2009**, *20*, 933.
- (455) Boyle, T. J.; Andrews, N. L.; Alam, T. M.; Rodriguez, M. A.; Santana, J. M.; Scott, B. L. *Polyhedron* **2002**, *21*, 2333.
- (456) Boyle, T. J.; Gallegos, J. J.; Pedrotty, D. M.; Mechenbier, E. R.; Scott, B. L. *J. Coord. Chem.* **1999**, *47*, 155.
- (457) Weinert, C. S.; Fanwick, P. E.; Rothwell, I. P. *Organometallics* **2005**, *24*, 5759.
- (458) Chang, H.-C.; Jiang, J.-C.; Hahndorf, I.; Lin, S. H.; Lee, Y. T.; Chang, H.-C. *J. Am. Chem. Soc.* **1999**, *121*, 4443.
- (459) Kimura, K.; Kubo, M. *J. Chem. Phys.* **1959**, *30*, 151.
- (460) Kolesnikov, S. P.; Lyudkovskaya, I. V.; Antipin, M. Y.; Struchkov, Y. T.; Nefedov, O. M. *Bull. Acad. Sci. USSR, Div. Chem. Sci.* **1985**, *34*, 74.
- (461) Castelvetro, V.; Bontà Pittaluga, G.; Ciardelli, F. *Macromol. Chem. Phys.* **2001**, *202*, 2093.
- (462) Rahman, M. S.; Hashimoto, T.; Kodaira, T. *J. Polym. Sci. Part A: Polym. Chem.* **2000**, *38*, 4362.
- (463) Zhang, X.; Goethals, E. J.; Loontjens, T.; Derks, F. *Macromol. Rapid Commun.* **2000**, *21*, 472.
- (464) Ouchi, M.; Sueoka, M.; Kamigaito, M.; Sawamoto, M. *J. Polym. Sci. Part A: Polym. Chem.* **2001**, *39*, 1067.
- (465) Ohgi, H.; Sato, T. *Macromolecules* **1999**, *32*, 2403.
- (466) Dainton, F. S.; Ivin, K. J. *Nature* **1948**, *162*, 705.
- (467) Sanli, O.; Pulat, E. *Commun. Ser. B: Chem. Chem. Eng.* **1981**, *27*, 190-197.
- (468) Matsuguma, Y.; Kunitake, T. *Polymer J.* **1971**, *2*, 353.
- (469) Banerjee, S.; Paira, T. K.; Mandal, T. K. *Macromol. Chem. Phys.* **2013**, *214*, 1332.
- (470) Koroskenyi, B.; Wang, L.; Faust, R. *Macromolecules* **1997**, *30*, 7667.
- (471) Brownstein, S.; Bywater, S.; Worsfold, D. J. *Macromol. Chem. Phys.* **1961**, *48*, 127.
- (472) Toman, L.; Pokorný, S.; Spěváček, J. *J. Polym. Sci. Part A: Polym. Chem.* **1989**, *27*, 2217.
- (473) Higashimura, T.; Ishihama, Y.; Sawamoto, M. *Macromolecules* **1993**, *26*, 744.
- (474) Lin, C. H.; Xiang, J. S.; Matyjaszewski, K. *Macromolecules* **1993**, *26*, 2785.
- (475) Frolov, A. N.; Kostjuk, S. V.; Vasilenko, I. V.; Kaputsky, F. N. *J. Polym. Sci. Part A: Polym. Chem.* **2010**, *48*, 3736.
- (476) Ouardad, S.; Deffieux, A.; Peruch, F. *Pure Appl. Chem.* **2012**, *84*, 2065.
- (477) Rozentsvet, V. A.; Kozlov, V. G.; Korovina, N. A.; Stotskaya, O. A.; Gnezdilov, O. I.; Kostjuk, S. V. *Macromol. Chem. Phys.* **2016**, *217*, 1860.
- (478) Ouardad, S.; Bakleh, M.-E.; Kostjuk, S. V.; Ganachaud, F.; Puskas, J. E.; Deffieux, A.; Peruch, F. *Polymer Int.* **2012**, *61*, 149.
- (479) Rozentsvet, V. A.; Kozlov, V. G.; Ziganshina, E. F.; Boreiko, N. P.; Kostjuk, S. V. *Polymer Int.* **2013**, *62*, 817.
- (480) Rozentsvet, V. A.; Korovina, N. A.; Stotskaya, O. A.; Kuznetsova, M. G.; Peruch, F.; Kostjuk, S. V. *J. Polym. Sci. Part A: Polym. Chem.* **2016**, *54*, 2430.
- (481) Rozentsvet, V. A.; Kozlov, V. G.; Ziganshina, E. F.; Boreiko, N. P.; Khachaturov, A. S. *Russ. J. Appl. Chem.* **2009**, *82*, 148.
- (482) Rozentsvet, V. A.; Kozlov, V. G.; Ziganshina, E. F.; Boreiko, N. P. *J. Polym. Sci. A* **2008**, *50*, 1038.

- (483) Puskas, J. E.; Peres, C.; Peruch, F.; Deffieux, A.; Dabney, D. E.; Wesdemiotis, C.; Hayat-Soytaş, S.; Lindsay, A. *J. Polym.Sci. Part A: Polym. Chem.* **2009**, *47*, 2181.
- (484) Puskas, J. E.; Peruch, F.; Deffieux, A.; Dabney, D. E.; Wesdemiotis, C.; Li, H.; Lindsay, A. *J. Polym.Sci. Part A: Polym. Chem.* **2009**, *47*, 2172.
- (485) Hasegawa, K.-i.; Asami, R.; Higashimura, T. *Macromolecules* **1977**, *10*, 585.
- (486) Lübbecke, H.; Boldt, P. *Tetrahedron* **1978**, *34*, 1577.
- (487) McManus, N. T.; Penlidis, A. *J. Appl. Polym. Sci.* **1998**, *70*, 1253.
- (488) Jackson, C.; Chen, Y.-J.; Mays, J. W. *J. Appl. Polym. Sci.* **1996**, *61*, 865.
- (489) Himmel, D.; Radtke, V.; Butschke, B.; Krossing, I. *Angew. Chem. Int. Ed.* **2018**, *10.1002/anie.201709057*.

## Appendices

### Appendix A

#### A.1 Supplementary Spectra for Chapter 2

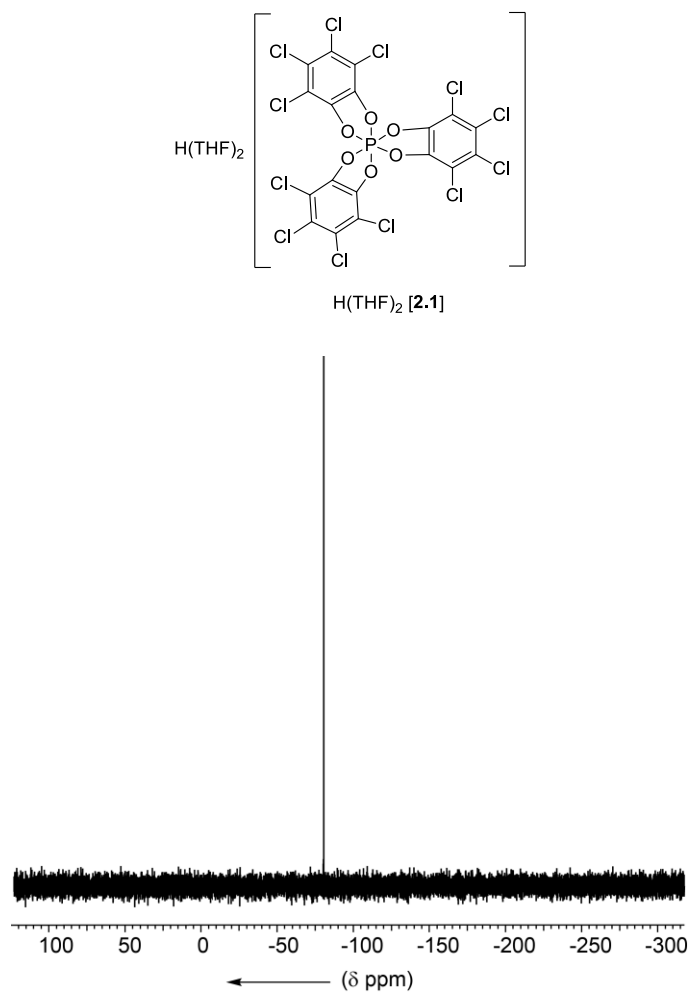
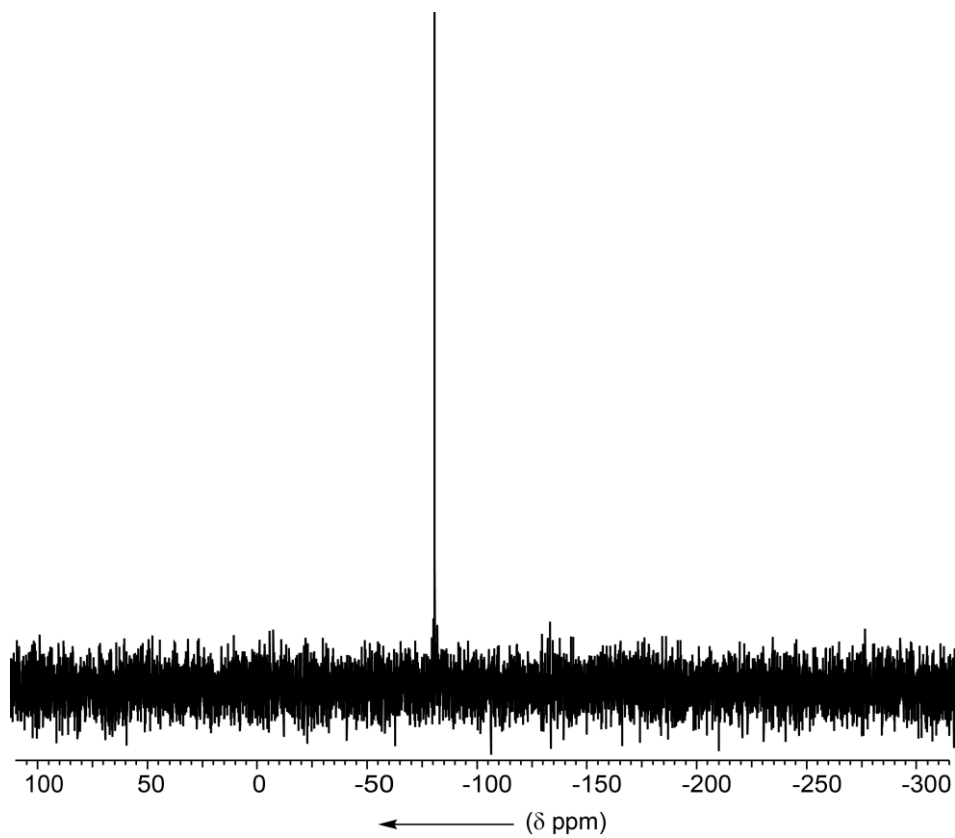
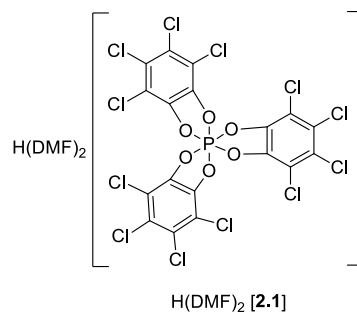


Figure A.1.  $^{31}\text{P}\{^1\text{H}\}$  NMR (121 MHz,  $\text{CD}_3\text{CN}$ , 25 °C) spectrum of  $\text{H(THF)}_2$ [2.1].



**Figure A.2.**  $^{31}\text{P}\{^1\text{H}\}$  NMR (121 MHz,  $\text{CD}_3\text{CN}$ , 25 °C) spectrum of  $\text{H(DMF)}_2[2.1]$ .

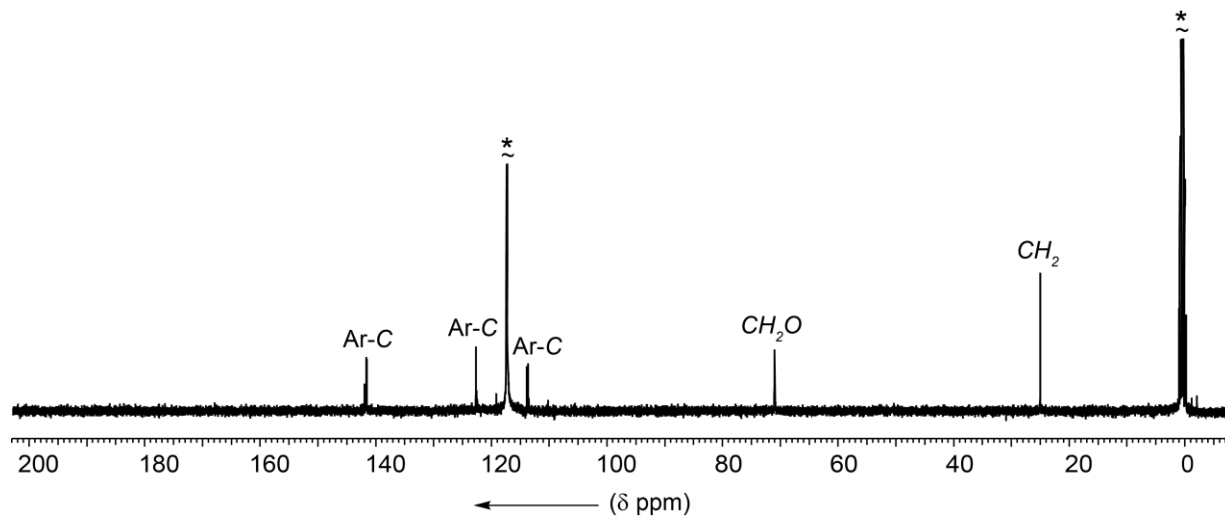
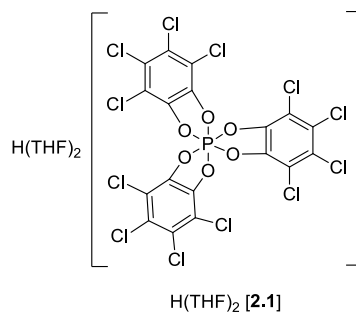


Figure A.3.  $^{13}\text{C}\{^1\text{H}\}$  NMR (75 MHz,  $\text{CD}_3\text{CN}$ , 25 °C) spectrum of  $\text{H}(\text{THF})_2[2.1]$ .

(\* indicates  $\text{CH}_3\text{CN}-d_3$  solvent.

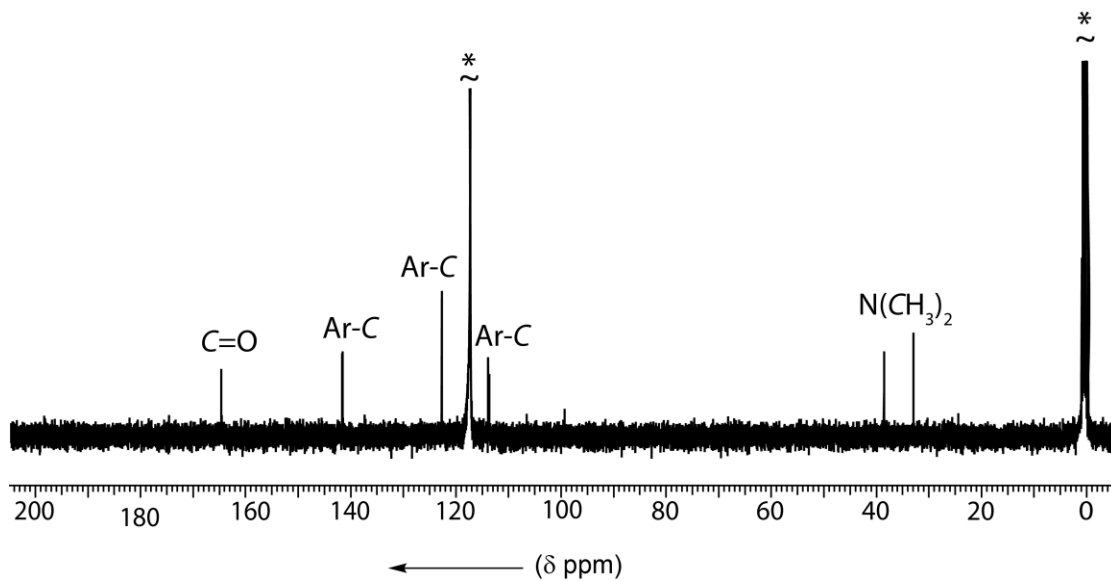
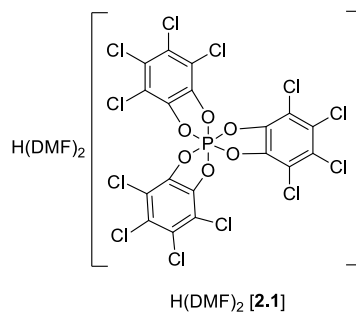


Figure A.4. <sup>13</sup>C{<sup>1</sup>H} NMR (75 MHz, CD<sub>3</sub>CN, 25 °C) spectrum of H(DMF)<sub>2</sub>[2.1].

(\* ) indicates CH<sub>3</sub>CN-*d*<sub>3</sub> solvent.

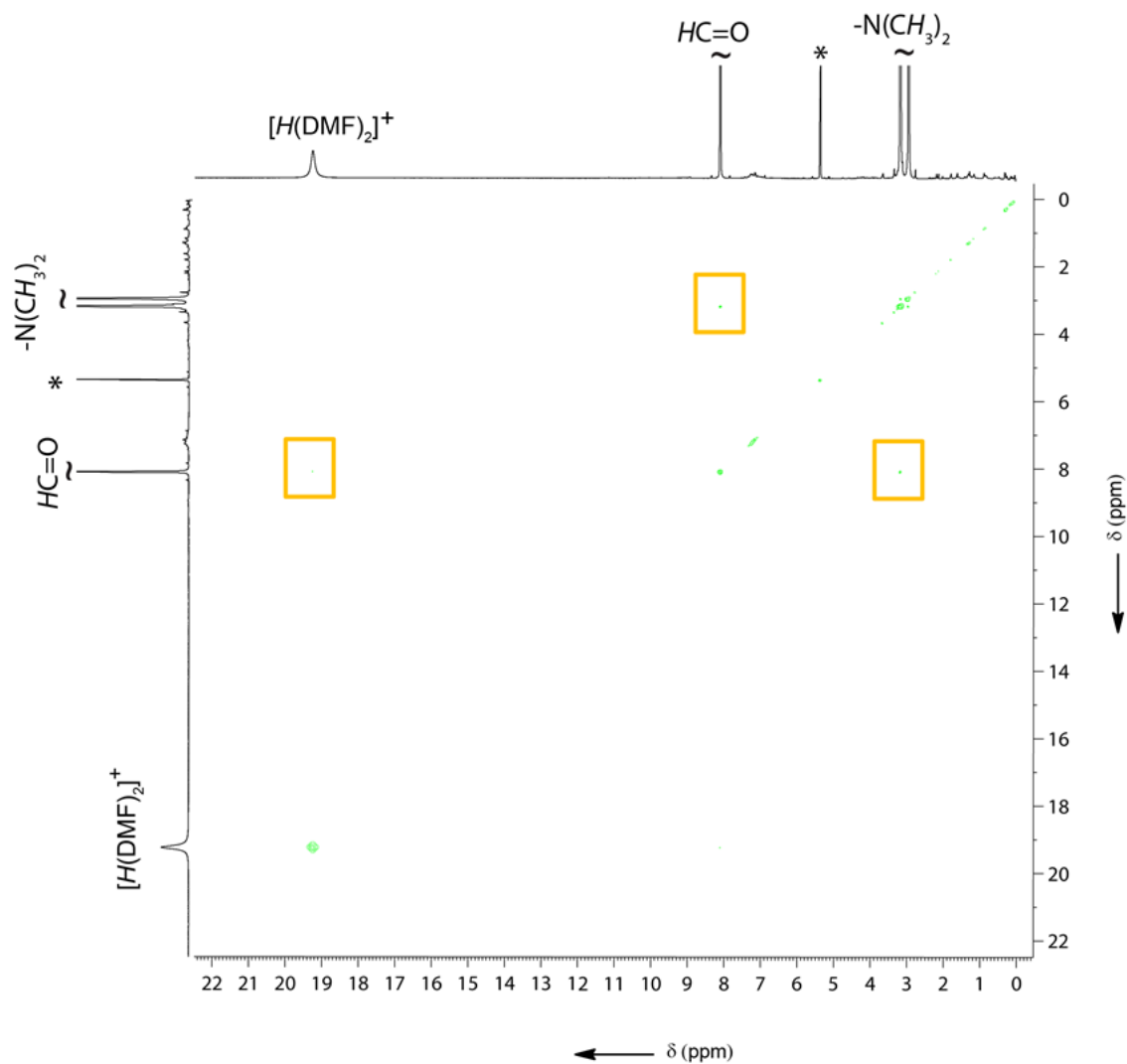
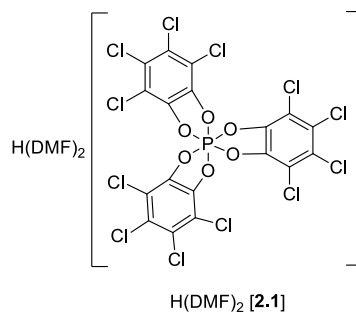


Figure A.5. <sup>1</sup>H-<sup>1</sup>H NOESY (400 MHz, CD<sub>2</sub>Cl<sub>2</sub>, -85 °C) spectrum of H(DMF)<sub>2</sub>[2.1].

\* indicates residual CHDCl<sub>2</sub> solvent.

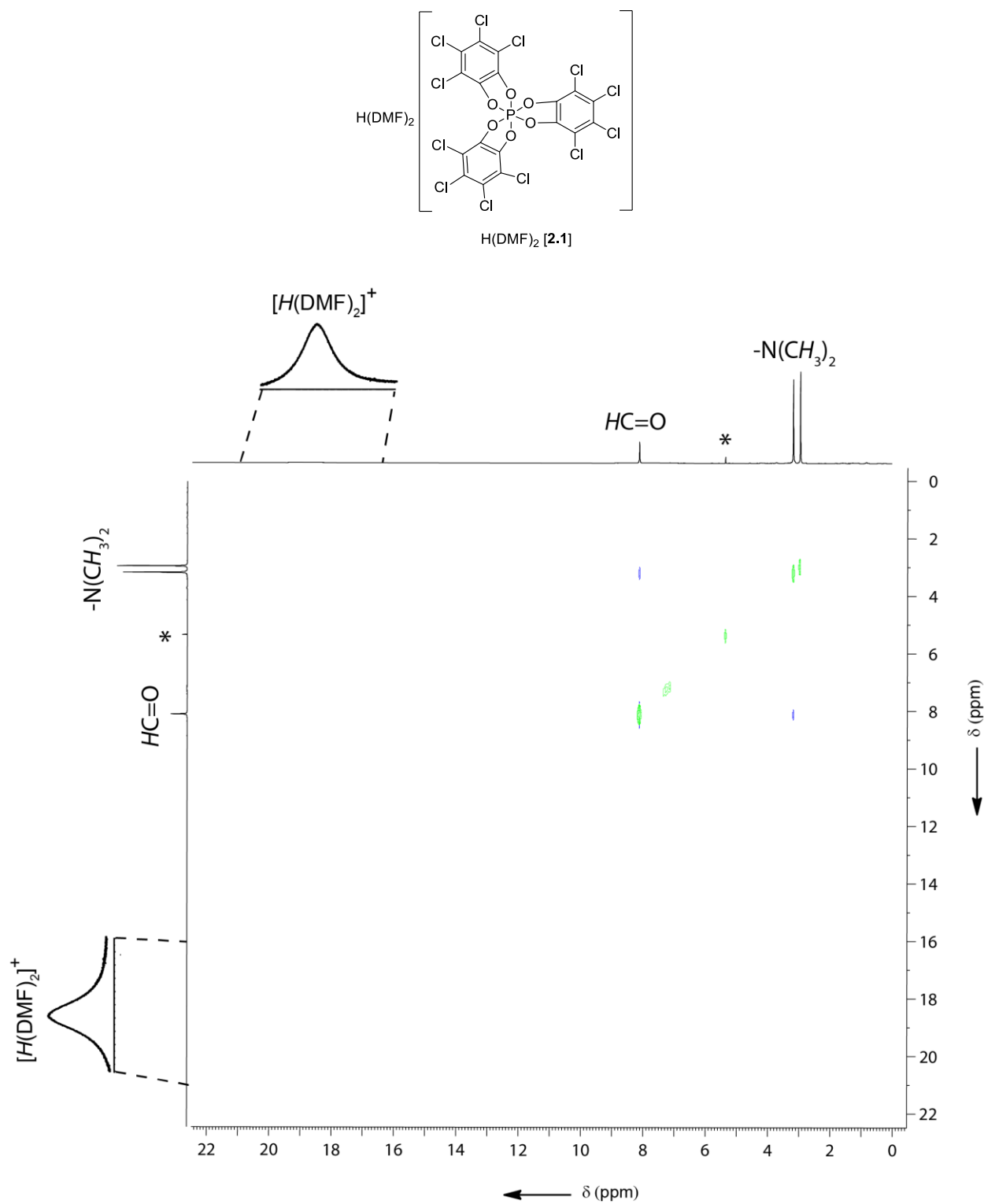


Figure A.6.  $^1\text{H}$ - $^1\text{H}$  ROESY (400 MHz,  $\text{CD}_2\text{Cl}_2$ ,  $-85^\circ\text{C}$ ) spectrum of  $\text{H(DMF)}_2$ [2.1].

\* indicates residual  $\text{CH}_2\text{Cl}_2$  solvent.

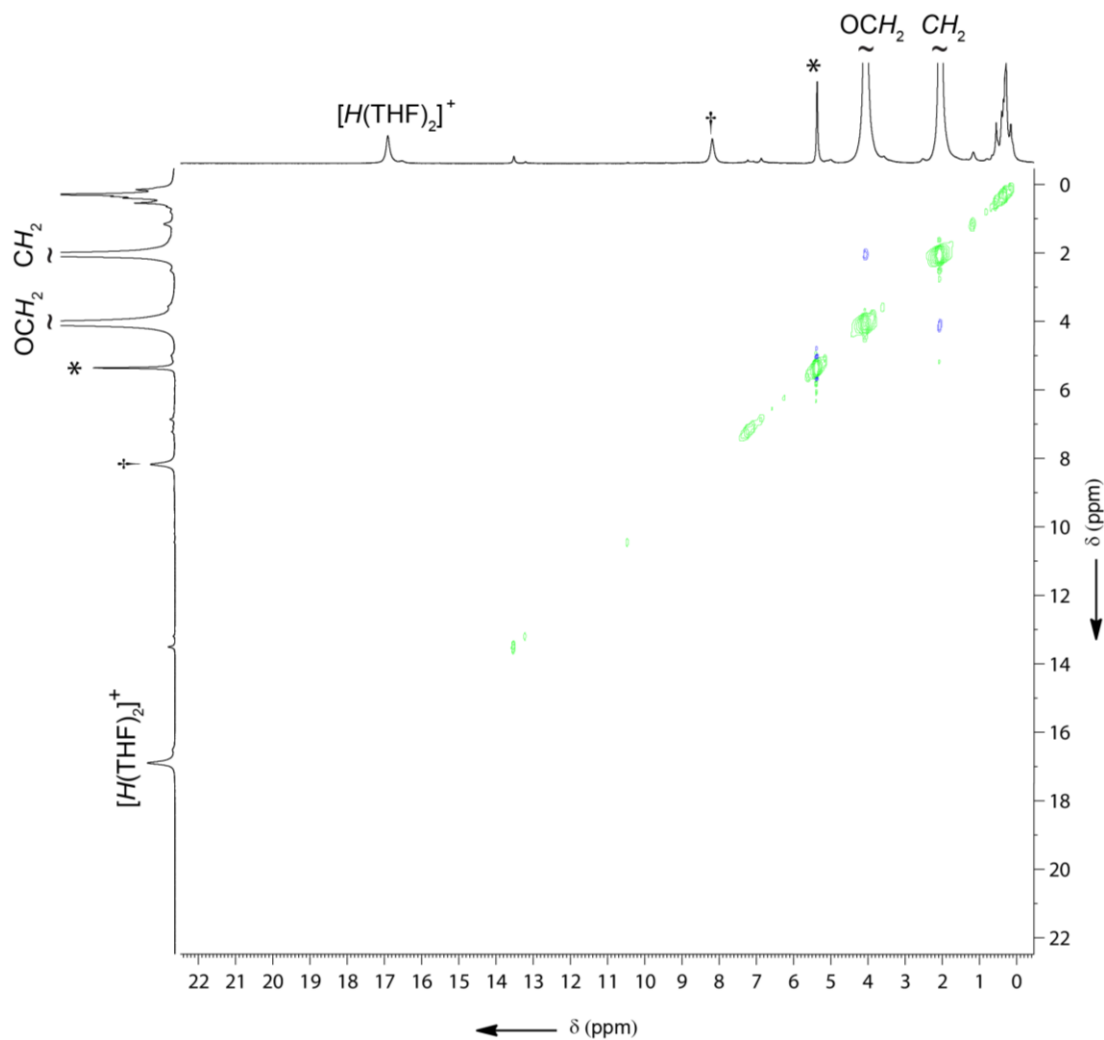
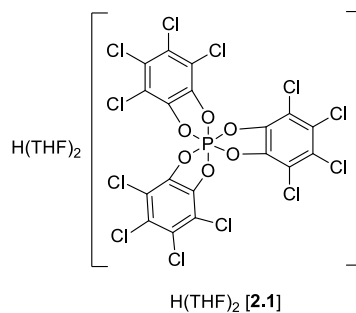


Figure A.7. <sup>1</sup>H-<sup>1</sup>H ROESY (400 MHz, CD<sub>2</sub>Cl<sub>2</sub>, -85 °C) spectrum of H(THF)<sub>2</sub>[2.1].

\* indicates residual CHDCl<sub>2</sub>. † indicates residual toluene solvent.

## Appendix B

### B.1 Supplementary Spectra for Chapter 3

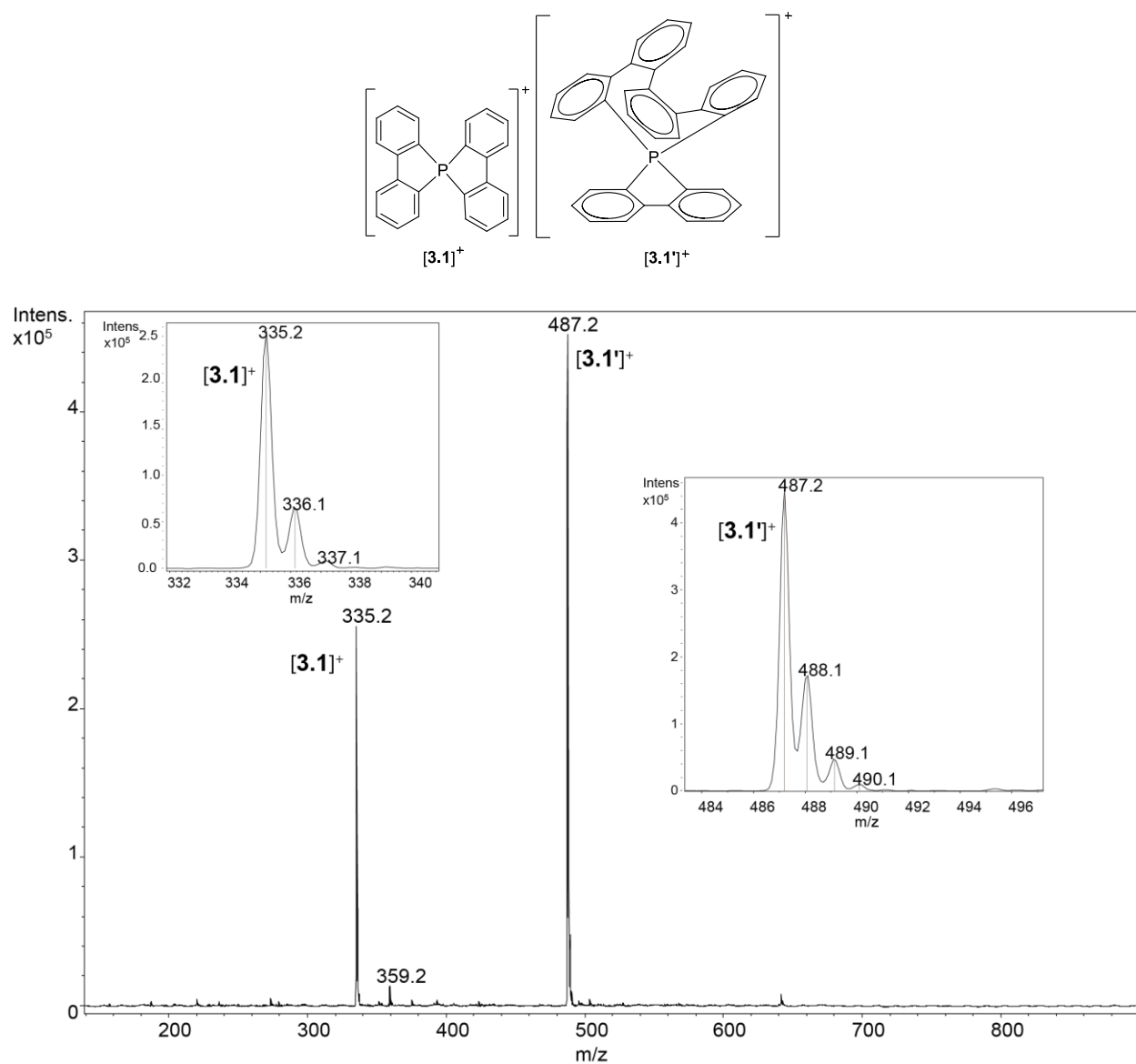


Figure B.1. LRMS (ESI; positive mode) mass spectrum of  $[3.1]^+$  and  $[3.1']^+$  via Route A.

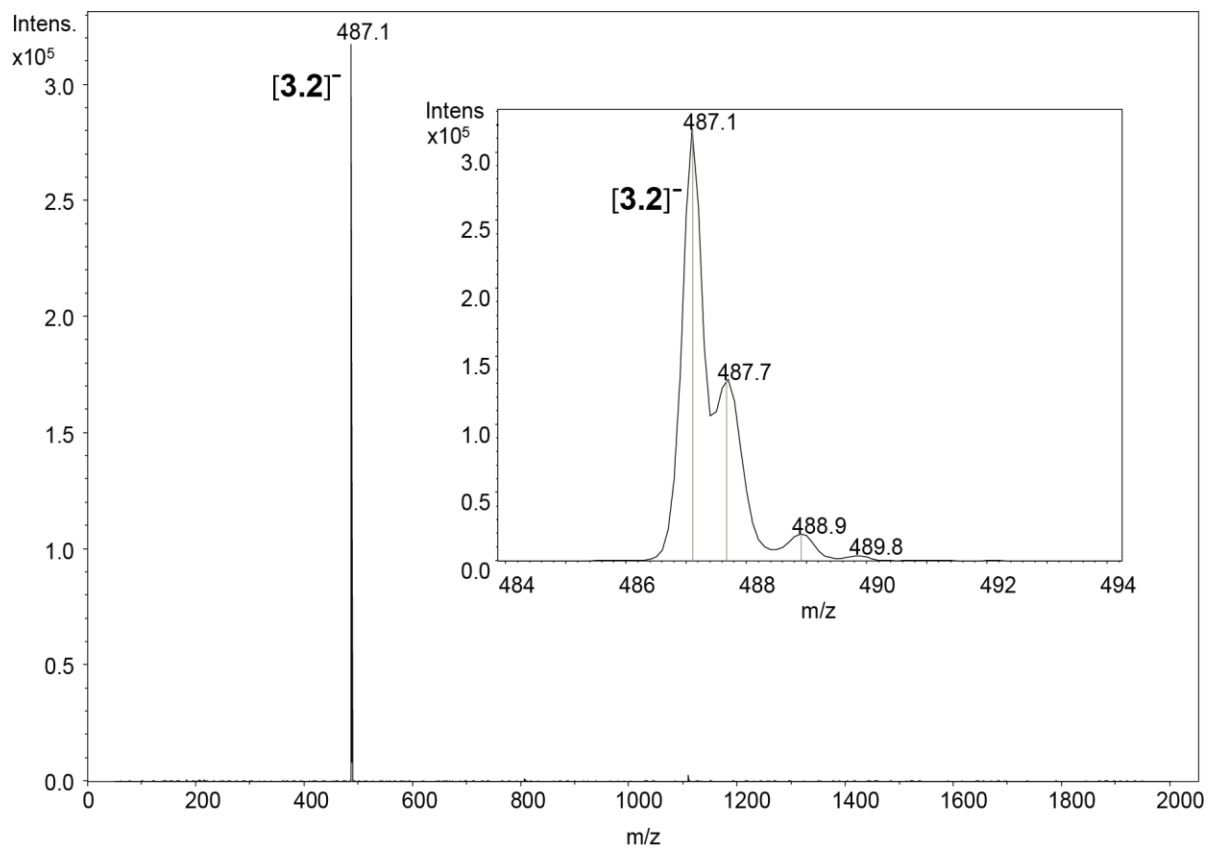
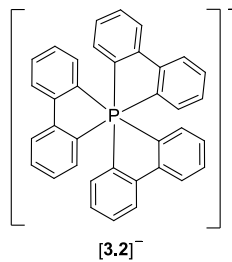
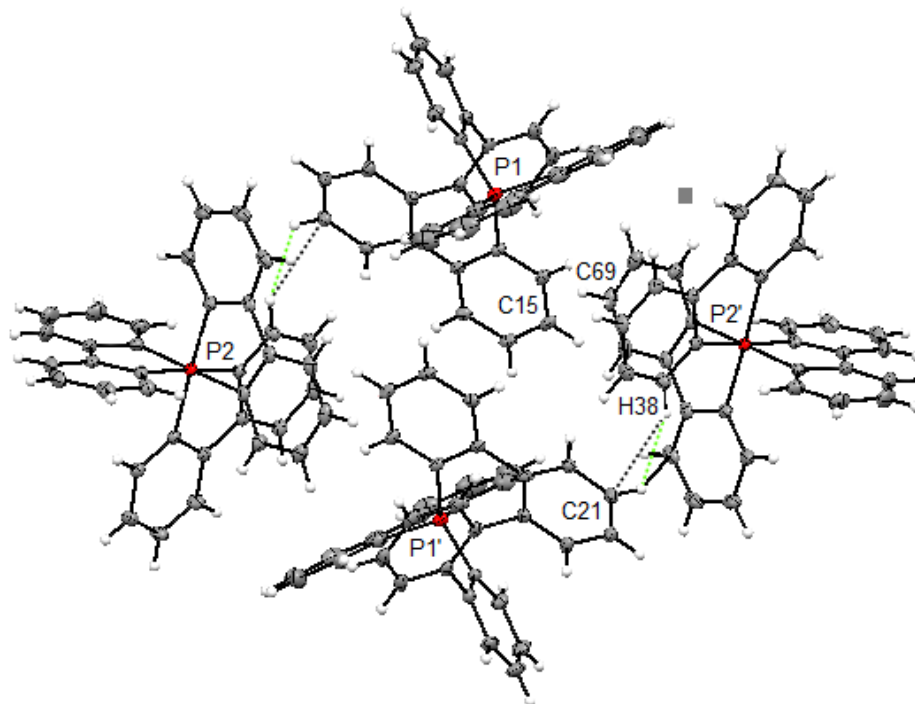


Figure B.2. LRMS (ESI; negative mode) mass spectrum of [3.2]⁻ via Route A .



**Figure B.3.** Crystal packing of the molecular structure of [3.1'] [3.2] is shown with 2 unit cells along the b axis (x,y,z). Solvent molecules have been omitted for clarity. Ellipsoids are drawn at the 50 % probability level. Dashed bonds represent H-bond interactions (green = H···H interaction and black = C···H interaction).  
**Black = carbon atom, red = phosphorus atom and white = hydrogen atom.**

## Appendix C

### C.1 Supplementary Spectra for Chapter 4

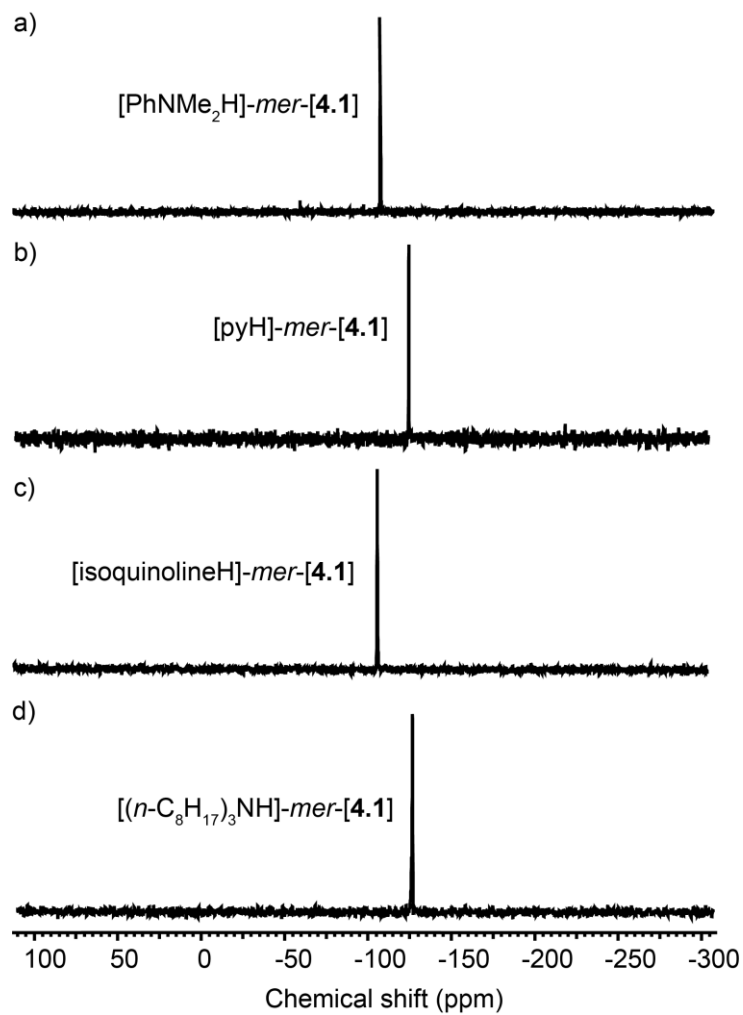


Figure C.1.  $^{31}\text{P}\{^1\text{H}\}$  NMR (162 MHz,  $(\text{CD}_3)_2\text{CO}$ , 25 °C) spectra of: a)  $[\text{PhNMe}_2\text{H}]\text{-mer-[4.1]}$ , b)  $[\text{pyH}]\text{-mer-[4.1]}$ , c)  $[\text{isoquinolineH}]\text{-mer-[4.1]}$ , and d)  $[(n\text{-C}_8\text{H}_{17})_3\text{NH}]\text{-mer-[4.1]}$ .

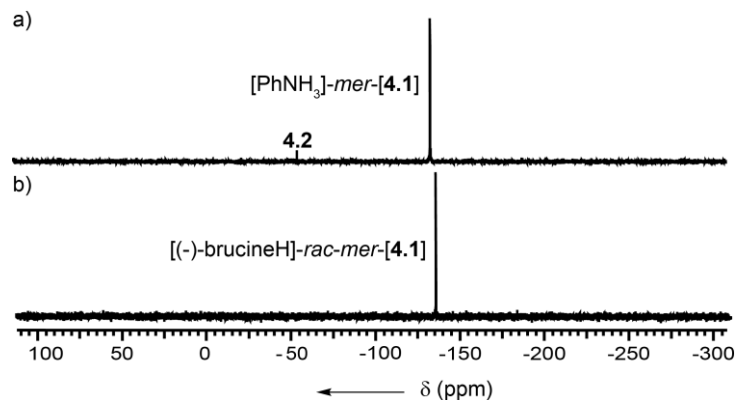


Figure C.2.  $^{31}\text{P}\{^1\text{H}\}$  NMR (162 MHz,  $(\text{CD}_3)_2\text{SO}$ , 25 °C) spectra of a)  $[\text{PhNH}_3]\text{-mer-[4.1]}$  and b)  $[(-)\text{-brucineH}]\text{-rac-mer-[4.1]}$ . 4.2 is phosphorane  $\text{P}(\text{C}_6\text{H}_4\text{CO}_2)_2(\text{C}_6\text{H}_4\text{COOH})$ .

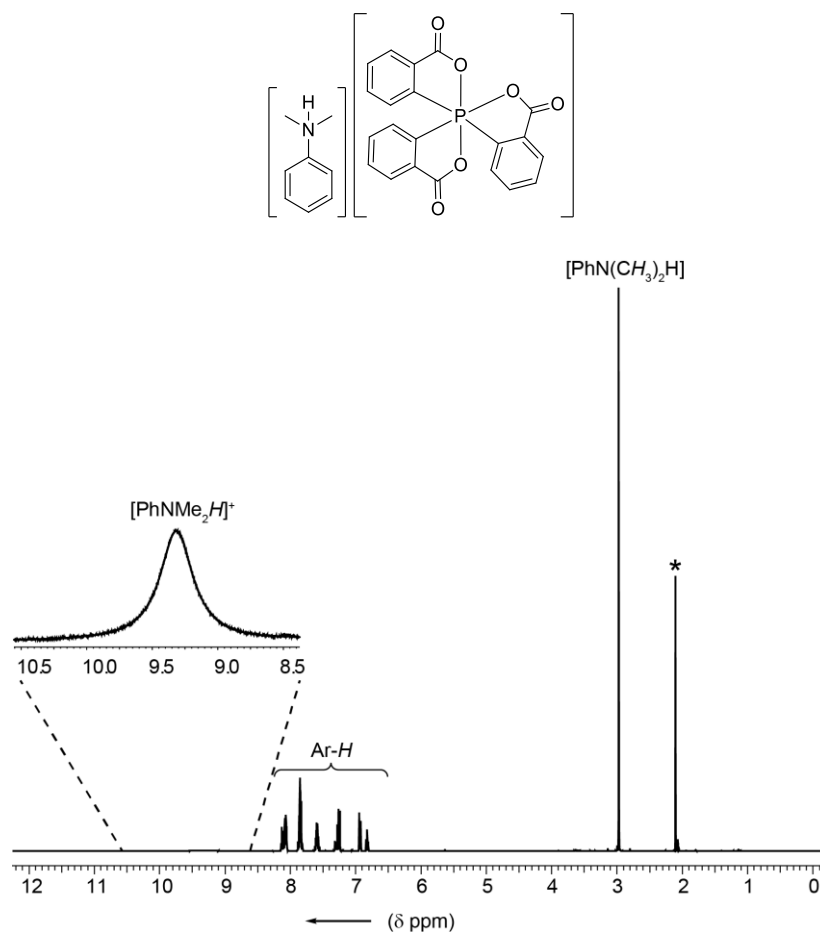


Figure C.3.  $^1\text{H}$  NMR (400 MHz,  $(\text{CD}_3)_2\text{CO}$ , 25 °C) spectrum of  $[\text{PhNMe}_2\text{H}]\text{-mer-[4.1]}$ .

\* indicates residual  $(\text{CHD}_2)(\text{CD}_3)\text{CO}$  solvent.

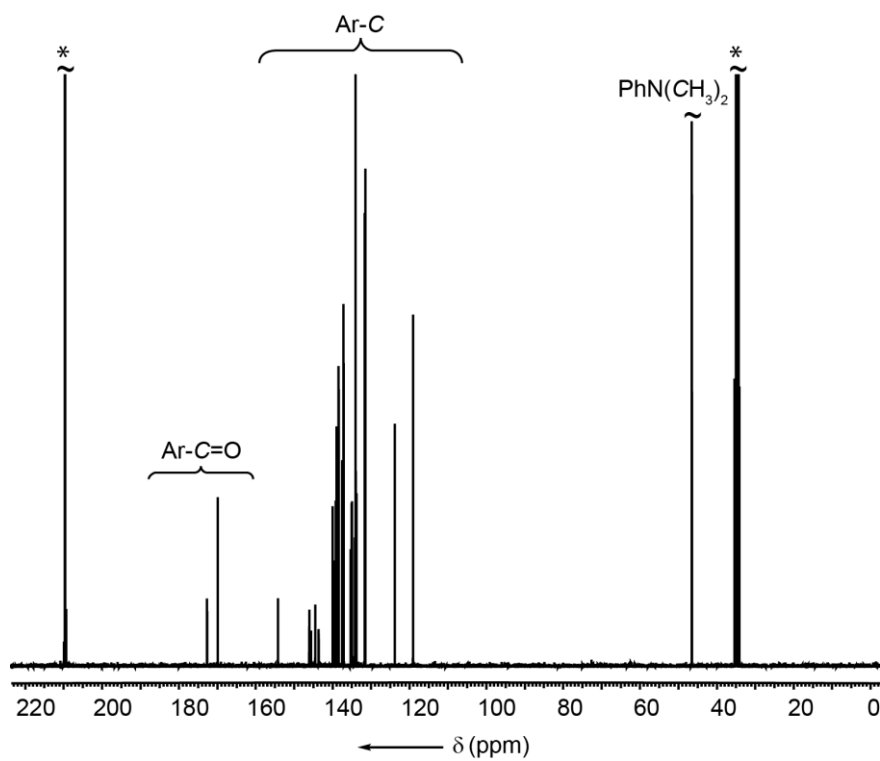


Figure C.4.  $^{13}\text{C}\{^1\text{H}\}$  NMR (101 MHz,  $(\text{CD}_3)_2\text{CO}$ , 25 °C) spectrum of  $[\text{PhNMe}_2\text{H}]\text{-mer-[4.1]}$ .

\* indicates  $(\text{CH}_3)_2\text{CO-}d_6$  solvent.

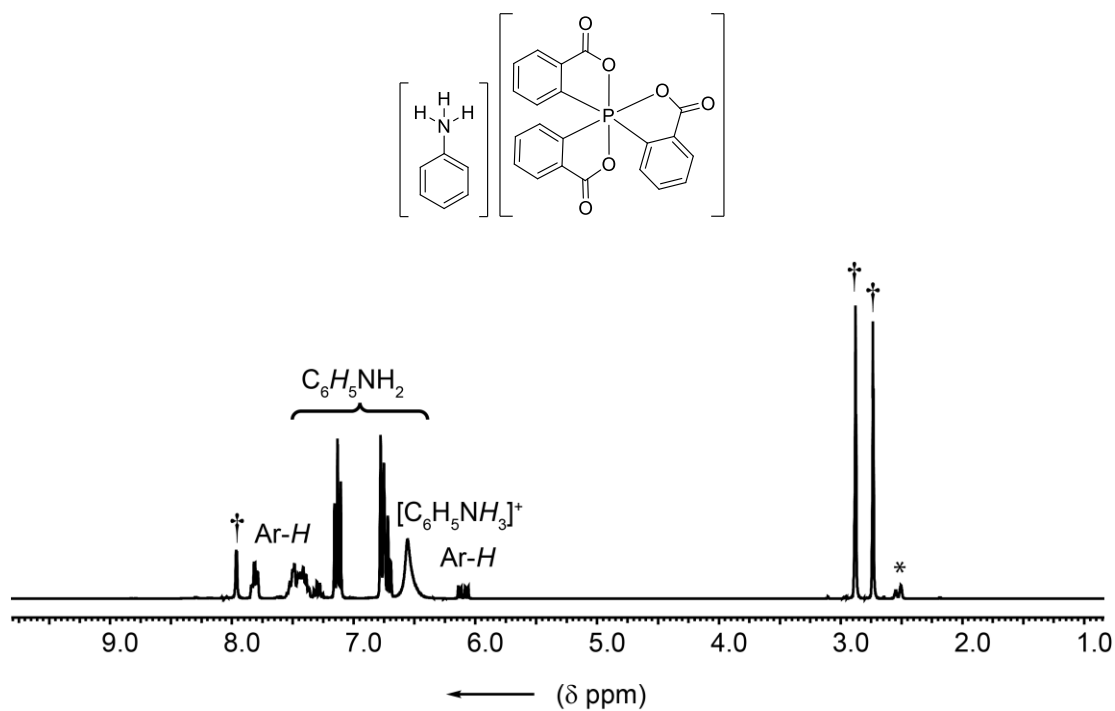


Figure C.5. <sup>1</sup>H NMR (400 MHz, (CD<sub>3</sub>)<sub>2</sub>SO, 25 °C) spectrum of [PhNH<sub>3</sub>]-mer-[4.1].

\* indicates residual (CHD<sub>2</sub>)(CD<sub>3</sub>)SO solvent. † indicates residual dimethylformamide solvent.

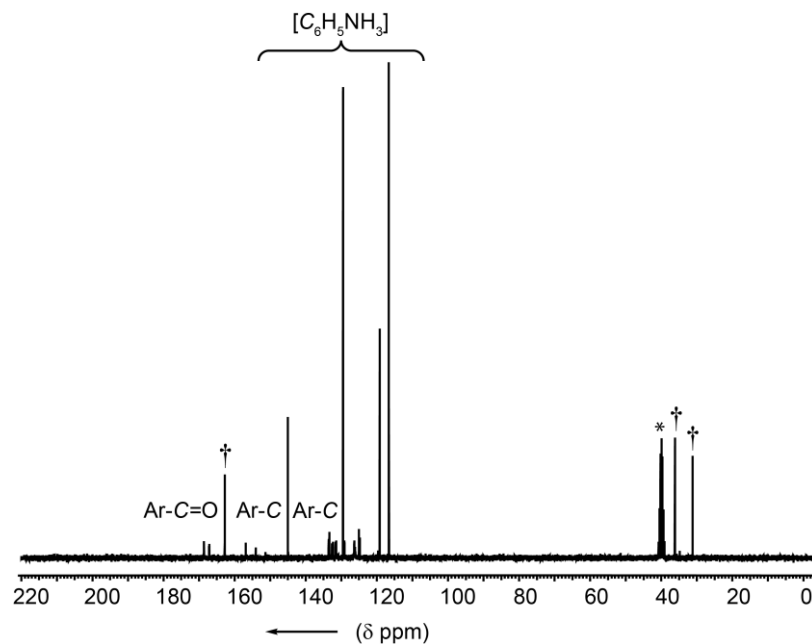
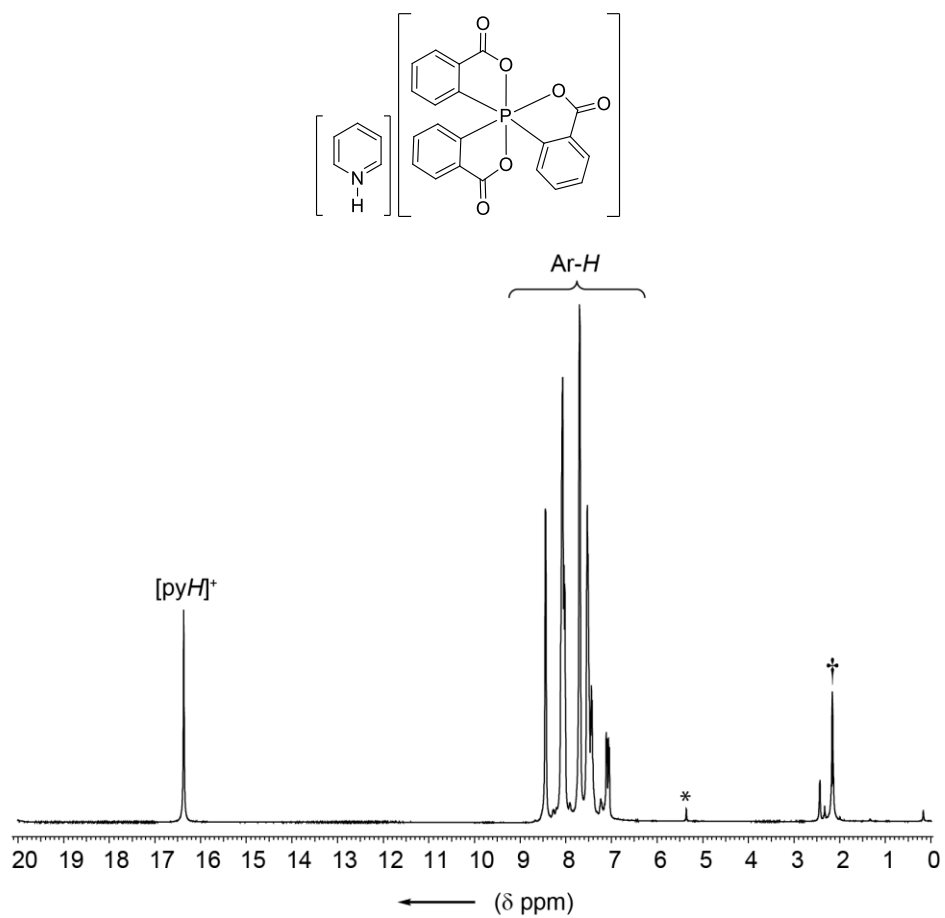


Figure C.6. <sup>13</sup>C{<sup>1</sup>H} NMR (101 MHz, (CD<sub>3</sub>)<sub>2</sub>SO, 25 °C) spectrum of [PhNH<sub>3</sub>]-mer-[4.1].

\* indicates (CH<sub>3</sub>)<sub>2</sub>SO-*d*<sub>6</sub> solvent. † indicates residual dimethylformamide solvent.



**Figure C.7.**  $^1\text{H}$  NMR (400 MHz,  $\text{CD}_2\text{Cl}_2$ , 25 °C) spectrum of  $[\text{pyH}]\text{-mer-[4.1]}$ .

$*$  indicates residual  $\text{CH}_2\text{Cl}_2$  solvent.  $\dagger$  indicates residual acetone solvent.

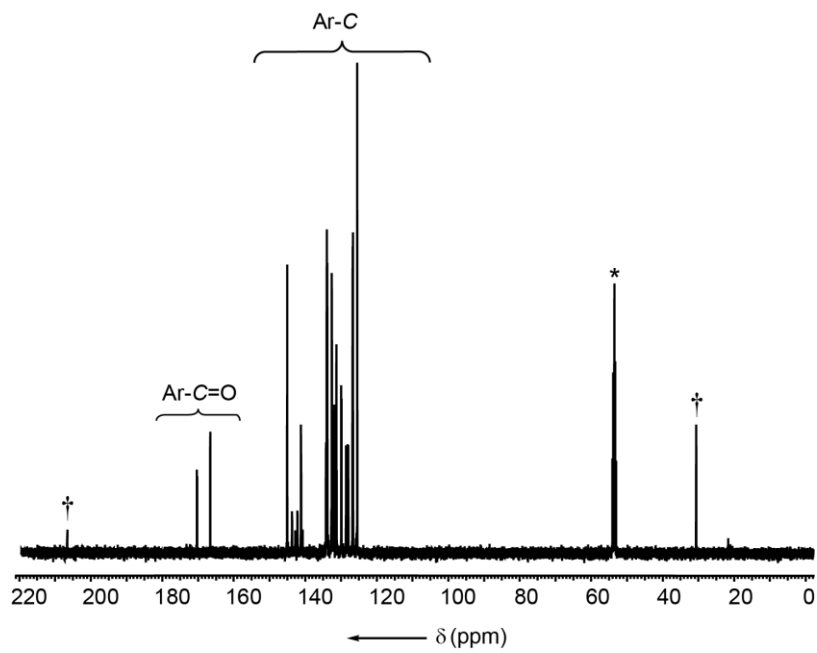


Figure C.8.  $^{13}\text{C}\{^1\text{H}\}$  NMR (101 MHz,  $\text{CD}_2\text{Cl}_2$ , 25 °C) spectrum of [pyH]-mer-[4.1].

\* indicates  $\text{CH}_2\text{Cl}_2\text{-}d_2$  solvent. † indicates residual acetone solvent.

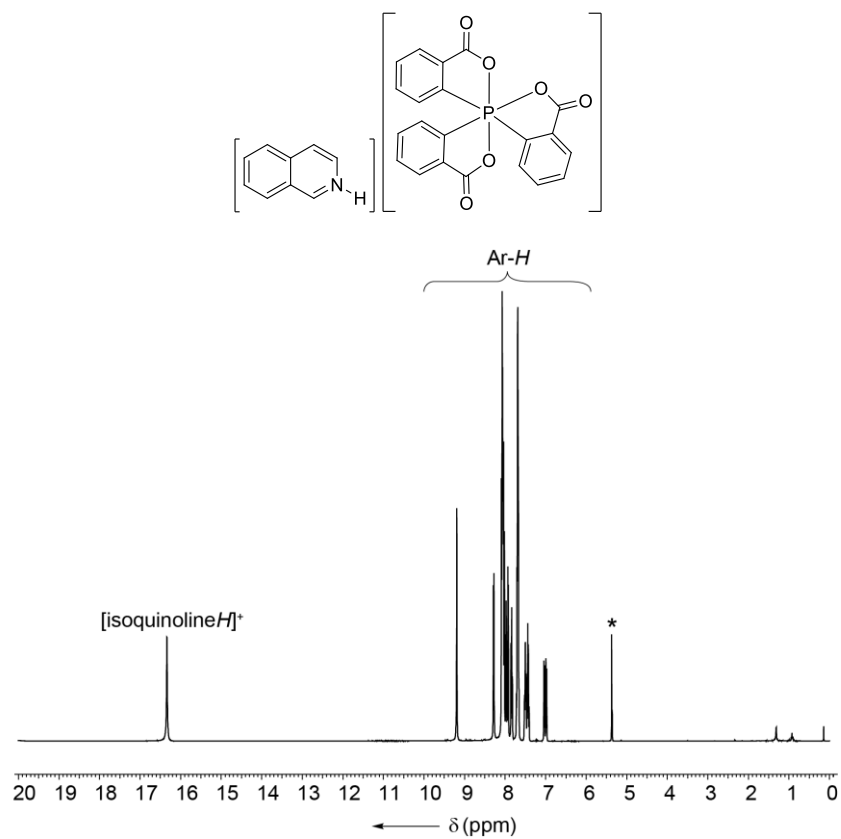


Figure C.9.  $^1\text{H}$  NMR (400 MHz,  $\text{CD}_2\text{Cl}_2$ , 25 °C) spectrum of [isoquinolineH]-mer-[4.1].

\* indicates residual  $\text{CH}_2\text{Cl}_2$  solvent.

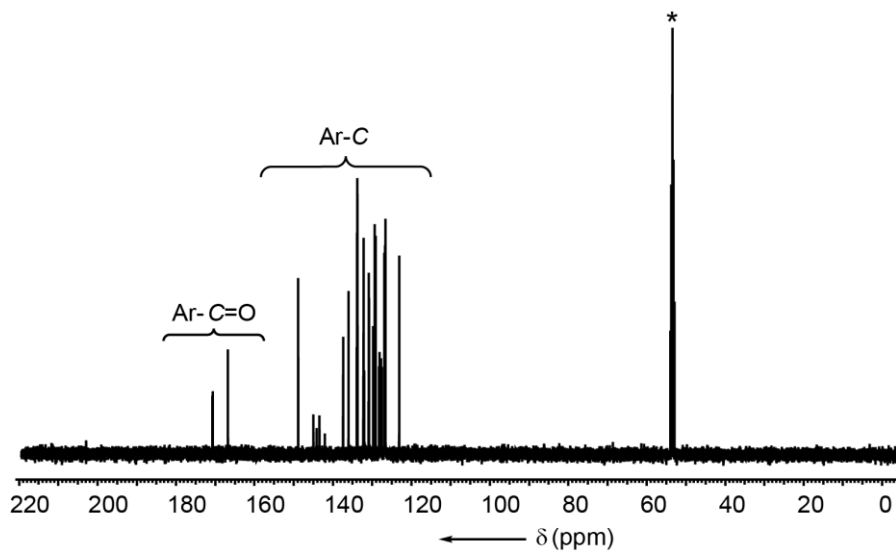


Figure C.10.  $^{13}\text{C}\{^1\text{H}\}$  NMR (101 MHz,  $\text{CD}_2\text{Cl}_2$ , 25 °C) spectrum of [isoquinolineH]-mer-[4.1].

\* indicates  $\text{CH}_2\text{Cl}_2-d_2$  solvent.

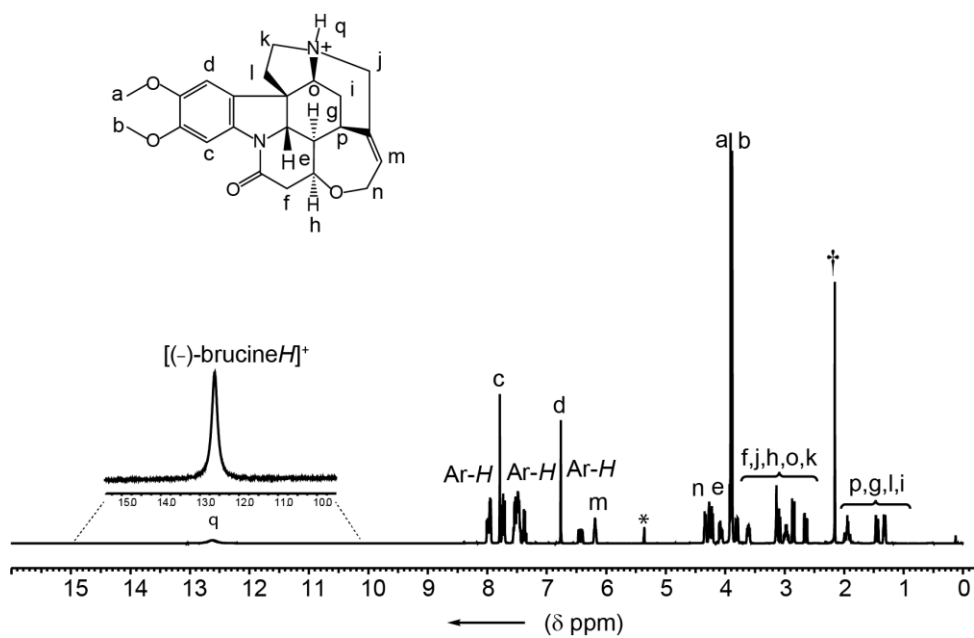
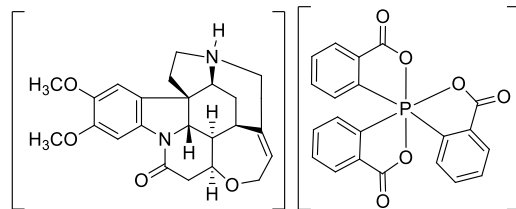
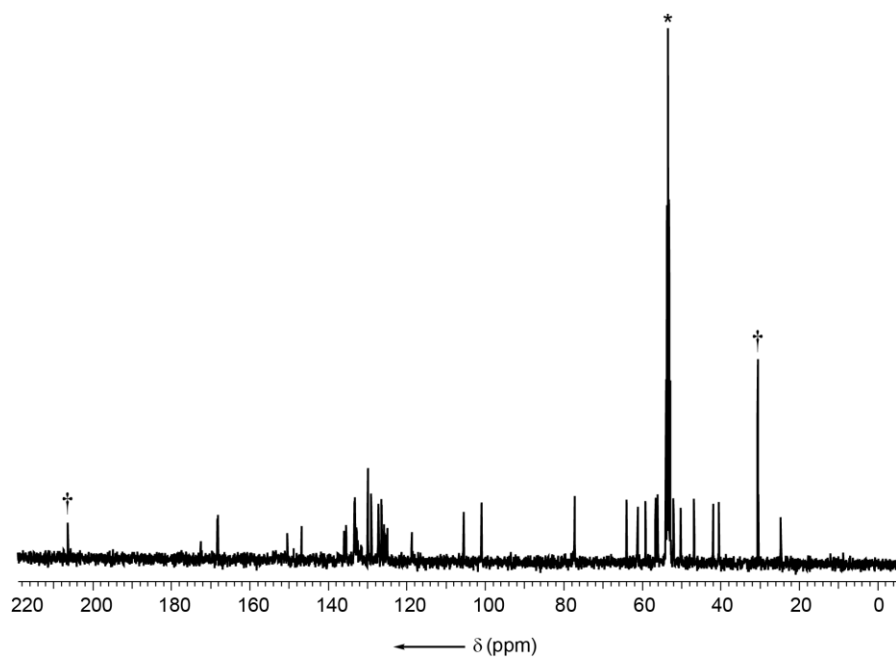


Figure C.11.  $^1\text{H}$  NMR (400 MHz,  $\text{CD}_2\text{Cl}_2$ , 25  $^\circ\text{C}$ ) spectrum of [(-)-brucineH] $^+$ - $\Lambda$ -mer-[4.1].

\* indicates residual  $\text{CH}_2\text{Cl}_2$  solvent. † indicates residual acetone solvent.



**Figure C.12.**  $^{13}\text{C}\{^1\text{H}\}$  NMR (101 MHz,  $\text{CD}_2\text{Cl}_2$ , 25 °C) spectrum of  $[(-)\text{-brucineH}]\text{-A-mer-[4.1]}$ .

\* indicates  $\text{CH}_2\text{Cl}_2\text{-}d_2$  solvent. † indicates residual acetone solvent.

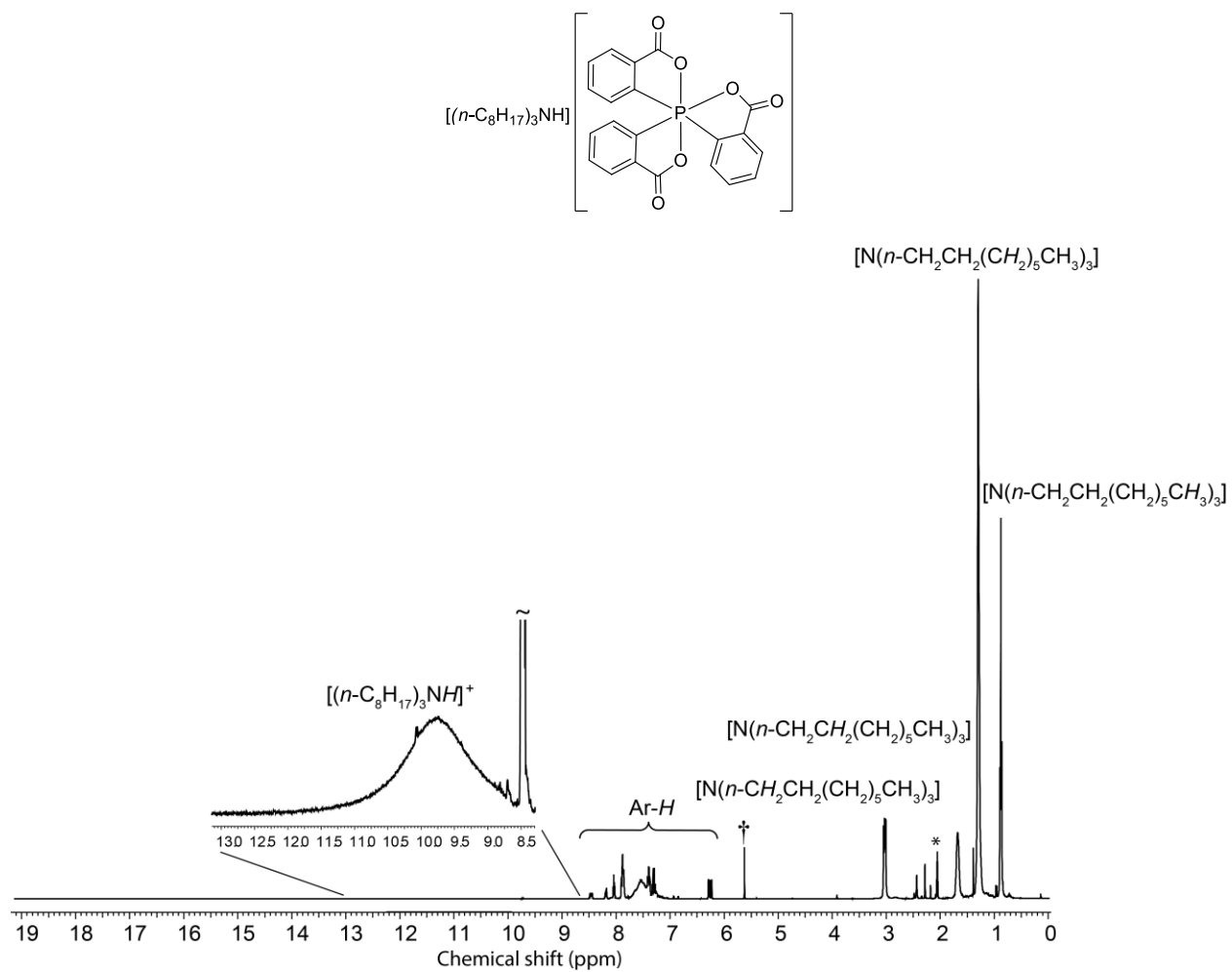


Figure C.13. <sup>1</sup>H NMR (400 MHz, (CD<sub>3</sub>)<sub>2</sub>CO, 25 °C) spectrum of [(n-C<sub>8</sub>H<sub>17</sub>)<sub>3</sub>NH]-mer-[4.1].

\* indicates residual (CHD<sub>2</sub>)(CD<sub>3</sub>)CO solvent. † indicates CH<sub>2</sub>Cl<sub>2</sub> solvent.

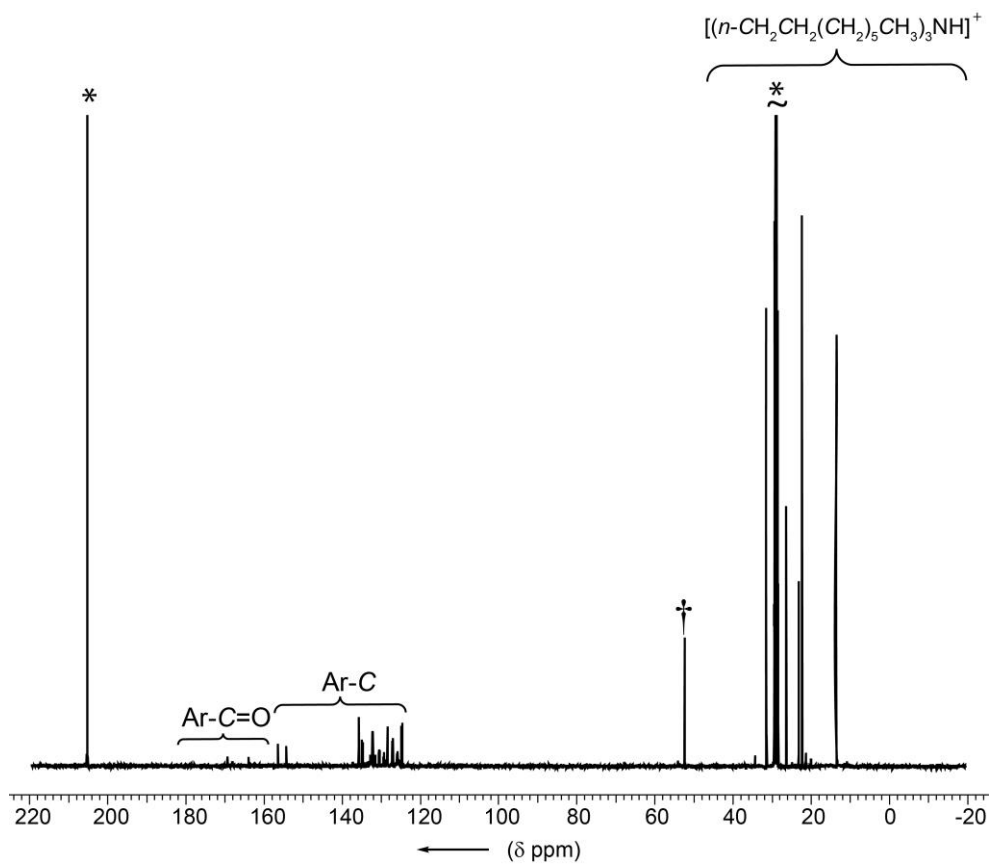


Figure C.14.  $^{13}\text{C}\{^1\text{H}\}$  NMR (101 MHz,  $(\text{CD}_3)_2\text{CO}$ , 25 °C) spectrum of  $[(n\text{-C}_8\text{H}_{17})_3\text{NH}]\text{-mer-[4.1]}$ .

\* indicates  $(\text{CH}_3)_2\text{CO-}d_6$  solvent. † indicates  $\text{CH}_2\text{Cl}_2$  solvent.

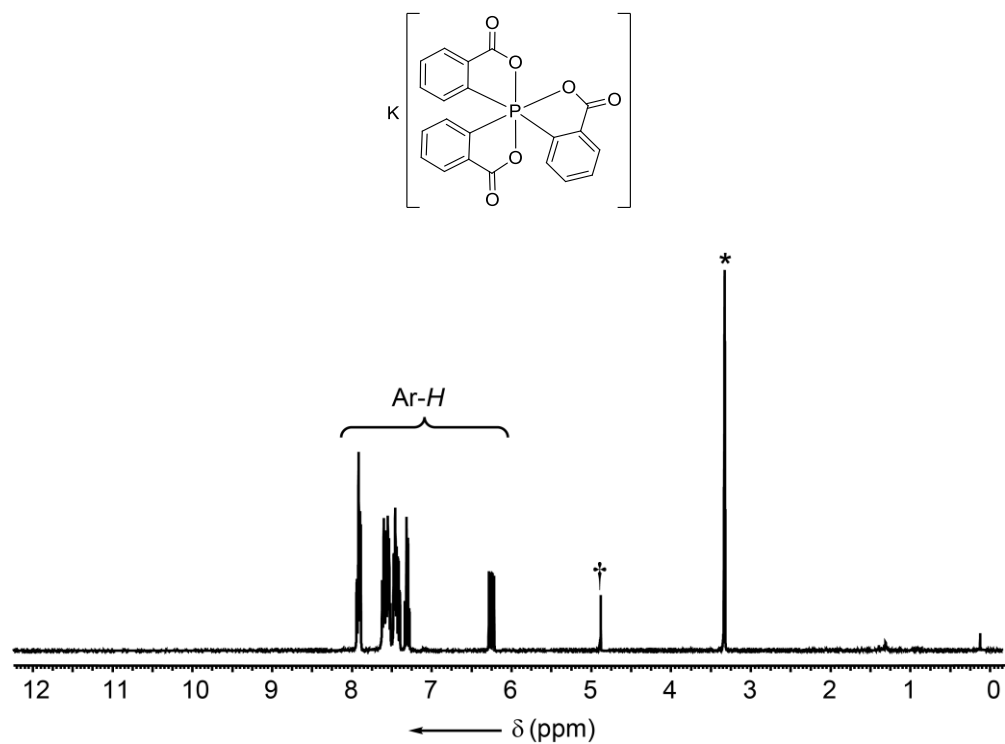


Figure C.15. <sup>1</sup>H NMR (400 MHz, CD<sub>3</sub>OD, 25 °C) spectrum of K-mer-[4.1].

\* indicates residual CHD<sub>2</sub>OD solvent. † indicates residual CH<sub>2</sub>Cl<sub>2</sub> solvent.

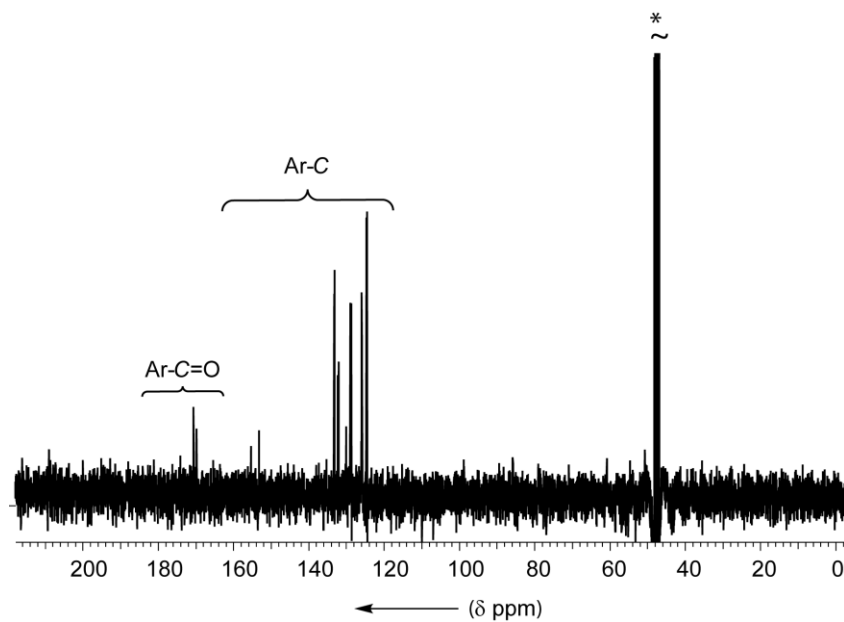


Figure C.16. <sup>13</sup>C{<sup>1</sup>H} NMR (101 MHz, CD<sub>3</sub>OD, 25 °C) spectrum of K-mer-[4.1].

\* indicates CH<sub>3</sub>OH-*d*<sub>3</sub> solvent.

**Table C-1. Selected bond lengths [Å] and bond angles [°] of [PhNMe<sub>2</sub>H]-*rac-mer*-[4.1], [pyH]-*rac-mer*-[4.1], [isoquinolineH]-*rac-mer*-[4.1], [(-)-brucineH]- $\Lambda$ -*mer*-[4.1], and K-*rac-mer*-[4.1].**

| Bond distances     | [PhNMe <sub>2</sub> H]- <i>rac-mer</i> -[4.1] | [pyH]- <i>rac-mer</i> -[4.1] | [isoquinolineH]- <i>rac-mer</i> -[4.1] | [(-)-brucineH]- $\Lambda$ - <i>mer</i> -[4.1] | K- <i>rac-mer</i> -[4.1] |
|--------------------|---|------------------------------|--|---|--------------------------|
| P1-O1              | 1.92(1)                                       | 1.926(2)                     | 1.838(3)                               | 1.908(6)                                      | 1.906(2)                 |
| P1-O3              | 1.778(1)                                      | 1.774(2)                     | 1.774(3)                               | 1.776(7)                                      | 1.765(2)                 |
| P1-O5              | 1.774(1)                                      | 1.769(2)                     | 1.77(3)                                | 1.765(8)                                      | 1.786(2)                 |
| P1-C1              | 1.861(2)                                      | 1.854(2)                     | 1.865(4)                               | 1.85(1)                                       | 1.85(3)                  |
| P1-C8              | 1.849(2)                                      | 1.87(2)                      | 1.857(4)                               | 1.85(1)                                       | 1.852(3)                 |
| P1-C15             | 1.849(2)                                      | 1.842(2)                     | 1.853(4)                               | 1.856(9)                                      | 1.841(3)                 |
| O1-C7              | 1.300(2)                                      | 1.303(3)                     | 1.333(5)                               | 1.30(1)                                       | 1.32(4)                  |
| C7-O2              | 1.239(2)                                      | 1.235(3)                     | 1.218(5)                               | 1.24(1)                                       | 1.217(4)                 |
| O3-C14             | 1.341(2)                                      | 1.38(2)                      | 1.337(5)                               | 1.33(1)                                       | 1.329(4)                 |
| O4-C14             | 1.216(2)                                      | 1.24(2)                      | 1.214(6)                               | 1.23(1)                                       | 1.217(4)                 |
| O5-C21             | 1.341(2)                                      | 1.339(3)                     | 1.341(5)                               | 1.35(1)                                       | 1.334(4)                 |
| O6-C21             | 1.212(2)                                      | 1.208(3)                     | 1.215(6)                               | 1.21(1)                                       | 1.213(4)                 |
| <b>Bond angles</b> |   |                              |  |   |                          |
| O1-P1-C15          | 83.2(6)                                       | 81.9(9)                      | 85.7(2)                                | 83.2(3)                                       | 89.9(1)                  |
| O1-P1-O3           | 86.8(5)                                       | 84.8(9)                      | 87.9(2)                                | 86.5(3)                                       | 91.5(9)                  |
| O3-P1-C8           | 88.3(6)                                       | 91.3(6)                      | 88.5(2)                                | 88.7(4)                                       | 87.5(1)                  |
| C8-P1-O5           | 95.4(6)                                       | 92.9(6)                      | 92.9(6)                                | 95.7(4)                                       | 92.7(1)                  |
| C8-P1-O3           | 92.6(6)                                       | 91.3(6)                      | 91.3(6)                                | 88.7(4)                                       | 87.5(1)                  |
| C8-P1-C15          | 97.0(7)                                       | 94.2(1)                      | 93.0(2)                                | 95.2(4)                                       | 92.9(1)                  |
| C15-P1-O5          | 87.7(6)                                       | 87.5(1)                      | 87.9(2)                                | 87.6(4)                                       | 87.9(1)                  |
| C1-P1-O3           | 90.3(6)                                       | 91.2(1)                      | 90.6(2)                                | 90.0(4)                                       | 87.7(1)                  |
| O5-P1-O3           | 176.3(5)                                      | 175.6(9)                     | 178.0(2)                               | 175.5(3)                                      | 175.6(1)                 |
| C1-P1-C8           | 97.0(7)                                       | 100.5(1)                     | 95.9(2)                                | 97.8(4)                                       | 167.7(1)                 |
| C8-P1-O1           | 174.9(6)                                      | 174.3(1)                     | 176.1(2)                               | 174.9(4)                                      | 84.5(1)                  |
| C15-P1-C1          | 166.9(7)                                      | 164.4(1)                     | 170.8(2)                               | 166.7(4)                                      | 171.5(1)                 |
| C7-O1-P1           | 115.8(1)                                      | 116.3(2)                     | 116.6(3)                               | 116.3(6)                                      | 115.9(2)                 |
| C1-P1-O1           | 84.3(6)                                       | 83.8(1)                      | 85.7(2)                                | 84.1(3)                                       | 84.3(1)                  |
| O1-C7-O2           | 123.8(2)                                      | 122.2(2)                     | 122.2(2)                               | 123.8(9)                                      | 122.5(3)                 |
| O3-C14-O4          | 122.3(1)                                      | 119.1(3)                     | 119.1(3)                               | 121.8(9)                                      | 122.0(3)                 |
| O5-C21-O6          | 122.8(2)                                      | 121.8(2)                     | 121.8(2)                               | 122.1(1)                                      | 121.0(3)                 |

## Appendix D

### D.1 Supplementary Spectra for Chapter 5

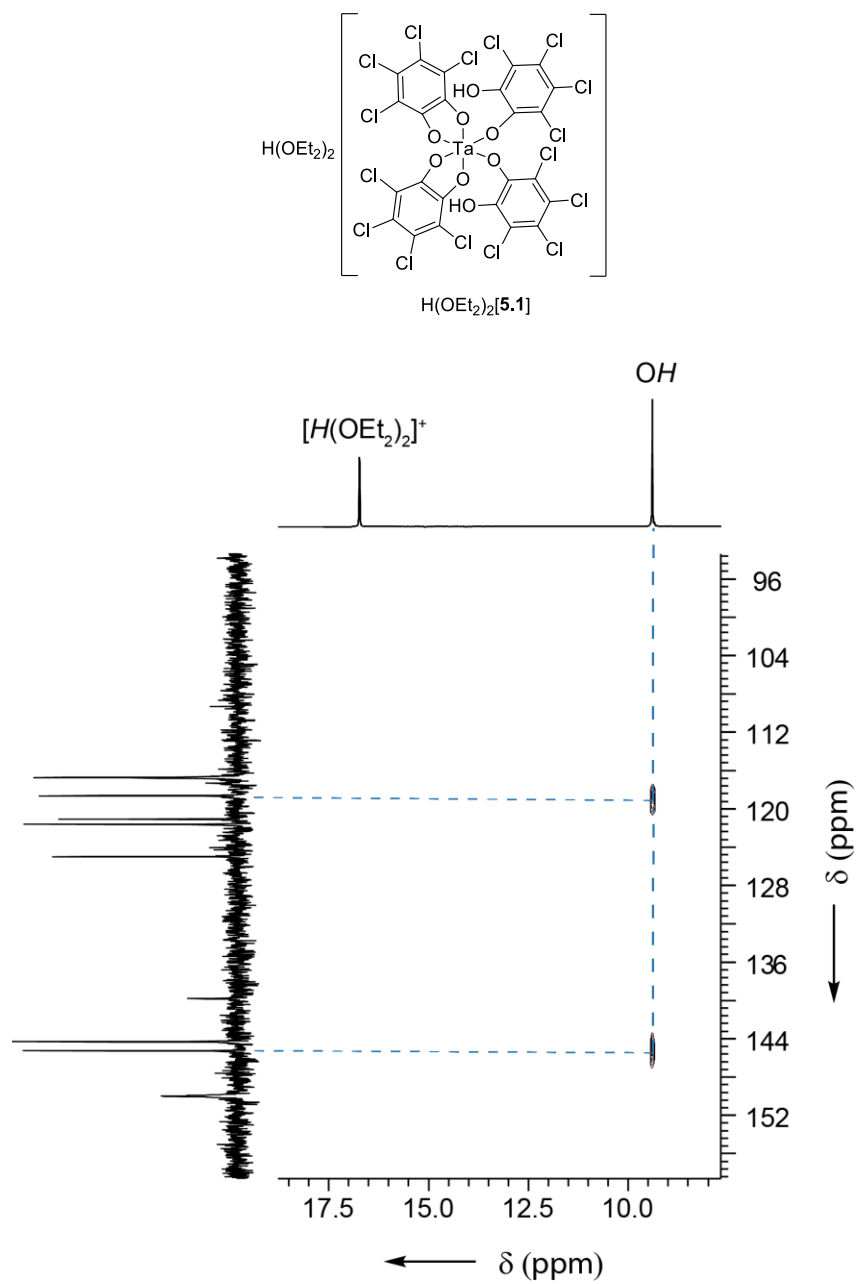


Figure D.1.  $^1\text{H}$ - $^{13}\text{C}$  HMBC NMR (400 MHz for  $^1\text{H}$ ,  $\text{CD}_2\text{Cl}_2$ ,  $-85^\circ\text{C}$ ) spectrum of  $\text{H}(\text{OEt}_2)_2[5.1]$ .

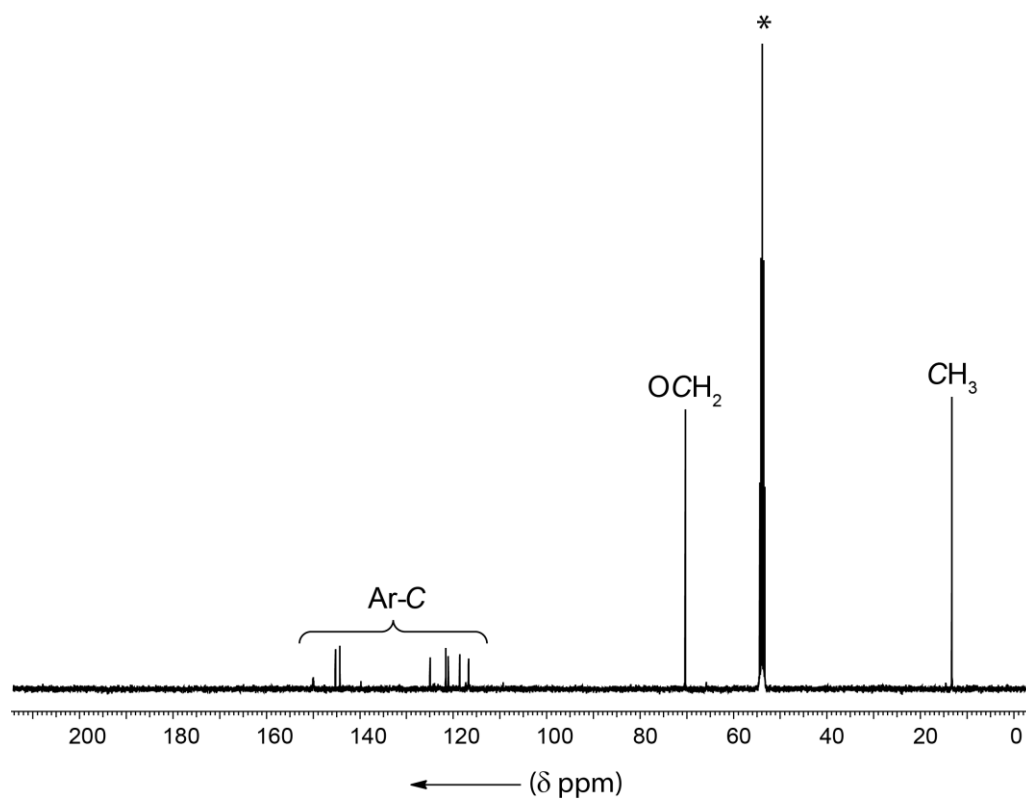
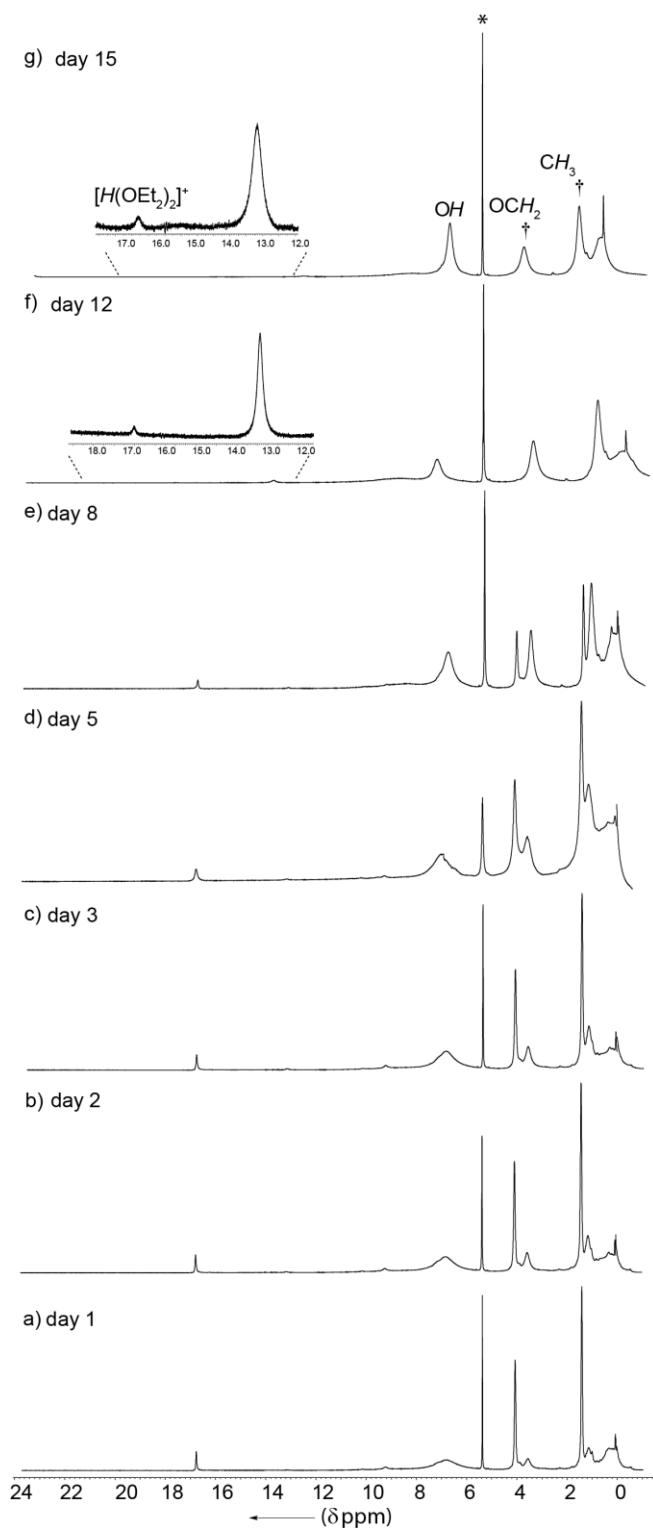


Figure D.2.  $^{13}\text{C}\{^1\text{H}\}$  NMR (400 MHz,  $\text{CD}_2\text{Cl}_2$ ,  $-85^\circ\text{C}$ ) spectrum of  $\text{H}(\text{OEt})_2[5.1]$ .

\* indicates  $\text{CH}_2\text{Cl}_2-d_2$  solvent.



**Figure D.3.** <sup>1</sup>H NMR (400 MHz, CD<sub>2</sub>Cl<sub>2</sub>, -85 °C) spectrum of H(OEt<sub>2</sub>)<sub>2</sub>[5.1]: a) day 1; b) day 2; c) day 3; d) day 5; e) day 8 (addition of CD<sub>2</sub>Cl<sub>2</sub> ca. 0.9 mL); f) day 12 and g) day 15. † indicates free Et<sub>2</sub>O.

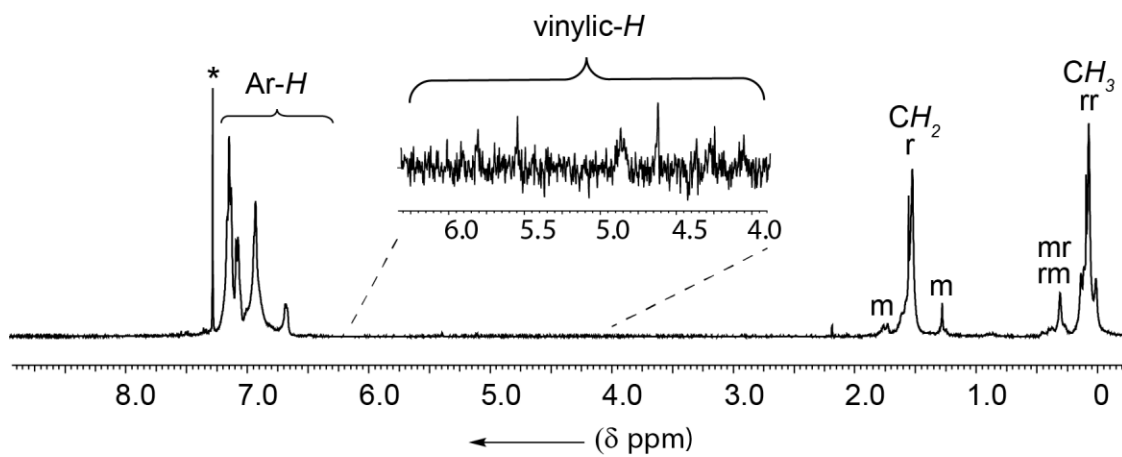


Figure D.4.  $^1\text{H}$  NMR (400 MHz,  $\text{CDCl}_3$ , 25  $^\circ\text{C}$ ) spectrum of syndiotactic-rich poly( $\alpha$ -methylstyrene) ( $rr = 86\%$ ); polymerization performed with initiator  $\text{H}(\text{OEt}_2)_2[5.2]$  at  $-78\text{ }^\circ\text{C}$ . \* indicates residual  $\text{CHCl}_3$  solvent.